UNIVERSIDADE FEDERAL DE SANTA MARIA
CENTRO DE TECNOLOGIA
PROGRAMA DE PÓS-GRADUAÇÃO EM ENGENHARIA QUÍMICA

Christian Luiz da Silveira

AVALIAÇÃO E APLICAÇÃO DE MODELOS TERMODINÂMICOS NO EQUILÍBRIO DE FASES EM UMA AMPLA FAIXA DE PRESSÃO EM SISTEMAS ENVOLVENDO ÁGUA, ÁLCOOL E HIDROCARBONETOS

Santa Maria, RS
2018

Christian Luiz da Silveira

AVALIAÇÃO E APLICAÇÃO DE MODELOS TERMODINÂMICOS NO EQUILÍBRIO DE FASES EM UMA AMPLA FAIXA DE PRESSÃO EM SISTEMAS ENVOLVENDO ÁGUA, ÁLCOOL E HIDROCARBONETOS

Tese apresentada ao Curso de Doutorado em Engenharia Química, da Universidade Federal de Santa Maria (UFSM, RS), como requisito parcial para obtenção do título de **Doutor em Engenharia Química**.

Orientadora: Profª. Drª. Nina Paula Gonçalves Salau

Santa Maria, RS
2018

Christian Luiz da Silveira

AVALIAÇÃO E APLICAÇÃO DE MODELOS TERMODINÂMICOS NO EQUILÍBRIO DE FASES EM UMA AMPLA FAIXA DE PRESSÃO EM SISTEMAS ENVOLVENDO ÁGUA, ÁLCOOL E HIDROCARBONETOS

Tese apresentada ao Curso de Doutorado em Engenharia Química, da Universidade Federal de Santa Maria (UFSM, RS), como requisito parcial para obtenção do título de **Doutor em Engenharia Química**.

Aprovado em 29 de Novembro de 2018:

_____
Nina Paula Gonçalves Salau, Dra. (UFSM)
(Presidente, Orientadora)

_____
Fernanda de Castilhos, Dra. (UFSM)
(Examinadora)

_____
Guilherme Luiz Dotto, Dr. (UFSM)
(Examinador)

_____
Rafael de Pelegrini Soares, Dr. (UFRGS)
(Examinador)

_____
Cauê Torres de Oliveira Guedes Costa, Dr. (UFF)
(Examinador, Participação por Videoconferência)

Santa Maria, RS
2018

AGRADECIMENTOS

Agradeço, primeiramente, aos meus pais e irmãos que me apoiaram em todas minhas decisões, que jamais lançaram âncoras quando eu resolvia velejar novos mares, que inúmeras vezes despenderam esforços custosos para que eu pudesse continuar. Obrigado pelo amor e compreensão, pela educação e formação. É evidente que cada um de vocês construiu um pouco de mim.

Agradeço à Débora Arsand, minha companheira, meu time, pelo amor e apoio incondicional nos últimos anos deste doutorado. Agradeço pela força que me mostraste existir dentro de mim mesmo. Agradeço pelo afeto quando o caminho se tornava difícil demais, segurando minha mão tu me fizeste atravessar por obstáculos que pareciam instransponíveis. Obrigado por me incentivar a ser melhor, a ter mais coragem, a enxergar a vida com olhos mais abertos.

Agradeço à Nina, minha orientadora e conselheira acadêmica desde 2010. Agradeço pela confiança em meu trabalho, pela liberdade que isso proporciona, e pela luz em momentos cruciais. Teus conselhos e auxílios me permitiram crescer como pesquisador e como pessoa.

Agradeço ao professor Stanley Sandler por me aceitar como pesquisador do seu grupo durante um ano na Universidade de Delaware. Minha percepção sobre a vida e sobre a ciência jamais voltariam a ser as mesmas depois daquele ano. E minha admiração pelo profissional dedicado e pessoa querida só cresceram ao longo daquele ano.

Agradeço ao meu amigo Cauê que, durante o ano de 2016 esteve trabalhando e me suportando diariamente na nossa sala na Universidade de Delaware. Obrigado por me ensinar tanto, teu vasto conhecimento me fez te admirar e querer aprender cada vez mais. Obrigado pela companhia, pelos ensinamentos e pela amizade que criamos.

Agradeço ao professor Rafael de Pelegrini Soares pela ajuda despendida em diversos pontos desta tese.

A ajuda de pessoas tão importantes na área da termodinâmica foi imprescindível para que meu caminho, no que até então era uma área nova para mim, fosse menos acidentado.

Minha mais sincera gratidão a todos que contribuíram para este trabalho.

Eis aqui o meu presente a todos vocês: gratidão sincera.

EPÍGRAFE

I am not what happened to me,
I am what I choose to become.

(C. G. Jung)

RESUMO

AVALIAÇÃO E APLICAÇÃO DE MODELOS TERMODINÂMICOS NO EQUILÍBRIO DE FASES EM UMA AMPLA FAIXA DE PRESSÃO EM SISTEMAS ENVOLVENDO ÁGUA, ÁLCOOL E HIDROCARBONETOS

AUTOR: Christian Luiz da Silveira
ORIENTADORA: Nina Paula Gonçalves Salau

Modelos termodinâmicos são essenciais para a descrição precisa de inúmeros processos industriais do escopo do engenheiro químico. Grande parte desses processos envolve, principalmente, equilíbrio de fases, como em equipamentos para processos de separação (destiladores, secadores, decantadores). Neste sentido, este trabalho apresenta uma revisão sobre diversos modelos termodinâmicos de energia de Gibbs em excesso, ou modelos de coeficiente de atividade. Também, investigou-se o uso destes através da união de modelos de coeficiente de atividade com equações cúbicas de estado através de regras de mistura. Os modelos foram abordados de maneiras diversas para a realização de cálculos de equilíbrio de fases, sejam elas líquido-vapor ou líquido-líquido. No que diz respeito à predição de dados de ELV do sistemas binários estudados neste trabalho, os modelos UNIQUAC e NRTL (tanto com parâmetros de literatura quanto com parâmetros otimizados) apresentaram os melhores resultados entre os modelos correlativos, já entre os modelos preditivos, o modelo UNIFAC (com parâmetros estimados) e o modelo COSMO-SAC apresentaram os resultados mais precisos. Ao se investigar a acurácia dos modelos na predição de coeficientes de atividade em diluição infinita dos mesmos sistemas, o modelo F-SAC se mostrou mais preciso. A predição do envelope de fases em diversos sistemas ternários de fase líquida foi mais precisa utilizando o modelo UNIFAC-LLE, porém, para diversos sistemas estudados, os modelos COSMO-SAC e F-SAC também apresentaram bons resultados. Quando regras de mistura foram utilizadas, o modelo UNIFAC tornou a oferecer excelentes resultados, sendo a combinação UNIFAC+VDW1+PRSV a mais precisa das 45 combinações testadas. O modelo COSMO-SAC revelou discrepâncias significativas na predição de ELV quando associado a EOS através da regra de mistura HVOS. Observou-se, também, uma tendência à deterioração das regras de mistura com o aumento do comprimento da cadeia carbônica do alcano presente na mistura.

Palavras-chave: Modelos de energia de Gibbs em excesso. Equilíbrio de fases. Regras de mistura.

ABSTRACT

ASSESMENT AND APPLICATION OF THERMODYNAMICS MODELS IN PHASE EQUILIBRIUM CALCULATION IN A WIDE RANGE OF PRESSURE IN SYSTEMS CONTAINING WATER, ALCOHOL AND HYDROCARBONS

AUTHOR: Christian Luiz da Silveira
ADVISOR: Nina Paula Gonçalves Salau

The role of thermodynamics models in describing several industrial processes for chemical engineers is essential. Many of those processes involve, mainly, phase equilibrium. This is the case of separation processes equipment, such as distillers, dryers, and decanters. In this manner, this work presents a review over several thermodynamics excess Gibbs energy models, or simply activity coefficients models. In addition, the use of these models was investigated when they were coupled to equations of state by using mixing rules. The models were addressed in different ways in order to perform phase equilibrium calculations, be them vapor-liquid or liquid-liquid. Concerning to the VLE data prediction for the binary systems studied in this work, the UNIQUAC and NRTL (either using literature parameters or optimized parameters) models presented the best results among the correlative models, and among the predictive models the UNIFAC (with estimated parameters) and the COSMO-SAC models yielded the most accurate results. When the predictions of infinite-dilution activity coefficients of the same systems were analyzed, the F-SAC has proved to be the most successful model. The phase-envelope prediction of several ternary liquid mixtures was best performed by the UNIFAC-LLE model, however, for several systems the COSMO-SAC and F-SAC models also presented reliable results. When the mixing rules were applied, the UNIFAC model offered, again, great results, and the UNIFAC+VDW1+PRSV combination the most accurate among the 45 combinations that were tested. The COSMO-SAC model has revealed significant unconformity in the VLE predictions when associated to an EOS by the HVOS mixing rule. It was also observed that the mixing rules results tend to deteriorate as the chain-length of the alkane present on the mixture becomes larger.

Keywords: Excess Gibbs energy models. Phase equilibrium. Mixing Rules.

LISTA DE ILUSTRAÇÕES

Capítulo 2

Capítulo 3

LISTA DE TABELAS

Capítulo 3

Capítulo 4

LISTA DE ABREVIATURAS E SIGLAS

ASOG – Analytical solution of groups

COSMO – Conductor-like screening model

COSMO-SAC - Conductor-like screening model segment activity coefficient

COSMO-RS - Conductor-like screening model for real solvents

EGE – Energia de Gibbs em Excesso

ELL – Equilíbrio Líquido-Líquido

ELLV – Equilíbrio Líquido-Líquido-Vapor

ELV – Equilíbrio Líquido-Vapor

EOS – Equação de Estado

F-SAC – Functional-segment activity coefficient

NRTL – Non-Random Two-Liquid model

UNIFAC – UNIQUAC Functional-group activity coefficients

UNIFAC-LLE – UNIFAC for Liquid-Liquid Equilibrium

UNIQUAC – Universal Quasichemical Theory

LISTA DE SÍMBOLOS

A – Área de superfície (modelo COSMO-SAC) ou energia de Helmholtz (capítulo 5)

a – Parâmetro de atração da espécie

b – Parâmetro de repulsão, ou volumétrico, da espécie

a_{mn} – Parâmetro de interação energética dos modelos UNIFAC

b_{mn} – Parâmetro de interação energética do modelo UNIFAC(Do)

c_{mn} – Parâmetro de interação energética do modelo UNIFAC(Do)

f - Fugacidade

G – Energia de Gibbs

g – Energia de Gibbs para descrição do modelo NRTL

K – Razão entre coeficientes de atividade

l – Parâmetro dos modelos UNIQUAC e UNIFAC

n_i – Número de segmentos i (modelo COSMO-SAC)

NC – Número de componentes do sistema

NF – Número de fases

P – Pressão

$p(\sigma)$ – Perfil sigma

Q – Parâmetro de superfície de grupo funcional

q – Parâmetro de área superficial

R – Constante universal dos gases ideais

r – Parâmetro volumétrico

T – Temperatura

u – Parâmetro de energia de interação molecular

V – Volume

X – Fração molar de grupo funcional

x – Fração molar da fase líquida

y – Fração molar da fase vapor

z – Fração de alimentação no problema de *flash* (capítulo 4) e média do número de coordenação (capítulo 3)

α – Parâmetro de equação de estado (capítulo 5) e constante de não-aleatoriedade (capítulo 3)

Δ - Variação de alguma propriedade

Γ – Coeficiente de atividade residual de grupo funcional

γ – Coeficiente de atividade

κ – Constante de Boltzmann

ν – Número de ocorrências de um grupo funcional em uma espécie química

τ – Parâmetro de interação binária

ϕ – Segmento ou fração volumétrica da espécie

ϕ' – Modificação da fração volumétrica de espécie do modelo UNIFAC(Do)

Θ – Parâmetro dos modelos UNIFAC

θ – Fração da área da espécie

ϱ – Propriedade termodinâmica

χ – Variável utilizada para descrever a variação do número de mols em um sistema

σ – Densidade de carga

μ – Potencial químico

ζ – Constante de dispersão

Ψ – Parâmetro de interação energética dos modelos UNIFAC

ω – Fator acêntrico

Sobrescritos

$\bar{}$ - Propriedade molar

I e II – Fases I e II de um sistema em equilíbrio

ex – Propriedade em excesso

L – Fase líquida

MI – Mistura ideal

sol – Solvatação

tot - Total

V – Fase vapor

vap – Vapor

Subscritos

c – Propriedade em condições críticas

$comb$ – Termo combinatorial

doa – Doador

EE – Equação de Estado

hb – Ligação de Hidrogênio

i – Componente de uma mistura

k – Número de iteração

mix - Mistura

par – Pares de segmentos

r – Propriedade reduzida

rec - Receptor

res – Termo residual

S - Segmento

SUMÁRIO

1 INTRODUÇÃO

A eficiência e a otimização de processos industriais estão diretamente ligadas à capacidade que possuímos de descrever um processo ou um fenômeno através de modelos matemáticos que possam nos direcionar e apontar os detalhes que podem ser melhorados. Neste sentido, Soares e Gerber (GERBER; SOARES, 2013) relatam que a predição acurada de propriedades de substâncias em solução são a chave para a otimização de processos, especialmente no que diz respeito a processos de separação.

No que diz respeito à termodinâmica, modelos são geralmente estacionários. Os modelos termodinâmicos estabelecem relações fundamentais entre variáveis de estado, portanto, são comumente utilizados como relações constitutivas para outros modelos de processos. Por exemplo, uma coluna de destilação pode ser descrita por diversos balanços de massa e energia, porém, o que estabelece o comportamento e equilíbrio das fases gás e líquido no processo são as equações termodinâmicas de equilíbrio.

Inúmeros modelos matemáticos termodinâmicos já foram propostos, muitos deles vêm sendo utilizados há décadas, como é o caso de algumas equações cúbicas de estado. Mathias e Klotz (MATHIAS; KLOTZ, 1994) relatam que equações de estado (EOS) vêm sendo utilizadas na indústria com bastante eficácia para modelagem e predição de propriedades termodinâmicas, tais como densidade, fugacidade, entalpia e entropia. Os autores ressaltam ainda a boa performance que EOSs baseadas na teoria de van der Waals possuem.

Equações de estado, no entanto, são aplicáveis a faixas que vão da Equação do tipo Virial (aplicável a baixas densidades) às Equações de Estado Cúbicas, essas que, apesar de seu bom desempenho em diversas faixas de pressão e temperatura, podem ser utilizadas para descrever apenas misturas relativamente simples, que não realizam pontes de hidrogênio, por exemplo. Para superar essa limitação, os chamados Modelos de Energia de Gibbs em Excesso (EGE) – também conhecidos como modelos de coeficiente de atividade -, os quais podem descrever o comportamento de moléculas de alta complexidade, porém com aplicação,

principalmente, em fases líquidas (SILVEIRA; SANDLER, 2017; WONG; ORBEY; SANDLER, 1992).

Propriedades em excesso são utilizadas para descrever mudanças nas propriedades de sistemas que, de alguma forma, excedem as mudanças esperadas em um sistema ideal (SANDLER, 2006); ou seja, propriedades em excesso são utilizadas para mensurar o afastamento da idealidade de um sistema. Destarte, a utilização de modelos de coeficiente de atividade se mostra interessante.

Modelos podem ser empíricos ou teóricos, e no caso dos modelos de energia livre de Gibbs em excesso não é diferente. Diversos modelos foram propostos para descrever a não-idealidade de sistemas, o cálculo de coeficientes de atividade passa por modelos que são completamente baseados em ajustes empíricos até modelos baseados em sólidos preceitos teóricos. Mais detalhes sobre modelos de coeficiente de atividade serão discutidos na seção 2.3 desta tese.

Um grande problema enfrentado pelos modelos de EGE é a necessidade de dados experimentais para ajustar parâmetros. Por exemplo, um dos modelos teóricos mais utilizados atualmente é o modelo UNIFAC (FREDENSLUND; JONES; PRAUSNITZ, 1975); este modelo, ainda que baseado em pressupostos teóricos, necessita de dados experimentais para ajustar seus parâmetros de energia de interação entre os grupos funcionais das moléculas envolvidas. Dados experimentais nem sempre estão disponíveis nas condições de temperatura e pressão necessárias para as estimações, ou ainda, em número suficiente para permitir estimações de parâmetros robustas. Assim, uma outra opção para a obtenção de coeficientes de atividade é o uso de modelos baseados na teoria COSMO (KLAMT; SCHÜÜRMANN, 1993), tais como COSMO-RS (KLAMT, 1995) e COSMO-SAC (LIN; SANDLER, 2002), os quais necessitam de apenas alguns dados experimentais para estimar parâmetros universais que serão utilizados pelo modelo, ademais, as informações subsequentes são obtidas por cálculos de química quântica. Esses cálculos são, geralmente, realizados por softwares especializados em química quântica e dinâmica molecular, como o GAMESS, o DMol3 e o ADF.

Dessa maneira, com uma necessidade de dados experimentais diminuída, o custo para o desenvolvimento e pesquisa de novos materiais, ou para a obtenção de

informações sobre o comportamento de diversas misturas e suas propriedades, se torna muito menor (HSIEH; LIN, 2012; XUE; MU; GMEHLING, 2012).

1.1 APLICAÇÕES DE MODELOS TERMODINÂMICOS

Os cálculos de necessidades de calor e de trabalho para processos químicos e físicos, a determinação das condições de equilíbrio para reações químicas e para transferência de espécies químicas entre fases diferentes, são da área de atuação do engenheiro químico e estão presentes em uma grande variedade de processos industriais (SMITH; VAN NESS; ABBOTT, 2007).

Um exemplo muito comum e nem por isso menos interessante é o problema de uma coluna de destilação. Uma hipótese que geralmente se faz em modelos matemáticos de colunas de destilação é que cada prato da coluna possui suas fases líquida e vapor em equilíbrio. Uma vez que se assume o equilíbrio de fases líquida e vapor em cada um dos pratos, pode-se inferir as composições nas duas fases através de balanços de massa e energia e por relações constitutivas de equilíbrio, como as que serão apresentadas no item 2.1 desta tese.

Exemplos da aplicação de modelos termodinâmicos podem ser vistos no trabalho de Jia e colaboradores (JIA et al., 2018), que utilizaram o modelo termodinâmico UNIQUAC. Souto e colaboradores investigaram a eficiência máxima de um processo de destilação extrativa utilizando os modelos termodinâmicos NRTL e UNIQUAC (SOUTO et al., 2018). Diversos outros trabalhos podem ser encontrados na literatura que evidenciam o papel dos modelos termodinâmicos em processos de separação, como processos de separação líquido-líquido, evaporadores, entre outros (OSUOLALE; ZHANG, 2017; SULEMAN et al., 2018; XU et al., 2017; YANG et al., 2018).

Os exemplos citados acima são os exemplos mais comuns do escopo do engenheiro químico. Modelos termodinâmicos, no entanto, podem ter seu uso estendido de processos de separação a buracos negros. O livro *Chemical, Biochemical, and Engineering Thermodynamics* (SANDLER, 2006), por exemplo, possui capítulos inteiros dedicados ao uso de modelos termodinâmicos, cujas

aplicações se estendem de equilíbrios líquido-vapor e líquido-líquido a reações químicas e desnaturação de proteínas.

1.2 OBJETIVOS

1.2.1 Objetivo Geral

Assim, o presente trabalho tem como objetivo principal investigar a precisão de modelos termodinâmicos de energia de Gibbs em excesso na predição de equilíbrios líquido-vapor e líquido-líquido. Essa análise é estendida para diferentes faixas de temperatura e pressão para diversos sistemas, binários e ternários em fase líquida e vapor, através do uso de regras de mistura e equações de estado.

1.2.2 Objetivos Específicos

i. Estudo e avaliação de modelos termodinâmicos de energia de Gibbs em excesso (modelos de coeficiente de atividade), correlativos e preditivos em cálculos de equilíbrio líquido-líquido e líquido-vapor;
ii. Estimação de parâmetros dos modelos Wilson, NRTL, UNIQUAC e UNIFAC;
iii. Avaliação do uso de três regras de mistura na extensão dos modelos para diferentes pressões e temperaturas em sistemas binários;
iv. Avaliação geral dos modelos com e sem regras de mistura na predição de equilíbrio de fases líquido-vapor e líquido-líquido.

1.3 ESTRUTURA DA TESE

Neste trabalho, serão apresentados estudos em equilíbrio de fases utilizando diferentes modelos e sistemas (binários e ternários), transitando entre EOSs e EGEs, por vezes utilizando regras de mistura.

Assim, a motivação e a importância deste trabalho foram discutidas neste capítulo de introdução (Capítulo 1). No Capítulo 2 serão apresentados: a) conceitos e fundamentos sobre equilíbrio de fases utilizados neste trabalho, tanto para equilíbrio líquido-vapor (ELV), quanto para equilíbrio líquido-líquido (ELL) e equilíbrio líquido-líquido-vapor (ELLV); b) uma revisão sobre equações cúbicas de estado será apresentada, onde serão discutidos alguns aspectos sobre limitações, vantagens e desvantagens, e características de algumas das principais equações cúbicas de estado utilizadas neste trabalho; c) os modelos de EGE, ou de coeficiente de atividade, utilizados neste trabalho, onde serão reportados detalhes sobre os modelos Wilson, UNIQUAC, UNIFAC, UNIFACLLE, UNIFAC(Do), COSMO-SAC e F-SAC - esses modelos voltarão a ser expostos brevemente no capítulo 3, constituído de um artigo científico onde os modelos citados são utilizados para previsão de ELV em diferentes sistemas binários; d) uma revisão sobre regras de mistura, com destaque para as regras de van der Waals, Huron-Vidal-Orbey-Sandler e Wong-Sandler - as regras de mistura serão abordadas, também, no capítulo 6 , que é composto por um artigo científico onde são feitas comparações de diferentes regras de mistura aplicadas a equações cúbicas de estado e modelos de coeficiente de atividade para previsão de dados ELV.

Os capítulos 3, 4 e 5 serão todos apresentados em forma de artigo científico. O capítulo 3, como mencionado anteriormente, tratar-se-á do uso de diferentes modelos de EGE na previsão do comportamento ELV em 32 sistemas binários. Os dados experimentais utilizados serão obtidos da literatura para diferentes condições de temperatura e pressão. Este artigo já se encontra publicado na revista *Fluid-Phase Equilibria* com o título *From Wilson to F-SAC: A comparative analysis of correlative and predictive activity coefficient models to determine VLE and IDAC of binary systems c*.

O capítulo 4, também em formato de artigo (*The UNIFAC(LLE), COSMO-SAC, and F-SAC performances on ternary LLE calculations*), trará comparações dos resultados de 3 modelos de EGE – UNIFACLLE, COSMO-SAC e F-SAC – na descrição de 55 sistemas ternários de ELL. Os 55 sistemas são compostos por diferentes componentes, e todos os dados utilizados foram obtidos da literatura, como serão especificadas no artigo. O artigo referente a este capítulo se encontra submetido à revista *Fluid-Phase Equilibria*.

No capítulo 5, serão utilizadas regras de mistura para estender os limites de aplicabilidade tanto das equações cúbicas de estado quanto dos modelos de coeficiente de atividade. Sistemas binários de ELV, com dados em diferentes condições de temperatura e pressão, serão utilizados na avaliação de desempenho dos modelos. As regras de mistura utilizadas neste artigo serão uma modificação de van der Waals, Huron-Vidal-Orbey-Sandler e Wong-Sandler; as equações de estado serão Peng-Robinson, PRSV e PRSV2; os modelos EGE utilizados serão UNIQUAC, UNIFAC, COSMO-SAC e F-SAC. O capítulo encontra-se publicado na revista *Fluid-Phase Equilibria* sob o nome de *On the mixing rules matter: The VLE predictions for binary systems*.

O capítulo 6 trará resultados e discussões gerais sobre todos os artigos elaborados nesta tese. Por fim, o capítulo 7 será composto de conclusões gerais sobre os trabalhos publicados nesta tese. Também serão discutidas formas de continuidade para este trabalho.

Nos apêndices poderão ser encontrados tabelas de resultados detalhadas, fluxogramas de algoritmos e demais informações relevantes ao trabalho:

- Apêndice A: um fluxograma para cálculo de ELV com regras de mistura é apresentado;
- Apêndice B: um fluxograma para cálculo de *flash* de ELL;
- Apêndice C: um fluxograma para cálculos de ELL com regras de mistura é apresentado;
- Apêndice D: a Tabela D1 do Apêndice D possui uma lista das equações dos parâmetros de EOS;
- Apêndice E: artigo científico produzido durante o período de colaboração com o professor Dr. Stanley Sandler. O artigo está publicado na revista da *American Institute of Chemical Engineers Journal* com o título *Extending the range of COSMO-SAC to high temperatures and high pressures*.

2 REVISÃO DE LITERATURA

2.1 EQUILÍBRIO DE FASES

2.1.1 Equilíbrio Líquido-Vapor (ELV)

No que diz respeito a equilíbrio de fases, Sandler (SANDLER, 2006) optaram por iniciar a abordagem através da definição de estabilidade de um sistema com apenas um componente. Um sistema isotérmico é dito instável quando a equação 2.1 é verdadeira:

$$\left(\frac{\partial P}{\partial \bar{V}}\right)_T > 0 \tag{2.1}$$

Ou seja, um fluido é dito estável quando há uma diminuição do volume ao aumentar-se a pressão à temperatura constante. Além disso, a condição de equilíbrio $\bar{G}^I = \bar{G}^{II}$ pode ser utilizada para que se encontre a posição da linha de coexistência de fases.

Uma condição necessária, mas não suficiente, ao equilíbrio químico é a variação da energia livre de Gibbs em relação ao número de mols do sistema seja zero:

$$\left(\frac{\partial G}{\partial \chi}\right)_{T,P} = 0 \tag{2.2}$$

Sendo χ uma variável que descreve a variação de número de mols do sistema. Isso resulta numa igualdade de potenciais químicos

$$\mu_i^I = \mu_i^{II} = \cdots = \mu_i^{NF} \tag{2.3}$$

Sendo μ_i^I e μ_i^I os potenciais químicos do componente i nas fases I e II e NF o número de fases no sistema. Sendo

$$\mu_i - \mu_i^o = RT \ln \frac{\bar{f}_i}{\bar{f}_i^o} \tag{2.4}$$

Onde o sobrescrito o se refere à um estado de referência. Então, rearranjando a equação 2.3 em termos de fugacidades, obtém-se:

$$\bar{f}_i^I = \bar{f}_i^{II} = \cdots = \bar{f}_i^{NF} \tag{2.5}$$

Onde $\bar{f}_i^I$, $\bar{f}_i^{II}$ e $\bar{f}_i^{NF}$ se referem às fugacidades nas fases I, II e NF. Quando tratamos de equilíbrio líquido-vapor em misturas, no entanto, um bom ponto inicial é o critério de equilíbrio representado pela equação 2.5, em termos mais comuns a problema de ELV:

$$\bar{f}_i^L(T, P, \bar{x}) = \bar{f}_i^V(T, P, \bar{y}) \tag{2.6}$$

Onde $\bar{f}_i^L$ e $\bar{f}_i^V$ representam as fugacidades da espécie i na mistura nas fases líquida e vapor, respectivamente; T representa a temperatura do sistema; P, a pressão; $\bar{x}$ e $\bar{y}$, o conjunto de frações molares nas fases líquida e vapor, respectivamente.

A fugacidade de uma espécie i em fase líquida pode ser obtida através de equações de estado, enquanto modelos de energia de Gibbs em excesso podem fornecer o coeficiente de atividade para corrigir a fugacidade de uma solução ideal. Assim, costuma-se utilizar uma notação para cada tipo de abordagem. Se a equação de estado é utilizada para descrever as fases líquida e vapor, diz-se que está se usando o método $\phi - \phi$. A outra opção é utilizar a equação de estado para descrever a fase vapor e um modelo de energia de Gibbs em excesso para a fase líquida, chamado de método $\gamma - \phi$.

A regra de Lewis-Randall estabelece uma relação entre a fugacidade de uma espécie numa mistura gasosa $\bar{f}_i^V$ e a fugacidade do componente puro na fase gás f_i^V (sob mesma temperatura e mesma pressão):

$$\bar{f}_i^V(T, P, \bar{y}) = y_i f_i^V(T, P) \tag{2.7}$$

Tendo em vista as equações 2.6 e 2.7, após uma série de substituições e manipulações algébricas, obtém-se:

$$x_i \gamma_i(T, P, \bar{x}) P_i^{vap}(T) = y_i P \tag{2.8}$$

Que é a equação característica para ELV de uma mistura não-ideal na fase líquida a baixas pressões, onde γ_i é o coeficiente de atividade da espécie i e P_i^{vap} é a pressão de vapor da espécie i.

Caso, porém, a mistura em fase líquida seja considerada ideal, o coeficiente de atividade se torna unitário e obtém-se a equação da lei de Raoult (ambas fases ideais):

$$x_i P_i^{vap}(T) = y_i P = P_i \tag{2.9}$$

Smith, Van Ness e Abbott (SMITH; VAN NESS; ABBOTT, 2007) ressaltaram que, assim como o gás ideal serve como base para prever o comportamento padrão de um gás ideal, a fase líquida ideal funciona da mesma maneira. Esses sistemas ideais levam em consideração misturas em que suas espécies moleculares não diferem tanto uma da outra em tamanho e possuem a mesma natureza química (e.g., hidrocarboneto + hidrocarboneto).

Em seu livro Introdução à Termodinâmica da Engenharia Química (SMITH; VAN NESS; ABBOTT, 2007), os autores indicaram diferentes tipos de algoritmos que podem ser programados para diferentes cálculos de equilíbrio de fases:

- BOL P: serve para calcular as composições da fase vapor e sua pressão, conhecidas as composições da fase líquida e temperatura;
- ORV P: serve para calcular as composições da fase líquida e sua pressão, conhecidas as composições da fase vapor e temperatura;
- BOL T: serve para calcular as composições da fase vapor e sua temperatura, conhecidas as composições da fase líquida e pressão;
- ORV T: serve para calcular as composições da fase líquida e sua temperatura, conhecidas as composições da fase vapor e pressão.

A maioria dos problemas abordados neste trabalho podem ser resolvidos com o algoritmo BOL P. Este método será visto novamente no capítulo 6 desta tese.

A maior parte dos sistemas, no entanto, não pode ser considerada ideal. É o caso de misturas como etanol + água, por exemplo, que é uma mistura azeotrópica. Um azeótropo é uma mistura cujas composições na fase líquida e na fase vapor se tornam idênticas, não podendo ser descritas pela equação 2.9, que considera ambas as fases ideais. Dessa forma, o desvio da lei de Raoult pode ser:

$$P > \sum_i^{NC} x_i P_i^{vap} \tag{2.10a}$$

$$P < \sum_i^{NC} x_i P_i^{vap} \tag{2.10b}$$

Onde NC é o número de componentes do Sistema. Em 2.10a, ao menos uma das espécies se desvia da idealidade positivamente ($\gamma_i > 1$); e em 2.10b, ao menos uma das espécies desvia da idealidade negativamente ($\gamma_i < 1$).

Os coeficientes de atividade das espécies em misturas podem ser obtidos através de diferentes modelos de energia de Gibbs em excesso. Detalhes sobre os modelos de coeficiente de atividade utilizados neste trabalho poderão ser encontrados no capítulo 4 (Modelos de Energia Livre de Gibbs em Excesso).

Modelos de coeficiente de atividade, ou de energia de Gibbs em excesso, são principalmente aplicáveis a misturas em fase líquida, com diferentes graus de complexidade molecular; equações cúbicas de estado, porém, são aplicáveis apenas a misturas relativamente simples, mas podem ser aplicáveis a condições mais severas de temperatura e pressão. Assim, para cálculos de ELV sob altas pressões, é aconselhável utilizar o método $\phi - \phi$ (SANDLER, 2006).

No entanto, uma outra maneira de estender a aplicabilidade de ambos os tipos de modelos (equações cúbicas de estado e EGEs) é fazer uso de regras de mistura. Mais detalhes sobre regras de mistura, seus conceitos e procedimentos de uso serão abordados no capítulo 5 deste trabalho (Regras de Mistura). Um fluxograma para cálculo de ELV utilizando regras de mistura é apresentado no Apêndice A deste trabalho.

2.1.2 Equilíbrio Líquido-Líquido (ELL)

Até agora tratamos apenas de equilíbrio líquido-vapor em sistemas não-críticos, cujos cálculos são relativamente diretos. Os algoritmos citados anteriormente envolvem procedimentos iterativos de fácil programação computacional e pouco esforço numérico. O mesmo não ocorre quando tratamos de equilíbrio líquido-líquido.

Os problemas de ELL envolvem um grau de dificuldade muito maior, com muitos problemas de convergência para a solução, ou convergência para soluções triviais. O problema de ELL é, portanto, um problema complexo de minimização.

Primeiramente, é importante que se entenda o ELL como qualquer outro problema de equilíbrio de fases. O requerimento básico para o equilíbrio é a igualdade das fugacidades de cada fase, assim, reescrevendo a equação 2.6 em termos para um problema de ELL:

$$\bar{f}_i^I(T,P,\bar{x}^I) = \bar{f}_i^{II}(T,P,\bar{x}^{II}) \tag{2.11}$$

Onde os sobrescritos I e II representam as diferentes fases em equilíbrio de um sistema líquido-líquido. Rearranjando a equação para que o coeficiente de atividade seja introduzido, obtém-se:

$$x_i^I \gamma_i^I(T,P,x_i^I) f_i(T,P) = x_i^{II} \gamma_i^{II}(T,P,x_i^{II}) f_i(T,P) \tag{2.12}$$

Sendo as fugacidades das espécies puras função apenas de temperatura e pressão, e supondo-se o sistema isotérmico e isobárico:

$$x_i^I \gamma_i^I(T,P,x_i^I) = x_i^{II} \gamma_i^{II}(T,P,x_i^{II}) \tag{2.13}$$

Pode-se perceber, portanto, que o problema de ELL pressupõe não-idealidade, uma vez que, caso o sistema fosse ideal, $\gamma_i^I = \gamma_i^{II} = 1$, existindo, portanto, apenas uma fase de composição $x_i^I = x_i^{II}$.

Lembrando que as frações molares de ambas as fases devem somar um,

$$\sum_{i=1}^{NC} x_i^I = \sum_{i=1}^{NC} x_i^{II} = 1 \tag{2.14}$$

Um problema de ELL com 2 componentes sendo resolvido com as equações 2.9 e 2.10 terá, portanto, 4 variáveis ($x_1^I, x_2^I, x_1^{II}, x_2^{II}$) e 4 equações (2.9 para componente e 2.10 para cada componente).

Um dos problemas dessa abordagem é a de que também são soluções do problema todas as respostas triviais, ou seja, todas aquelas em que a mistura apresenta uma única fase, com composições iguais e, portanto, coeficientes de atividade iguais.

Na subseção anterior, expressamos um critério necessário para o equilíbrio na forma da equação 2.2. Porém, o critério suficiente para que um sistema fechado a temperatura e pressão constantes é o de que a energia de Gibbs do sistema seja um mínimo. É importante, no entanto, que o mínimo seja o mínimo global, o que gera

problemas na minimização da função, uma vez que, dependendo dos chutes iniciais dados, a equação pode convergir para mínimos locais.

Uma abordagem diferente para o problema de ELL é o método de Rachford-Rice (RACHFORD; RICE, 1952), originalmente desenvolvido para cálculos de *flash* (ELV). O método foi recentemente aplicado por Possani (POSSANI, 2014) em seu trabalho de dissertação.

O procedimento para o cálculo de *flash* pode ser descrito pela equação 2.15:

$$1 - \sum_i^{NC} \frac{K_i z_i}{1+v(K_i-1)} = 0 \tag{2.15}$$

Onde z_i representa a fração molar do componente i de alimentação; v, a fração da alimentação na fase de composição mais leve; e K_i é dados por:

$$K_i = \frac{\gamma_i^{II}}{\gamma_i^{I}} \tag{2.16}$$

Assim, chutam-se valores iniciais para as frações molares das duas fases, calcula-se os coeficientes de atividade para o conjunto de frações, sob as mesmas condições de temperatura e pressão, para se obter K_i. Finalmente, pode-se utilizar algum método numérico para resolver a equação 2.15 para v. De posse de v, recalcula-se as frações molares de cada fase através das equações 2.17a e 2.17b:

$$x_i^I = \frac{z_i}{\frac{1-v}{K_i}+v} \tag{2.17a}$$

$$x_i^{II} = \frac{z_i - v x_i^I}{1-v} \tag{2.17b}$$

Com os novos valores das frações molares, calcula-se novamente os coeficientes de atividade para se obter um novo K_i e continua-se o procedimento iterativo até que se atinja um a tolerância ε desejada:

$$\left| x_{i,k}^I - x_{i,k-1}^I \right| < \varepsilon \tag{2.18}$$

Onde o subscrito k indica o número de iterações do algoritmo.

Possani também ressalta que $v = 1$ significa que as fases I e II são, na verdade, a mesma fase; portanto, $v = 1$ é uma solução trivial do sistema. Para que isso não ocorra, z_i deve estar contido no envelope de fases. Na verdade, isso acontece porque o método descrito satisfaz apenas a condição necessária ao

equilíbrio líquido-líquido, e não a condição suficiente – que é a de que a energia de Gibbs esteja em seu mínimo global. Um fluxograma para o algoritmo deste método pode ser visualizado no Apêndice B e no capítulo 7 deste trabalho.

Dessa maneira, percebe-se que o problema de ELL é de difícil resolução. Michelsen apresentou dois trabalhos publicados em sequência (Partes I e II) onde o autor discorre sobre análises de estabilidade dos sistemas e também métodos para cálculo de separação de fases, para assim obter o envelope de fases (MICHELSEN, 1982a, 1982b). Outros trabalhos interessantes foram publicados neste sentido, com destaque para Segtovich et al. (SEGTOVICH; BARRETO; TAVARES, 2016), (WASYLKIEWICZ et al., 1996) e a Tese de Li (LI, 2015).

Os métodos acima descritos podem ser utilizados para descrição de diversos sistemas de ELL, porém, quando se deseja previsões dos mesmos sistemas para diferentes faixas de temperatura, o procedimento não é capaz de contabilizar os efeitos da pressão. Dessa maneira, o método mais comum de resolução de problemas ELL, o método $\gamma - \gamma$, só consegue contabilizar os efeitos da pressão no equilíbrio do sistema caso ocorra uma otimização dos parâmetros para os dados experimentais nas condições desejadas, uma vez que modelos como UNIQUAC, UNIFAC e COSMO-SAC são funções da temperatura e composição do sistema (ESCOBEDO-ALVARADO; SANDLER, 1998).

Assim, para que se possa mensurar os efeitos da pressão sem incorrer em um procedimento de estimação de parâmetros, pode-se utilizar de uma regra de mistura. Dessa forma, usa-se uma regra de mistura para “unir” uma equação cúbica de estado com um modelo de EEG. A equação de estado contabiliza a pressão no cálculo das fugacidades – agora sim, como funções de temperatura, pressão e composição -, permitindo que o efeito da pressão seja também visualizado, considerando que as fugacidades na fase líquida leve são diferentes daquelas na fase líquida pesada.

O método é descrito no trabalho de Escobedo-Alvarado e Sandler (ESCOBEDO-ALVARADO; SANDLER, 1998). Este método será revisitado no capítulo 10 desta tese. O fluxograma do algoritmo para este método pode ser encontrado no Apêndice C.

2.2. EQUAÇÕES CÚBICAS DE ESTADOS

Equações cúbicas de estado são equações polinomiais simples capazes de descrever o comportamento PVT de líquidos e vapores (SMITH; VAN NESS; ABBOTT, 2007).

Desde o surgimento da equação cúbica de estado de van der Waals (WAALS, 1873), muitas outras modificações foram propostas. Uma das versões mais promissoras foi aquela proposta por Redlich e Kwong (RK) (REDLICH; KWONG, 1949). As formas das equações de van der Waals (VDW) e RK podem ser vistas nas equações 3.1 e 3.2, respectivamente.

$$P = \frac{RT}{\bar{V}-b} - \frac{a}{\bar{V}^2} \tag{3.1}$$

$$P = \frac{RT}{\bar{V}-b} - \frac{a}{\sqrt{T}\,\bar{V}(\bar{V}+b)} \tag{3.2}$$

Onde P é a pressão do sistema, R é a constante universal dos gases ideais, T é a temperatura, $\bar{V}$ é o volume molar, e a e b são parâmetros específicos das espécies. Os parâmetros a e b são também conhecidos como parâmetros de atração e repulsão (ou volumétrico) das espécies, respectivamente, e são obtidos de maneiras diferentes para cada uma das equações cúbicas de estado apresentadas neste trabalho, assim, as formas mais importante serão apresentadas no Apêndice D

O sucesso da equação de Redlich-Kwong se deve, principalmente, a dois fatores. O primeiro deles é a capacidade de RK descrever com maior precisão, em relação às demais equações da época, o segundo coeficiente de Virial, garantindo boa performance para fluidos em baixa densidade. O segundo fator é a descrição razoável da região de alta densidade de fluidos sob pressão crítica (ABBOTT, 1979).

No entanto, observou-se que RK falhava para fatores acêntricos diferentes de zero. Abbott (ABBOTT, 1979) citou alguns trabalhos realizados que tentaram suplantar essas falhas, no entanto, com pouco sucesso. Então, em 1971 Giorgio Soave propôs a equação conhecida como SRK, na qual o autor modificou o termo atrativo de RK, na forma:

$$P = \frac{RT}{\bar{V}-b} - \frac{\alpha(T)\,a}{\bar{V}(\bar{V}+b)} \tag{3.3}$$

A equação de SRK fornecia melhores resultados na descrição de ELV. No entanto, a equação continuava fornecendo problemas no cálculo de densidades para líquidos, o mesmo problema encontrado em RK. Assim, Peng e Robinson (PENG; ROBINSON, 1976) apresentaram uma nova equação cúbica de estado que pudesse oferecer maior precisão na descrição do comportamento volumétrico em cálculos de ELV, porém, mantendo a simplicidade de sua predecessora. A equação característica de Peng-Robinson (PR) está denotada na equação 3.4.

$$P = \frac{RT}{\bar{V}-b} - \frac{\alpha(T)\,a}{\bar{V}^2+2b\bar{V}-b^2} \tag{3.4}$$

Onde $a = 0.4572\ R^2T_c^2/P_c$, $b = 0.0778\ RT_c/P_c$ e $\alpha(T) = [1 + k(1 - \sqrt{T_r})]^2$.

Sandler (SANDLER, 2006) reportou que as equações de estado mais utilizadas são as equações SRK e PR. Neste trabalho, a equação cúbica de estado de Peng-Robinson foi utilizada e seus resultados podem ser verificados no capítulo 9 e Apêndice E (SILVEIRA; SANDLER, 2017).

Tendo em vista que a equação PR é uma das mais comuns, além de a utilizarmos, utilizou-se também duas variações propostas para a referida equação, ambas propostas por Stryjek e Vera no ano de 1986 (STRYJEK; VERA, 1986a, 1986b).

A primeira das modificações propostas foi batizada pelos próprios autores de PRSV (STRYJEK; VERA, 1986a). A equação PRSV introduz um novo parâmetro por espécie utilizada, e esta modificação permitiu melhores predições em regiões de temperaturas reduzidas baixas (abaixo de 0.7). A introdução desse parâmetro também permitiu a melhoria nas predições de misturas contendo componentes polares e aromáticos. A equação 3.4 se mantém para PRSV, sendo que a modificação reside na determinação do parâmetro k (que consta na função de $\alpha(T)$), agora conforme equação 3.5.

$$k = k_0 + k_1(1 + \sqrt{T_r})(0.7 - T_r) \tag{3.5}$$

Onde

$$k_0 = 0.37889 + 1.4897153\omega - 0.17131848\omega^2 + 0.0196554\omega^3 \tag{3.6}$$

Sendo ω o fator acêntrico e k_1 um fator ajustável característico de cada espécie.

A segunda modificação (PRSV2) proposta pelos autores em seu artigo subsequente (STRYJEK; VERA, 1986b) permitiu maior precisão na descrição do comportamento de ELV, principalmente para misturas contendo componentes polares e hidrocarbonetos saturados. A modificação proposta em PRSV2 consiste numa mudança na equação 3.5, conforme equação 3.7:

$$k = k_0 + \left[k_1 + k_2(k_3 - T_r)(1 - \sqrt{T_r})\right] \times (1 - \sqrt{T_r})(0.7 - T_r) \qquad (3.5)$$

Onde k_0 é dado pela equação 3.6, e k_1, k_2 e k_3 são parâmetros ajustáveis de cada espécie.

Abbott (ABBOTT, 1979) ofereceu uma revisão sobre diversas equações de estado. Uma revisão mais recente, porém, menos abrangente também foi publicada por Valderrama (VALDERRAMA, 2003). Outras equações de estado podem ser citadas, ainda que não sejam cúbicas, sem, no entanto, serem do escopo deste trabalho. Dentre as mais importantes, destacam-se os modelos: SAFT (*Statistical Associating Fluid Theory*), desenvolvido por Chapman e colegas (CHAPMAN et al., 1989) através de uma expansão da expressão da energia de Helmholtz; PC-SAFT (*Perturbed-Chain SAFT*), desenvolvido por Gross e Sadowski (GROSS; SADOWSKI, 2001), que relatam melhorias em relação ao modelo SAFT; e PC-SAFT para eletrólitos (*electrolyte PC-SAFT*),desenvolvido por Cameretti e Sadowski (CAMERETTI; SADOWSKI, 2005) através do uso do termo de Debye-Hückel para interações eletrostáticas.

2.3 MODELOS DE ENERGIA LIVRE DE GIBBS EM EXCESSO

Nos casos em que misturas não podem ser descritas por equações de estado – misturas com moléculas bastante complexas ou que possuem ligações de hidrogênio -, a alternativa para efetuar cálculos de equilíbrio e propriedades termodinâmicas é obter diretamente a energia livre de Gibbs em excesso (SANDLER, 2006; SILVEIRA; SANDLER, 2017).

Neste capítulo trataremos de modelos para o cálculo da energia de Gibbs em excesso, ou modelos de coeficiente de atividade, para misturas líquidas simples. Uma mistura líquida é dita simples quando todos os componentes envolvidos na mistura

estejam na fase líquida quando puros, submetidos às mesmas condições de pressão e temperatura. Por exemplo, uma mistura de água e açúcar em condições de ambiente não é uma mistura líquida simples, pois o açúcar puro está em fase sólida nessas condições (SANDLER, 2006).

A variação de energia de Gibbs para formar uma mistura líquida é dada pela equação 4.1:

$$\Delta_{mix}\bar{G} = \Delta_{mix}\bar{G}^{MI} + \bar{G}^{ex} = RT\sum_{i=1}^{NC} x_i \ln x_i + \bar{G}^{ex}(\bar{x}) \tag{4.1}$$

Onde $\Delta_{mix}\bar{G}$ é a variação na energia de Gibbs no processo de mistura, $\Delta_{mix}\bar{G}^{MI}$ é a variação na energia de Gibbs para uma mistura ideal, $\bar{G}^{ex}$ é a energia de Gibbs em excesso e $\bar{x}$ é o conjunto $[x_1, x_2, \dots, x_{NC}]$.

É importante que se defina, neste ponto, o que é uma propriedade em excesso. Uma propriedade em excesso é a diferença entre a propriedade em uma mistura real e a propriedade em uma mistura ideal, conforme equação 4.2.

$$\bar{\varrho}^{ex} = \Delta_{mix}\bar{\varrho}(T, P, \bar{x}) - \Delta_{mix}\bar{\varrho}^{MI}(T, P, \bar{x}) \tag{4.2}$$

Onde $\bar{\varrho}$ é uma propriedade molar qualquer - como entalpia, entropia, volume molar e energia de Gibbs -, as demais notações seguem a equação 4.1.

Dessa maneira, e tendo em vista a própria definição de coeficiente de atividade (conforme equação 4.3), a energia de Gibbs em excesso pode ser obtida por modelos a fim de se encontrar o coeficiente de atividade de um componente em uma mistura não-ideal.

$$RT\ln\gamma_i(T, P, \bar{x}) = \bar{G}_i^{ex} = \left(\frac{\partial N\bar{G}^{ex}}{\partial N_i}\right)_{T,P,N_{j\neq i}} \tag{4.3}$$

Relembrando a equação 2.8, por exemplo, para determinarmos o equilíbrio de fases de uma mistura, é preciso obter primeiramente o coeficiente de atividade γ_i de cada componente. Para que esse coeficiente de atividade seja obtido, a energia de Gibbs em excesso deve ser calculada diretamente, e para isso, diversos modelos foram propostos.

A seguir, apresentamos uma série de modelos que são comumente utilizados em cálculos de engenharia química. Os modelos citados nesta tese não

compreendem a totalidade dos modelos existentes, porém, abrangem uma boa parte dos modelos mais clássicos e promissores.

2.3.1 Wilson

Wilson (WILSON, 1964) propôs uma equação para representar a energia livre de Gibbs em excesso par uma mistura de NC componentes que pode ser ajustada com $NC(NC-1)$ parâmetros binários. O modelo de coeficiente de atividade de Wilson é derivado da equação de Flory-Huggins – portanto, de composição local -, conforme equação 4.4.

$$\bar{G}^M = RT \sum_i x_i \ln \xi_i \tag{4.4}$$

Onde $\bar{G}^M$ é a energia livre de Gibbs de mistura, e ξ_i é a fração de volume local do componente i em torno de uma molécula central da mesma espécie, dado por:

$$\xi_i = \frac{x_i \bar{V}_i \exp(-g_{ii}/\kappa T)}{\sum_j x_j \bar{V}_j \exp(-g_{ij}/\kappa T)} \tag{4.5}$$

Onde g_{ii} e g_{ij} são termos proporcionais de energia de interação entre as moléculas $i-i$ e $i-j$, respectivamente, e κ é a constante de Boltzmann. Substituindo a equação 4.5 em 4.4 e rearranjando os termos, obtém-se a equação proposta por Wilson:

$$\frac{\bar{G}^{ex}}{RT} = -\sum_i x_i \ln\left(1 - \sum_j x_j \, \Lambda_{j/i}\right) \tag{4.6}$$

Onde $\Lambda_{j/i}$ é o parâmetro binário ajustável da equação, com as restrições

$$\Lambda_{i/i} = 0 \tag{4.7a}$$

$$\Lambda_{j/i} \neq \Lambda_{i/j} \tag{4.7b}$$

Portanto, para uma mistura binária, a equação do modelo de Wilson terá dois parâmetros ajustáveis: $\Lambda_{1/2}$ e $\Lambda_{2/1}$. Se o desvio da idealidade for positivo, os parâmetros também devem ser positivos; se o desvio for negativo, os parâmetros são negativos. Caso um parâmetro seja positivo e outro negativo, o desvio da idealidade

dependerá de qual parâmetro tem maior efeito sobre a equação. Por fim, se um parâmetro for unitário (igual a um), significa que as moléculas não têm interação.

Assim, para um sistema binário, a equação 4.6 se torna:

$$\frac{\bar{G}^{ex}}{RT} = -x_1 \ln\left(x_1 + x_2\Lambda_{1/2}\right) - x_2 \ln\left(x_2 + x_1\Lambda_{2/1}\right) \tag{4.8}$$

Obtendo-se, finalmente:

$$\ln \gamma_1 = -\ln\left(x_1 + x_2\Lambda_{1/2}\right) + x_2\left[\frac{\Lambda_{1/2}}{x_1+x_2\Lambda_{1/2}} - \frac{\Lambda_{2/1}}{x_1\Lambda_{2/1}+x_2}\right] \tag{4.9a}$$

$$\ln \gamma_2 = -\ln\left(x_2 + x_1\Lambda_{2/1}\right) + x_1\left[\frac{\Lambda_{1/2}}{x_1+x_2\Lambda_{1/2}} - \frac{\Lambda_{2/1}}{x_1\Lambda_{2/1}+x_2}\right] \tag{4.9b}$$

2.3.2 NRTL

O modelo conhecido como NRTL (*Non-Random Two-Liquid*) foi desenvolvido por Renon e Prausnitz (RENON; PRAUSNITZ, 1968) levando em consideração o modelo proposto por Wilson. O modelo publicado por Wilson (WILSON, 1964) supõe que a distribuição de moléculas ao redor de uma molécula central é dada por

$$\frac{x_{ji}}{x_{ki}} = \frac{x_j\, exp\left(-g_{ji}/\kappa T\right)}{x_k\, exp(-g_{ki}/\kappa T)} \tag{4.10}$$

Utilizando a equação 4.10 e levando em consideração a não-aleatoriedade de mistura, Renon e Prausnitz propuseram

$$\frac{x_{21}}{x_{11}} = \frac{x_2\, \exp(-\frac{\alpha_{12}g_{21}}{RT})}{x_1 \exp(-\frac{\alpha_{12}g_{11}}{RT})} \tag{4.11}$$

Onde x_{21} e x_{11}representam frações molares locais e α_{12} é uma constante característica da não-aleatoriedade da mistura. Da mesma maneira:

$$\frac{x_{12}}{x_{22}} = \frac{x_1\, \exp(-\frac{\alpha_{12}g_{12}}{RT})}{x_2 \exp(-\frac{\alpha_{12}g_{22}}{RT})} \tag{4.12}$$

As frações molares locais relacionadas por:

$$x_{21} + x_{11} = 1 \tag{4.13a}$$

$$x_{12} + x_{22} = 1 \tag{4.13b}$$

Rearrajando as equações 4.11 em 4.13a e 4.12 em 4.13b, e sendo $g_{21} = g_{12}$:

$$x_{21} = \frac{x_2 \exp(-\alpha_{12}(g_{21}-g_{11})/RT)}{x_1+x_2 \exp(-\alpha_{12}(g_{21}-g_{11})/RT)} \tag{4.14a}$$

$$x_{12} = \frac{x_1 \exp(-\alpha_{12}(g_{12}-g_{22})/RT)}{x_2+x_1 \exp(-\alpha_{12}(g_{12}-g_{22})/RT)} \tag{4.14b}$$

Introduzindo as equações 4.14a e 4.14b na Teoria de Dois Líquidos (*Two-Liquid Theory*) (SCOTT, 1956), desenvolveu-se o modelo NRTL, para o qual a energia de Gibbs residual é dada por:

$$g_1 = x_{11}g_{11} + x_{21}g_{21} \tag{4.15a}$$

$$g_2 = x_{12}g_{12} + x_{22}g_{22} \tag{4.15b}$$

É interessante notar que, caso consideremos um líquido puro do componente 1, por exemplo, a energia residual de Gibbs se tornaria $g_{1,puro} = g_{11}$.

A definição geral de uma propriedade residual é muito semelhante àquela da propriedade em excesso, sendo a propriedade residual a diferença entre o valor real da propriedade sendo um gás não-ideal e o valor da propriedade sendo gás-ideal sob as mesmas condições de pressão e temperatura (SMITH; VAN NESS; ABBOTT, 2007).

Sendo a energia de Gibbs em excesso para uma mistura binária a soma das mudanças nas energias de Gibbs residual:

$$\bar{G}^{ex} = x_1\left(g_1 - g_{1,puro}\right) + x_2(g_2 - g_{2,puro}) \tag{4.16}$$

Substituindo as equações 4.13 e 4.15 em 4.16, e rearranjando os termos, obtém-se a equação característica do modelo NRTL:

$$\frac{\bar{G}^{ex}}{RT} = x_1x_2\left(\frac{\tau_{21}G_{21}}{x_1+x_2G_{21}} + \frac{\tau_{12}G_{12}}{x_2+x_1G_{12}}\right) \tag{4.17}$$

Sendo:

$$G_{12} = exp(-\alpha\tau_{12}) \tag{4.18a}$$

$$G_{21} = exp(-\alpha\tau_{21}) \tag{4.18b}$$

$$\tau_{12} = (g_{12} - g_{22})/RT \tag{4.18c}$$

$$\tau_{21} = (g_{21} - g_{11})/RT \tag{4.18d}$$

Assim, através do modelo NRTL, os coeficientes de atividade podem ser obtidos por:

$$\ln \gamma_1 = x_2^2 \left[\tau_{21} \left(\frac{G_{21}}{x_1 + x_2 G_{21}} \right)^2 + \frac{\tau_{12} G_{12}}{(x_2 + x_1 G_{12})^2} \right] \quad (4.19a)$$

$$\ln \gamma_2 = x_1^2 \left[\tau_{12} \left(\frac{G_{12}}{x_2 + x_1 G_{12}} \right)^2 + \frac{\tau_{21} G_{21}}{(x_1 + x_2 G_{21})^2} \right] \quad (4.19b)$$

2.3.3 UNIQUAC

O modelo semi-teórico UNIQUAC, proposto por Abrams e Prausnitz (ABRAMS; PRAUSNITZ, 1975) como uma extensão da teoria de Guggenheim para misturas contendo moléculas de diferentes tamanhos e formas, utiliza-se, também, do conceito de composição local introduzido por Wilson (WILSON, 1964).

A teoria de Guggenheim leva em consideração apenas misturas de moléculas esféricas de tamanhos semelhantes, assumindo que a molécula de um componente 1, por exemplo, seria vizinha de uma molécula de um componente 2. Essa simples consideração seria verdadeira se existisse, de fato, uma tendência à aleatoriedade na mistura. No entanto, se as moléculas do componente 1, por exemplo, tiverem uma tendência a se agregarem e a repelir moléculas diferentes, a presunção da aleatoriedade se tornaria inapropriada.

Para superar essa suposição, Abrams e Prausnitz propuseram a fração de área local. Os autores consideraram que uma molécula de um componente é descrita por uma série de segmentos interligados, e o número de segmentos por molécula é representado por r_i. Os segmentos, ainda que possuam tamanhos iguais, por definição, podem diferir na área externa de contato; assim, utilizou-se o parâmetro q_i como um parâmetro de proporcionalidade para a área de superfície externa, ou área de contato, possibilitando que o modelo UNIQUAC considere a degeneração das moléculas.

Abrams e Prausnitz obtiveram a equação característica do modelo UNIQUAC como a soma de duas contribuições diferentes: a parte combinatorial, relacionada às diferenças de tamanho e forma das moléculas, o que afeta a entropia da mistura; e a

parte residual, ou predominantemente entálpica, que está relacionada às diferenças energéticas entre as moléculas. Assim:

$$\frac{\bar{G}^{ex}}{RT} = \frac{\bar{G}^{ex}_{comb}}{RT} + \frac{\bar{G}^{ex}_{res}}{RT} \tag{4.20}$$

Onde os subscritos $comb$ e res representam as partes combinatorial e residual, respectivamente.

Para uma mistura de NC componentes, os termos combinatorial e residual tomam a forma das equações 4.21 e 4.22:

$$\frac{\bar{G}^{ex}_{comb}}{RT} = \sum_{i=1}^{NC} x_i \ln\left(\frac{\phi}{x_i}\right) + \frac{z}{2}\sum_{i=1}^{NC} x_i q_i \ln\left(\frac{\theta_i}{\phi_i}\right) \tag{4.21}$$

$$\frac{\bar{G}^{ex}_{res}}{RT} = -\sum_{i=1}^{NC} q_i x_i \ln\left(\sum_{j=1}^{NC} \theta_j \tau_{ji}\right) \tag{4.22}$$

Onde ϕ_i e θ_i representam a fração volumétrica e a fração de área da espécie i, respectivamente (obtidos pelas equações 4.23a e 4.23b), z representa o número de coordenação (geralmente assumido como 10) e τ_{ji} o termo que contabiliza a interação energética de uma espécie i com uma espécie j (obtido pela equação 4.23c).

$$\phi_i = \frac{x_i r_i}{\sum_j x_j r_j} \tag{4.23a}$$

$$\theta_i = \frac{x_i q_i}{\sum_j x_j q_j} \tag{4.23b}$$

$$\tau_{ji} = \exp\left(-\frac{u_{ij} - u_{jj}}{RT}\right) \tag{4.23c}$$

Onde r_i e q_i são parâmetros relacionados ao volume e à área superficial da espécie i, respectivamente; u_{ij} é a energia de interação média das espécies i e j.

Pode-se perceber que, para uma mistura binária, o termo combinatorial possui 2 parâmetros estruturais por componente (r_i e q_i), 2 variáveis de composição (ϕ_i e θ_i) e nenhum parâmetro de interação binária ajustável. Já o termo residual possui apenas uma variável de composição (θ_i) e dois parâmetros de interação binária ajustáveis ($(u_{21} - u_{11})$ e $(u_{12} - u_{22})$, sendo $u_{21} = u_{12}$).

Da mesma maneira, o coeficiente de atividade pode ser dividido em partes residual e combinatória:

$$\ln \gamma_i = \ln \gamma_{i,comb} + \ln \gamma_{i,res} \tag{4.24a}$$

$$\ln \gamma_{i,comb} = \ln \frac{\phi_i}{x_i} - \frac{z}{2} q_i \ln \frac{\phi_i}{\theta_i} + l_i - \frac{\phi_i}{x_i} \sum_j x_j l_j \quad (4.24b)$$

$$\ln \gamma_{i,res} = q_i \left[1 - \ln\left(\sum_j \theta_j \tau_{ji}\right) - \sum_j \frac{\theta_j \tau_{ij}}{\sum_k \theta_k \tau_{kj}} \right] \quad (4.24c)$$

Onde $l_i = (r_i - q_i)\frac{z}{2} - (r_i - 1)$.

Os parâmetros estruturais r e q estão disponíveis na literatura para diversos componentes.

Abrams e Prausnitz reportaram que o modelo NRTL (3 parâmetros) é melhor aplicável à predição da entalpia em excesso do que à predição da energia de Gibbs em excesso. Além disso, os autores relatam que, ainda que o modelo UNIQUAC não tenha oferecido grandes melhorias em relação ao modelo de Wilson para predição de ELV de misturas completamente miscíveis, ele pode representar ELL para misturas de dois ou mais componentes utilizando apenas dois parâmetros ajustáveis por par de espécies.

2.3.4 UNIFAC

O modelo UNIFAC foi desenvolvido por Fredenslund e colaboradores (FREDENSLUND; JONES; PRAUSNITZ, 1975) e teve como base o modelo conhecido como ASOG (DERR; DEAL, 1969) e o modelo UNIQUAC (ABRAMS; PRAUSNITZ, 1975). O modelo UNIFAC, no entanto, contabiliza a contribuição dos grupos funcionais que compõem as moléculas de uma mistura, dessa maneira as espécies passam a ser estudadas no nível dos grupos funcionais das quais são constituídas. O modelo UNIFAC é, por conseguinte, um modelo de contribuição de grupos.

Da mesma maneira que o modelo UNIQUAC, o modelo UNIFAC é dividido em termos residual (dependente da área superficial dos grupos e interações entre eles) e combinatorial (dependente do tamanho e da forma das moléculas). Assim, também podemos escrever os coeficientes de atividade como a soma das contribuições combinatorial e residual.

$$\ln \gamma_i = \ln \gamma_{i,comb} + \ln \gamma_{i,res} \quad (4.25a)$$

$$\ln \gamma_{i,comb} = \ln \frac{\phi_i}{x_i} - \frac{z}{2} q_i \ln \frac{\theta_i}{\phi_i} + l_i - \frac{\phi_i}{x_i} \sum_j x_j l_j \quad (4.25b)$$

$$\ln \gamma_{i,res} = \sum_k \nu_k^{(i)} \left(\ln \Gamma_{\mathrm{k}} - \ln \Gamma_{\mathrm{k}}^{(i)} \right) \quad (4.25c)$$

Onde Γ_{k} representa o coeficiente de atividade residual do grupo funcional k; $\Gamma_{\mathrm{k}}^{(i)}$, o coeficiente de atividade residual do grupo funcional k em uma solução de referência que contém apenas moléculas da espécie i; ν_k é o número de grupos funcionais do tipo k presentes na espécie i.

Assim, os modelos UNIQUAC e UNIFAC diferem pelo fato de que este último utiliza um conceito de solução de grupos para a contribuição residual. O coeficiente de atividade residual de grupo Γ_{k} é obtido pela equação 4.26:

$$\Gamma_{\mathrm{k}} = Q_k \left[1 - \ln(\sum_m \Theta_m \Psi_{\mathrm{mk}}) - \sum_m \left(\frac{\Theta_m \Psi_{\mathrm{km}}}{\sum_n \Theta_n \Psi_{nm}} \right) \right] \quad (4.26)$$

A equação 4.26 também é utilizada para calcular $\Gamma_{\mathrm{k}}^{(i)}$, e Θ_m e Ψ_{mn} são dados por:

$$\Theta_m = \frac{Q_m X_m}{\sum_n Q_n X_n} \quad (4.27)$$

$$\Psi_{\mathrm{mn}} = exp\left(-\frac{(u_{mn} - u_{nn})}{RT} \right) = exp\left(-\frac{a_{mn}}{T} \right) \quad (4.28)$$

Onde Q_k é um parâmetro de superfície do grupo k; X_m é a fração molar do grupo m na mistura, u_{mn} é uma medida de interação energética entre os grupos m e n, e a_{mn} é o parâmetro que deve ser estimado através de dados experimentais e possui unidades de graus Kelvin – é importante notar que $a_{mn} \neq a_{nm}$.

Fredenslund e colaboradores mostraram em seu trabalho que o uso do modelo UNIFAC para novas misturas, sem estimações de parâmetros prévias, pode fornecer resultados satisfatórios se os grupos contidos na mistura já tiverem sido estudados. Por exemplo, se a mistura binária heptano + 2-butanona for estudada e incluída na base de dados, o modelo UNIFAC pode, prontamente, ser utilizado para predições da mistura hexano + 2-butanona. Essa capacidade proporciona uma grande vantagem ao modelo UNIFAC sobre seus predecessores, de forma que nem toda mistura precisa constar no banco de dados, apenas as interações entre os grupos funcionais, o que é muito mais simples.

2.3.5 UNIFAC-LLE

O modelo UNIFAC-LLE, na verdade, é o mesmo modelo UNIFAC, porém com parâmetros otimizados especialmente para cálculos de ELL. Os parâmetros foram estimados e publicados por Magnussen e colaboradores (MAGNUSSEN; RASMUSSEN; FREDENSLUND, 1981) como forma de trazer melhorias para os resultados desse tipo de problema. Os autores apresentaram uma tabela com 32 grupos funcionais cujos parâmetros de interação foram otimizados para cálculos de ELL.

Magnussen e colaboradores ainda discutem o fato do conceito de solução de grupos do modelo UNIFAC ser, na verdade, uma aproximação pois, caso não fosse, não deveriam haver diferenças entre os parâmetros para ELV e ELL. Além disso, os autores relatam a falta de melhorias no modelo para extensão do mesmo para diferentes temperaturas.

2.3.6 UNIFAC(DO)

O modelo UNIFAC-Dortmund, ou simplesmente UNIFAC(Do), foi proposto por Weidlich em sua tese de doutorado (1985), orientado pelo doutor Gmehling, e publicado em 1987 (WEIDLICH; GMEHLING, 1987).

Weidlich e Gmehling propuseram algumas modificações para o bem-sucedido modelo UNIFAC. A primeira das modificações reside na contribuição combinatorial do modelo. Enquanto a parte combinatorial do modelo UNIFAC pode descrita pela equação 4.29 (equação 4.25b rearranjada):

$$\ln \gamma_{i,comb} = 1 - \phi_i + \ln \phi_i - 5q_i \left(1 - \frac{\phi_i}{\theta_i} + \ln \frac{\phi_i}{\theta_i}\right) \tag{4.29}$$

Onde as definições dos parâmetros ϕ_i e θ_i se mantêm, a parte combinatorial do modelo UNIFAC(Do) é expressa por:

$$\ln \gamma_{i,comb} = 1 - \phi_i' + \ln \phi_i' - 5q_i \left(1 - \frac{\phi_i}{\theta_i} + \ln \frac{\phi_i}{\theta_i}\right) \tag{4.30}$$

Onde ϕ_i' representa uma alteração empírica em ϕ_i e é descrito por:

$$\phi_i' = \frac{r_i^{3/4}}{\sum_j r_j^{3/4} x_j} \tag{4.31}$$

Outra modificação proposta por Weidlich e Gmehling reside no termo que descreve a interação energética entre os grupos funcionais. Enquanto no modelo UNIFAC essa relação é dada pela equação 4.28, o modelo UNIFAC(Do) busca descrever as interações como uma função diferente da temperatura, descrita pela equação 4.32.

$$\Psi_{\mathrm{mn}} = exp\left(-\frac{a_{mn}+b_{mn}T+c_{mn}T^2}{T}\right) \tag{4.32}$$

Outras diferenças entre os dois modelos propostos residem no fato de que Weidlich e Gmehling: estimaram os parâmetros estruturais de volume e superfície juntamente dos parâmetros a_{mn}, b_{mn} e c_{mn}; adicionaram parâmetros estruturais especiais para os grupos funcionais cíclicos CH_2 e CH, de forma que os cálculos para sistemas com alcanos cíclicos sejam mais precisos; separaram os parâmetros de volume e área de álcoois em álcoois primários, secundários e terciários.

Os autores reportam melhorias significativas nos resultados do modelo modificado em comparação ao original, chegando a ser 73% mais preciso em cálculos de coeficientes de atividade em diluição infinita (WEIDLICH; GMEHLING, 1987).

2.3.7 COSMO-SAC

O desenvolvimentos dos modelos baseados na teoria COSMO iniciou com os trabalhos de Klamt e colaboradores (KLAMT; ECKERT, 2000; KLAMT; SCHÜÜRMANN, 1993). Klamt e Schüürmann começaram o desenvolvimento através da introdução de um método de varredura para a obtenção da energia de solvatação de uma molécula em um condutor perfeito (KLAMT; SCHÜÜRMANN, 1993), e mais tarde aplicando este método a problemas de termodinâmica em fase líquida através do chamado modelo COSMO-RS (KLAMT, 1995; KLAMT; ECKERT, 2000).

Lin e Sandler desenvolveram o que ficou conhecido como modelo COSMO-SAC em 2002 (LIN; SANDLER, 2002), ainda baseados nos cálculos COSMO

propostos por Klamt e Schüürmann, porém, afirmando agora consistência termodinâmica, uma vez que o modelo predecessor COSMO-RS falhava em satisfazer algumas restrições termodinâmicas.

O modelo COSMO-SAC estima a energia livre de solvatação $\Delta G_{i/S}^{*sol}$ – que é a energia necessária para transferir uma molécula de soluto em uma posição fixa em um gás ideal para uma posição fixa em uma solução S. Lin e Sandler (LIN; SANDLER, 2002) descreveram um processo de duas etapas para o cálculo da energia de solvatação:

i. Primeiro, considera-se que o soluto possui suas cargas de superfície "desligadas", então as propriedades dielétricas do solvente são igualadas àquelas de um condutor perfeito para a varredura e só depois as cargas do soluto são "ligadas" (um processo de solvatação ideal);
ii. As propriedades do solvente retornam ao normal e as cargas de varredura são removidas, tendo agora as informações da densidade de carga na superfície da molécula do soluto.

Durante o processo de varredura de cargas, o potencial eletrostático da molécula é obtido. Cada molécula é, então, dividida em diversos segmentos e a probabilidade de encontrar um segmento com densidade de carga σ é calculado. A probabilidade de encontrar um segmento com densidade de carga σ, $p(\sigma)$, é a soma ponderada dos perfis-sigma (σ-*profile*) de todos os componentes, conforme equação 4.33:

$$p(\sigma) = \frac{\sum_i x_i n_i p_i(\sigma)}{\sum_i x_i n_i} = \frac{\sum_i x_i A_i p_i(\sigma)}{\sum_i x_i A_i} \tag{4.33}$$

Onde $p(\sigma)$ representa o perfil sigma da solução, x_i a fração molar da espécie i, n_i o número de segmentos da espécie, $p_i(\sigma)$ o perfil sigma da espécie i e A_i a área de superfície. As cargas ideais de varredura devem então ser removidas, e isso é feito através da adição de segmentos de pareamento para toda a superfície de carga oposta àquelas varridas idealmente. Neste ponto, a energia do sistema é dada por:

$$E^{tot} = \sum_i \left(E_i^{COSMO} + \zeta A_i\right) + \sum_{m,n} E_{par}(\sigma_m, \sigma_n) \tag{4.44}$$

Onde σ_m e σ_n são as densidades de carga dos segmentos m e n e E_{par} a energia de contato entre os segmentos; E_i^{COSMO} é a energia eletrostática das moléculas obtida pelos cálculos COSMO; ζA_i formam uma energia de dispersão, onde ζ representa uma constante de dispersão e A_i a área superficial da molécula; o primeiro somatório abrange todas as moléculas; e o segundo somatório abrange todos os pares de segmentos $m-n$. Assim, o potencial químico dos segmentos é calculado:

$$\mu_S(\sigma_m) = -\kappa T \ln\left[exp\left(\frac{-E_{par}(\sigma_m,\sigma_n)+\mu_S(\sigma_n)}{\kappa T}\right)\right] + \kappa T \ln p_S(\sigma_m) \tag{4.45}$$

Da equação 4.45 pode-se obter o coeficiente de atividade de segmento:

$$\ln \Gamma_S(\sigma_m) = -\ln\left[\sum_{\sigma_n} p_S(\sigma_n)\, \Gamma_S(\sigma_n)\, exp\left(\frac{-\Delta W(\sigma_m,\sigma_n)}{\kappa T}\right)\right] \tag{4.46}$$

Onde $\Delta W(\sigma_m,\sigma_n) = E_{par}(\sigma_m,\sigma_n) - E_{par}(0{,}0)$, a energia de troca, é a energia necessária para obter um par de segmentos $m-n$ de um par neutro. A energia livre de restauração da molécula, $\Delta G_{i/s}^{*res}$, pode ser obtida pela soma das contribuições dos segmentos:

$$\frac{\Delta G_{i/s}^{*res}}{RT} = \sum_{\sigma_m}\left[n_i(\sigma_m)\frac{\Delta G_{\sigma m/s}^{*res}}{RT}\right] = n_i \sum_{\sigma_m} p_i(\sigma_m) \ln \Gamma_S(\sigma_m) \tag{4.47}$$

Chegando, então, à equação característica do coeficiente de atividade obtido pelo modelo COSMO-SAC:

$$\ln \gamma_{i/S} = n_i \sum_{\sigma_m} p_i(\sigma_m)[\ln \Gamma_S(\sigma_m) - \ln \Gamma_i(\sigma_m)] + \ln \gamma_{i/S}^{SG} \tag{4.48}$$

Onde $\ln \gamma_{i/S}^{SG}$ representa o termo combinatorial de Staverman-Guggenheim, dado por:

$$\ln \gamma_{i/S}^{SG} = \ln \frac{\phi_i}{x_i} + \frac{z}{2} q_i \ln \frac{\theta_i}{\phi_i} + l_i - \frac{\phi_i}{x_i}\sum_j x_j l_j \tag{4.49}$$

Sendo:

$$\phi_i = \frac{x_i r_i}{\sum_j x_j r_j} \tag{4.50a}$$

$$\theta_i = \frac{x_i q_i}{\sum_j x_j q_j} \tag{4.50b}$$

$$l_i = \frac{z}{2}[(r_i - q_i) - (r_i - 1)] \tag{4.50c}$$

É importante notar que a energia de contato entre os segmentos E_{par} (chamado de *self-energy* na publicação de Lin e Sandler) possui contribuições das interações eletrostáticas (*misfit energy*), das interações por ponte de hidrogênio e das interações não-eletrostáticas:

$$E_{par}(\sigma_m, \sigma_n) = E_{mf}(\sigma_m, \sigma_n) + E_{hb}(\sigma_m, \sigma_n) + E_{ne}(\sigma_m, \sigma_n) = \left(\frac{\alpha\prime}{2}\right)(\sigma_m + \sigma_n)^2 + c_{hb} \max[0, \sigma_{rec} - \sigma_{hb}] \min[0, \sigma_{doa} + \sigma_{hb}] + c_{ne} \quad (4.51)$$

Onde α' é uma constante de proporcionalidade da interações eletrostáticas, c_{hb} é a constante das interações por ligação de hidrogênio, σ_{rec} e σ_{doa} são o maior e o menor valor de σ_m e σ_n, max e min indicam que o maior e o menor valor são utilizados, respectivamente, e c_{ne} é a contribuição das interações não-eletrostáticas, consideradas constantes nesta versão do modelo.

Uma vez que a contribuição não-eletrostática é considerada constante, a energia de troca ΔW se torna:

$$\Delta W(\sigma_m, \sigma_n) = \left(\frac{\alpha\prime}{2}\right)(\sigma_m + \sigma_n)^2 + c_{hb} \max[0, \sigma_{rec} - \sigma_{hb}] \min[0, \sigma_{doa} + \sigma_{hb}] \quad (4.52)$$

2.3.8 F-SAC

O modelo F-SAC é baseado, da mesma maneira que o modelo UNIFAC, na contribuição de grupos, no entanto, as energias de interação provêm do modelo COSMO-SAC. Essa abordagem, proposta por Soares e colaboradores (SOARES et al., 2013; SOARES; GERBER, 2013), introduz um grau de empirismo maior, consequentemente diminuindo o aspecto preditivo do modelo, se comparado ao COSMO-SAC.

Os autores relatam que a principal diferença entre o modelo F-SAC e os modelos COSMO-SAC ou COSMO-RS reside no fato de que os últimos se baseiam em propriedades moleculares obtidas por cálculos de química quântica, enquanto o primeiro se baseia em propriedades moleculares ajustadas (SOARES; GERBER, 2013).

O modelo F-SAC possui a mesma forma dos modelos UNIFAC e COSMO-SAC, uma soma das contribuições residual e combinatorial. A parte combinatorial do modelo é dada pela equação 4.53:

$$\ln \gamma_{i,comb} = 1 - V_i' + \ln V_i' - 5\frac{q_i}{q}\left(1 - \frac{V_i}{F_i} + \ln \frac{V_i}{F_i}\right) \tag{4.53}$$

Onde,

$$V_i' = \frac{r_i^{3/4}}{\sum_j x_j r_j^{3/4}} \tag{4.54a}$$

$$V_i = \frac{r_i}{\sum_j x_j r_j} \tag{4.54b}$$

$$r_i = \sum_k \nu_k^{(i)} R_k \tag{4.54c}$$

$$F_i = \frac{q_i}{\sum_j x_j q_j} \tag{4.54d}$$

$$q_i = \sum_k \nu_k^{(i)} Q_k \tag{4.54e}$$

$\nu_k^{(i)}$ representa o número de subgrupos do tipo k na espécie i, x_i é a fração molar da espécie, R_k e Q_k representam os parâmetros de volume e área superficial do grupo funcional k, respectivamente, sendo o primeiro obtido através de cálculos COSMO e o último por otimização de parâmetros

Da mesma maneira que o modelo COSMO-SAC, o modelo F-SAC utiliza a contribuição residual como uma diferença entre a energia livre de restauração das cargas da molécula do soluto i em uma solução S e a energia livre de restauração das cargas da molécula i em um líquido puro em i. No entanto, os autores introduziram um fator empírico β à equação do termo residual:

$$\ln \gamma_{i,res} = \frac{\beta\left(\Delta G_{i/S}^{*res} - \Delta G_{i/i}^{*res}\right)}{RT} \tag{4.55}$$

E para o cálculo da energia livre de restauração das cargas da molécula do soluto:

$$\frac{\Delta G_{i/S}^{*res}}{RT} = n_i \sum_{\sigma_m} p_i(\sigma_m) \ln \Gamma_S(\sigma_m) \tag{4.56}$$

Onde $\Gamma_S(\sigma_m)$ representa o coeficiente de atividade de um segmento de carga σ_m, expresso por:

$$\ln \Gamma_S(\sigma_m) = -\ln\left\{\sum_{\sigma_n} p_S(\sigma_n)\Gamma_S(\sigma_n) exp\left[\frac{-\Delta W(\sigma_m,\sigma_n)}{RT}\right]\right\} \quad (4.57)$$

Sendo

$$\Delta W(\sigma_m,\sigma_n) = \frac{\alpha'}{2}(\sigma_m + \sigma_n)^2 + \frac{E_{hb}(\sigma_m,\sigma_n)}{2} \quad (4.58)$$

Onde E_{hb} é um termo que contabiliza os efeitos das ligações de hidrogênio, negligenciado na versão publicada por Gerber e Soares em 2013 (SOARES; GERBER, 2013).

É importante ressaltar que neste trabalho a versão do modelo F-SAC utilizada não utiliza o termo de contribuição energética das ligações de hidrogênio. Dessa maneira, as predições para sistemas onde ligações de hidrogênio ocorrem foram compromissadas (ainda que com excelentes resultados do modelo).

2.4 REGRAS DE MISTURA

Nos capítulos 3 e 4 tratamos de equações cúbicas de estado e modelos de energia de Gibbs em excesso. Equações cúbicas de estado são bastante eficientes e vêm sendo utilizadas em aplicações industriais para muitas abordagens, como as predições de densidade, de fugacidade e de entalpia, por exemplo. Mathias e Klotz (MATHIAS; KLOTZ, 1994) ressaltam a surpreendente performance dos modelos de equação de estado, especialmente aqueles baseados na equação de van der Waals, apesar de uma base teórica pouco robusta.

No entanto, apesar dos bons resultados, as equações cúbicas de estado fornecem bons resultados para fluidos puros e resultados apenas razoáveis para misturas relativamente simples, que não fazem ligação de hidrogênio ou se associam de outra maneira (SILVEIRA; SANDLER, 2017). Wong e colaboradores (WONG; ORBEY; SANDLER, 1992) relataram ainda que o principal problema para a descrição de misturas complexas pelas equações cúbicas de estado reside nas regras de mistura utilizadas. A Figura 5.1 representa regiões de aplicabilidades de diferentes tipos de modelos termodinâmicos, conforme reportado por Wong e colaboradores (adaptada nesta tese).

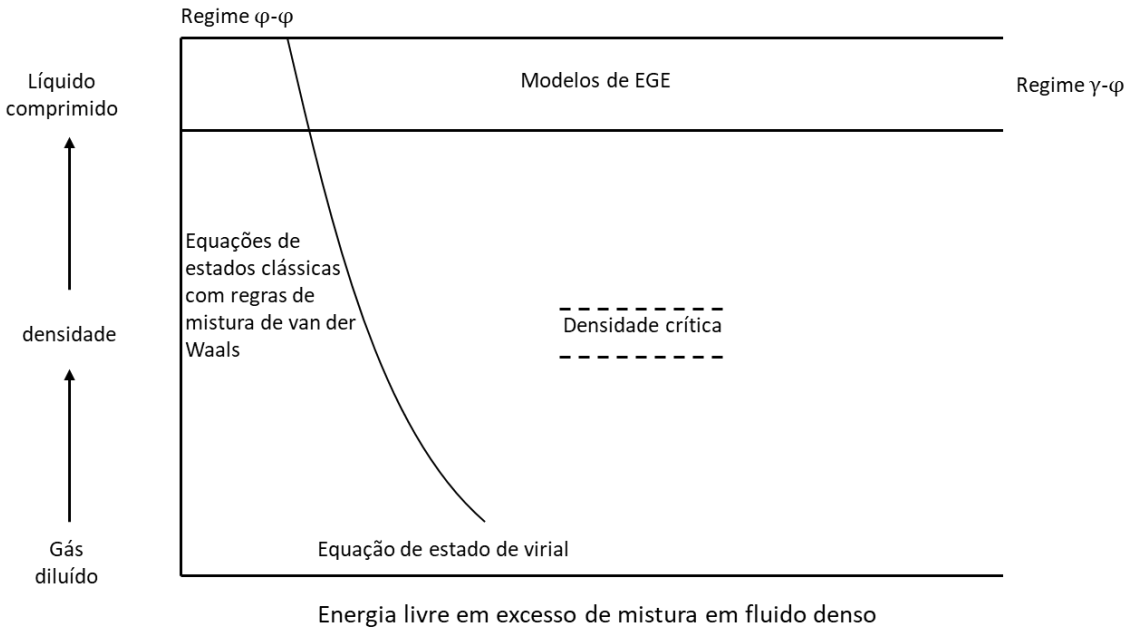

Figura 2.1. Diagrama esquemático da região aproximada de aplicação de diferentes modelos termodinâmico (Adaptado de: (WONG; ORBEY; SANDLER, 1992)).

Pode-se perceber, pela Figura 2.1, que conforme andamos no sentido positivo do eixo de energia livre em excesso, as equações de estado clássicas deixam de ser aplicáveis, mesmo em densidades baixas (região de gás diluído). Já os modelos de energia de Gibbs em excesso, são aplicáveis em toda região do eixo da energia livre em excesso (ou seja, se estendem de misturas simples a misturas muito complexas), no entanto, apenas na região de líquido comprimido. Dessa maneira, ainda que os modelos de EGE sejam capazes de descrever misturas complexas, são principalmente aplicáveis em regiões de alta densidade (SILVEIRA; SANDLER, 2017; WONG; ORBEY; SANDLER, 1992).

Uma maneira de estender a aplicabilidade de ambos os modelos (EGEs e equações de estados cúbicas) é utilizar regra de mistura. Regras de mistura são utilizadas para descrever misturas de diferentes graus de complexidade sob diferentes condições de pressão e temperatura. Diversos trabalhos foram publicados nesta área, como por exemplos os trabalhos de Asselineau e colaboradores (ASSELINEAU; BOGDANIC; VIDAL, 1978), de Wong e Sandler (WONG; SANDLER, 1992), de Orbey e Sandler (ORBEY; SANDLER, 1997), de Silveira e Sandler (SILVEIRA; SANDLER, 2017), entre outros.

Diversas regras de misturas foram desenvolvidas ao longo dos anos desde a regra de um fluido de van der Waals, algumas delas possuem falhas para diferentes regiões de composição ou de condições temperatura e pressão, seja pelo alcance de sua aplicabilidade ou por causa da complexidade dos componentes da mistura, como misturas com componentes altamente polares (HURON; VIDAL, 1979; LUEDECKE; PRAUSNITZ, 1985; MATHIAS; KLOTZ; PRAUSNITZ, 1991; MICHELSEN, 1990; PANAGIOTOPOULOS; REID, 1986; SCHWARTZENTRUBER; RENON, 1991; WONG; SANDLER, 1992).

Shibata e Sandler (SHIBATA; SANDLER, 1989) descreveram um método de aplicação de uma regra de mistura para expandir o uso de uma equação cúbica de estado de componentes puros a misturas. O método, descrito abaixo, foi utilizado como exemplo aplicando a regra de mistura clássica de um fluido de van der Waals e foi apresentado por Wong e Sandler, conforme equações 5.1-5.4:

$$a_{mix} = \sum_{i=1}^{NC} \sum_{j=1}^{NC} x_i x_j a_{ij} \tag{5.1}$$

$$b_{mix} = \sum_{i=1}^{NC} \sum_{j=1}^{NC} x_i x_j b_{ij} \tag{5.2}$$

$$a_{ij} = a_{ji} = \sqrt{a_{ii} - a_{jj}}\left(1 - k_{ij}\right) \tag{5.3}$$

$$b_{ij} = \frac{b_i + b_j}{2} \tag{5.4}$$

Onde a_{mix} e b_{mix} são os parâmetros obtidos para a mistura, a_{ii} e b_{ii} são os parâmetros das espécies puras, a_{ij} e b_{ij} são os parâmetros cruzados, e k_{ij} é o parâmetro de interação binária.

Ainda que existam diversas regras de mistura, este trabalho explorou apenas três delas: van der Waals de um fluido modificada (VDW1), Huron-Vidal-Orbey-Sandler (HVOS) e Wong-Sandler (WS). A escolha destas três regras foi feita devido à simplicidade de uso e programação computacional, à robustez comprovada por diversos testes publicados em trabalhos científicos, e satisfação da dependência quadrática do segundo coeficiente de virial na composição (ORBEY; SANDLER, 1995).

As três regras de mistura mencionadas anteriormente serão detalhadas a seguir.

2.4.1 VDW1

A regra de mistura de van der Waals de um fluido (VDW1) é facilmente aplicável e razoavelmente boa para misturas relativamente simples. Apenas uma modificação foi proposta para esta regra: a energia de Gibbs em excesso será determinada pelo modelo de coeficiente de atividade, em vez da própria equação de estado. Assim,

$$\bar{G}_{EGE}^{ex} = C^* \left(\frac{a_{mix}}{b_{mix}} - \sum_{i=1}^{NC} x_i \frac{a_{ii}}{b_{ii}} \right) \tag{5.5}$$

Onde $\bar{G}_{EGE}^{ex}$ representa a energia de Gibbs em excesso obtida pelo modelo EGE e C^* é uma constante que depende da equação de estado utilizada. Para a equação de van der Waals, $C^* = 1$; para a equação de Peng-Robinson (e consequentemente PRSV e PRSV2), $C^* = -0.62323$. Mais detalhes sobre a obtenção da constante C^* podem ser vistos no trabalho de Wong e Sandler (WONG; SANDLER, 1992) (especialmente na seção de Apêndice).

Com a aplicação da regra de mistura, e o uso da energia de Gibbs em excesso obtida pelo modelo de EGE, obtém-se as fugacidades da mistura para cálculos de equilíbrio de fases (ELV ou ELL).

2.4.2 HVOS

Orbey e Sandler (ORBEY; SANDLER, 1995) propuseram uma modificação na regra de mistura de Huron-Vidal que se tornou conhecida como HVOS (Huron-Vidal-Orbey-Sandler). O ponto de partida para a obtenção da regra é a equação para energia de Gibbs em excesso de uma equação de estado, dada por:

$$\frac{\bar{G}_{EE}^{ex}(T,P,x_i)}{RT} = ln\, \phi_{mix}(T,P,x_i) - \sum_i x_i\, ln\, \phi_i(T,P) = [Z_{mix}(T,P,x_i) - \sum_i x_i Z_i(T,P)] - [ln\, Z_{mix}(T,P,x_i) - \sum_i x_i\, ln\, Z_i(T,P)] - \left[\int_{\infty}^{V_{mix}(T,P,x_i)} \frac{Z_{mix}-1}{V_{mix}} dV - \sum_i x_i \int_{\infty}^{V_i(T,P)} \frac{Z_i-1}{V_i} dV \right] \tag{5.6}$$

Ou, equivalentemente, em termos de energia de Helmholtz em excesso ($\bar{A}^{ex}$):

$$\frac{\bar{A}_{EE}^{ex}(T,P,x_i)}{RT} = -\left[\sum_i x_i \ln \frac{Z_{mix}(T,P,x_i)}{Z_i(T,P)}\right] - \left[\int_{\infty}^{V_{mix}(T,P,x_i)} \frac{Z-1}{V} dV - \sum_i x_i \int_{\infty}^{V(T,P)} \frac{Z_i-1}{V_i} dV\right] \quad (5.7)$$

Os autores propõem, então, que fluidos podem ser descritos por uma função algébrica linear u, que relaciona o volume da espécie com o seu parâmetro volumétrico b na forma $V = ub$, sendo u positivo e maior que 1 para qualquer temperatura. Assim, após uma série de manipulações algébricas e fazendo $u = 1$, os autores propõem a seguinte equação:

$$\frac{A_{EE}^{ex}}{RT} = -\sum_i x_i \ln \frac{b_{mix}}{b_{ii}} + C^* \left(\frac{a_{mix}}{b_{mix}RT} - \sum_i x_i \frac{a_{ii}}{b_{ii}RT}\right) \quad (5.8)$$

É importante notar que quando os autores impõem $u = 1$, na verdade o que se obtém é que $V = b$. Essa asserção é válida quando a pressão do sistema tende a infinito:

$$\lim_{P\to\infty} \bar{V} = b \quad (5.9)$$

O que é possível porque a energia de Helmholtz é uma função fracamente dependente da pressão, ao contrário da energia de Gibbs (WONG; SANDLER, 1992).

2.4.3 WS

A regra de mistura de Wong-Sandler (WONG; SANDLER, 1992), ou simplesmente WS, foi desenvolvida com o intuito de permitir uma maior extensão do método nas faixas de pressão e temperatura. Os autores se valem do fato de que

$$\bar{G}^{ex} = \bar{A}^{ex} + P\bar{V}^{ex} \quad (5.10)$$

De forma que para que a energia em excesso de Gibbs pudesse ser calculada a pressões muito altas, o volume molar em excesso tenderia a zero, caso contrário o termo $P\bar{V}^{ex}$ se torna infinito.

Assim, os autores utilizam a energia de Helmholtz em excesso, justificada por:

$$\bar{G}^{ex}(T, x, P = baixa) = \bar{A}^{ex}(T, x, P = baixa) = \bar{A}^{ex}(T, x, P = \infty) \quad (5.11)$$

Os autores propõem, então, a equação:

$$\bar{A}_{\infty}^{ex}(x) = -\frac{a_{mix}}{b_{mix}} + \sum_i x_i \frac{a_i}{b_i} \tag{5.12}$$

A equação 5.12 é muito semelhante àquela obtida por Huron-Vidal na sua regra de mistura original, porém aqui se considera a energia de Helmholtz em excesso, o que permite satisfazer a necessidade do segundo coeficiente de virial ser quadrático em sua composição.

Mais detalhes sobre esta regra de mistura e as demais serão abordados no capítulo 9. A regra de mistura WS também voltará a aparecer no capítulo 10 como alternativa para o cálculo de ELL em diferentes faixas de pressão.

3 DE WILSON A F-SAC: UMA ANÁLISE COMPARATIVA DE MODELOS DE COEFICIENTE DE ATIVIDADE CORRELATIVOS E PREDITIVOS PARA DETERMINAR ELV E COEFICIENTES DE ATIVIDADE DE DILUIÇÃO INFINITA DE SISTEMAS BINÁRIOS

From Wilson to F-SAC: A comparative analysis of correlative and predictive activity coefficient models to determine VLE and IDAC of binary systems

Christian Luiz da Silveira[1]

Nina Paula Gonçalves Salau

Chemical Engineering Department
Universidade Federal de Santa Maria

ABSTRACT

Several activity coefficient models are available in literature nowadays, with attention to the recently developed COSMO-SAC and F-SAC models. This work used isothermal data for 11 different binary systems, a total of 1818 experimental points, plus 129 IDAC experimental points of the same systems, to compare the accuracy of 10 activity coefficient models – Wilson, Wilson (literature), NRTL, NRTL (literature), UNIQUAC, UNIQUAC (literature), UNIFAC, UNIFAC (literature), F-SAC, and COSMO-SAC. Amongst the correlative models, the UNIQUAC and NRTL had the best performances, either with literature parameters or with the optimized parameters. When comparing the predictive models, both UNIFAC (with estimated parameters) and COSMO-SAC presented the most accurate results. However, the F-SAC model was particularly good to predict infinite-dilution activity coefficients, outperforming both COSMO-SAC and UNIFAC.

Keywords: vapor-liquid equilibria, COSMO-SAC, F-SAC, binary systems, infinite-dilution activity coefficient, thermodynamic models.

[1] To whom all correspondence should be addressed. E−mail: christiansilveira86@gmail.com
Address: Chemical Engineering Department, UFSM − Av. Roraima, 1000, Cidade Universitária −Bairro Camobi. 97105-900 Santa Maria, RS − Brazil.
Phone: +55-55-3220-8448- Fax: +55-55-3220-8030.

1 INTRODUCTION

A large number of chemical engineering processes is related to mixtures and their separation operations that are often based on phase-contact, such as distillation, absorption, and extraction[1]. The design of these processes requires quantitative information about the fluid phase equilibria of the multicomponent mixture, this information can be frequently obtained from extrapolation or interpolation of the available experimental data of the referred mixture. In this case, models like Wilson and NRTL can be used to predict the mixture behavior.

Several times, however, the experimental data for that particular mixture is either limited or not even available. In such scenario, the engineer can only make a reasonable guess about the behavior of the mixture. In this case, models like UNIQUAC and UNIFAC can provide better insights about the vapor-liquid or liquid-liquid equilibrium of the mixture. Fredenslund *et al*.[2] proposed the UNIFAC model claiming its applicability to reduce the uncertainty of the estimations of activity coefficients in nonelectrolyte liquid mixtures.

In 2002, 27 years after the UNIFAC model had been proposed. Lin and Sandler[3] published an innovative approach with the model called COSMO-SAC (**Co**nductor-like **S**creening **Mo**del Segment Activity Coefficient). This new model was a thermodynamic consistent version of the COSMO-RS (COSMO for Real Solvents), proposed by Klamt[4]. The great advantage of the COSMO-SAC model is that it only needs the atomic radius of each atom of the components of the mixture and two universal parameters. The remaining information is obtained by quantum mechanical calculations (COSMO).

More details about the models used in this work can be found in Section 3.

Gerber and Soares[5] used a large database to compare the UNIFAC model to the COSMO-SAC variants. They reported a very good agreement of the COSMO-SAC model with

optimized parameters when predicting Infinite-Dilution Activity Coefficients for aqueous systems, while the UNIFAC model better described nonaqueous systems.

Hiseh et al.[6] also compared their modified COSMO-SAC model to the previous COSMO-SAC, to the UNIFAC, and to the UNIFAC-LLE for VLE and LLE predictions. They have shown that their modifications on the temperature dependence of the electrostatic interaction parameter and the hydrogen-bond approach resulted in a better performance for both VLE and LLE predictions of binary systems.

Chen et al.[7] also compared the COSMO-SAC model to the NRTL and UNIQUAC for LLE data. Their results showed good agreement of the COSMO-SAC model when compared to the NRTL and UNIQUAC models.

Soares and Gerber[8,9] also proposed a new approach. As an alternative to improve the COSMO-based models quantitative performance, their approach uses group-contribution, like UNIFAC, but the interaction energies between the groups are obtained from the COSMO-SAC formulation. By doing so, they increase the empiricism of the model decreasing its predictive strength. The authors report a performance slightly better than UNIFAC (Do) and significantly better than COSMO-SAC. This new approach was called by the authors as F-SAC (Functional Segment Activity Coefficient).

This work uses 1818 experimental points for vapor-liquid equilibrium (VLE), available in literature, for 11 different binary mixtures. The main novelties of this work are: (i) to use the VLE data available in a parameters estimation procedure, which was performed in order to obtain optimized parameters for the models, as it will be described with more details in Section 3, these models with optimized parameters were compared to the models with parameters found in literature; (ii) to bring a straightforward comparison in predicting VLE and Infinite-Dilution Activity Coefficients (IDAC) data by the already well-known UNIFAC and COSMO-SAC models and the new F-SAC model.

In order to validate the results of the comparisons, we also have used 129 IDAC experimental points, available in literature (cf. Table 1), that were not used in the previous parameter estimation.

Furthermore, the comparisons were divided in two sections. One section is exclusively comparing the correlative models, i.e., Wilson, NRTL, and UNIQUAC. The other section compares the predictive models UNIFAC, F-SAC, and COSMO-SAC.

2 MATERIAL AND METHODS

The first part of this work was to collect several experimental VLE data for different binary systems. One of the requirements was that this data was isothermally obtained (the pressure varies) for different temperatures. So, for example, the ethanol/water system data was isothermally obtained for 7 different temperatures (150, 200, 250, 275, 300, 325, and 350°C).

There were gathered 1818 VLE and 129 IDAC experimental points for 11 different binary systems. Table 1 presents the systems, the Antoine coefficients used to estimate the vapor pressure of the pure components, and the number of experimental points and their sources.

Table 1. Antoine coefficients and data information on the tested systems.

Systems	A	B	C	VLE Exp. Data Source	NP	IDAC Exp. Data Source	NP
Acetone (1)	4.4244	1312.2530	-32.4450	[10]	117	[5]	3
Methanol (2)	5.1585	1569.6130	-34.8460				
Methanol (1)	5.1585	1569.6130	-34.8460	[10]	153	[11,12]	30
Water (2)	3.5596	643.7480	-198.0430				

2-propanol (1)	7.9584	1519.6600	216.8290	[13]	231	[5,11,12,14]	20
Water (2)	3.5596	643.7480	-198.0430				
Methanol (1)	5.1585	1569.6130	-34.8460	[15]	210	[16]	2
Benzene (2)	4.6036	1701.0730	20.8060				
Acetone (1)	4.4244	1312.2530	-32.4450	[10]	216	[5,11,12]	11
Water (2)	3.5596	643.7480	-198.0430				
Ethanol (1)	4.9253	1432.5260	-61.8190	[13]	252	[5,12,14,17]	49
Water (2)	3.5596	643.7480	-198.0430				
Butane (1)	4.3557	1175.5810	-2.0710	[18,19]	138	[20]	8
Methanol (2)	5.1585	1569.6130	-34.8460				
Butanol (1)	4.5460	1351.5550	-93.3400	[21]	126	[22]	1
n-Decane (2)	0.2102	440.6160	-156.8960				
Butanol (1)	4.5460	1351.5550	-93.3400	[23,24]	93	[22,25,26]	4
n-Hexane (2)	4.0026	1171.5300	-48.7840				
Heptane (1)	4.0283	1268.6360	-56.1990	[27]	183	[22]	1
1-Pentanol (2)	4.3242	1297.6890	-110.6690				
Pentane (1)	3.9892	1070.6170	-40.4540	[28]	99		0
Methanol (2)	5.1585	1569.6130	-34.8460				

*$log_{10}P^{vap} = A - \frac{B}{T+C}$, with pressure given in bar (and then converted to Pa) and temperature in K.

After assembling all the data, a Bubble Point Pressure algorithm was programmed in Matlab. For each model, different parameters were estimated using the available VLE data. Hence, for Wilson, the parameters $\Lambda_{1,2}$ and $\Lambda_{2,1}$were estimated; for NRTL, $\tau_{1,2}$, $\tau_{2,1}$, and α; for UNIQUAC, $u_{1,2} - u_{2,2}$ and $u_{2,1} - u_{1,1}$; for UNIFAC, $a_{m,n}$, where m and n are the functional

groups contained in the mixture. The COSMO-SAC and F-SAC models were used with no parameters adjustment, according to the version published by Xiong *et al*.[29] and Soares and Gerber[8].

The *fminsearch* function, implemented in Matlab, was used. This function uses the simplex method, as proposed by Lagarias *et al*.[30]. The algorithm begins by applying the simplex method around the initial guess vector x_0 with a perturbation of 5%. It uses $n+1$points for a $n-dimensional$ vector x. After this initial step, the algorithm modifies the simplex repeatedly with expansions and reflections over solution plane. More details about the algorithm can be seen in the Lagarias *et al*. work[30] and in the Section 3.

After the parameters optimization, the new parameters were used to predict the VLE data with each model. The same simulation was performed using literature parameters (Table 15). Both results were then compared. However, it is unfair to compare each model with the literature found parameters to the same model with parameters optimized using the same data used for validation. So, to keep investigating the strength of the estimated parameters, IDAC data was collected to validate and compare the results obtained with both set of parameters. The results will be discussed in Section 4.

The computer used for this work was a desktop Intel(R) Core(TM) i7-3770 CPU @ 3.40GHz 8GB RAM running on Xubuntu 16.04.2 LTS. The optimization and simulation were performed in Matlab and the statistical analysis was made with the LibreOffice Calc.

3 THEORY AND CALCULATION

The activity coefficient models that were used in this work were programmed in Matlab. The Wilson model, as proposed by Wilson[31]; the NRTL, as developed by Renon and Prausnitz[32]; the UNIQUAC, as described by Abrams and Prausnitz[33]; the UNIFAC, according

to Fredenslund et al.[2]; the F-SAC model, as proposed by Soares and coworkers[8,9]; and the COSMO-SAC, as Xiong and Sandler[29].

Further information about each of the referred models can be found in the Supplementary Information section (Appendix A).

The optimization method used in this work is the Nelder-Mead *simplex*[34], the *fminsearch* function on Matlab. The Nelder-Mead *simplex* is a direct search optimization method for nonlinear unconstrained problems. The method attempts to minimize a scalar-valued nonlinear function of η variables using only the function values, i. e. not using the any derivative information. Lagarias *et al*.[30] described the algorithm in detail, including the application for one iteration of the algorithm.

The results obtained with the 6 models tested were computed using the following definitions of Average Relative Deviation (AR), Root Mean Square Deviation ($RMSD$), and Average Absolute Deviation (AAD):

$$AR = \frac{\sum_{i=1}^{NP} |\theta_{i,exp} - \theta_{i,calc}|}{\theta_{i,exp}} \quad (1)$$

$$RMSD = \frac{\sum_{i=1}^{NP} \sqrt{(\theta_{i,exp} - \theta_{i,calc})^2}}{NP} \quad (2)$$

And

$$AAD = \frac{\sum_{i=1}^{NP} |\theta_{i,exp} - \theta_{i,calc}|}{NP} \quad (3)$$

With θ being either the vapor-phase composition or pressure, NP the number of points, and the subscripts exp and $calc$ indicating the experimental and calculated values, respectively. The SD indicates the standard deviation of the obtained results; so, even though it may not hold significant statistical meaning for the $RMSD$ and AAD for pressure, since it has

different order of magnitude depending on the system and its conditions, it does measure the standard deviation for the vapor phase fraction results and all AR results.

4 RESULTS AND DISCUSSION

4.1 VLE Results

The overall results of each model for every binary system can be seen in Table 2. If only the correlative models are compared, the UNIQUAC model offered the best results, followed by the NRTL, both with optimized parameters. When comparing only the models with the literature obtained parameters, the NRTL model performance is slightly more accurate than the UNIQUAC. The difference of performance between these two predictive models, however, is not very significative, while NRTL resulted in RMSD for vapor-phase composition and pressure of 3.4301 and $1.75\times10^{+07}$, respectively, the UNIQUAC RMSDs were 3.7100 and $2.12\times10^{+07}$.

When comparing the predictive models, there is a clear difference of performance between COSMO-SAC and UNIFAC with literature parameters. Whilst the COSMO-SAC yielded in RMSD for vapor-phase composition and pressure of 2.5993 and $1.42\times10^{+07}$, respectively, the UNIFAC model resulted in 3.7685 and $1.64\times10^{+07}$. The UNIFAC was also outperformed by the F-SAC model in the vapor-phase composition predictions, the RMSD of the latter was 3.3841 while the former resulted in 3.7685; concerning to the equilibrium pressure, the UNIFAC results are more satisfying than the F-SAC results.

The UNIFAC model could offer better results with the optimized parameters. In fact, when the parameters of the model were estimated, its performance was comparable to COSMO-SAC performance. While the UNIFAC predicted with more accuracy the equilibrium pressure – RMSD of $7.76\times10^{+06}$ against $1.42\times10^{+07}$ of COSMO-SAC -, it was less accurate for the vapor-phase composition predictions, resulting in a RMSD of 2.6803 in comparison to 2.5993 obtained by COSMO-SAC.

Table 2. Overall results for Vapor-Liquid Equilibrium.

Model		Residual y	Residual P [Pa]	AR y	AR P	RMSD y	RMSD P [Pa]	AAD y	AAD P [Pa]
Wilson	Sum	33.8177	$8.72\times10^{+07}$	10.5673	2.2744	3.2628	$1.12\times10^{+07}$	2.8295	$9.49\times10^{+06}$
	Average	0.7686	$1.98\times10^{+06}$	0.2402	0.0517	0.0742	$2.54\times10^{+05}$	0.0643	$2.16\times10^{+05}$
	SD	0.5691	$2.94\times10^{+06}$	0.5847	0.0407	0.0589	$5.64\times10^{+05}$	0.0556	$5.11\times10^{+05}$
Wilson Literature	Sum	63.6271	$3.53\times10^{+08}$	12.3125	9.6870	5.8853	$3.79\times10^{+07}$	4.6977	$3.52\times10^{+07}$
	Average	1.4461	$8.01\times10^{+06}$	0.2798	0.2202	0.1338	$8.62\times10^{+05}$	0.1068	$7.99\times10^{+05}$
	SD	1.0559	$1.05\times10^{+07}$	0.3550	0.1492	0.0914	$1.31\times10^{+06}$	0.0672	$1.27\times10^{+06}$
NRTL	Sum	28.2565	$4.40\times10^{+07}$	10.2567	1.3989	2.9297	$5.83\times10^{+06}$	2.5467	$4.36\times10^{+06}$
	Average	0.6422	$1.00\times10^{+06}$	0.2331	0.0318	0.0666	$1.32\times10^{+05}$	0.0579	$9.92\times10^{+04}$
	SD	0.5224	$1.24\times10^{+06}$	0.7088	0.0216	0.0641	$2.19\times10^{+05}$	0.0631	$1.61\times10^{+05}$
NRTL Literature	Sum	32.7036	$1.35\times10^{+08}$	8.5213	4.8416	3.4301	$1.75\times10^{+07}$	2.7159	$1.65\times10^{+07}$
	Average	0.7433	$3.07\times10^{+06}$	0.1937	0.1100	0.0780	$3.98\times10^{+05}$	0.0617	$3.75\times10^{+05}$
	SD	0.5287	$4.58\times10^{+06}$	0.3809	0.1143	0.0558	$8.62\times10^{+05}$	0.0455	$8.56\times10^{+05}$
UNIQUAC	Sum	26.6478	$6.26\times10^{+07}$	9.9703	1.6057	2.7850	$8.09\times10^{+06}$	2.3964	$6.54\times10^{+06}$
	Average	0.6056	$1.42\times10^{+06}$	0.2266	0.0365	0.0633	$1.84\times10^{+05}$	0.0545	$1.49\times10^{+05}$
	SD	0.4823	$2.06\times10^{+06}$	0.6936	0.0245	0.0605	$3.80\times10^{+05}$	0.0580	$3.02\times10^{+05}$
UNIQUAC Literature	Sum	37.8304	$1.84\times10^{+08}$	8.2364	7.0711	3.7100	$2.12\times10^{+07}$	3.0308	$2.04\times10^{+07}$
	Average	0.8598	$4.19\times10^{+06}$	0.1872	0.1607	0.0843	$4.83\times10^{+05}$	0.0689	$4.64\times10^{+05}$
	SD	0.5255	$5.35\times10^{+06}$	0.3472	0.1054	0.0543	$8.95\times10^{+05}$	0.0434	$8.93\times10^{+05}$
UNIFAC	Sum	25.9953	$4.65\times10^{+07}$	9.9085	1.4233	2.6803	$7.76\times10^{+06}$	2.3314	$6.15\times10^{+06}$
	Average	0.5908	$1.06\times10^{+06}$	0.2252	0.0323	0.0609	$1.76\times10^{+05}$	0.0530	$1.40\times10^{+05}$
	SD	0.5068	$1.84\times10^{+06}$	0.6495	0.0274	0.0599	$4.91\times10^{+05}$	0.0563	$4.08\times10^{+05}$
UNIFAC Literature	Sum	38.8365	$1.62\times10^{+08}$	11.6405	3.3511	3.7685	$1.64\times10^{+07}$	3.2595	$1.43\times10^{+07}$
	Average	0.8826	$3.67\times10^{+06}$	0.2646	0.0762	0.0856	$3.74\times10^{+05}$	0.0741	$3.26\times10^{+05}$
	SD	0.6956	$5.66\times10^{+06}$	0.6824	0.0560	0.0672	$5.82\times10^{+05}$	0.0636	$5.06\times10^{+05}$
COSMO-SAC	Sum	25.2157	$1.24\times10^{+08}$	8.3902	2.9399	2.5993	$1.42\times10^{+07}$	2.1606	$1.33\times10^{+07}$
	Average	0.5731	$2.81\times10^{+06}$	0.1907	0.0668	0.0591	$3.22\times10^{+05}$	0.0491	$3.03\times10^{+05}$
	SD	0.4471	$5.01\times10^{+06}$	0.5178	0.0411	0.0489	$7.00\times10^{+05}$	0.0461	$6.73\times10^{+05}$
F-SAC	Sum	34.8912	$1.61\times10^{+08}$	12.2316	3.1599	3.3841	$2.23\times10^{+07}$	2.8251	$1.99\times10^{+07}$
	Average	0.7929	$3.67\times10^{+06}$	0.2779	0.0718	0.0769	$5.07\times10^{+05}$	0.0642	$4.53\times10^{+05}$
	SD	0.8754	$7.35\times10^{+06}$	0.6882	0.0988	0.0786	$1.42\times10^{+06}$	0.0679	$1.22\times10^{+06}$

In Figure 1, the results for the binary system of Methanol + Water under 250°C can be seen. The Wilson model with literature parameters is completely off the experimental data, however, when the same model with optimized parameters is analyzed the results are much better, being as accurate as the UNIQUAC and NRTL models, as it can be seen in Table 3.

As expected, amongst the models using literature parameters, the UNIQUAC model presented the most reliable results.

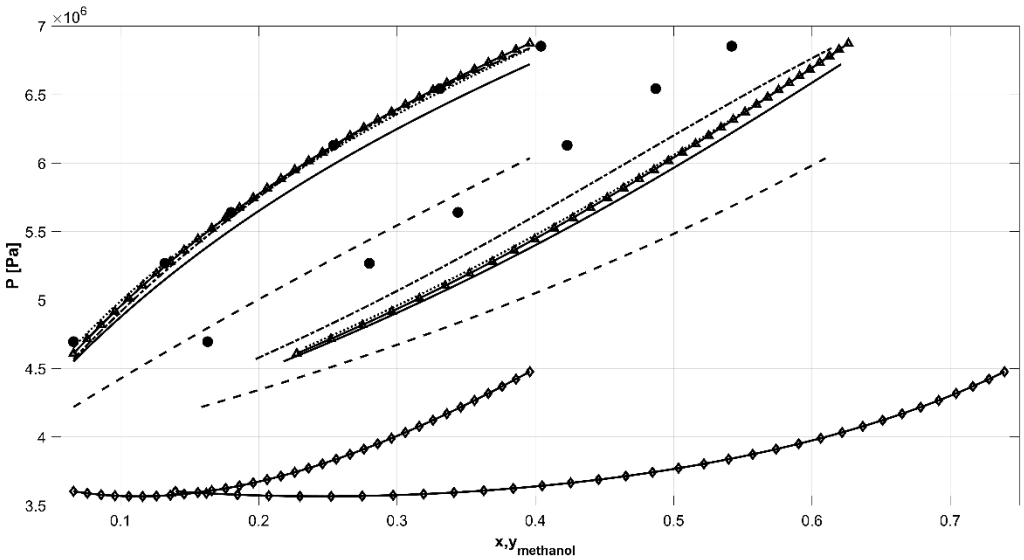

Figure 1. Methanol + Water VLE correlative models results (● Experimental Data, – – NRTL Literature, ····· NRTL, ◆ Wilson Literature, – – – Wilson, —— UNIQUAC Literature, ▲ UNIQUAC).

When the predictive models are compared, the F-SAC results are more accurate than the other, including the UNIFAC optimized for the data. As it can be seen in Figure 2, all the predictive models are very reliable, at least qualitatively, although it should be noted that neither COSMO-SAC nor F-SAC had any parameter adjustment. More details about the results can be seen in the Supplementary Information section (Appendix B).

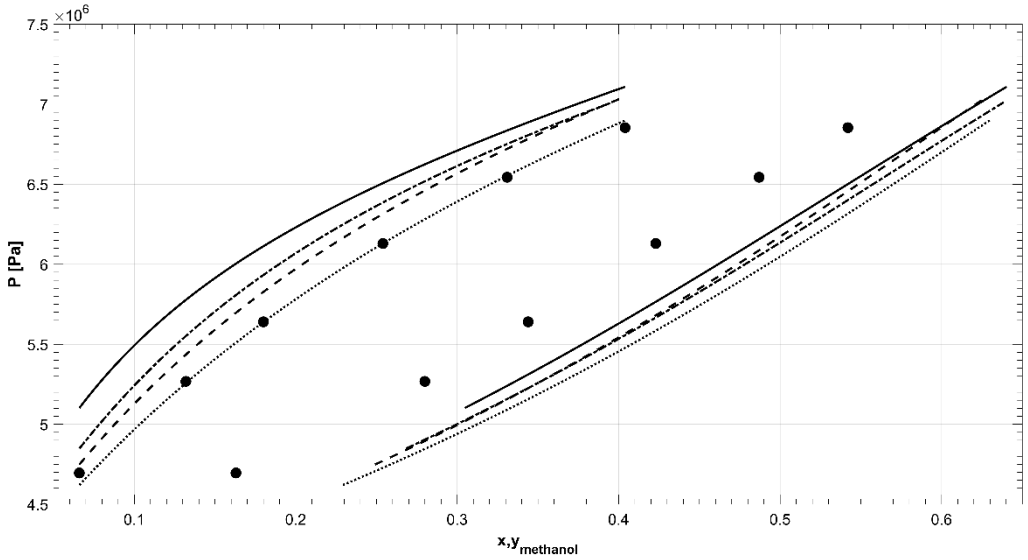

Figure 2. Methanol + Water VLE predictive models results (● Experimental Data, ━ ━ UNIFAC Literature, ┅┅┅ UNIFAC, ━ ━ ━ F-SAC, ━━━ COSMO-SAC).

Table 3. Methanol + Water results for 250°C.

Model	Residual y	Residual P [Pa]	AR y	AR P	RMSD y	RMSD P [Pa]	AAD y	AAD P [Pa]
Wilson	0.3487	$2.5735\times10^{+05}$	0.1516	0.0064	0.0600	$6.0049\times10^{+04}$	0.0581	$4.2892\times10^{+04}$
Wilson Literature	0.5705	$1.1830\times10^{+07}$	0.2848	0.3406	0.1208	$2.0246\times10^{+06}$	0.0951	$1.9717\times10^{+06}$
NRTL	0.4908	$1.2535\times10^{+05}$	0.2000	0.0035	0.0820	$2.4764\times10^{+04}$	0.0818	$2.0892\times10^{+04}$
NRTL Literature	0.1954	$4.3229\times10^{+06}$	0.0991	0.1234	0.0425	$7.3117\times10^{+05}$	0.0326	$7.2048\times10^{+05}$
UNIQUAC	0.5086	$1.9297\times10^{+05}$	0.2103	0.0052	0.0853	$4.3869\times10^{+04}$	0.0848	$3.2162\times10^{+04}$
UNIQUAC Literature	0.4540	$7.5927\times10^{+05}$	0.1898	0.0211	0.0764	$1.2757\times10^{+05}$	0.0757	$1.2655\times10^{+05}$
UNIFAC	0.5067	$1.4376\times10^{+05}$	0.2084	0.0038	0.0849	$3.6481\times10^{+04}$	0.0844	$2.3959\times10^{+04}$
UNIFAC Literature	0.5681	$9.6289\times10^{+05}$	0.2267	0.0278	0.0949	$1.6779\times10^{+05}$	0.0947	$1.6048\times10^{+05}$
COSMO-SAC	0.5271	$7.0375\times10^{+05}$	0.2052	0.0192	0.0882	$1.2364\times10^{+05}$	0.0879	$1.1729\times10^{+05}$
F-SAC	0.5051	$1.6973\times10^{+05}$	0.2023	0.0046	0.0843	$3.5640\times10^{+04}$	0.0842	$2.8300\times10^{+04}$

The NRTL and UNIQUAC models offered the best results for the Ethanol + Water system when only the correlative models are compared. The UNIQUAC with literature parameters resulted in the lowest RMSD for the vapor-phase compositions, followed by the

NRTL with literature parameters. The equilibrium pressure was better described by the NRTL with optimized parameters, followed by the UNIQUAC with optimized parameters, making it evident that the residuals reduction was the main goal with the optimization. Figure 3 represents the VLE diagram of that system for 250°C.

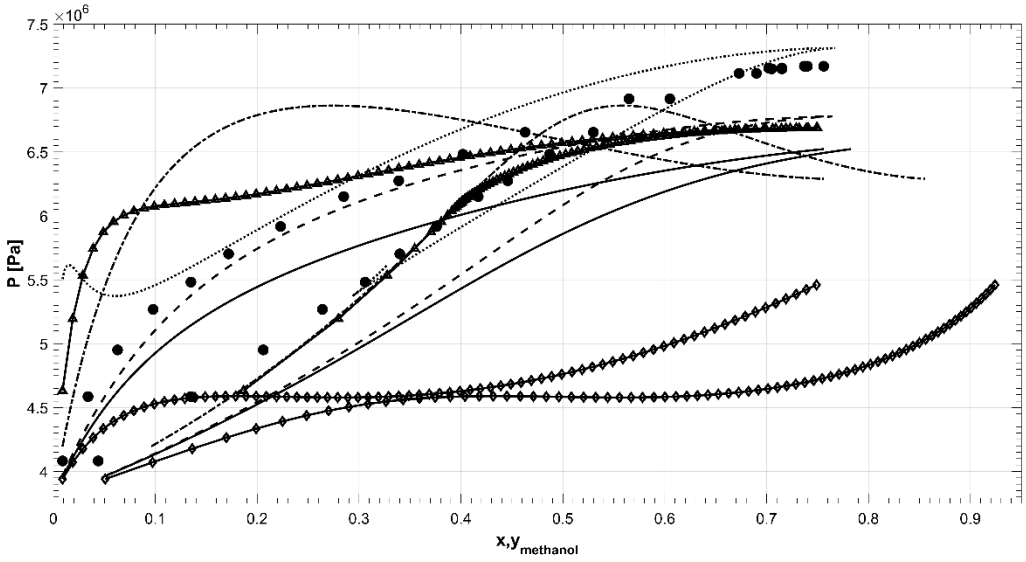

Figure 3. Ethanol + Water VLE correlative models results (● Experimental Data, ━ ━ NRTL Literature, ┅┅┅ NRTL, ◆ Wilson Literature, ▬ ▬ Wilson, ▬▬ UNIQUAC Literature, ▲ UNIQUAC).

The predictive models are qualitatively similar, as it can be seen from Figure 4. The F-SAC model has been shown to be more accurate when it comes to vapor-phase composition predictions, however it was the least accurate for the equilibrium pressure, in which case the UNIFAC with optimized parameters offered better results. Once again, both COSMO-SAC and F-SAC with no optimized parameters were more accurate than UNIFAC. The quantitative results can be seen in Table 4.

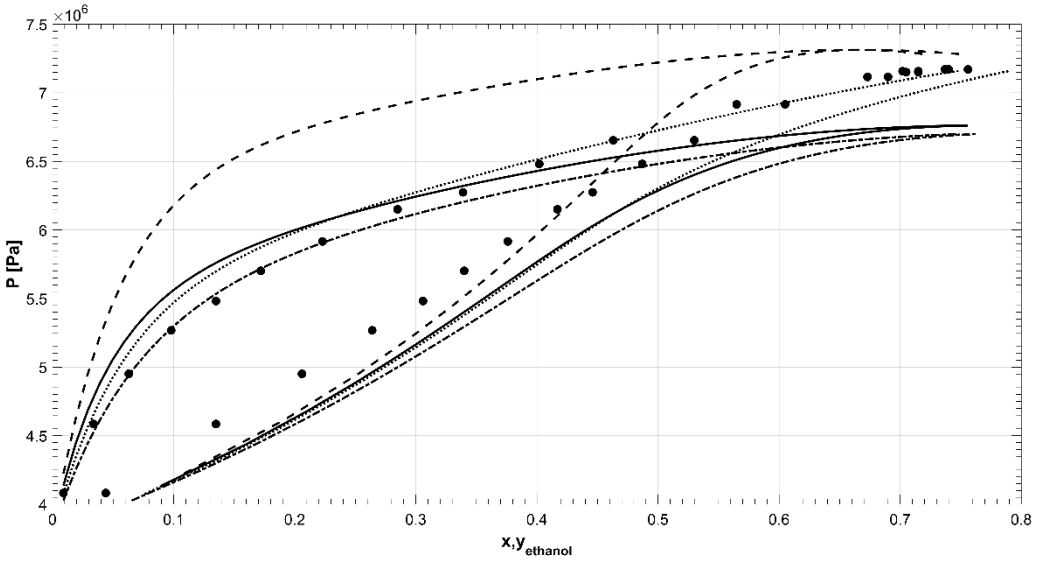

Figure 4. Ethanol + Water VLE predictive models results (● Experimental Data, ━ ━ UNIFAC Literature, ┅┅┅ UNIFAC, ━━━ F-SAC, ——— COSMO-SAC).

Table 4. Ethanol + Water overall results.

Model	Residual y	Residual P [Pa]	AR y	AR P	RMSD y	RMSD P [Pa]	AAD y	AAD P [Pa]
Wilson	11.1705	$5.0094\times10^{+07}$	7.0843	0.7359	1.1509	$7.2519\times10^{+06}$	1.0918	$6.2304\times10^{+06}$
Wilson Literature	9.9037	$1.4107\times10^{+08}$	5.0886	1.7140	1.0192	$1.7787\times10^{+07}$	0.8702	$1.7223\times10^{+07}$
NRTL	9.1268	$2.0870\times10^{+07}$	7.2396	0.2651	1.1032	$3.1116\times10^{+06}$	1.0421	$2.2737\times10^{+06}$
NRTL Literature	5.1943	$6.3356\times10^{+07}$	4.4132	0.7263	0.6462	$1.0005\times10^{+07}$	0.5756	$9.8537\times10^{+06}$
UNIQUAC	8.8009	$3.5185\times10^{+07}$	7.1131	0.4513	1.0898	$5.1534\times10^{+06}$	0.9814	$4.0382\times10^{+06}$
UNIQUAC Literature	4.6719	$7.7518\times10^{+07}$	4.0492	0.8959	0.5865	$1.1205\times10^{+07}$	0.5196	$1.1112\times10^{+07}$
UNIFAC	8.2398	$2.6522\times10^{+07}$	7.0909	0.4024	0.9797	$5.3632\times10^{+06}$	0.9223	$4.2918\times10^{+06}$
UNIFAC Literature	9.4475	$4.6256\times10^{+07}$	7.4702	0.6163	1.1011	$6.5505\times10^{+06}$	1.0266	$5.5249\times10^{+06}$
COSMO-SAC	6.2031	$4.3386\times10^{+07}$	5.6335	0.5314	0.7735	$7.2214\times10^{+06}$	0.7190	$6.8160\times10^{+06}$
F-SAC	5.2162	$5.9650\times10^{+07}$	4.6288	0.6938	0.6467	$9.3861\times10^{+06}$	0.5942	$9.1955\times10^{+06}$

One last example of the binary systems studied in this work is the Acetone + Water system at 250°C. In this case, the Wilson model with literature parameters was excluded from the diagram because of its huge inaccuracy. Although the UNIQUAC model with literature

parameters had the lowest RMSD for the vapor-phase composition predictions (Table 5), its predictions for the equilibrium pressure were very poor, as seen in Figure 5. The NRTL with literature parameters, and the NRTL and UNIQUAC with optimized parameters, have shown good agreement with the experimental data.

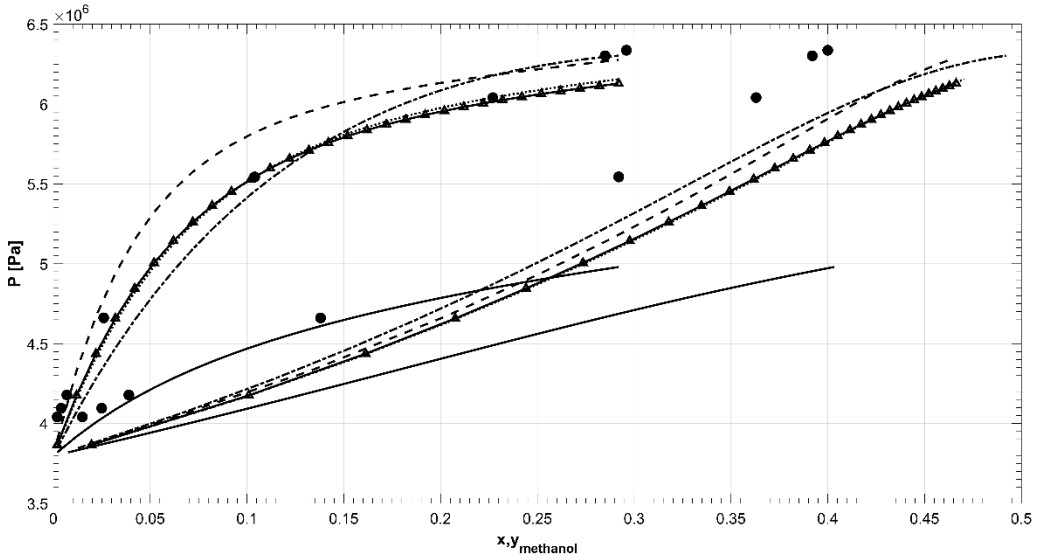

Figure 5. Acetone + Water VLE correlative models results (● Experimental Data, ▬ ▬ NRTL Literature, ▪▪▪▪▪▪▪ NRTL, ▬▬▬ Wilson, ▬▬ UNIQUAC Literature, ▬▲▬ UNIQUAC).

When the predictive models are compared, the UNIFAC with optimized parameters offered the best results. Once again, considering that, in this case, the number of parameters to be optimized on the UNIFAC model is 6, the COSMO-SAC model presented accurate results, its performance was superior to the UNIFAC with literature parameters. The overall results (Appendix B) also show that the COSMO-SAC was very close to the optimized UNIFAC performance. Figure 6 shows the overestimation of equilibrium pressure by the UNIFAC (Optimized), F-SAC, and more critically by the UNIFAC (Literature).

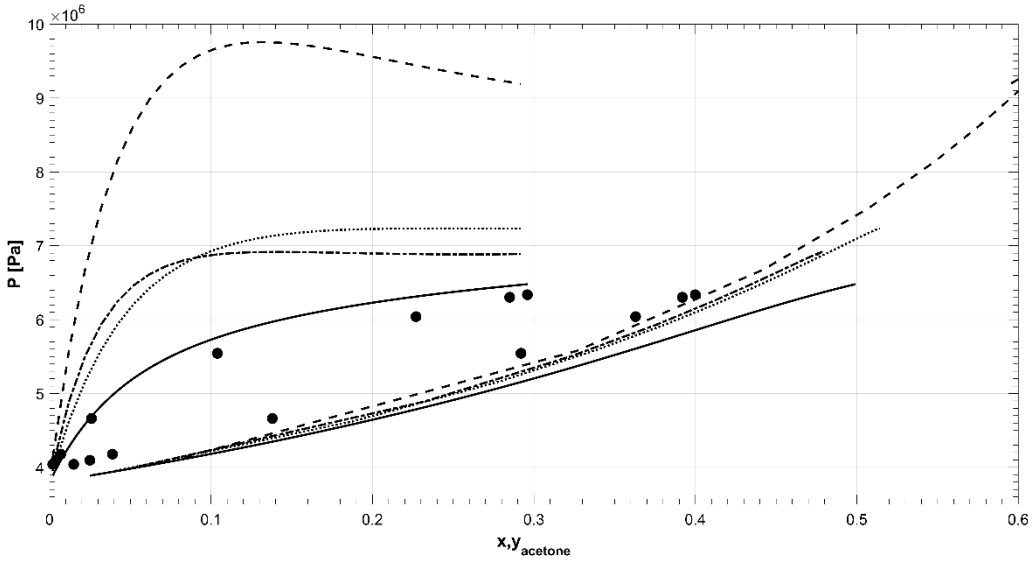

Figure 6. Acetone + Water VLE predictive models results (● Experimental Data, ▬ ▬ UNIFAC Literature, ▪▪▪▪▪▪▪ UNIFAC, ▬▬▬ F-SAC, ▬▬▬ COSMO-SAC).

Table 5. Acetone + Water results for 250°C.

Model	Residual y	Residual P [Pa]	AR y	AR P	RMSD y	RMSD P [Pa]	AAD y	AAD P [Pa]
Wilson	0.3170	1.1806E+06	0.2097	0.0250	0.0572	1.7501E+05	0.0396	1.4757E+05
Wilson Literature	0.7497	1.8784E+07	0.3902	0.5007	0.1162	2.9166E+06	0.0937	2.3480E+06
NRTL	0.3825	9.9602E+05	0.2123	0.0224	0.0566	1.4397E+05	0.0478	1.2450E+05
NRTL Literature	0.4828	9.2799E+05	0.2253	0.0216	0.0662	1.3693E+05	0.0604	1.1600E+05
UNIQUAC	0.3768	1.0332E+06	0.2038	0.0238	0.0547	1.4705E+05	0.0471	1.2915E+05
UNIQUAC Literature	0.1772	6.3408E+06	0.0676	0.1648	0.0316	9.1780E+05	0.0221	7.9260E+05
UNIFAC	0.3719	1.0647E+06	0.1974	0.0249	0.0533	1.5130E+05	0.0465	1.3308E+05
UNIFAC Literature	0.9764	6.0863E+06	0.4668	0.1609	0.1351	9.5596E+05	0.1221	7.6079E+05
COSMO-SAC	0.5303	1.1207E+06	0.2799	0.0274	0.0753	1.5575E+05	0.0663	1.4009E+05
F-SAC	0.8755	4.6344E+06	0.3415	0.1163	0.1212	7.0891E+05	0.1094	5.7930E+05

The remaining results can be seen in detail in the Appendix B of the Supplementary Information.

Also, it should be noted that the parameters used to produce these results were estimated, according to the Nelder-Mead *simplex*[30,34]. The parameters optimized for the

experimental data available are presented in Tables 6-9. The COSMO-SAC and F-SAC models were not included in the referred Tables because no parameters estimations were performed for these two models in this work.

Table 6. Wilson optimized parameters, obtained from the VLE data, and literature parameters.

	Wilson (opt)		Wilson (literature)		Parameters Reference
System	λ_{12}	λ_{21}	λ_{12}	λ_{21}	
Acetone(1) / Methanol(2)	-1871.80	3127.60	-767.72	2692.4	37
Methanol(1) / Water(2)	-2455.20	4844.10	389.37	368.45	38
2-Propanol(1) / Water(2)	-1100.90	9496.10	2095.82	5300.58	39
Methanol(1) / Benzene(2)	2481.00	1016.10	7476.31	730.83	37
Acetone(1) / Water(2)	-1869.20	9010.80	0.15716	0.45981	40
Ethanol(1) / Water(2)	1564.80	7697.00	1883.5	3871.3	41
Butane(1) / Methanol(2)	-12561.00	25639.00	273.83	1187.44	12
Butanol(1)/Decane(2)	5027.30	5516.30	5695.3	918.43	13
Butanol(1)/hexane(2)	-639.12	598.18	1968.86	-60.3	42
Heptane(1)/1-Pentanol(2)	438.32	5322.80	717.616	5880.91	16
Pentane(1)/Methanol(2)	461.66	11619.00	0.1773	0.1587	17

Table 7. NRTL optimized parameters, obtained from the VLE data, and literature parameters.

	NRTL (opt)			NRTL (literature)			Parameters Reference
System	g_{12}	g_{21}	α	g_{12}	g_{21}	α	
Acetone(1) / Methanol(2)	1179.30	4358.80	1.8544	770.1500	1023.1800	0.1099	37
Methanol(1) / Water(2)	1139.10	824.79	-3.2481	-436.5000	1159.5500	0.2410	38
2-Propanol(1) / Water(2)	-37980.0	54483.00	0.0216	111.4600	6726.0800	0.3000	39
Methanol(1) / Benzene(2)	6952.00	2169.50	0.7184	3352.1000	5003.9500	0.5020	37
Acetone(1) / Water(2)	-17.09	8207.50	0.3651	1594.1753	8631.6566	0.5466	43
Ethanol(1) / Water(2)	6201.80	16507.00	0.7376	227.5600	5196.9000	0.4000	41

Butane(1) / Methanol(2)	219.68	5856.60	-53.0640	763.9300	570.9200	0.4408	12
Butanol(1)/Decane(2)	8283.20	28748.00	0.3463	1905.4000	1816.3000	-1.1217	13
Butanol(1)/hexane(2)	-8613.40	16334.00	0.0550	660.3830	300.9060	0.52897	42
Heptane(1)/1-Pentanol(2)	1229.70	2070.60	-1.3447	1267.7400	2112.9200	-1.1732	44
Pentane(1)/Methanol(2)	446.29	7170.90	-0.0090	1.91080	1.8215	0.4889	17

Table 8. UNIQUAC optimized parameters, obtained from the VLE data, and literature parameters.

	UNIQUAC (opt)		UNIQUAC (literature)		Parameters Reference
System	u_{12}	u_{21}	u_{12}	u_{21}	
Acetone(1) / Methanol(2)	-565.14	2184.90	190.42	-43.506	45
Methanol(1) / Water(2)	1443.10	-954.55	-164.8	256.6	46
2-Propanol(1) / Water(2)	3037.90	-111.81	1319.93	426.02	39
Methanol(1) / Benzene(2)	2199.80	754.02	-123.69	935.05	47
Acetone(1) / Water(2)	1069.90	599.65	-81.56071	-179.9613	48
Ethanol(1) / Water(2)	-1740.80	6157.30	1359.8	-24.504	41
Butane(1) / Methanol(2)	5681.80	206.53	592.24	50.984	12
Butanol(1)/Decane(2)	334.23	1100.10	502.24	-91.59	49
Butanol(1)/hexane(2)	-952.61	2853.90	968.65	-327.3	49
Heptane(1)/1-Pentanol(2)	2069.30	-663.00	-282.37	720.62	49
Pentane(1)/Methanol(2)	6464.00	64.59	0.1595	0.9963	17

Table 9. UNIFAC optimized parameters, obtained from the VLE data.

System	a_{12}	a_{13}	a_{14}	a_{21}	a_{23}	a_{24}
	a_{31}	a_{32}	a_{34}	a_{41}	a_{42}	a_{43}
Acetone(1) / Methanol(2)	-182.2634	-49.5369	----	-667.326	-72.3480	----
	-454.6260	270.3275	----	----	----	----
Methanol(1) / Water(2)	109.4681	----	----	-79.0500	----	----
	----	----	----	----	----	----
	0	48.7320	235591.0173	0	48.7320	235591.0173

2-propanol(1) / Water(2)	-14.1970	-14.1970	320.8800	-20.4438	-20.4438	-644.2425
Methanol(1) / Benzene(2)	231.4919	----	----	77.9522	----	----
	----	----	----	----	----	---
Acetone(1) / Water(2)	-710.0073	343.8687	---	577.3874	129.4777	----
	166.12	-392.4707	----	----	----	----
Ethanol(1) / Water(2)	0	-1218.130	3339554.736	0	-1218.130	3339554.7366
	-201.5477	-201.5477	56858.3279	94.1953	94.1953	-1927.953
Butane(1) / Methanol(2)	0	683.0499	----	0	683.0499	----
	1.9104	1.9104	----	----	----	----
Butanol(1)/Decane(2)	0	939.9078	----	0	939.9078	----
	6424.4588	6424.4588	----	----	----	----
Butanol(1)/hexane(2)	0	1019.1050	----	0	1019.1050	----
	133.6714	133.6714	----	----	----	----
Heptane(1)/1-Pentanol(2)	0	962.0424	----	0	962.0424	----
	4840.7884	4840.7884	----	----	----	----
Pentane(1)/Methanol(2)	0	784.3499	----	0	784.3499	----
	-35.2190	-35.2190	----	----	----	----

Table 10. UNIFAC parameters (published in Skjold-Jørgensen et al., 1979[50]).

System	a_{12}	a_{13}	a_{14}	a_{21}	a_{23}	a_{24}
	a_{31}	a_{32}	a_{34}	a_{41}	a_{42}	a_{43}
Acetone(1) / Methanol(2)	476.40	697.20	----	26.76	108.65	----
	16.51	23.39	----	----	----	----
Methanol(1) / Water(2)	-180.95	----	----	289.60	----	----
	----	----	----	----	----	----
2-propanol(1) / Water(2)	0	986.50	1318.00	0	986.50	1318.00
	156.40	156.40	353.50	300.00	300.00	-229.10
Methanol(1) / Benzene(2)	-50.00	----	----	637.35	----	----
	----	----	----	----	----	---
	476.40	1318.00	---	26.76	472.50	----

Acetone(1) / Water(2)	300.00	-195.40	----	----	----	----
Ethanol(1) / Water(2)	0	986.50	1318.00	0	986.50	1318.00
	156.40	156.40	353.50	300.00	300.00	-229.10
Butane(1) / Methanol(2)	0	697.20	----	0	697.20	----
	16.51	16.51	----	----	----	----
Butanol(1)/Decane(2)	0	986.50	----	0	986.50	----
	156.40	156.40	----	----	----	----
Butanol(1)/hexane(2)	0	986.50	----	0	986.50	----
	156.40	156.40	----	----	----	----
Heptane(1)/1-Pentanol(2)	0	986.50	----	0	986.50	----
	156.40	156.40	----	----	----	----
Pentane(1)/Methanol(2)	0	697.20	----	0	697.20	----
	16.51	16.51	----	----	----	----

It is important to say that different results could be obtained if the models were compared for ternary mixtures. This kind of comparison was not performed in this work but it is going to be developed in a future work.

4.2 IDAC Results

In addition to the VLE data tested earlier, 129 IDAC experimental points were collected to evaluate the 10 models and compare their prediction accuracy. The data was obtained from different sources than those of the VLE data, assuring no correlation between them. Therefore, no model was favored by the parameters estimation performed in the first part of this work.

After the IDAC data collection, each model was used to predict them. The sum of the residuals of the 129 $\ln \gamma_i^{\infty}$ obtained by each model is given in Table 11. It can be seen that the

F-SAC model has the lowest deviation (residuals) from the experimental data, followed by the UNIQUAC with literature parameters, COSMO-SAC, and UNIFAC with optimized parameters. The RMSD obtained by the F-SAC model was the smallest and its coefficient of determination the bigger, reassuring its good results described by the residuals.

Table 11. IDAC results for the tested models (a is the linear regression parameter with its lower and upper boundaries, R^2 is the coefficient of determination, RMSD is the root-mean-squared deviation, and the sum of the prediction residuals).

Model	Residual	a* (lower, upper)	R^2	RMSD
Wilson	38.5452	0.9959 (0.9082, 1.0835)	0.0890	0.3742
Wilson Literature	137.5733	0.7757 (0.6273, 0.9240)	0.0702	0.5796
NRTL	149.2676	1.9896 (1.6858, 2.2933)	-0.4631	1.2965
NRTL Literature	37.9457	1.0280 (0.9363, 1.1198)	0.3026	0.3916
UNIQUAC	67.4864	1.5164 (1.3749, 1.6579)	-0.0230	0.6040
UNIQUAC Literature	29.7691	0.7107 (0.6410, 0.7804)	-0.0954	0.2976
UNIFAC	32.0968	0.7260 (0.6687, 0.7832)	0.2465	0.2444
UNIFAC Literature	39.6401	1.3275 (1.2603, 1.3948)	0.4787	0.2871
COSMO-SAC	31.5010	1.1045 (1.0228, 1.1861)	0.2004	0.3487
F-SAC	22.1765	1.1527 (1.0959, 1.2095)	0.6361	0.2425

* The parameter a was obtained by the adjustment of ($\ln \gamma_{i,model}^{\infty} = a \ln \gamma_{i,exp}^{\infty}$).

The UNIFAC model with its original parameters provided results with less accuracy than the other predictive models. Thus, considering only the predictive models for IDAC predictions, the F-SAC model is absolutely recommended, and so is the COSMO-SAC, although not as accurate as the former.

The linear regression of the results, depicted in Table 10, can be seen in the Figures presented in the Appendix C of the Supplementary Information. The linear fitting of the

predicted to the experimental values are a measure of how good is the performance of the model. The prediction boundaries were obtained by the 95% confidence interval of the linear regression parameters.

5 CONCLUSIONS

The activity coefficient models were divided in two classes of models: correlative and predictive. The correlative models that were found to be the most reliable for VLE predictions of the 11 binary systems tested were the NRTL and UNIQUAC models. Both models presented lower residuals and RMSD than the Wilson model, either when comparing only the literature parameters approach or when the estimated parameters were used. The NRTL model was especially good when equilibrium pressure predictions were performed, while the UNIQUAC model offered higher accuracy for vapor-phase compositions when the optimized parameters are used.

Still concerning to the correlative models, the UNIQUAC model with the optimized parameters had the best performance in 7 of the 11 binary systems; while, when comparing only the models with literature parameters, the NRTL model has shown to be the most reliable model. For the Ethanol + Water system, however, the best results were obtained by the UNIQUAC and NRTL models with the literature parameters, which overperformed the reliability of the models with optimized parameters.

The VLE results are biased, however, favoring the models with optimized parameters. To overcome this, the Infinite Dilution Activity Coefficient was used. When predictions of IDAC are performed, the correlative model with the lowest residuals is the UNIQUAC model with literature parameters, leading to conclude that the literature parameters are still superior for predictions of these systems. Although the UNIQUAC (literature) had the lowest residuals and RMSD for the linear regression of the correlative models, its determination coefficient is

negative, showing that the null-hypothesis, a horizontal line, fits better the data than the linear model adjusted.

Concerning to the predictive models, the most reliable results for VLE predictions were obtained by the UNIFAC with the estimated parameters. However, comparing only the UNIFAC with literature parameters and the COSMO-SAC and F-SAC models, it can be seen that the former was less accurate for vapor-phase composition predictions than both other, and more accurate than F-SAC for equilibrium pressure. The last comparison is valid for the VLE data used, since neither UNIFAC (literature), nor F-SAC, nor COSMO-SAC were parametrized for the experimental data. So, in general, the COSMO-SAC model presented better results for almost every binary system tested in this work.

Still, the IDAC predictions were performed with the predictive models. The F-SAC presented the lowest residuals of the 4 models. Also, it presented the lowest RMSD and the highest coefficient of determination, both good indicators of the goodness of fit of the model. Therefore, the F-SAC model was the most successful when it comes to describe IDAC.

Nomenclature

A_i – Total surface area from all segments in molecule i

$a_{m,n}$ – Energy parameters for a $m - n$ group interaction (UNIFAC)

α – Non-randomness parameter for the NRTL model

α' - Constant for the misfit energy

c_{hb} - Constant for the hydrogen-bond interaction

c_{ne} – Nonelectrostatic constant

E – Energy

ξ_i – Local volume fraction of the component i around a central molecule of the same type

g_{ji} – Constant of proportionality of the interaction energy between molecules j and i

$\Delta G_{i/S}^{*sol}$ – Solvation free energy

$\Delta G_{i/S}^{*res}$ – Restoring free energy

$\bar{G}^{E}$ – Molar excess Gibbs free energy

$\bar{G}^{M}$ – Molar free energy of mixing

γ_i – Activity coefficient of the component i

κ – Boltzmann Constant

$\Lambda_{1,2}$ and $\Lambda_{2,1}$ – Binary interaction parameters for the Wilson equation

n_i – Number of segments in a single molecule i

η – Number of variables in the Nelder-Mead optimization method

P - Pressure

$p_s(\sigma)$ – Probability of a segment s to have a charge density σ

Φ_i – Average segment/volume fraction of the component i

Ψ_{mn} – Group interaction parameter

q_i – UNIQUAC and UNIFAC surface area parameter for component i

R – Universal constant of gases

r_i – UNIQUAC and UNIFAC volume parameter for component i

σ – Charge density

T – Temperature

Γ_k - Residual activity coefficient of group k (UNIFAC)

Γ_s – Segment activity coefficient (COSMO-SAC)

$\tau_{1,2}$ and $\tau_{2,1}$ - Binary interaction parameters for the NRTL model

θ_i – Average area fraction of the component i

Θ_m – Area fraction of group m

U_{mn} - Measure of the energy of interaction between the groups m and n

$u_{1,2} - u_{2,2}$ and $u_{2,1} - u_{1,1}$ – Average interaction energy for species $i - j$ (UNIQUAC model)

μ_s – Chemical potential of segment s

$\bar{V}_i$ – Molar volume of the component i

x_i – Mole fraction of the component i in the mixture

X_m - Mole fraction of group m in the mixture

z – Average coordination number (usually taken to be 10)

ζ – Dispersion constant

ΔW – Exchange energy

Subscripts

acc – Acceptor

$calc$ - Calculated

$comb$ – Combinatorial contribution

don – Donor

exp - Experimental

hb – Hydrogen-bond

i – Component

i/S – Component i in solvent S

j – Component

k – Functional group

m – Functional group (for UNIFAC) or segment (for COSMO-SAC)

mf - Misfit

n – Functional group (for UNIFAC) or segment (for COSMO-SAC)

ne - Nonelectrostatic

res – Residual contribution

s – Segment

tot - Total

Superscripts

$\bar{}$ - Molar property

E – Excess property

M – Mixing

NP – Number of points

SG – Staverman-Guggenheim

$* res$ – Restoring process for a solute

Abbreviations

ASOG - Analytical solutions of groups

AAD – Average Absolute Deviation

AR – Average Relative Deviation

COSMO-RS – Conductor-like Screening Model for Real Solvents

COSMO-SAC – Conductor-like Screening Model Segment Activity Coefficient model

IDAC – Infinite Dilution Activity Coefficient

NRTL – Non-Random Two-Liquid Model

RMSD – Root Mean Square Deviation

UNIFAC – UNIQUAC Functional-group Activity Coefficients

UNIQUAC – Universal Quasichemical Theory

VLE – Vapor-Liquid Equilibrium

SUPPLEMENTARY INFORMATION

Appendix A - Activity Coefficient models

A.1 Wilson

The local composition activity coefficient model proposed by Wilson(WILSON, 1964) is derived from an equation similar to the Flory-Huggins equation:

$$\frac{\bar{G}^M}{RT} = \sum_i x_i \, ln\xi_i \tag{A.1}$$

Where x_i is the mole fraction of component i and ξ_i is the local volume fraction of component i about a central molecule of the same type, given by:

$$\xi_i = \frac{x_i \bar{V}_i e^{(-g_{ii}/\kappa T)}}{\sum_j x_j \bar{V}_j e^{(-g_{ij}/\kappa T)}} \tag{A.2}$$

Where $\bar{V}_i$ is the molar volume of component i. Equation A.2 is obtained based on the assumption that the distribution of molecules about a central molecule is of the type

$$\frac{x_{ji}}{x_{ki}} = \frac{x_j e^{(-g_{ji}/\kappa T)}}{x_k e^{(-g_{ki}/\kappa T)}} \tag{A.3}$$

Substituting equation A.2 into equation A.1 and rearranging:

$$\frac{\bar{G}^E}{RT} = -\sum_i x_i \, ln\left(1 - \sum_j x_j \, \Lambda_{j/i}\right) \tag{A.4}$$

Where $\Lambda_{j/i} = 1 - \left(\bar{V}_j/\bar{V}_i\right) exp\left(-\left(g_{ji} - g_{ii}\right)/\kappa \, T\right)$. Equation A.4 is the Wilson equation, with $\Lambda_{j/i}$ as adjustable parameters ($\Lambda_{i/i} = 0$ and $\Lambda_{j/i} \neq \Lambda_{i/j}$). The number of parameters to be adjusted for the Wilson equation is given by $n(n-1)$, where n is the number of components.

For a binary mixture, there will be two adjustable parameters, $\Lambda_{2/1}$and $A_{1/2}$. If the deviation from ideality is positive, so are the parameters; if the deviation from ideality is negative, the parameters are negative. If one parameter is positive and the other is negative, the deviation from ideality will depend upon which one has the greater effect. If a parameter is equal to unity, it means that the molecules have zero interaction.

The activity coefficients are derived from equation 4, thus, for a binary mixture:

$$ln\gamma_1 = -ln(x_1 + x_2\Lambda_{12}) + x_2\left(\frac{\Lambda_{12}}{x_1 + x_2\Lambda_{12}} - \frac{\Lambda_{21}}{x_1\Lambda_{21} + x_2}\right) \tag{A.5}$$

$$ln\gamma_2 = -ln(x_2 + x_1\Lambda_{21}) + x_1\left(\frac{\Lambda_{12}}{x_1+x_2\Lambda_{12}} - \frac{\Lambda_{21}}{x_1\Lambda_{21}+x_2}\right) \quad \text{(A.6)}$$

A.2 NRTL

To develop the NRTL model, Renon and Prausnitz(RENON; PRAUSNITZ, 1968) used a modification of equation A.3, which takes into account the non-randomness of mixing. Thus, for a binary mixture, the relation between the local mole fractions x_{21} and x_{11} is given by:

$$\frac{x_{21}}{x_{11}} = \frac{x_2}{x_1}\frac{e^{(-\alpha_{12}g_{21}/RT)}}{e^{(-\alpha_{12}g_{11}/RT)}} \quad \text{(A.7)}$$

In the same manner

$$\frac{x_{12}}{x_{22}} = \frac{x_1}{x_2}\frac{e^{(-\alpha_{12}g_{12}/RT)}}{e^{(-\alpha_{12}g_{22}/RT)}} \quad \text{(A.8)}$$

Where α_{12} is a nonrandomness constant and $g_{12} = g_{21}$.

The local mole fractions are related by

$$x_{21} + x_{11} = 1$$
$$x_{12} + x_{22} = 1 \quad \text{(A.9)}$$

Rearranging equations A.7 and A.8 into equation A.9, we obtain

$$x_{21} = \frac{x_2 e^{(-\alpha_{12}(g_{21}-g_{11})/RT)}}{x_1+x_2 e^{(-\alpha_{12}(g_{21}-g_{11})/RT)}} \quad \text{(A.10)}$$

$$x_{12} = \frac{x_1 e^{(-\alpha_{12}(g_{12}-g_{22})/RT)}}{x_2+x_1 e^{(-\alpha_{12}(g_{12}-g_{22})/RT)}} \quad \text{(A.11)}$$

According to the Scott's two-liquid theory of binary mixture, used by Renon and Prausnitz to develop the NRTL model, the residual Gibbs energy is given by

$$g_1 = x_{11}g_{11} + x_{21}g_{21} \tag{A.12}$$

$$g_2 = x_{12}g_{12} + x_{22}g_{22} \tag{A.13}$$

It should be noted that, for example, if we consider only pure liquid of component 1, the residual Gibbs energy would be $g_{1,pure} = g_{11}$.

Since the molar excess Gibbs energy for a binary mixture is the sum of two changes in the residual Gibbs energy, the molar excess Gibbs energy is

$$g^E = x_1\left(g_1 - g_{1,pure}\right) + x_2\left(g_2 - g_{2,pure}\right) \tag{A.14}$$

Substituting equations A.9, A.12, and A.13 into equation A.14 we obtain the NRTL characteristic equation:

$$g^E = x_1x_{21}(g_{21} - g_{11}) + x_2x_{12}(g_{12} - g_{22}) \tag{A.15}$$

By differentiation of equation A.15, we obtain the activity coefficients expressions for the NRTL model:

$$ln(\gamma_1) = {x_2}^2\left(\tau_{21}\frac{e^{(-2\alpha_{12}\tau_{21})}}{\left[x_1+x_2e^{(-\alpha_{12}\tau_{21})}\right]^2} + \tau_{12}\frac{e^{(-\alpha_{12}\tau_{12})}}{\left[x_2+x_1e^{(-\alpha_{12}\tau_{12})}\right]^2}\right) \tag{A.16}$$

$$ln(\gamma_2) = {x_1}^2\left(\tau_{12}\frac{e^{(-2\alpha_{12}\tau_{12})}}{\left[x_2+x_1e^{(-\alpha_{12}\tau_{12})}\right]^2} + \tau_{21}\frac{e^{(-\alpha_{12}\tau_{21})}}{\left[x_1+x_2e^{(-\alpha_{12}\tau_{21})}\right]^2}\right) \tag{A.17}$$

Where $\tau_{12} = (g_{12} - g_{22})/RT$, $\tau_{21} = (g_{21} - g_{11})/RT$, and $g_{12} = g_{21}$.

A.3 UNIQUAC

The UNIQUAC model was proposed by Abrams and Prausnitz(ABRAMS; PRAUSNITZ, 1975) as an extension of the Guggenheim's theory to mixtures containing molecules of different shapes and sizes by using the local-composition concept introduced by Wilson(WILSON, 1964).

The theory of Guggenheim takes into account only mixtures of spherical molecules with about the same size, therefore it was assumed that a molecule of component 1, for instance, would be neighbor of a molecule of component 2. This is true if there is a random tendency on the mixture. However, if the molecules tend to be near to each other or to segregate from different molecules, let us say molecule of component 1 is attracted by other molecules of component 1, this approach is not appropriate.

To overcome this, Abrams and Prausnitz proposed the local area fraction. They considered that a molecule of a component is described by a set of bonded segments, and the number of segments per molecule is represented by r_i. The segments, although they have the same size, by definition, may differ in their external contact area, the parameter q_i is a proportionality parameter for the external surface area. Hence, the UNIQUAC theory considers the degeneracy of the molecules.

Abrams and Prausnitz obtained the characteristic equation of the UNIQUAC model as a sum of a combinatorial (that accounts for shape and size differences between molecules, affecting the entropy of the mixture) and a residual (enthalpic) terms

$$g^E = g^E_{combinatorial} + g^E_{residual} \tag{A.18}$$

For a binary mixture, the combinatorial and residual terms are given as:

$$\frac{g^E_{comb}}{RT} = x_1 ln\frac{\Phi_1}{x_1} + x_2 ln\frac{\Phi_2}{x_2} + \left(\frac{z}{2}\right)\left(q_1 x_1 ln\frac{\theta_1}{\Phi_1} + q_2 x_2 ln\frac{\theta_2}{\Phi_2}\right) \tag{A.19}$$

$$\frac{g^E_{res}}{RT} = -q_1 x_1 ln(\theta_1 + \theta_2\tau_{21}) - q_2 x_2 ln(\theta_2 + \theta_1\tau_{12}) \tag{A.20}$$

Where

$$\begin{aligned} \tau_{21} &\equiv e^{-\left(\frac{u_{21}-u_{11}}{RT}\right)} \\ \tau_{12} &\equiv e^{-\left(\frac{u_{12}-u_{22}}{RT}\right)} \end{aligned} \tag{A.21}$$

$$\begin{aligned} \theta_1 &\equiv \frac{q_1 N_1}{q_1 N_1 + q_2 N_2} = \frac{q_1 x_1}{q_1 x_1 + q_2 x_2} \\ \theta_2 &\equiv \frac{q_2 N_2}{q_1 N_1 + q_2 N_2} = \frac{q_2 x_2}{q_1 x_1 + q_2 x_2} \end{aligned} \tag{A.22}$$

$$\begin{aligned} \Phi_1 &\equiv \frac{r_1 N_1}{r_1 N_1 + r_2 N_2} = \frac{r_1 x_1}{r_1 x_1 + r_2 x_2} \\ \Phi_2 &\equiv \frac{r_2 N_2}{r_1 N_1 + r_2 N_2} = \frac{r_2 x_2}{r_1 x_1 + r_2 x_2} \end{aligned} \tag{A.23}$$

The authors pointed out that the combinatorial term contains 2 structural parameters per component (r_i and q_i), 2 composition variables (θ and Φ) and no adjustable binary parameters. The residual term, however, has only one composition variable (θ) and two adjustable binary parameters, $(u_{21} - u_{11})$ and $(u_{12} - u_{22})$, where $u_{21} = u_{12}$.

In the same way, the activity coefficient equation can be divided into combinatorial and residual parts:

$$ln\,\gamma_i = ln\,\gamma_{i,comb} + ln\,\gamma_{i,res}$$
$$ln\,\gamma_{i,comb} = ln\frac{\phi_i}{x_i} - \frac{z}{2}q_i ln\frac{\theta_i}{\phi_i} + l_i - \frac{\phi_i}{x_i}\sum_j x_j\,l_j$$
$$ln\,\gamma_{i,res} = q_i\left[1 - ln\left(\sum_j \theta_j\,\tau_{ji}\right) - \sum_j \frac{\theta_j\tau_{ij}}{\sum_k \theta_k\tau_{kj}}\right]$$

(A.24)

Where $l_j = (z/2)\left(r_j - q_j\right) - \left(r_j - 1\right)$.

The structural parameters r and q of several components are readily available in literature.

In their work, the authors report that the NRTL (3 parameters) model is more properly applicable to excess enthalpy than to excess Gibbs energy. Also, it is shown that the UNIQUAC model has no major improvements over Wilson's model for VLE, which is the scope of the present work.

A.4 UNIFAC

The UNIFAC method was based on the ASOG model(DERR; DEAL, 1969) and on the UNIQUAC method(ABRAMS; PRAUSNITZ, 1975). The UNIFAC model development is very similar to the development of the UNIQUAC model. The UNIFAC model(FREDENSLUND; JONES; PRAUSNITZ, 1975) ends up with the activity coefficients given by the summation of the combinatorial and residual parts, being the combinatorial contribution dependent on the molecules sizes and shapes, and the residual contribution depends on the groups areas and interactions.

So, similar to equation A.24, the UNIFAC model is given by

$$ln\,\gamma_i = ln\,\gamma_{i,comb} + ln\,\gamma_{i,res}$$
$$ln\,\gamma_{i,comb} = ln\frac{\phi_i}{x_i} - \frac{z}{2}q_i ln\frac{\theta_i}{\phi_i} + l_i - \frac{\phi_i}{x_i}\sum_j x_j\,l_j$$
$$ln\,\gamma_{i,res} = \sum_k \nu_k\left(ln\,\Gamma_k - ln\,\Gamma_k^{(i)}\right)$$

(A.25)

Where Γ_k is the group residual activity coefficient, and $\Gamma_k^{(i)}$ is the residual activity coefficient of group k in a solution containing only molecules of type i. Therefore, the difference between the UNIQUAC and UNIFAC is that the latter uses a solution-of-groups concept for the residual contribution. The group residual activity coefficient Γ_k is computed as

$$ln\,\Gamma_k = Q_k\left[1 - ln(\sum_m \Theta_m\Psi_{mk}) - \sum_m\left(\frac{\Theta_m\Psi_{km}}{\sum_n \Theta_n\Psi_{nm}}\right)\right]$$

(A.26)

Equation A.26 is true for $\Gamma_k^{(i)}$ as well, and Θ_m and Ψ_{mn} are given by

$$\Theta_m = \frac{Q_m X_m}{\sum_n Q_n X_n} \tag{A.27}$$

$$\Psi_{mn} = e^{-\left(\frac{U_{mn}-U_{nn}}{RT}\right)} = e^{-\left(\frac{a_{mn}}{T}\right)} \tag{A.28}$$

Where X_m is the mole fraction of group m in the mixture, U_{mn} is a measure of the energy of interaction between the groups m and n, and a_{mn} is the parameter that must be evaluated from experimental data and has units of degrees Kelvin.

Fredenslund *et al*. showed in their work that the use of the UNIFAC method for new mixtures, without previous parameters estimation, can provide satisfactory results if the groups contained in the mixture have already been studied. For example, if the binary mixture heptane + 2-butanone was studied and included in the database, the UNIFAC model can promptly be used for hexane + 2-butanone. This would provide a great advantage, meaning that not every mixture needs to be in the database, only its groups interactions, which is much more feasible.

Nevertheless, some mixtures are still not accurately predictable with this approach.

A.5 COSMO-SAC

The COSMO-based models development began with the work of Klamt and coworkers(KLAMT; ECKERT, 2000; KLAMT; SCHÜÜRMANN, 1993). Klamt and Schüürmann began by introducing the screening method to obtain the solvation energy of molecule in a conductor(KLAMT; SCHÜÜRMANN, 1993), and later applying this method for liquid-phase thermodynamics in the COSMO-RS(KLAMT, 1995; KLAMT; ECKERT, 2000). Lin and Sandler(LIN; SANDLER, 2002) developed the COSMO-SAC model, still based on the COSMO calculation, but thermodynamically consistent, since the COSMO-RS model failed to satisfy some thermodynamics boundaries.

The COSMO-SAC model estimates the solvation free energy, $\Delta G_{i/S}^{*sol}$, i. e. the energy necessary to transfer a solute molecule from a fixed position in an ideal gas to a fixed position in a solution S. Lin and Sandler described a two steps process to calculate the solvation free energy, first an ideal solvation process is conducted (the dielectric properties of the solvent are increased to that of a perfect conduction and the solute charges are turned on), then the solvent properties are restored to their normal values and the screening charges are removed.

During the ideal screening process, the electrostatic potential of the molecule is obtained. Each molecule is then divided in several segments and the probability of finding a segment with charge density σ is calculated. The probability of finding a segment with charge density σ, $p_s(\sigma)$, is the weighted sum of the σ-profiles of all the components

$$p_s(\sigma) = \frac{\sum_i x_i n_i p_i(\sigma)}{\sum_i x_i n_i} = \frac{\sum_i x_i A_i p_i(\sigma)}{\sum_i x_i A_i} \tag{A.28}$$

The ideal screening charges must then be removed, this is done by adding paired segments to all surfaces with opposite charges to those that were ideally screened. At this point, the energy of a system is given by

$$E_{tot} = \sum_i \left(E_i^{COSMO} + \zeta A_i\right) + \sum_{m,n} E_{pair}\,(\sigma_m, \sigma_n)$$

(A.29)

Where σ_m and σ_n are the charge densities of the paired segments m and n, the first summation is for all molecules, and the second for all segment pairs. Then, the chemical potential of the segments is calculated

$$\mu_s(\sigma_m) = -kT ln\left[e^{\left(\frac{-E_{pair}(\sigma_m,\sigma_n)+\mu_s(\sigma_n)}{kT}\right)}\right] + kT \ln p_s(\sigma_m) \quad \text{(A.30)}$$

Which leads to the segment activity expression

$$ln\Gamma_s(\sigma_m) = -ln\left\{\sum_{\sigma_n} p_s\,(\sigma_n)\Gamma_s(\sigma_n) e^{\frac{-\Delta W(\sigma_m,\sigma_n)}{kT}}\right\} \quad \text{(A.31)}$$

Where $\Delta W(\sigma_m, \sigma_n) = E_{pair}(\sigma_m, \sigma_n) - E_{pair}(0,0)$, the exchange energy, is the energy required to obtain one pair m-n from a neutral pair. The restoring free energy can be obtained by the summation of the segments contributions

$$\frac{\Delta G_{i/s}^{*res}}{RT} = \sum_{\sigma_m}\left[n_i(\sigma_m)\frac{\Delta G_{\sigma_{m/s}}^{*res}}{RT}\right] = n_i \sum_{\sigma_m} p_i\,(\sigma_m) ln\,\Gamma_s(\sigma_m)$$

(A.32)

And the final COSMO-SAC equation is given by

$$ln\,\gamma_{i/s} = n_i \sum_{\sigma_m} p_i\,(\sigma_m)[ln\,\Gamma_s(\sigma_m) - ln\Gamma_i(\sigma_m)] + ln\,\gamma_{i/s}^{SG}$$

(A.33)

Where $ln\,\gamma_{i/s}^{SG}$ is the Staverman-Guggenheim combinatorial term

$$ln\,\gamma_{i/s}^{SG} = ln\frac{\phi_i}{x_i} + \frac{z}{2} q_i ln\frac{\theta_i}{\phi_i} + l_i - \frac{\phi_i}{x_i}\sum_j x_j\, l_j$$

(A.34)

With $\phi_i = (x_i r_i)/\left(\sum_j x_j\, r_j\right)$, $\theta_i = (x_i q_i)/\left(\sum_j x_j\, q_j\right)$, $l_i = (z/2)[(r_i - q_i) - (r_i - 1)]$.

It is important to notice that the self-energy term contains contributions from electrostatic interactions (misfit energy), hydrogen-bond interactions, and nonelectrostatic interactions

$$E_{pair}(\sigma_m, \sigma_n) = E_{mf}(\sigma_m, \sigma_n) + E_{hb}(\sigma_m, \sigma_n) + E_{ne}(\sigma_m, \sigma_n)$$

$$= \left(\frac{\alpha'}{2}\right)(\sigma_m + \sigma_n)^2 + c_{hb} max[0, \sigma_{acc} - \sigma_{hb}] min[0, \sigma_{don} + \sigma_{hb}] + c_{ne} \quad \text{(A.35)}$$

Where α' is a constant for the misfit energy; c_{hb} is a constant for the hydrogen-bond interaction, and σ_{hb} is a cutoff value for the hydrogen-bonding interactions; σ_{acc} and σ_{don} are the larger and smaller values of σ_m and σ_n; the nonelectrostatic contribution is assumed to be a constant c_{ne}.

Since the nonelectrostatic contribution is assumed to be constant, the exchange energy, to be used in equation A.31, becomes

$$\Delta W(\sigma_m, \sigma_n) = \frac{\alpha\prime}{2}(\sigma_m + \sigma_n)^2 + c_{hb} max[0, \sigma_{acc} - \sigma_{hb}] min[0, \sigma_{don} + \sigma_{hb}] \quad \text{(A.36)}$$

A.6 F-SAC

The F-SAC model is based, as UNIFAC is, on group contributions, however, the interaction energies come from the COSMO-SAC model. This approach proposed by Soares and coworkers(GERBER; SOARES, 2013; SOARES et al., 2013) introduces a higher degree of empiricism, decreasing the predictive aspect, if compared to COSMO-SAC.

The authors report that the main difference between the F-SAC and the COSMO-SAC or the COSMO-RS is that the former relies on fitted molecular properties, while the latter on molecular properties obtained by quantum chemistry calculations(GERBER; SOARES, 2013).

The F-SAC model follows the same formulation as the UNIFAC and COSMO-SAC models by summing the residual and combinatorial contributions, cf. equation A.24. The combinatorial part is given by

$$\ln \gamma_{i,comb} = 1 - V_i' + \ln V_i' - \frac{5q_i}{q}\left(1 - \frac{V_i}{F_i} + \ln \frac{V_i}{F_i}\right) \quad \text{(A.37)}$$

Where $V_i' = r_i^{3/4} / \sum_j x_j r_j^{3/4}$, $V_i = r_i / \sum_j x_j r_j$, $r_i = \sum_k v_k^{(i)} R_k$, $F_i = q_i / \sum_j x_k q_j$, and $q_i = \sum_k v_k^{(i)} Q_k$. The $v_k^{(i)}$ represents the number of subgroups of type k in molecule i, x_i is the mole fraction, R_k and Q_k are the functional groups volumes and surface areas, respectively, the formar obtained by COSMO calculations and the latter by parameters optimization.

Just like the COSMO-SAC model, the F-SAC uses the residual contribution as the difference between the free energy to restore the charge around the solute molecule i in solution s and the free energy to restore the charge around the solute molecule i in a pure liquid i. However, the authors introduced an empirical factor β to the equation:

$$\ln \gamma_{i,res} = \frac{\beta\left(\Delta G_{i/s}^{*res} - \Delta G_{i/i}^{*res}\right)}{RT} \quad \text{(A.38)}$$

And to calculate the free energy to restore the charge around the solute molecule:

$$\frac{\Delta G_{i/s}^{*res}}{RT} = n_i \sum_{\sigma_m} p_i(\sigma_m) \ln \Gamma_s(\sigma_m) \quad \text{(A.39)}$$

Where $\Gamma_s(\sigma_m)$ is the activity coefficient of a segment with charge σ_m, expressed by

$$\ln \Gamma_s(\sigma_m) = -\ln\left\{\sum_{\sigma_n} p_s(\sigma_n) \Gamma_s(\sigma_n) exp\left[\frac{-\Delta W(\sigma_m, \sigma_n)}{RT}\right]\right\} \quad \text{(A.40)}$$

And

$$\Delta W(\sigma_m, \sigma_n) = \frac{\alpha'}{2}(\sigma_m + \sigma_n)^2 + E^{HB}\frac{(\sigma_m, \sigma_n)}{2} \quad (A.41)$$

As it can be seen, the sigma profile is still necessary to obtain the activity coefficient. However, the sigma profile obtainment is essentially different than the COSMO-SAC, Soares and Gerber(GERBER; SOARES, 2013) propose that each functional group has its own, empirically calibrated, sigma profile $p_k(\sigma)$.

Appendix B – Results details

Table B.1. Acetone + Methanol system results.

	Temperature (°C)	Residual y	Residual P [Pa]	AR y	AR P	RMSD y	RMSD P [Pa]	AAD y	AAD P [Pa]
Wilson	100	0.1549	1.8706×10^5	0.0210	0.0353	0.0128	1.5481×10^4	0.0110	1.3362×10^4
	150	0.2370	3.5504×10^5	0.0384	0.0177	0.0248	2.6800×10^4	0.0158	2.3669×10^4
	200	0.2413	9.1061×10^5	0.0659	0.0238	0.0371	1.1330×10^5	0.0241	9.1061×10^4
Wilson Literature	100	0.5597	1.1949×10^5	0.0658	0.0224	0.0417	1.0191×10^4	0.0399	8.5352×10^3
	150	0.6721	7.2559×10^5	0.0844	0.0355	0.0507	5.8545×10^4	0.0448	4.8373×10^4
	200	0.4473	1.7338×10^6	0.1086	0.0472	0.0571	1.9932×10^5	0.0447	1.7338×10^5
NRTL	100	0.3008	8.1970×10^4	0.0328	0.0153	0.0224	6.6218×10^3	0.0214	5.8550×10^3
	150	0.2595	1.1887×10^5	0.0327	0.0059	0.0219	9.8997×10^3	0.0173	7.9245×10^3
	200	0.2087	8.9843×10^5	0.0485	0.0231	0.0289	1.2264×10^5	0.0208	8.9843×10^4
NRTL Literature	100	0.3224	8.5534×10^4	0.0291	0.0156	0.0257	6.6466×10^3	0.0230	6.1096×10^3
	150	0.3410	3.3723×10^5	0.0352	0.0172	0.0248	3.0502×10^4	0.0227	2.2482×10^4
	200	0.1870	1.1333×10^6	0.0444	0.0305	0.0273	1.4032×10^5	0.0187	1.1333×10^5
UNIQUAC	100	0.2563	5.0602×10^4	0.0204	0.0091	0.0248	4.6067×10^3	0.0183	3.6144×10^3
	150	0.3346	1.9167×10^5	0.0363	0.0094	0.0273	1.5287×10^4	0.0223	1.2778×10^4
	200	0.2503	8.7954×10^5	0.0560	0.0228	0.0327	1.1411×10^5	0.0250	8.7954×10^4
UNIQUAC Literature	100	0.5494	4.9568×10^5	0.0677	0.0930	0.0433	3.9386×10^4	0.0392	3.5406×10^4
	150	0.5607	1.8375×10^6	0.0724	0.0929	0.0447	1.3324×10^5	0.0373	1.2250×10^5
	200	0.4086	2.9246×10^6	0.0901	0.0833	0.0492	3.1197×10^5	0.0408	2.9246×10^5
UNIFAC	100	0.2566	5.3095×10^4	0.0203	0.0096	0.0250	4.8624×10^3	0.0183	3.7925×10^3
	150	0.3343	1.8780×10^5	0.0366	0.0092	0.0273	1.5057×10^4	0.0222	1.2520×10^4
	200	0.2498	8.7138×10^5	0.0562	0.0225	0.0327	1.1278×10^5	0.0249	8.7138×10^4
UNIFAC Literature	100	0.3112	1.2195×10^5	0.0243	0.0227	0.0270	9.3852×10^3	0.0222	8.7106×10^3
	150	0.3469	3.5788×10^5	0.0312	0.0180	0.0265	2.8346×10^4	0.0231	2.3858×10^4
	200	0.2361	1.1644×10^6	0.0490	0.0307	0.0288	1.5024×10^5	0.0236	1.1644×10^5
COSMO-SAC	100	0.3659	1.4766×10^5	0.0427	0.0271	0.0287	1.1694×10^4	0.0261	1.0547×10^4
	150	0.3390	7.1703×10^5	0.0446	0.0366	0.0263	5.6489×10^4	0.0226	4.7802×10^4

	200	0.1660	1.5547×10^{6}	0.0506	0.0434	0.0299	1.6488×10^{5}	0.0166	1.5547×10^{5}
F-SAC	100	0.3350	1.0383×10^{5}	0.0298	0.0191	0.0271	8.0143×10^{3}	0.0239	7.4167×10^{3}
	150	0.3420	3.5311×10^{5}	0.0369	0.0181	0.0246	3.3671×10^{4}	0.0228	2.3541×10^{4}
	200	0.1724	1.1683×10^{6}	0.0456	0.0320	0.0280	1.4078×10^{5}	0.0172	1.1683×10^{5}

Table B.2. Methanol + Water system results.

	Temperature (°C)	Residual y	Residual P [Pa]	AR y	AR P	RMSD y	RMSD P [Pa]	AAD y	AAD P [Pa]
Wilson	100	0.2326	2.6791×10^{5}	0.0169	0.0570	0.0174	1.9019×10^{4}	0.0145	1.6745×10^{4}
	150	0.2123	6.6108×10^{5}	0.0091	0.0492	0.0232	5.7163×10^{4}	0.0152	4.7220×10^{4}
	200	0.2100	1.9689×10^{6}	0.0184	0.0465	0.0156	1.4811×10^{5}	0.0140	1.3126×10^{5}
	250	0.3487	2.5735×10^{5}	0.1516	0.0064	0.0600	6.0049×10^{4}	0.0581	4.2892×10^{4}
Wilson Literature	100	1.0652	8.1235×10^{5}	0.0993	0.1934	0.0846	5.4847×10^{4}	0.0666	5.0772×10^{4}
	150	1.0905	2.3472×10^{6}	0.0922	0.1555	0.0925	1.9307×10^{5}	0.0779	1.6766×10^{5}
	200	1.0809	6.9492×10^{6}	0.0997	0.1528	0.0887	5.4478×10^{5}	0.0721	4.6328×10^{5}
	250	0.5705	1.1830×10^{7}	0.2848	0.3406	0.1208	2.0246×10^{6}	0.0951	1.9717×10^{6}
NRTL	100	1.1608	1.2804×10^{5}	0.0684	0.0296	0.0930	1.0627×10^{4}	0.0726	8.0027×10^{3}
	150	0.2406	6.2134×10^{5}	0.0187	0.0419	0.0208	4.8013×10^{4}	0.0172	4.4382×10^{4}
	200	0.2799	1.7618×10^{6}	0.0187	0.0384	0.0239	1.2504×10^{5}	0.0187	1.1746×10^{5}
	250	0.4908	1.2535×10^{5}	0.2000	0.0035	0.0820	2.4764×10^{4}	0.0818	2.0892×10^{4}
NRTL Literature	100	0.4776	5.2954×10^{5}	0.0434	0.1223	0.0375	3.4639×10^{4}	0.0299	3.3096×10^{4}
	150	0.5047	1.1230×10^{6}	0.0323	0.0788	0.0448	8.6721×10^{4}	0.0361	8.0212×10^{4}
	200	0.4653	2.8651×10^{6}	0.0349	0.0673	0.0349	2.1153×10^{5}	0.0310	1.9101×10^{5}
	250	0.1954	4.3229×10^{6}	0.0991	0.1234	0.0425	7.3117×10^{5}	0.0326	7.2048×10^{5}
UNIQUAC	100	0.6464	3.2624×10^{5}	0.0512	0.0731	0.0497	2.1519×10^{4}	0.0404	2.0390×10^{4}
	150	0.2097	4.3340×10^{5}	0.0148	0.0357	0.0195	4.5602×10^{4}	0.0150	3.0957×10^{4}
	200	0.2201	1.4507×10^{6}	0.0177	0.0345	0.0197	1.1308×10^{5}	0.0147	9.6713×10^{4}
	250	0.5086	1.9297×10^{5}	0.2103	0.0052	0.0853	4.3869×10^{4}	0.0848	3.2162×10^{4}
UNIQUAC Literature	100	0.5896	3.6838×10^{5}	0.0485	0.0840	0.0445	2.3841×10^{4}	0.0369	2.3024×10^{4}
	150	0.2216	5.6949×10^{5}	0.0148	0.0447	0.0207	5.1123×10^{4}	0.0158	4.0678×10^{4}
	200	0.2031	1.3391×10^{6}	0.0175	0.0338	0.0172	1.1756×10^{5}	0.0135	8.9273×10^{4}
	250	0.4540	7.5927×10^{5}	0.1898	0.0211	0.0764	1.2757×10^{5}	0.0757	1.2655×10^{5}
UNIFAC	100	0.6532	3.2908×10^{5}	0.0512	0.0744	0.0500	2.1527×10^{4}	0.0408	2.0567×10^{4}
	150	0.1970	4.4913×10^{5}	0.0140	0.0369	0.0184	4.6645×10^{4}	0.0141	3.2081×10^{4}
	200	0.2187	1.4797×10^{6}	0.0175	0.0352	0.0192	1.1555×10^{5}	0.0146	9.8645×10^{4}
	250	0.5067	1.4376×10^{5}	0.2084	0.0038	0.0849	3.6481×10^{4}	0.0844	2.3959×10^{4}
UNIFAC Literature	100	0.7473	3.0005×10^{5}	0.0535	0.0691	0.0571	1.9447×10^{4}	0.0467	1.8753×10^{4}
	150	0.1670	5.2476×10^{5}	0.0124	0.0399	0.0149	4.7132×10^{4}	0.0119	3.7483×10^{4}
	200	0.2684	1.8374×10^{6}	0.0176	0.0408	0.0238	1.3243×10^{5}	0.0179	1.2249×10^{5}

	250	0.5681	9.6289×10^{5}	0.2267	0.0278	0.0949	1.6779×10^{5}	0.0947	1.6048×10^{5}
COSMO-SAC	100	0.7034	3.5318×10^{5}	0.0498	0.0840	0.0526	2.2307×10^{4}	0.0440	2.2074×10^{4}
	150	0.1130	5.9852×10^{5}	0.0094	0.0451	0.0107	5.1588×10^{4}	0.0081	4.2752×10^{4}
	200	0.2715	1.8994×10^{6}	0.0166	0.0418	0.0235	1.3899×10^{5}	0.0181	1.2662×10^{5}
	250	0.5271	7.0375×10^{5}	0.2052	0.0192	0.0882	1.2364×10^{5}	0.0879	1.1729×10^{5}
F-SAC	100	0.6811	3.3709×10^{5}	0.0514	0.0786	0.0519	2.1580×10^{4}	0.0426	2.1068×10^{4}
	150	0.1635	5.3227×10^{5}	0.0114	0.0419	0.0141	5.0043×10^{4}	0.0117	3.8020×10^{4}
	200	0.2354	1.7031×10^{6}	0.0168	0.0393	0.0201	1.2905×10^{5}	0.0157	1.1354×10^{5}
	250	0.5051	1.6973×10^{5}	0.2023	0.0046	0.0843	3.5640×10^{4}	0.0842	2.8288×10^{4}

Table B.3. 2-Propanol + Water system results.

	Temperature (°C)	Residual y	Residual P [Pa]	AR y	AR P	RMSD y	RMSD P [Pa]	AAD y	AAD P [Pa]
Wilson	150	0.9093	1.7023×10^{6}	0.0655	0.1142	0.0550	1.1333×10^{5}	0.0479	8.9596×10^{4}
	200	0.7925	2.6429×10^{6}	0.0780	0.0587	0.0477	2.0381×10^{5}	0.0440	1.4683×10^{5}
	250	1.1987	4.3477×10^{6}	0.1614	0.0469	0.0830	3.2050×10^{5}	0.0749	2.7173×10^{5}
	275	2.3989	4.0414×10^{6}	0.4394	0.0245	0.1400	2.9924×10^{5}	0.1333	2.2452×10^{5}
	300	0.8578	6.1214×10^{6}	0.7076	0.0859	0.1625	1.1535×10^{6}	0.1430	1.0202×10^{6}
Wilson Literature	150	2.0397	2.0760×10^{6}	0.1916	0.1409	0.1231	1.2675×10^{5}	0.1074	1.0927×10^{5}
	200	1.9517	7.3082×10^{6}	0.2145	0.1692	0.1324	4.7748×10^{5}	0.1084	4.0601×10^{5}
	250	1.9743	2.1681×10^{7}	0.3102	0.2383	0.1532	1.4916×10^{6}	0.1234	1.3550×10^{6}
	275	2.5515	4.3157×10^{7}	0.4941	0.2862	0.1621	2.5066×10^{6}	0.1418	2.3976×10^{6}
	300	0.7994	1.8919×10^{7}	0.6648	0.2926	0.1576	3.2966×10^{6}	0.1332	3.1532×10^{6}
NRTL	150	0.9749	1.1271×10^{6}	0.0686	0.0742	0.0605	6.5817×10^{4}	0.0513	5.9323×10^{4}
	200	0.2539	6.8283×10^{5}	0.0231	0.0151	0.0160	4.6435×10^{4}	0.0141	3.7935×10^{4}
	250	0.8649	1.4144×10^{6}	0.0877	0.0142	0.0636	1.2663×10^{5}	0.0541	8.8400×10^{4}
	275	2.3283	2.5932×10^{6}	0.3947	0.0157	0.1308	1.9687×10^{5}	0.1294	1.4407×10^{5}
	300	0.9230	3.9270×10^{6}	0.7539	0.0514	0.1740	9.4059×10^{5}	0.1538	6.5450×10^{5}
NRTL Literature	150	0.5745	8.0517×10^{5}	0.0356	0.0530	0.0417	4.6427×10^{4}	0.0302	4.2377×10^{4}
	200	0.4250	1.6876×10^{6}	0.0361	0.0383	0.0269	1.0166×10^{5}	0.0236	9.3755×10^{4}
	250	0.5998	2.2246×10^{6}	0.0698	0.0206	0.0486	1.9282×10^{5}	0.0375	1.3904×10^{5}
	275	1.9323	1.0599×10^{7}	0.3553	0.0665	0.1136	6.2416×10^{5}	0.1074	5.8883×10^{5}
	300	0.7797	9.2106×10^{6}	0.6429	0.1348	0.1469	1.5804×10^{6}	0.1300	1.5351×10^{6}
UNIQUAC	150	0.4905	1.2083×10^{6}	0.0412	0.0814	0.0290	7.2917×10^{4}	0.0258	6.3597×10^{4}
	200	0.6053	3.4894×10^{6}	0.0545	0.0768	0.0366	2.0041×10^{5}	0.0336	1.9386×10^{5}
	250	0.9448	2.7340×10^{6}	0.0916	0.0289	0.0686	1.8964×10^{5}	0.0590	1.7087×10^{5}
	275	2.2244	2.2100×10^{6}	0.3742	0.0137	0.1242	1.6295×10^{5}	0.1236	1.2278×10^{5}
	300	0.8231	5.5470×10^{6}	0.6686	0.0780	0.1543	1.0295×10^{6}	0.1372	9.2450×10^{5}
UNIQUAC Literature	150	0.6046	4.4895×10^{5}	0.0364	0.0279	0.0444	3.0765×10^{4}	0.0318	2.3629×10^{4}

	200	0.2313	1.0871×10^{6}	0.0140	0.0241	0.0186	6.5675×10^{4}	0.0129	6.0393×10^{4}
	250	0.3560	6.2103×10^{6}	0.0381	0.0662	0.0261	3.9814×10^{5}	0.0223	3.8815×10^{5}
	275	1.3190	1.7248×10^{7}	0.2328	0.1123	0.0746	9.6256×10^{5}	0.0733	9.5823×10^{5}
	300	0.6136	1.0805×10^{7}	0.4985	0.1616	0.1134	1.8076×10^{6}	0.1023	1.8009×10^{6}
UNIFAC	150	0.9334	9.8241×10^{5}	0.0632	0.0637	0.0609	5.9038×10^{4}	0.0491	5.1706×10^{4}
	200	0.1132	3.2679×10^{5}	0.0089	0.0069	0.0085	2.4017×10^{4}	0.0063	1.8155×10^{4}
	250	0.8279	1.3196×10^{6}	0.0770	0.0136	0.0607	9.7358×10^{4}	0.0517	8.2472×10^{4}
	275	2.2882	1.5212×10^{6}	0.3809	0.0094	0.1276	1.0758×10^{5}	0.1271	8.4510×10^{4}
	300	0.8715	3.4626×10^{6}	0.7050	0.0455	0.1661	8.2059×10^{5}	0.1453	5.7711×10^{5}
UNIFAC Literature	150	1.2792	2.9730×10^{6}	0.0928	0.1877	0.0788	1.6685×10^{5}	0.0673	1.5647×10^{5}
	200	1.9055	1.0602×10^{7}	0.1416	0.2240	0.1221	6.2822×10^{5}	0.1059	5.8899×10^{5}
	250	2.1095	1.9168×10^{7}	0.1849	0.1945	0.1583	1.2765×10^{6}	0.1318	1.1980×10^{6}
	275	3.4733	2.8671×10^{7}	0.5282	0.1821	0.2039	1.6558×10^{6}	0.1930	1.5928×10^{6}
	300	1.2364	9.6245×10^{6}	0.9564	0.1485	0.2242	1.7230×10^{6}	0.2061	1.6041×10^{6}
COSMO-SAC	150	0.2617	2.0647×10^{5}	0.0163	0.0117	0.0192	1.5414×10^{4}	0.0138	1.0867×10^{4}
	200	0.7716	3.2134×10^{6}	0.0423	0.0677	0.0612	1.8692×10^{5}	0.0429	1.7852×10^{5}
	250	1.2260	1.3320×10^{7}	0.0959	0.1371	0.0970	8.4848×10^{5}	0.0766	8.3253×10^{5}
	275	2.3285	2.5653×10^{7}	0.3642	0.1648	0.1333	1.4358×10^{6}	0.1294	1.4252×10^{6}
	300	0.7558	1.1037×10^{7}	0.6000	0.1726	0.1455	1.9976×10^{6}	0.1260	1.8395×10^{6}
F-SAC	150	0.3770	7.6174×10^{5}	0.0274	0.0499	0.0263	4.4336×10^{6}	0.0198	4.0091×10^{4}
	200	0.7829	3.5616×10^{6}	0.0466	0.0770	0.0591	2.0206×10^{5}	0.0435	1.9787×10^{5}
	250	1.0326	1.0486×10^{7}	0.0850	0.1094	0.0800	6.6566×10^{5}	0.0645	6.5536×10^{5}
	275	2.0566	1.8556×10^{7}	0.3328	0.1199	0.1156	1.0383×10^{6}	0.1143	1.0309×10^{6}
	300	1.6703	3.9469×10^{7}	1.3854	0.6396	0.3308	8.2325×10^{6}	0.2784	6.5782×10^{6}

Table B.4. Methanol + Benzene system results.

	Temperature (°C)	Residual y	Residual P [Pa]	AR y	AR P	RMSD y	RMSD P [Pa]	AAD y	AAD P [Pa]
Wilson	100	0.9719	2.7100×10^{5}	0.1237	0.0657	0.1269	3.2356×10^{4}	0.0972	2.7100×10^{4}
	120	0.8722	3.6059×10^{5}	0.1050	0.0506	0.1115	4.4908×10^{4}	0.0872	3.6059×10^{4}
	140	0.8855	6.0053×10^{5}	0.1089	0.0534	0.1054	7.0934×10^{4}	0.0885	6.0053×10^{4}
	160	0.7596	8.1725×10^{5}	0.0865	0.0475	0.0907	9.3803×10^{4}	0.0760	8.1725×10^{4}
	180	0.6403	8.0409×10^{5}	0.0773	0.0331	0.0707	8.7492×10^{4}	0.0640	8.0409×10^{4}
	200	0.5006	1.0884×10^{6}	0.0609	0.0331	0.0550	1.2220×10^{5}	0.0501	1.0884×10^{5}
	220	0.3673	1.8826×10^{6}	0.0499	0.0413	0.0406	2.3470×10^{5}	0.0367	1.8826×10^{5}
Wilson Literature	100	0.5438	4.8875×10^{5}	0.0865	0.1266	0.0650	5.3319×10^{4}	0.0544	4.8875×10^{4}
	120	0.4690	7.5168×10^{5}	0.0727	0.1133	0.0561	8.0775×10^{4}	0.0469	7.5168×10^{4}
	140	0.4869	1.1740×10^{6}	0.0710	0.1093	0.0555	1.2714×10^{5}	0.0487	1.1740×10^{5}
	160	0.5476	1.7226×10^{6}	0.0709	0.1029	0.0592	1.8559×10^{5}	0.0548	1.7226×10^{5}

	180	0.6348	2.7118×10^{6}	0.0722	0.1059	0.0727	3.0362×10^{5}	0.0635	2.7118×10^{5}
	200	0.7400	4.1419×10^{6}	0.0837	0.1140	0.0833	4.6168×10^{5}	0.0740	4.1419×10^{5}
	220	0.7663	5.6117×10^{6}	0.0775	0.1073	0.0907	6.4947×10^{5}	0.0766	5.6117×10^{5}
NRTL	100	0.5629	3.3370×10^{5}	0.0743	0.0823	0.0702	3.7030×10^{4}	0.0563	3.3370×10^{4}
	120	0.4197	3.7497×10^{5}	0.0533	0.0531	0.0508	4.4477×10^{4}	0.0420	3.7497×10^{4}
	140	0.2972	5.3029×10^{5}	0.0400	0.0473	0.0339	6.0540×10^{4}	0.0297	5.3029×10^{4}
	160	0.2909	4.8222×10^{5}	0.0417	0.0269	0.0328	5.7222×10^{4}	0.0291	4.8222×10^{4}
	180	0.3624	1.4694×10^{5}	0.0516	0.0057	0.0406	1.7906×10^{4}	0.0362	1.4694×10^{4}
	200	0.4526	5.7133×10^{5}	0.0605	0.0173	0.0531	6.8143×10^{4}	0.0453	5.7133×10^{4}
	220	0.5413	1.8871×10^{6}	0.0614	0.0390	0.0641	2.4385×10^{5}	0.0541	1.8871×10^{5}
NRTL Literature	100	0.2911	1.1600×10^{5}	0.0449	0.0283	0.0314	1.3320×10^{4}	0.0291	1.1600×10^{4}
	120	0.3109	2.2085×10^{5}	0.0439	0.0300	0.0326	2.9556×10^{4}	0.0311	2.2085×10^{4}
	140	0.3742	5.2981×10^{5}	0.0458	0.0440	0.0469	6.8452×10^{4}	0.0374	5.2981×10^{4}
	160	0.4573	9.7817×10^{5}	0.0482	0.0526	0.0609	1.2192×10^{5}	0.0457	9.7817×10^{4}
	180	0.6307	1.8227×10^{6}	0.0638	0.0646	0.0829	2.3016×10^{5}	0.0631	1.8227×10^{5}
	200	0.7142	2.9503×10^{6}	0.0684	0.0742	0.0942	3.6293×10^{5}	0.0714	2.9503×10^{5}
	220	0.7144	4.2207×10^{6}	0.0592	0.0747	0.1013	5.3348×10^{5}	0.0714	4.2207×10^{5}
UNIQUAC	100	0.4749	1.8765×10^{5}	0.0634	0.0443	0.0606	2.5922×10^{4}	0.0475	1.8765×10^{4}
	120	0.3872	2.1360×10^{5}	0.0495	0.0282	0.0474	3.2820×10^{4}	0.0387	2.1360×10^{4}
	140	0.3078	3.7451×10^{5}	0.0418	0.0317	0.0349	4.7613×10^{4}	0.0308	3.7451×10^{4}
	160	0.3312	4.2245×10^{5}	0.0456	0.0224	0.0372	5.4834×10^{4}	0.0331	4.2245×10^{4}
	180	0.3797	3.1120×10^{5}	0.0551	0.0124	0.0435	3.6765×10^{4}	0.0380	3.1120×10^{4}
	200	0.4386	7.4329×10^{5}	0.0605	0.0227	0.0530	8.3276×10^{4}	0.0439	7.4329×10^{4}
	220	0.4968	1.6972×10^{6}	0.0586	0.0359	0.0608	2.2665×10^{5}	0.0497	1.6972×10^{5}
UNIQUAC Literature	100	1.0579	9.5263×10^{5}	0.1425	0.2419	0.1292	9.6506×10^{4}	0.1058	9.5263×10^{4}
	120	0.9121	1.4419×10^{6}	0.1167	0.2154	0.1107	1.4698×10^{5}	0.0912	1.4419×10^{5}
	140	0.8579	2.2364×10^{6}	0.1102	0.2114	0.0989	2.2970×10^{5}	0.0858	2.2364×10^{5}
	160	0.7292	2.9517×10^{6}	0.0868	0.1836	0.0853	3.0805×10^{5}	0.0729	2.9517×10^{5}
	180	0.5416	3.7698×10^{6}	0.0650	0.1613	0.0607	3.9654×10^{5}	0.0542	3.7698×10^{5}
	200	0.5050	4.8438×10^{6}	0.0650	0.1479	0.0543	5.1095×10^{5}	0.0505	4.8438×10^{5}
	220	0.4259	5.4672×10^{6}	0.0606	0.1182	0.0453	5.6970×10^{5}	0.0426	5.4672×10^{5}
UNIFAC	100	0.4677	2.1152×10^{5}	0.0619	0.0505	0.0610	2.7328×10^{4}	0.0468	2.1152×10^{4}
	120	0.3806	2.4291×10^{5}	0.0483	0.0327	0.0473	3.4376×10^{4}	0.0381	2.4291×10^{4}
	140	0.3046	4.0976×10^{5}	0.0410	0.0352	0.0345	4.9839×10^{4}	0.0305	4.0976×10^{4}
	160	0.3248	4.4699×10^{5}	0.0444	0.0240	0.0367	5.6541×10^{4}	0.0325	4.4699×10^{4}
	180	0.3759	3.1323×10^{5}	0.0544	0.0125	0.0431	3.6803×10^{4}	0.0376	3.1323×10^{4}
	200	0.4383	7.5530×10^{5}	0.0603	0.0231	0.0530	8.4609×10^{4}	0.0438	7.5530×10^{4}
	220	0.4993	1.7306×10^{6}	0.0587	0.0365	0.0610	2.3085×10^{5}	0.0499	1.7306×10^{5}
UNIFAC Literature	100	0.4513	2.0327×10^{5}	0.0688	0.0486	0.0484	2.6469×10^{4}	0.0451	2.0327×10^{4}
	120	0.5000	4.4125×10^{5}	0.0703	0.0612	0.0540	5.5932×10^{4}	0.0500	4.4125×10^{4}
	140	0.5761	9.0361×10^{5}	0.0736	0.0762	0.0683	1.1358×10^{5}	0.0576	9.0361×10^{4}

	160	0.6662	1.5439×10^{6}	0.0758	0.0845	0.0813	1.8998×10^{5}	0.0666	1.5439×10^{5}
	180	0.8321	2.7740×10^{6}	0.0902	0.1017	0.1029	3.4012×10^{5}	0.0832	2.7740×10^{5}
	200	0.9172	4.1149×10^{6}	0.0958	0.1044	0.1131	5.1535×10^{5}	0.0917	4.1149×10^{5}
	220	0.9015	6.0181×10^{6}	0.0836	0.1092	0.1177	7.5442×10^{5}	0.0902	6.0181×10^{5}
COSMO-SAC	100	0.3528	3.4891×10^{5}	0.0460	0.0909	0.0454	3.6337×10^{4}	0.0353	3.4891×10^{4}
	120	0.2042	4.7376×10^{5}	0.0261	0.0737	0.0268	5.0308×10^{4}	0.0204	4.7376×10^{4}
	140	0.2001	6.9836×10^{5}	0.0250	0.0688	0.0248	7.7184×10^{4}	0.0200	6.9836×10^{4}
	160	0.2107	9.9261×10^{5}	0.0204	0.0629	0.0320	1.0420×10^{5}	0.0211	9.9261×10^{4}
	180	0.3290	1.4403×10^{6}	0.0266	0.0581	0.0532	1.5346×10^{5}	0.0329	1.4403×10^{5}
	200	0.4775	2.2012×10^{6}	0.0406	0.0617	0.0671	2.3817×10^{5}	0.0477	2.2012×10^{5}
	220	0.5241	2.9811×10^{6}	0.0378	0.0568	0.0792	3.2988×10^{5}	0.0524	2.9811×10^{5}
F-SAC	100	0.2848	1.1391×10^{5}	0.0431	0.0288	0.0294	1.1929×10^{4}	0.0285	1.1391×10^{4}
	120	0.2202	1.8551×10^{5}	0.0324	0.0267	0.0232	2.1079×10^{4}	0.0220	1.8551×10^{4}
	140	0.2324	4.0207×10^{5}	0.0285	0.0361	0.0296	4.5190×10^{4}	0.0232	4.0207×10^{4}
	160	0.2854	6.3397×10^{5}	0.0299	0.0371	0.0381	7.1217×10^{4}	0.0285	6.3397×10^{4}
	180	0.4453	1.1068×10^{6}	0.0461	0.0418	0.0569	1.2930×10^{5}	0.0445	1.1068×10^{5}
	200	0.5177	1.8003×10^{6}	0.0527	0.0496	0.0655	2.0445×10^{5}	0.0518	1.8003×10^{5}
	220	0.5278	2.6699×10^{6}	0.0463	0.0517	0.0725	3.0754×10^{5}	0.0528	2.6699×10^{5}

Table B.5. Acetone + Water system results.

	Temperature (°C)	Residual y	Residual P [Pa]	AR y	AR P	RMSD y	RMSD P [Pa]	AAD y	AAD P [Pa]
Wilson	100	0.7988	5.0804×10^{5}	0.0489	0.0612	0.0406	3.0572×10^{4}	0.0363	2.3093×10^{4}
	150	0.6093	6.9266×10^{5}	0.0419	0.0365	0.0420	5.8586×10^{4}	0.0358	4.0745×10^{4}
	200	0.9652	2.7517×10^{6}	0.0541	0.0413	0.0440	1.4110×10^{5}	0.0386	1.1007×10^{5}
	250	0.3170	1.1806×10^{6}	0.2097	0.0250	0.0572	1.7501×10^{5}	0.0396	1.4757×10^{5}
Wilson Literature	100	3.8965	2.6129×10^{6}	0.2229	0.3846	0.2157	1.4351×10^{5}	0.1771	1.1877×10^{5}
	150	2.8822	5.2789×10^{6}	0.2013	0.2823	0.1939	3.8859×10^{5}	0.1695	3.1052×10^{5}
	200	4.2345	2.0922×10^{7}	0.2257	0.3189	0.1976	1.0390×10^{6}	0.1694	8.3688×10^{5}
	250	0.7497	1.8784×10^{7}	0.3902	0.5007	0.1162	2.9166×10^{6}	0.0937	2.3480×10^{6}
NRTL	100	1.2263	5.4618×10^{5}	0.0577	0.0823	0.0656	3.0101×10^{4}	0.0557	2.4827×10^{4}
	150	0.1334	3.5585×10^{5}	0.0078	0.0179	0.0126	2.3535×10^{4}	0.0078	2.0933×10^{4}
	200	0.4475	1.5418×10^{6}	0.0224	0.0197	0.0216	8.4576×10^{4}	0.0179	6.1672×10^{4}
	250	0.3825	9.9602×10^{5}	0.2123	0.0224	0.0566	1.4397×10^{5}	0.0478	1.2450×10^{5}
NRTL Literature	100	1.5851	5.1409×10^{5}	0.0613	0.0812	0.0982	3.0505×10^{4}	0.0721	2.3368×10^{4}
	150	0.2422	4.3767×10^{5}	0.0105	0.0191	0.0278	4.1664×10^{4}	0.0142	2.5745×10^{4}
	200	0.6734	2.7784×10^{6}	0.0286	0.0361	0.0380	1.4886×10^{5}	0.0269	1.1114×10^{5}

	250	0.4828	9.2799×10^{5}	0.2253	0.0216	0.0662	1.3693×10^{5}	0.0604	1.1600×10^{5}
UNIQUAC	100	0.9617	5.7909×10^{5}	0.0546	0.0807	0.0462	2.9166×10^{4}	0.0437	2.6322×10^{4}
	150	0.1148	2.0897×10^{5}	0.0072	0.0111	0.0095	1.3607×10^{4}	0.0068	1.2292×10^{4}
	200	0.4105	1.3454×10^{6}	0.0218	0.0173	0.0189	7.1032×10^{4}	0.0164	5.3815×10^{4}
	250	0.3768	1.0332×10^{6}	0.2038	0.0238	0.0547	1.4705×10^{5}	0.0471	1.2915×10^{5}
UNIQUAC Literature	100	1.8148	1.6359×10^{6}	0.1019	0.2359	0.0988	8.7793×10^{4}	0.0825	7.4358×10^{4}
	150	1.1488	2.3409×10^{6}	0.0759	0.1250	0.0863	1.6652×10^{5}	0.0676	1.3770×10^{5}
	200	1.1435	7.1398×10^{6}	0.0549	0.1092	0.0570	3.4234×10^{5}	0.0457	2.8559×10^{5}
	250	0.1772	6.3408×10^{6}	0.0676	0.1648	0.0316	9.1780×10^{5}	0.0221	7.9260×10^{5}
UNIFAC	100	1.0483	4.9544×10^{5}	0.0571	0.0686	0.0511	2.4956×10^{4}	0.0477	2.2520×10^{4}
	150	0.1105	1.7271×10^{5}	0.0071	0.0088	0.0097	1.1498×10^{4}	0.0065	1.0159×10^{4}
	200	0.4169	1.3809×10^{6}	0.0217	0.0177	0.0193	7.3760×10^{4}	0.0167	5.5238×10^{4}
	250	0.3719	1.0647×10^{6}	0.1974	0.0249	0.0533	1.5130×10^{5}	0.0465	1.3308×10^{5}
UNIFAC Literature	100	1.6758	4.2149×10^{5}	0.0776	0.0583	0.0929	2.2658×10^{4}	0.0762	1.9159×10^{4}
	150	1.0041	2.4304×10^{6}	0.0716	0.1286	0.0675	1.5549×10^{5}	0.0591	1.4297×10^{5}
	200	1.9566	1.1755×10^{7}	0.1025	0.1733	0.0907	5.0824×10^{5}	0.0783	4.7021×10^{5}
	250	0.9764	6.0863×10^{6}	0.4668	0.1609	0.1351	9.5596×10^{5}	0.1221	7.6079×10^{5}
COSMO-SAC	100	0.8494	6.9704×10^{5}	0.0557	0.0892	0.0489	4.1532×10^{4}	0.0386	3.1684×10^{4}
	150	0.4327	7.0510×10^{5}	0.0317	0.0382	0.0295	4.3294×10^{4}	0.0255	4.1476×10^{4}
	200	0.8542	4.1758×10^{6}	0.0512	0.0623	0.0382	1.7189×10^{5}	0.0342	1.6703×10^{5}
	250	0.5303	1.1207×10^{6}	0.2799	0.0274	0.0753	1.5575×10^{5}	0.0663	1.4009×10^{5}
F-SAC	100	1.9616	4.3663×10^{5}	0.0758	0.0579	0.1229	3.4076×10^{4}	0.0892	1.9847×10^{4}
	150	0.9131	1.8831×10^{6}	0.0539	0.0913	0.0747	1.4764×10^{5}	0.0537	1.1077×10^{5}
	200	1.6981	8.7298×10^{6}	0.0727	0.1207	0.0910	4.2592×10^{5}	0.0679	3.4919×10^{5}
	250	0.8755	4.6344×10^{6}	0.3415	0.1163	0.1212	7.0891×10^{5}	0.1094	5.7930×10^{5}

Table B.6. Ethanol + Water system results.

	Temperature (°C)	Residual y	Residual P [Pa]	AR y	AR P	RMSD y	RMSD P [Pa]	AAD y	AAD P [Pa]
Wilson	150	0.9840	2.3070×10^{6}	0.0778	0.1512	0.0611	1.5558×10^{5}	0.0578	1.3570×10^{5}
	200	1.4300	6.7545×10^{6}	0.1339	0.1514	0.0865	4.3839×10^{5}	0.0841	3.9732×10^{5}
	250	2.1410	1.1353×10^{7}	0.2217	0.1076	0.1287	7.3352×10^{5}	0.1259	6.6781×10^{5}
	275	2.2807	7.1709×10^{6}	0.4696	0.0633	0.1801	6.3667×10^{5}	0.1754	5.5161×10^{5}
	300	1.8575	3.7954×10^{6}	0.8885	0.0348	0.2179	5.7364×10^{5}	0.2063	4.2172×10^{5}
	325	1.6541	5.8064×10^{6}	1.7646	0.0526	0.2515	1.2548×10^{6}	0.2363	8.2949×10^{5}
	350	0.8231	1.2907×10^{7}	3.5280	0.1747	0.2249	3.4593×10^{6}	0.2057	3.2267×10^{6}
Wilson Literature	150	1.3192	2.1192×10^{6}	0.1290	0.1521	0.0929	1.3884×10^{5}	0.0775	1.2466×10^{5}
	200	1.3157	6.3994×10^{6}	0.1716	0.1625	0.1011	4.5326×10^{5}	0.0773	3.7643×10^{5}
	250	2.2240	2.3291×10^{7}	0.2878	0.2323	0.1494	1.4943×10^{6}	0.1308	1.3701×10^{6}

	275	2.1428	2.9480×10^{7}	0.5104	0.2741	0.1886	2.4360×10^{6}	0.1648	2.2677×10^{6}
	300	1.3818	2.7093×10^{7}	0.7490	0.2763	0.1832	3.1448×10^{6}	0.1535	3.0103×10^{6}
	325	1.0642	2.8923×10^{7}	1.2110	0.2894	0.1727	4.1758×10^{6}	0.1520	4.1319×10^{6}
	350	0.4560	2.3767×10^{7}	2.0296	0.3269	0.1311	5.9442×10^{6}	0.1140	5.9417×10^{6}
NRTL	150	0.8527	6.7561×10^{5}	0.0642	0.0436	0.0600	4.8933×10^{4}	0.0501	3.9742×10^{4}
	200	0.7099	2.5923×10^{6}	0.0631	0.0562	0.0520	1.9522×10^{5}	0.0417	1.5249×10^{5}
	250	1.1432	4.7520×10^{6}	0.0825	0.0384	0.0918	4.4000×10^{5}	0.0672	2.7953×10^{5}
	275	1.7260	2.9657×10^{6}	0.2928	0.0207	0.1419	4.6638×10^{5}	0.1327	2.2813×10^{5}
	300	1.7058	3.9922×10^{6}	0.6503	0.0370	0.1947	5.5841×10^{5}	0.1895	4.4358×10^{5}
	325	1.7418	3.1989×10^{6}	1.5343	0.0327	0.2502	5.5792×10^{5}	0.2488	4.5699×10^{5}
	350	1.2473	2.6931×10^{6}	4.5522	0.0364	0.3124	8.4474×10^{5}	0.3118	6.7327×10^{5}
NRTL Literature	150	0.2260	3.3281×10^{5}	0.0176	0.0243	0.0172	2.6587×10^{4}	0.0132	1.9577×10^{4}
	200	0.2271	1.1884×10^{6}	0.0246	0.0283	0.0156	8.1844×10^{4}	0.0133	6.9907×10^{4}
	250	0.7275	3.7006×10^{6}	0.0697	0.0365	0.0510	2.5166×10^{5}	0.0427	2.1768×10^{5}
	275	1.2685	7.8743×10^{6}	0.2753	0.0690	0.1033	6.1848×10^{5}	0.0975	6.0571×10^{5}
	300	1.1625	1.2086×10^{7}	0.5973	0.1164	0.1440	1.3691×10^{6}	0.1291	1.3429×10^{6}
	325	1.0842	1.8159×10^{7}	1.2149	0.1775	0.1723	2.6287×10^{6}	0.1548	2.5942×10^{6}
	350	0.4983	2.0015×10^{7}	2.2137	0.2740	0.1426	5.0288×10^{6}	0.1245	5.0037×10^{6}
UNIQUAC	150	0.9186	9.6476×10^{5}	0.0592	0.0590	0.0709	8.2938×10^{4}	0.0540	5.6750×10^{4}
	200	1.1469	4.6526×10^{6}	0.0813	0.0961	0.0877	3.4775×10^{5}	0.0674	2.7368×10^{5}
	250	0.9259	7.8111×10^{6}	0.0474	0.0691	0.0868	5.4411×10^{5}	0.0544	4.5948×10^{5}
	275	1.3698	6.4874×10^{6}	0.2041	0.0564	0.1220	5.8887×10^{5}	0.1053	4.9903×10^{5}
	300	1.6089	4.9795×10^{6}	0.6362	0.0475	0.1850	6.0118×10^{5}	0.1787	5.5328×10^{5}
	325	1.7390	3.5127×10^{6}	1.6812	0.0326	0.2535	8.0864×10^{5}	0.2484	5.0182×10^{5}
	350	1.0917	6.7769×10^{6}	4.4035	0.0902	0.2836	2.1799×10^{6}	0.2729	1.6942×10^{6}
UNIQUAC Literature	150	0.4046	7.3091×10^{5}	0.0240	0.0515	0.0343	4.6434×10^{4}	0.0238	4.2995×10^{4}
	200	0.2189	1.3307×10^{6}	0.0136	0.0338	0.0179	9.8689×10^{4}	0.0128	7.8277×10^{4}
	250	0.5679	7.9646×10^{6}	0.0639	0.0784	0.0364	4.9572×10^{5}	0.0334	4.6850×10^{5}
	275	1.0327	1.2288×10^{7}	0.2284	0.1106	0.0847	9.5950×10^{5}	0.0794	9.4524×10^{5}
	300	0.9879	1.5038×10^{7}	0.5065	0.1479	0.1223	1.6734×10^{6}	0.1097	1.6709×10^{6}
	325	0.9770	1.9929×10^{7}	1.0846	0.1961	0.1538	2.8552×10^{6}	0.1395	2.8470×10^{6}
	350	0.4828	2.0237×10^{7}	2.1280	0.2773	0.1367	5.0761×10^{6}	0.1207	5.0593×10^{6}
UNIFAC	150	1.1013	1.6067×10^{6}	0.0869	0.1132	0.0715	1.0215×10^{5}	0.0647	9.4509×10^{4}
	200	0.2260	1.2810×10^{6}	0.0275	0.0309	0.0166	9.0175×10^{4}	0.0132	7.5355×10^{4}
	250	1.0402	1.4491×10^{6}	0.0999	0.0129	0.0639	1.0702×10^{5}	0.0611	8.5243×10^{4}
	275	1.5920	2.0565×10^{6}	0.3143	0.0163	0.1256	2.1523×10^{5}	0.1224	1.5819×10^{5}
	300	1.6418	3.5732×10^{6}	0.7654	0.0322	0.1906	5.8171×10^{5}	0.1824	3.9702×10^{5}
	325	1.6930	6.1341×10^{6}	1.7828	0.0567	0.2553	1.2361×10^{6}	0.2418	8.7630×10^{5}
	350	0.9454	1.0421×10^{7}	4.0139	0.1399	0.2558	3.0308×10^{6}	0.2363	2.6052×10^{6}
UNIFAC Literature	150	0.6055	1.3599×10^{6}	0.0504	0.0890	0.0391	8.6683×10^{4}	0.0356	7.9992×10^{4}
	200	1.0264	5.7037×10^{6}	0.0861	0.1280	0.0694	3.6138×10^{5}	0.0603	3.3551×10^{5}

	250	1.3865	8.7671×10^{6}	0.1099	0.0786	0.0974	6.0246×10^{5}	0.0815	5.1571×10^{5}
	275	1.7857	8.0298×10^{6}	0.3227	0.0697	0.1449	6.8511×10^{5}	0.1373	6.1768×10^{5}
	300	1.8288	6.6263×10^{6}	0.8200	0.0650	0.2105	7.8990×10^{5}	0.2032	7.3626×10^{5}
	325	1.8212	6.5583×10^{6}	1.8905	0.0626	0.2724	1.1999×10^{6}	0.2601	9.3690×10^{5}
	350	0.9933	9.2111×10^{6}	4.1904	0.1230	0.2671	2.8251×10^{6}	0.2483	2.3028×10^{6}
COSMO-SAC	150	0.3084	4.8923×10^{5}	0.0238	0.0347	0.0222	3.5324×10^{5}	0.0181	2.8778×10^{4}
	200	0.3119	1.9452×10^{6}	0.0260	0.0432	0.0217	1.2679×10^{5}	0.0183	1.1442×10^{5}
	250	0.7695	3.5369×10^{6}	0.0581	0.0354	0.0553	2.5183×10^{5}	0.0452	2.0806×10^{5}
	275	1.3168	4.1620×10^{6}	0.2519	0.0384	0.1042	3.9548×10^{5}	0.1012	3.2015×10^{5}
	300	1.3658	6.9026×10^{6}	0.6330	0.0660	0.1582	8.1511×10^{5}	0.1517	7.6695×10^{5}
	325	1.3851	1.1292×10^{7}	1.4605	0.1087	0.2090	1.7191×10^{6}	0.1978	1.6131×10^{6}
	350	0.7454	1.5058×10^{7}	3.1800	0.2049	0.2027	3.8778×10^{6}	0.1863	3.7645×10^{6}
F-SAC	150	0.2043	3.5686×10^{5}	0.0169	0.0255	0.0143	2.8055×10^{4}	0.0120	2.0991×10^{4}
	200	0.2158	1.5353×10^{6}	0.0222	0.0352	0.0139	9.9927×10^{4}	0.0127	9.0311×10^{4}
	250	0.7043	3.6605×10^{6}	0.0619	0.0381	0.0476	2.8347×10^{5}	0.0414	2.1532×10^{5}
	275	1.2051	7.6934×10^{6}	0.2476	0.0692	0.0958	6.1622×10^{5}	0.0927	5.9180×10^{5}
	300	1.1745	1.1206×10^{7}	0.5753	0.1089	0.1400	1.2563×10^{6}	0.1305	1.2451×10^{6}
	325	1.1492	1.6497×10^{7}	1.2508	0.1612	0.1776	2.3886×10^{6}	0.1642	2.3567×10^{6}
	350	0.5631	1.8701×10^{7}	2.4542	0.2558	0.1574	4.7135×10^{6}	0.1408	4.6753×10^{6}

Table B.7. Butane + Methanol system results.

	Temperature (°C)	Residual y	Residual P [Pa]	AR y	AR P	RMSD y	RMSD P [Pa]	AAD y	AAD P [Pa]
Wilson	0	0.3951	1.2329×10^{5}	0.0429	0.1532	0.0572	1.7639×10^{4}	0.0395	1.2329×10^{4}
	50	0.2456	7.3715×10^{4}	0.0275	0.0194	0.0326	9.7177×10^{3}	0.0246	7.3715×10^{3}
	50	0.2530	1.6570×10^{5}	0.0112	0.0130	0.0150	9.2456×10^{3}	0.0097	6.3730×10^{3}
Wilson Literature	0	3.8339	3.6916×10^{5}	0.4703	0.5271	0.5309	4.9430×10^{4}	0.3834	3.6916×10^{4}
	50	2.2993	1.6261×10^{6}	0.2714	0.3858	0.3502	2.1660×10^{5}	0.2299	1.6261×10^{5}
	50	4.2708	6.6571×10^{6}	0.1795	0.5307	0.2724	3.0087×10^{5}	0.1643	2.5604×10^{5}
NRTL	0	0.3293	5.3979×10^{4}	0.0356	0.0894	0.0425	1.0579×10^{4}	0.0329	5.3979×10^{3}
	50	0.1589	2.3766×10^{5}	0.0212	0.0568	0.0194	2.6461×10^{4}	0.0159	2.3766×10^{4}
	50	0.3874	5.3591×10^{5}	0.0174	0.0429	0.0181	2.3547×10^{4}	0.0149	2.0612×10^{4}
NRTL Literature	0	1.5123	2.7382×10^{5}	0.1727	0.3876	0.2093	3.6361×10^{4}	0.1512	2.7382×10^{4}
	50	1.2468	1.1000×10^{6}	0.1406	0.2669	0.1754	1.4327×10^{5}	0.1247	1.1000×10^{5}
	50	2.2359	4.3712×10^{6}	0.0941	0.3483	0.1363	1.9322×10^{5}	0.0860	1.6812×10^{5}
UNIQUAC	0	0.2277	3.8794×10^{4}	0.0256	0.0490	0.0278	5.4158×10^{3}	0.0228	3.8794×10^{3}
	50	0.1424	1.6076×10^{5}	0.0188	0.0371	0.0180	1.8567×10^{4}	0.0142	1.6076×10^{4}

	50	0.3866	3.5411×10^{5}	0.0173	0.0282	0.0168	1.5352×10^{4}	0.0149	1.3620×10^{4}
UNIQUAC Literature	0	1.6671	2.8774×10^{5}	0.1919	0.4107	0.2286	3.8234×10^{4}	0.1667	2.8774×10^{4}
	50	1.3583	1.1693×10^{6}	0.1543	0.2855	0.1910	1.5308×10^{5}	0.1358	1.1693×10^{5}
	50	2.5445	4.7265×10^{6}	0.1073	0.3778	0.1526	2.0926×10^{5}	0.0979	1.8179×10^{5}
UNIFAC	0	0.2071	4.1525×10^{4}	0.0237	0.0509	0.0254	5.7749×10^{3}	0.0207	4.1525×10^{3}
	50	0.1423	1.6094×10^{5}	0.0188	0.0372	0.0180	1.8586×10^{4}	0.0142	1.6094×10^{4}
	50	0.3865	3.5457×10^{5}	0.0173	0.0282	0.0168	1.5371×10^{4}	0.0149	1.3637×10^{4}
UNIFAC Literature	0	0.2955	3.3342×10^{4}	0.0317	0.0494	0.0375	5.5952×10^{3}	0.0295	3.3342×10^{3}
	50	0.2005	1.1204×10^{5}	0.0231	0.0291	0.0271	1.5690×10^{4}	0.0200	1.1204×10^{4}
	50	0.4262	5.0446×10^{5}	0.0187	0.0414	0.0195	2.3590×10^{4}	0.0164	1.9402×10^{4}
COSMO-SAC	0	0.2832	9.0693×10^{4}	0.0337	0.1088	0.0322	1.3164×10^{4}	0.0283	9.0693×10^{3}
	50	0.2616	2.8882×10^{5}	0.0295	0.0601	0.0317	4.2611×10^{4}	0.0262	2.8882×10^{4}
	50	0.5333	9.1106×10^{5}	0.0231	0.0680	0.0252	4.2794×10^{4}	0.0205	3.5041×10^{4}
F-SAC	0	0.2537	4.3699×10^{4}	0.0277	0.0635	0.0322	5.9267×10^{3}	0.0254	4.3699×10^{3}
	50	0.1537	9.7049×10^{4}	0.0182	0.0215	0.0216	1.4495×10^{4}	0.0154	9.7049×10^{3}
	50	0.4167	3.6735×10^{5}	0.0184	0.0298	0.0185	1.8669×10^{4}	0.0160	1.4129×10^{4}

Table B.8. Butanol + Decane system results.

	Temperature (°C)	Residual y	Residual P [Pa]	AR y	AR P	RMSD y	RMSD P [Pa]	AAD y	AAD P [Pa]
Wilson	85	0.9390	1.2726×10^{4}	0.0725	0.0222	0.0926	1.6539×10^{3}	0.0671	9.0898×10^{2}
	100	0.9902	2.2539×10^{4}	0.0766	0.0223	0.0981	2.7188×10^{3}	0.0707	1.6099×10^{3}
	115	1.0257	3.9867×10^{4}	0.0791	0.0243	0.1024	4.5452×10^{3}	0.0733	2.8476×10^{3}
Wilson Literature	85	1.0538	3.0841×10^{4}	0.0824	0.0743	0.0985	2.7040×10^{3}	0.0753	2.2029×10^{3}
	100	1.0769	5.7295×10^{4}	0.0840	0.0743	0.1026	4.8587×10^{3}	0.0769	4.0925×10^{3}
	115	1.0921	9.8439×10^{4}	0.0848	0.0732	0.1058	8.1047×10^{3}	0.0780	7.0314×10^{3}
NRTL	85	0.9812	1.1616×10^{4}	0.0747	0.0208	0.1028	1.4489×10^{3}	0.0701	8.2973×10^{2}
	100	0.9965	2.0360×10^{4}	0.0766	0.0212	0.1014	2.5385×10^{3}	0.0712	1.4543×10^{3}
	115	1.0236	3.8699×10^{4}	0.0787	0.0240	0.1038	4.4838×10^{3}	0.0731	2.7642×10^{3}
NRTL Literature	85	1.0127	2.7842×10^{4}	0.0785	0.0659	0.0982	2.4858×10^{3}	0.0723	1.9887×10^{3}
	100	1.0488	5.5265×10^{4}	0.0814	0.0710	0.1024	4.7474×10^{3}	0.0749	3.9475×10^{3}
	115	1.0734	1.0003×10^{5}	0.0831	0.0740	0.1057	8.3201×10^{3}	0.0767	7.1451×10^{3}
UNIQUAC	85	0.9894	1.7021×10^{4}	0.0762	0.0341	0.0983	1.8941×10^{3}	0.0707	1.2158×10^{3}
	100	1.0395	3.0170×10^{4}	0.0801	0.0340	0.1036	3.1179×10^{3}	0.0742	2.1550×10^{3}
	115	1.0706	5.1744×10^{4}	0.0824	0.0351	0.1072	5.1694×10^{3}	0.0765	3.6960×10^{3}
UNIQUAC Literature	85	0.8783	5.3814×10^{4}	0.0713	0.1316	0.0789	5.2998×10^{3}	0.0627	3.8439×10^{3}
	100	0.9795	1.0191×10^{5}	0.0775	0.1321	0.0889	9.8604×10^{3}	0.0700	7.2794×10^{3}
	115	1.0335	1.7756×10^{5}	0.0808	0.1299	0.0970	1.6693×10^{4}	0.0738	1.2683×10^{3}
UNIFAC	85	1.0179	1.7707×10^{4}	0.0781	0.0410	0.1017	1.6692×10^{3}	0.0727	1.2648×10^{3}

	100	1.0511	3.3987×10^{4}	0.0809	0.0436	0.1047	3.1699×10^{3}	0.0751	2.4277×10^{3}
	115	1.0759	6.3359×10^{4}	0.0827	0.0472	0.1075	5.7841×10^{3}	0.0769	4.5256×10^{3}
UNIFAC Literature	85	1.0220	2.1323×10^{4}	0.0785	0.0512	0.1016	1.8850×10^{3}	0.0730	1.5231×10^{3}
	100	1.0534	4.0423×10^{4}	0.0812	0.0531	0.1044	3.5808×10^{3}	0.0752	2.8874×10^{3}
	115	1.0774	7.0813×10^{4}	0.0829	0.0541	0.1072	6.4007×10^{3}	0.0770	5.0581×10^{3}
COSMO-SAC	85	1.0275	3.2599×10^{4}	0.0790	0.0812	0.0992	2.8735×10^{3}	0.0734	2.3285×10^{3}
	100	1.0543	6.2483×10^{4}	0.0812	0.0828	0.1020	5.3713×10^{3}	0.0753	4.4631×10^{3}
	115	1.0775	1.0902×10^{5}	0.0827	0.0823	0.1052	9.0992×10^{3}	0.0770	7.7870×10^{3}
F-SAC	85	1.0217	2.1101×10^{4}	0.0785	0.0501	0.1014	1.8559×10^{3}	0.0730	1.5072×10^{3}
	100	1.0524	4.3116×10^{4}	0.0812	0.0557	0.1038	3.6937×10^{3}	0.0752	3.0797×10^{3}
	115	1.0766	8.0188×10^{4}	0.0829	0.0597	0.1066	6.7250×10^{3}	0.0769	5.7277×10^{3}

Table B.9. Butanol + Hexane system results.

	Temperature (°C)	Residual y	Residual P [Pa]	AR y	AR P	RMSD y	RMSD P [Pa]	AAD y	AAD P [Pa]
Wilson	25	0.1921	4.3180×10^{3}	0.0107	0.0127	0.0131	3.6102×10^{2}	0.0113	2.5400×10^{2}
	50	0.3089	2.6135×10^{3}	0.1975	0.0040	0.0237	2.8060×10^{2}	0.0221	1.8668×10^{2}
Wilson Literature	25	1.1272	5.9275×10^{4}	0.1190	0.1919	0.1159	4.2111×10^{3}	0.0663	3.4868×10^{3}
	50	0.5618	1.6147×10^{5}	0.7265	0.2293	0.0691	1.2673×10^{4}	0.0401	1.1534×10^{4}
NRTL	25	0.2122	1.3309×10^{4}	0.0238	0.0407	0.0237	9.6830×10^{2}	0.0125	7.8289×10^{2}
	50	0.0563	1.1874×10^{4}	0.0623	0.0175	0.0057	1.1354×10^{3}	0.0040	8.4811×10^{2}
NRTL Literature	25	0.8637	6.4185×10^{4}	0.0886	0.2230	0.0857	4.3065×10^{3}	0.0508	3.7756×10^{3}
	50	0.5020	1.8946×10^{5}	0.6084	0.2768	0.0563	1.4165×10^{4}	0.0359	1.3533×10^{4}
UNIQUAC	25	0.1711	1.0956×10^{4}	0.0195	0.0336	0.0187	7.7680×10^{2}	0.0101	6.4444×10^{2}
	50	0.0453	8.9690×10^{3}	0.0454	0.0133	0.0041	8.5593×10^{2}	0.0032	6.4064×10^{2}
UNIQUAC Literature	25	0.4445	4.9020×10^{4}	0.0429	0.1779	0.0405	3.2600×10^{3}	0.0261	2.8835×10^{3}
	50	0.3305	1.4964E+05	0.3488	0.2218	0.0307	1.1100×10^{4}	0.0236	1.0688×10^{4}
UNIFAC	25	0.1176	7.3233×10^{3}	0.0136	0.0220	0.0127	5.3078×10^{2}	0.0069	4.3079×10^{2}
	50	0.0276	4.5951×10^{3}	0.0227	0.0070	0.0021	4.4346×10^{2}	0.0020	3.2822×10^{2}
UNIFAC Literature	25	0.1185	7.5411×10^{3}	0.0136	0.0233	0.0126	5.3136×10^{2}	0.0070	4.4359×10^{2}
	50	0.0214	6.4813×10^{3}	0.0189	0.0099	0.0017	5.8787×10^{2}	0.0015	4.6295×10^{2}
COSMO-SAC	25	0.1550	1.0650×10^{4}	0.0181	0.0321	0.0172	7.8054×10^{2}	0.0091	6.2645×10^{2}
	50	0.0644	2.8234×10^{4}	0.0691	0.0402	0.0064	2.1692×10^{3}	0.0046	2.0167×10^{3}
F-SAC	25	3.9485	3.9183×10^{4}	0.3172	0.1311	0.3122	2.7060×10^{3}	0.2323	2.3049×10^{3}
	50	4.1814	5.4731×10^{4}	3.7280	0.0785	0.3181	4.3599×10^{3}	0.2987	3.9094×10^{3}

Table B.10. Heptane + 1-Pentanol system results.

	Temperature (°C)	Residual y	Residual P [Pa]	AR y	AR P	RMSD y	RMSD P [Pa]	AAD y	AAD P [Pa]

Wilson	75	0.6603	1.7025×10^{4}	0.0366	0.0208	0.0391	9.5886×10^{2}	0.0314	8.1071×10^{2}
	85	0.6655	2.0278×10^{4}	0.0392	0.0203	0.0411	1.2214×10^{3}	0.0333	1.0139×10^{3}
	95	0.6542	3.2135×10^{4}	0.0390	0.0235	0.0406	2.0413×10^{3}	0.0327	1.6068×10^{3}
Wilson Literature	75	0.5415	1.9124×10^{4}	0.0307	0.0244	0.0317	1.1357×10^{3}	0.0258	9.1068×10^{2}
	85	0.5332	3.3828×10^{4}	0.0331	0.0310	0.0337	2.1411×10^{3}	0.0267	1.6914×10^{3}
	95	0.5140	5.7428×10^{4}	0.0328	0.0375	0.0337	3.7500×10^{3}	0.0257	2.8714×10^{3}
NRTL	75	0.0819	3.0747×10^{3}	0.0028	0.0038	0.0079	1.7114×10^{2}	0.0039	1.4642×10^{2}
	85	0.0609	3.9885×10^{3}	0.0027	0.0034	0.0048	2.4999×10^{2}	0.0030	1.9943×10^{2}
	95	0.0564	4.3850×10^{3}	0.0030	0.0027	0.0037	3.1599×10^{2}	0.0028	2.1925×10^{2}
NRTL Literature	75	0.0865	5.4470×10^{3}	0.0032	0.0073	0.0078	3.2416×10^{2}	0.0041	2.5938×10^{2}
	85	0.0617	6.2714×10^{3}	0.0028	0.0060	0.0048	3.6863×10^{2}	0.0031	3.1357×10^{2}
	95	0.0403	6.3243×10^{3}	0.0017	0.0044	0.0034	3.7354×10^{2}	0.0020	3.1622×10^{2}
UNIQUAC	75	0.1106	1.1645×10^{4}	0.0055	0.0136	0.0074	6.5846×10^{2}	0.0053	5.5453×10^{2}
	85	0.0779	1.1415×10^{4}	0.0043	0.0106	0.0054	6.5738×10^{2}	0.0039	5.7074×10^{2}
	95	0.0639	1.4720×10^{4}	0.0036	0.0100	0.0040	8.6405×10^{2}	0.0032	7.3598×10^{2}
UNIQUAC Literature	75	1.1296	1.1263×10^{5}	0.0557	0.1282	0.0730	6.7932×10^{3}	0.0538	5.3636×10^{3}
	85	1.1248	1.4538×10^{5}	0.0589	0.1267	0.0742	9.1776×10^{3}	0.0562	7.2691×10^{3}
	95	1.1172	1.8999×10^{5}	0.0591	0.1211	0.0722	1.1901×10^{4}	0.0559	9.4997×10^{3}
UNIFAC	75	0.0943	8.4041×10^{3}	0.0042	0.0084	0.0074	5.0384×10^{2}	0.0045	4.0020×10^{2}
	85	0.0678	8.0251×10^{3}	0.0033	0.0064	0.0056	4.7119×10^{2}	0.0034	4.0126×10^{2}
	95	0.0726	9.2527×10^{3}	0.0041	0.0056	0.0041	6.5336×10^{2}	0.0036	4.6264×10^{2}
UNIFAC Literature	75	0.1687	1.5302×10^{4}	0.0075	0.0148	0.0145	9.6508×10^{3}	0.0080	7.2866×10^{2}
	85	0.1514	1.5525×10^{4}	0.0066	0.0112	0.0134	1.0768×10^{3}	0.0076	7.7626×10^{2}
	95	0.1359	1.5830×10^{4}	0.0059	0.0079	0.0112	1.1480×10^{3}	0.0068	7.9152×10^{2}
COSMO-SAC	75	0.3197	2.4736×10^{4}	0.0148	0.0234	0.0239	1.7420×10^{3}	0.0152	1.1779×10^{3}
	85	0.3154	3.1331×10^{4}	0.0151	0.0234	0.0237	2.2167×10^{3}	0.0158	1.5665×10^{3}
	95	0.3033	3.9909×10^{4}	0.0147	0.0223	0.0217	2.6697×10^{3}	0.0152	1.9954×10^{3}
F-SAC	75	0.0590	4.2079×10^{3}	0.0025	0.0045	0.0047	3.0851×10^{2}	0.0028	2.0038×10^{2}
	85	0.0386	5.3528×10^{3}	0.0022	0.0049	0.0025	4.1694×10^{2}	0.0019	2.6764×10^{2}
	95	0.0484	8.4250×10^{3}	0.0031	0.0058	0.0028	6.0116×10^{2}	0.0024	4.2125×10^{2}

Table B.11. Pentane + Methanol system results.

	Temperature (°C)	Residual y	Residual P [Pa]	AR y	AR P	RMSD y	RMSD P [Pa]	AAD y	AAD P [Pa]
Wilson	99.55	0.4096	4.2014×10^{5}	0.0513	0.0514	0.0447	4.5280×10^{4}	0.0372	3.8195×10^{4}
	124.55	0.2179	6.4381×10^{5}	0.0295	0.0457	0.0244	6.8343×10^{4}	0.0198	5.8529×10^{4}
	149.45	0.2083	1.1485×10^{6}	0.0291	0.0507	0.0235	1.2018×10^{5}	0.0189	1.0441×10^{5}
Wilson Literature	99.55	2.2103	3.4705×10^{6}	0.2960	0.4755	0.2355	3.7126×10^{5}	0.2009	3.1550×10^{5}
	124.55	1.9416	6.4112×10^{6}	0.2541	0.4886	0.2113	6.8790×10^{5}	0.1765	5.8284×10^{5}

	149.45	1.9131	1.0645×10^{7}	0.2744	0.4890	0.2044	1.1287×10^{6}	0.1739	9.6777×10^{5}
NRTL	99.55	0.3599	2.5701×10^{5}	0.0473	0.0307	0.0414	3.2019×10^{4}	0.0327	2.3364×10^{4}
	124.55	0.4330	3.0162×10^{5}	0.0552	0.0202	0.0473	2.9784×10^{4}	0.0394	2.7420×10^{4}
	149.45	0.5896	4.2957×10^{5}	0.0846	0.0174	0.0644	4.8899×10^{4}	0.0536	3.9052×10^{4}
NRTL Literature	99.55	1.7953	2.7422×10^{6}	0.2343	0.3743	0.1988	2.8721×10^{5}	0.1632	2.4929×10^{5}
	124.55	1.5277	4.7899×10^{6}	0.1943	0.3637	0.1712	5.0258×10^{5}	0.1389	4.3545×10^{5}
	149.45	1.2213	7.6725×10^{6}	0.1662	0.3510	0.1332	7.9725×10^{5}	0.1110	6.9750×10^{5}
UNIQUAC	99.55	0.2778	1.9737×10^{5}	0.0361	0.0225	0.0303	2.1743×10^{4}	0.0253	1.7943×10^{4}
	124.55	0.4234	1.9275×10^{5}	0.0552	0.0127	0.0460	2.2788×10^{4}	0.0385	1.7523×10^{4}
	149.45	0.6267	5.1994×10^{5}	0.0885	0.0214	0.0691	5.4219×10^{4}	0.0570	4.7267×10^{4}
UNIQUAC Literature	99.55	1.9919	2.9201×10^{6}	0.2606	0.3994	0.2196	3.0759×10^{5}	0.1811	2.6547×10^{5}
	124.55	1.7243	5.1501×10^{6}	0.2186	0.3917	0.1924	5.4351×10^{5}	0.1568	4.6819×10^{5}
	149.45	1.4090	8.3145×10^{6}	0.1919	0.3812	0.1524	8.6930×10^{5}	0.1281	7.5587×10^{5}
UNIFAC	99.55	0.2597	2.0758×10^{5}	0.0331	0.0236	0.0284	2.3422×10^{4}	0.0236	1.8871×10^{4}
	124.55	0.4138	1.9537×10^{5}	0.0542	0.0129	0.0448	2.2959×10^{4}	0.0376	1.7761×10^{4}
	149.45	0.6318	5.2896×10^{5}	0.0893	0.0217	0.0697	5.5300×10^{4}	0.0574	4.8087×10^{4}
UNIFAC Literature	99.55	0.3534	2.9827×10^{5}	0.0458	0.0363	0.0434	3.5517×10^{4}	0.0321	2.7115×10^{4}
	124.55	0.5203	4.5223×10^{5}	0.0631	0.0304	0.0595	5.7101×10^{4}	0.0473	4.1112×10^{4}
	149.45	0.7382	7.5698×10^{5}	0.0978	0.0299	0.0816	9.0946×10^{4}	0.0671	6.8816×10^{4}
COSMO-SAC	99.55	0.2768	6.8163×10^{5}	0.0313	0.0878	0.0339	6.9286×10^{4}	0.0252	6.1967×10^{4}
	124.55	0.2323	1.0957×10^{6}	0.0365	0.0807	0.0293	1.1310×10^{5}	0.0211	9.9611×10^{4}
	149.45	0.3139	1.6660×10^{6}	0.0491	0.0742	0.0377	1.6964×10^{5}	0.0285	1.5145×10^{5}
F-SAC	99.55	0.2460	1.7247×10^{5}	0.0328	0.0199	0.0281	1.8888×10^{4}	0.0224	1.5679×10^{4}
	124.55	0.3620	2.8845×10^{5}	0.0471	0.0208	0.0416	3.3746×10^{4}	0.0329	2.6223×10^{4}
	149.45	0.5006	7.3590×10^{5}	0.0690	0.0328	0.0565	8.1066×10^{4}	0.0455	6.6900×10^{4}

Appendix C – IDAC Figures

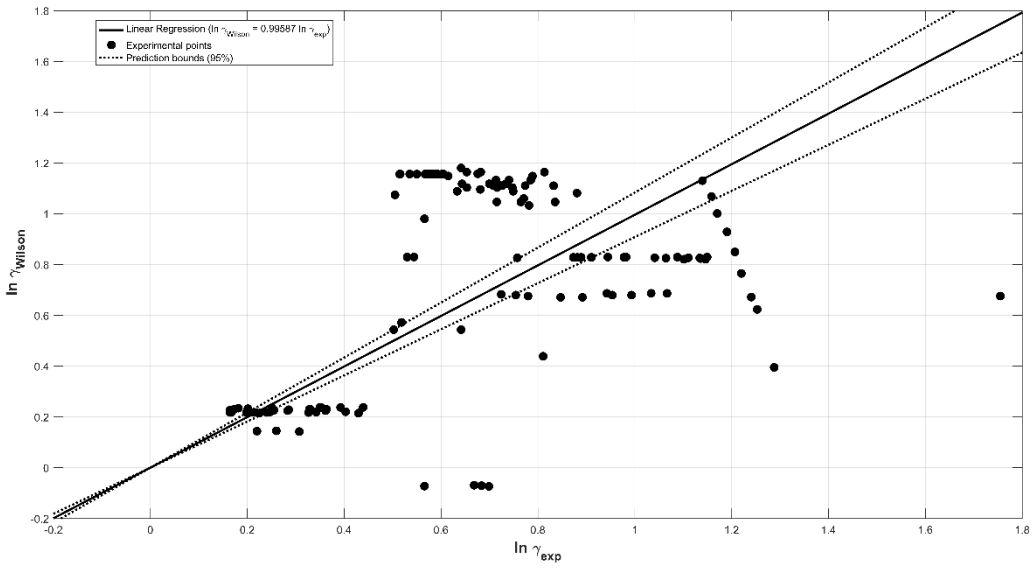

Figure C.1. IDAC predictions of the Wilson model with the estimated parameters vs. experimental IDAC.

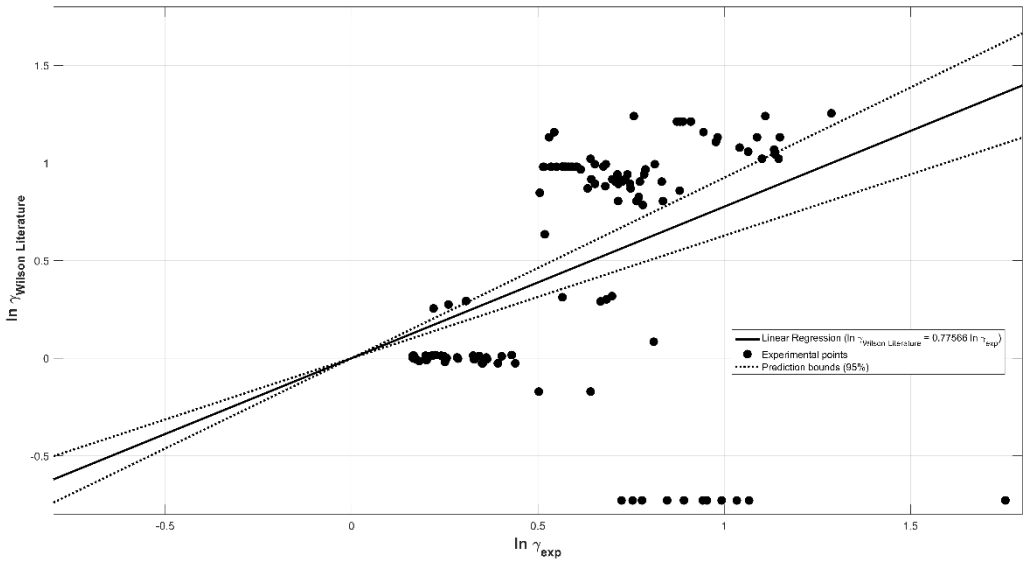

Figure C.2. IDAC predictions of the Wilson model with the literature parameters vs. experimental IDAC.

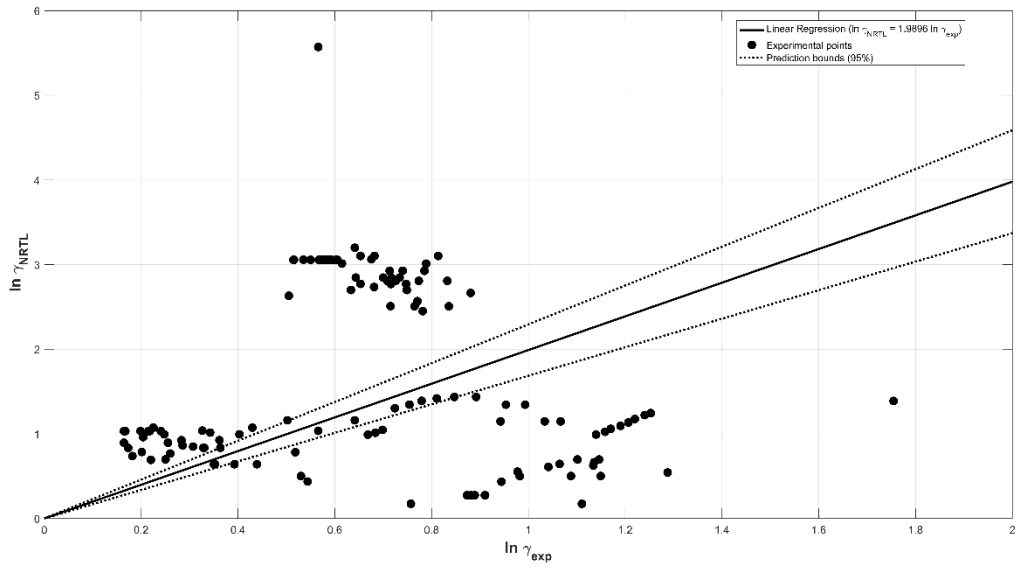

Figure C.3. IDAC predictions of the NRTL model with the estimated parameters vs. experimental IDAC.

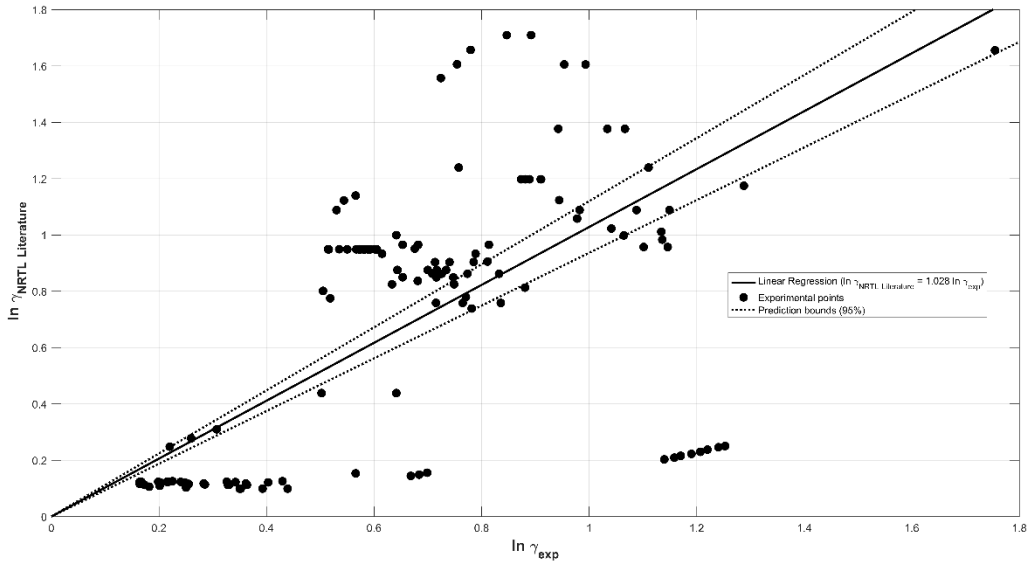

Figure C.4. IDAC predictions of the NRTL model with the literature parameters vs. experimental IDAC.

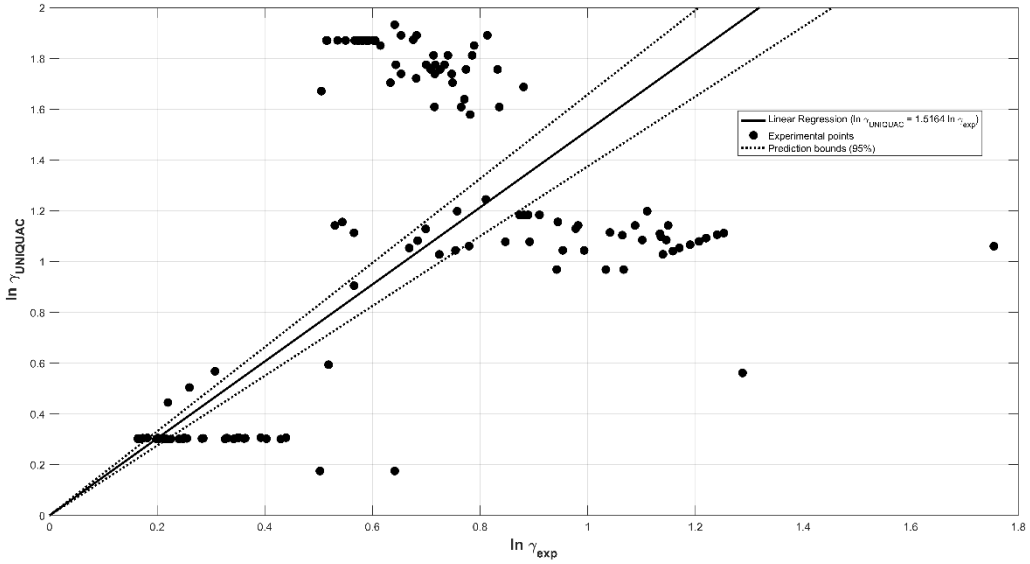

Figure C.5. IDAC predictions of the UNIQUAC model with the estimated parameters vs. experimental IDAC.

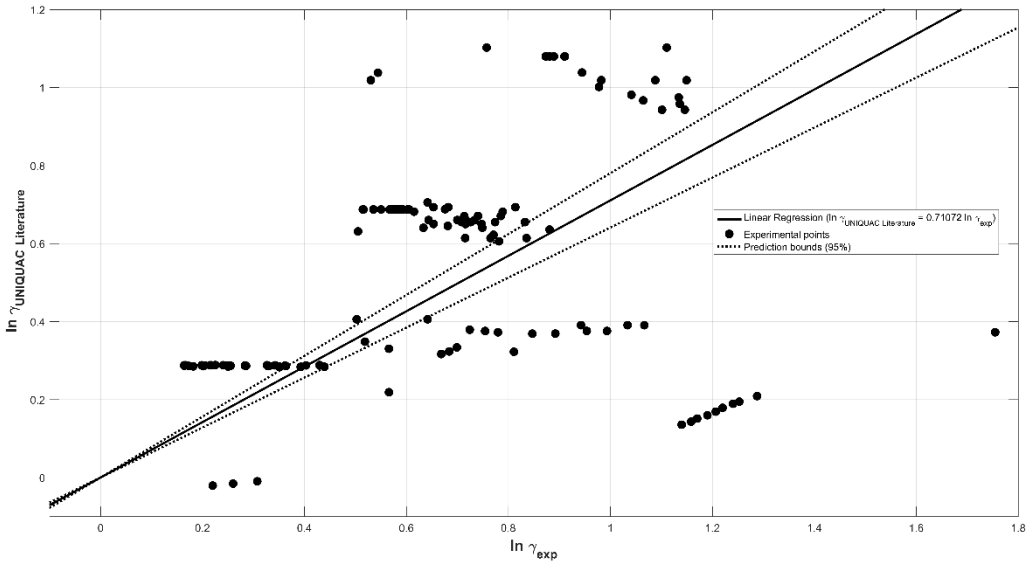

Figure C.6. IDAC predictions of the UNIQUAC model with the literature parameters vs. experimental IDAC.

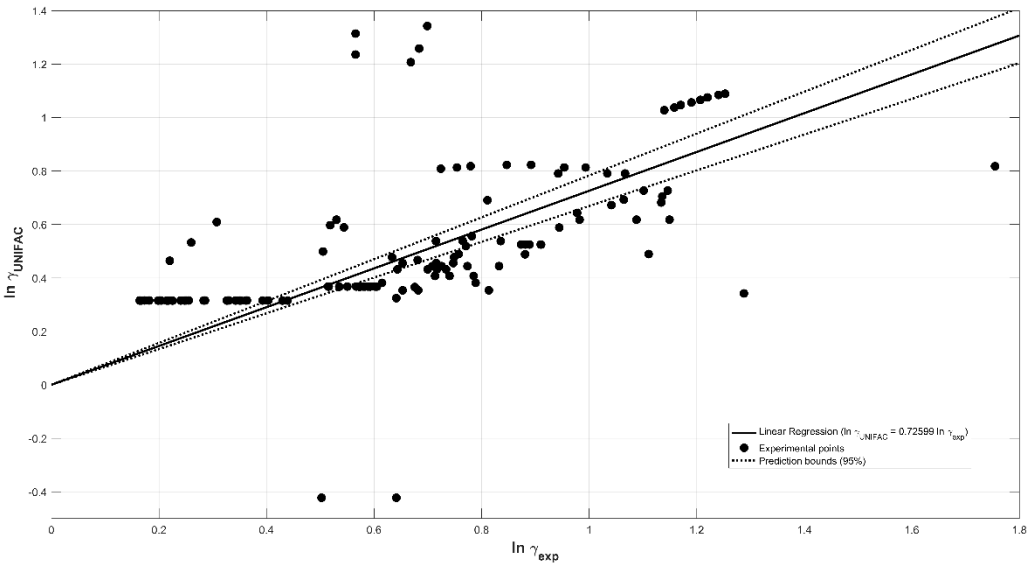

Figure C.7. IDAC predictions of the UNIFAC model with the estimated parameters vs. experimental IDAC.

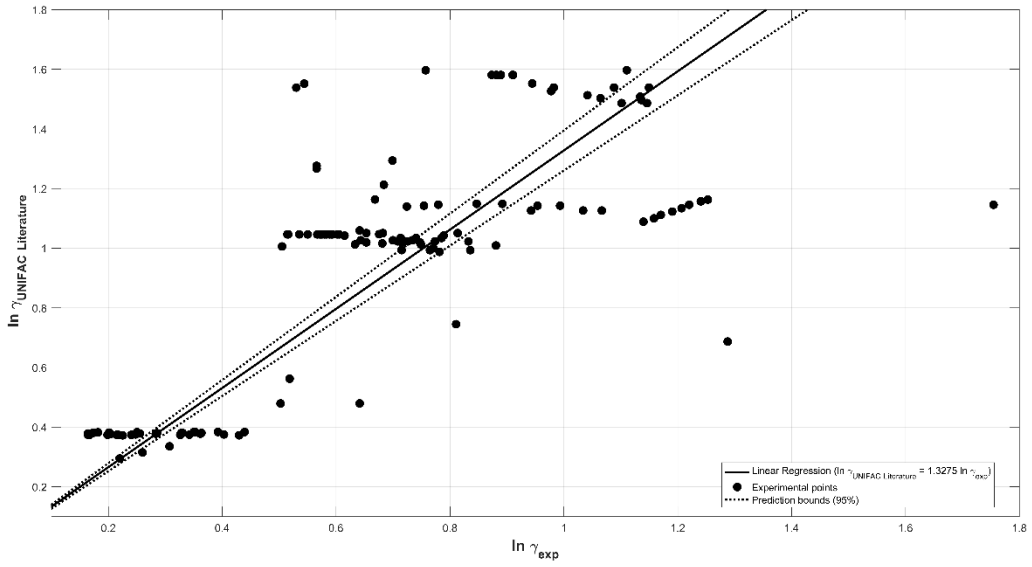

Figure C.8. IDAC predictions of the UNIFAC model with the literature parameters vs. experimental IDAC.

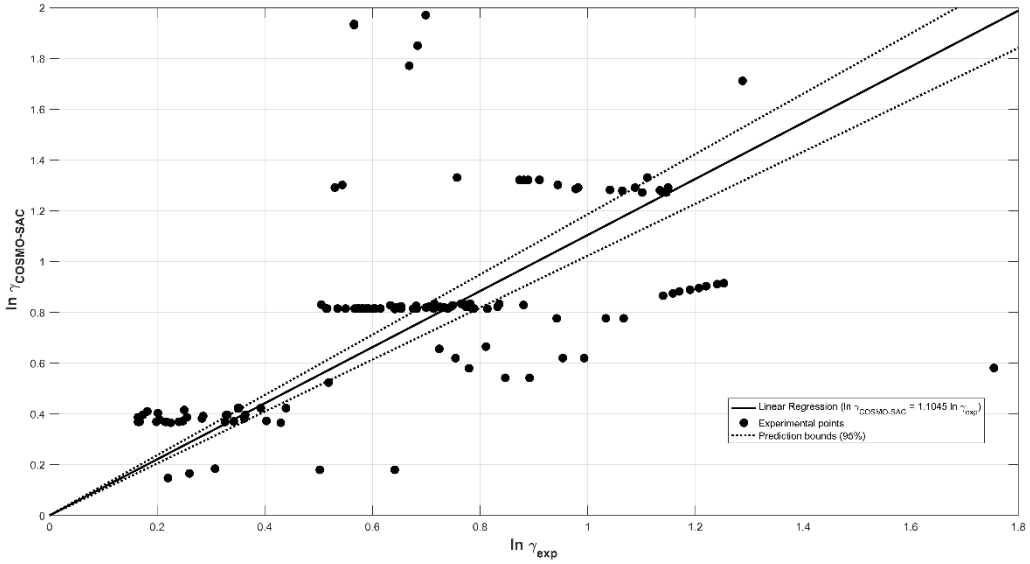

Figure C.9. IDAC predictions of the COSMO-SAC model vs. experimental IDAC.

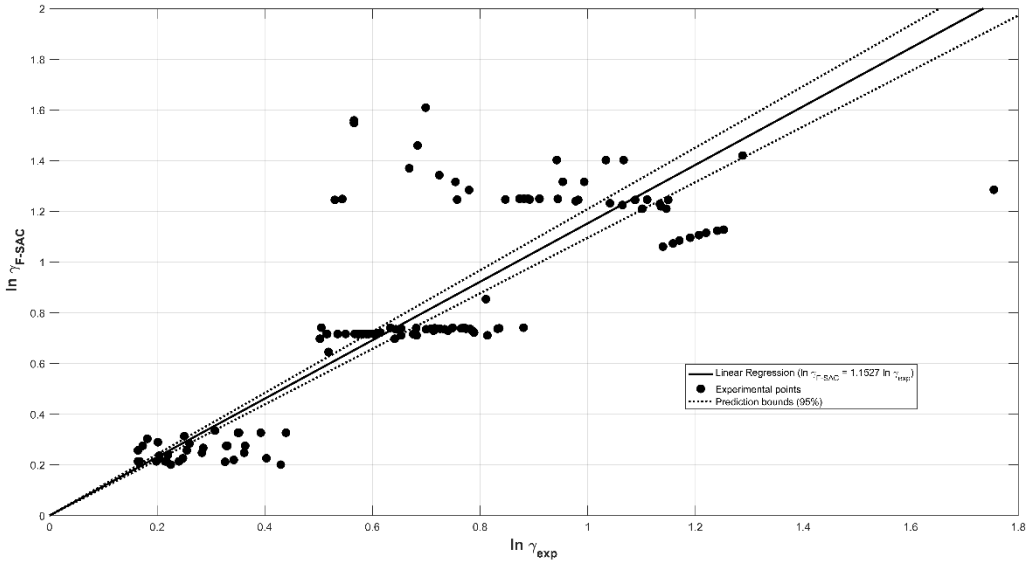

Figure C.10. IDAC predictions of the F-SAC model vs. experimental IDAC.

REFERENCES

1. Fredenslund A, Gmehling J, Michelsen ML, Rasmussen P, Prausnitz JM. Computerized Design of Multicomponent Distillation Columns Using the UNIFAC Group

Contribution Method for Calculation of Activity Coefficients. Ind Eng Chem Process Des Dev. 1977;16(4):450-462. doi:10.1021/i260064a004.

2. Fredenslund A, Jones RL, Prausnitz JM. Group-contribution estimation of activity coefficients in nonideal liquid mixtures. AIChE J. 1975;21(6):1086-1099. doi:10.1002/aic.690210607.

3. Lin S-T, Sandler SI. A Priori Phase Equilibrium Prediction from a Segment Contribution Solvation Model. Ind Eng Chem Res. 2002;41(5):899-913. doi:10.1021/ie001047w.

4. Klamt A. Conductor-like Screening Model for Real Solvents: A New Approach to the Quantitative Calculation of Solvation Phenomena. J Phys Chem. 1995;99(7):2224-2235. doi:10.1021/j100007a062.

5. Gerber RP, Soares RDP. Prediction of infinite-dilution activity coefficients using UNIFAC and COSMO-SAC variants. Ind Eng Chem Res. 2010;49(16):7488-7496. doi:10.1021/ie901947m.

6. Hsieh CM, Sandler SI, Lin ST. Improvements of COSMO-SAC for vapor-liquid and liquid-liquid equilibrium predictions. Fluid Phase Equilib. 2010;297(1):90-97. doi:10.1016/j.fluid.2010.06.011.

7. Chen Y, Zhou S, Wang Y, Li L. Screening solvents to extract phenol from aqueous solutions by the COSMO-SAC model and extraction process simulation. Fluid Phase Equilib. 2017;451:12-24. doi:10.1016/j.fluid.2017.08.007.

8. Gerber RP, Soares R de P. Functional-Segment Activity Coefficient Model. 1. Model Formulation. Ind Eng Chem Res. 2013;52:1159-11171. doi:10.1021/ie400170a.

9. Soares R de P, Gerber RP, Possani LFK, Staudt PB. Functional-Segment Activity Coefficient Model. 2. Associating Mixtures. Ind Eng Chem Res. 2013;52(32):11172-11181.

10. Griswold J, Wong SY. Phase-equilibria of the acetone-methanol-water system from 100°C into the critical region. Chem Eng Prog Symp Ser. 1952;48(3):18-34.

11. Bergmann DL, Eckert CA. Measurement of limiting activity coefficients for aqueous systems by differential ebuliometry. Fluid Phase Equilib. 1991;63:141-150.

12. Kojima K, Zhang S, Hiaki T. Measuring methods of infinite dilution activity coefficients and a database for systems including water. Fluid Phase Equilib. 1997;131(1-2):145-179. doi:10.1016/s0378-3812(96)03210-4.

13. Barr-David F, Dodge BF. Vapor-Liquid Equilibrium at High Pressures. The Systems Ethanol - Water and 2-Propanol - Water. J Chem Eng Data. 1959;4(2):107-121. doi:10.1021/je60002a003.

14. Pividal KA, Birtigh A, Sandler SI. Infinite Dilution Activity Coefficients for Oxygenate Systems Determined Using a Differential Static Cell. J Chem Eng Data. 1992;37:484-487.

15. Butcher KL, Medani MS. Thermodynamic properties of methanol–benzene mixtures at elevated temperatures. J Appl Chem. 1968;18(4):100-107. doi:10.1002/jctb.5010180402.

16. Endler I, Hradetzky G, Bittrich HJ. Grenzaktivitätskoeffizienten in binären Systemen Benzen-Alkanol. J Prakt Chem. 1985;327:693-697.

17. Schmidt TW. Determination of Infinite Dilution Activity Coefficients (gamma infinite) using molecular beams. US-Patent. 1980:1-16.

18. Gmehling J, Onken U. Vapor-Liquid Equilibrium Data Collection. Alcohols: Methanol. Supplement 5 - DECHEMA - Chemistry Data Series 1(2g).; 2005.

19. Moilanen P, Uusi-Kyyny P, Pokki JP, Pakkanen M, Aittamaa J. Vapor-liquid equilibrium for butane + methanol, + ethanol, + 2-propanol, + 2-butanol, and + 2-methyl-2-propanol (TBA) at 323 K. J Chem Eng Data. 2008;53(1):83-88. doi:10.1021/je7003947.

20. Miyano Y, Nakanishi K, Fukuchi K. Henry’s constants of butane, isobutane, 1-butene and isobutene in methanol at 255-320 K. Fluid Phase Equilib. 2003;208(1-2):223-238. doi:10.1016/S0378-3812(03)00036-0.

21. Bernatová S, Linek J, Wichterle I. Vapour-liquid equilibrium in the butyl alcohol – n-decane system at 85, 100 and 115°C. Fluid Phase Equilib. 1992;74:127-132.

22. Dohnal V, Vrbka P. Limiting activity coefficients in the 1-alkanol + n-alkane systems: Survey, critical evaluation and recommended values, interpretation in terms of association models. Fluid Phase Equilib. 1997;133(1-2):73-87. doi:10.1016/S0378-3812(97)00008-3.

23. Heintz A, Dolch E, Lichtenthaler RN. New experimental VLE-data for alkanol/alkane mixtures and their description by an extended real association (ERAS) model. Fluid Phase Equilib. 1986;27(C):61-79. doi:10.1016/0378-3812(86)87041-8.

24. Rodriguez V, Pardo J, López MC, Royo FM, Urieta JS. Vapor pressures of binary mixtures of hexane + 1-butanol, + 2-butanol, + 2-methyl-1-propanol, or + 2-methyl-2-propanol at 298.15 K. J Chem Eng Data. 1993;38(1):350-352.

25. Thomas ER, Newman BA, Long TC, Wood DA, Eckert CA. Limiting activity coefficients of nonpolar and polar solutes in both volatile and nonvolatile solvents by gas chromatography. J Chem Eng Data. 1982;27:399-405.

26. Landau I, Belfer AJ, Locke DC. Measurement of limiting activity coefficients using non-steady-state gas chromatography. Ind Eng Chem Res. 1991;30:1900-1906.

27. Máchová I, Linek J, Wichterle I. Vapour-liquid equilibria in the heptane – 1-pentanol and heptane – 3-methyl-1-butanol systems at 75, 85 and 95°C. Fluid Phase Equilib. 1988;41:257-267.

28. Wilsak RA, Campbell SW, Thodos G. Vapor-liquid equilibrium measurements for the n-pentane-methanol-acetone ternary at 372.7 K and their prediction from the constituent binaries. Fluid Phase Equilib. 1987;33(1-2):173-190. doi:10.1016/0378-3812(87)87010-3.

29. Xiong R, Sandler SI, Burnett RI. An improvement to COSMO-SAC for predicting thermodynamic properties. Ind Eng Chem Res. 2014;53(19):8265-8278. doi:10.1021/ie404410v.

30. Lagarias JC, Reeds JA, Wright MH, Wright PE. Convergence Properties of the Nelder--Mead Simplex Method in Low Dimensions. SIAM J Optim. 1998;9(1):112-147. doi:10.1137/S1052623496303470.

31. Wilson GM. Vapor-Liquid Equilibrium. XI. A New Expression for the Excess Free Energy of Mixing. J Am Chem Soc. 1964;86(2):127-130. doi:10.1021/ja01056a002.

32. Renon H, Pruasnitz JM. Local compositions in thermodynamics excess functions for liquids mixtures. AIChE J. 1968;14(1):116-128.

33. Abrams DS, Prausnitz JM. Statistical thermodynamics of liquid mixtures: A new expression for the excess Gibbs energy of partly or completely miscible systems. AIChE J. 1975;21(1):116-128. doi:10.1002/aic.690210115.

34. Nelder J a., Mead R. A simplex method for function minimization. Comput J. 1964;7:308-313. doi:10.1093/comjnl/7.4.308.

35. Derr EL, Deal CH. Analytical solutions of groups: correlation of activity coefficients through structural groups parameters. Chem Eng Symp Ser. 1969;32:3-40.

36. Klamt A, Schüürmann G. COSMO: a new approach to dielectric screening in solvents with explicit expressions for the screening energy and its gradient. J Chem Soc, Perkin Trans 2. 1993;(5):799-805. doi:10.1039/P29930000799.

37. Klamt A, Eckert F. COSMO-RS: a novel and efficient method for the a priori prediction of thermophysical data of liquids. Fluid Phase Equilib. 2000;172(1):43-72. doi:10.1016/S0378-3812(00)00357-5.

4 PERFORMANCES DOS MODELOS UNIFAC(LLE), COSMO-SAC E F-SAC EM CÁLCULOS DE ELL

The UNIFAC(LLE), COSMO-SAC, and F-SAC performances on ternary LLE calculations.

Christian Luiz da Silveira[2]

Nina Paula Gonçalves Salau

Chemical Engineering Department
Universidade Federal de Santa Maria

ABSTRACT

The reliable description of a liquid-liquid equilibrium system is irrefragably important, given that liquid-liquid equilibrium has several important applications in industry, such as extraction of propionic acid for thermoplastics production through esterification and acid acetic, a toxic compound released during the 2nd generation ethanol production, and the proper calculation of fuel blends equilibrium composition. The use of accurate models is one of the main necessities to achieve good predictions of a system. In this work, the use of the UNIFAC(LLE), COSMO-SAC, and F-SAC excess Gibbs energy models in liquid-liquid equilibrium is analyzed. Liquid-liquid equilibrium predictions of 55 ternary systems are performed, the models are compared and their accuracy evaluated. The UNIFAC(LLE) model yielded the most reliable results, although some systems were better described by the COSMO-SAC and F-SAC models. The performance of the models for systems containing ethanol + water + 3rd compound

[1]To whom all correspondence should be addressed. E−mail: christiansilveira86@gmail.com
Address: Chemical Engineering Department, UFSM − Av. Roraima, 1000, Cidade Universitária −Bairro Camobi. 97105-900 Santa Maria, RS − Brazil.
Phone: +55-55-3220-8448- Fax: +55-55-3220-8030.

was also analyzed, and the influence of the different compounds (hydrocarbons and alcohols) over the phase-equilibrium and the accuracy of the models was evaluated.

Keywords: liquid-liquid equilibrium; ternary systems; COSMO-SAC; F-SAC; UNIFAC(LLE).

1. INTRODUCTION

The COSMO-SAC model is predictive excess Gibbs energy model for liquid phase nonideality. The COSMO-SAC model is based on COSMO calculations [1], a quantum mechanical calculation method used to obtain the charge-density profile of different molecules (more details about the COSMO and its derivative COSMO-RS model can be seen in Klamt and coworkers works [1–6]).

The COSMO-SAC (**Co**nductor-like **S**creening **M**odel – **S**egment **A**ctivity **C**oefficient) model was firstly proposed by Lin and Sandler [7], based on the COSMO calculations and on the solvation theory published in their previous work [8] and in [9]. The characteristic equation of the model is

$$\ln \gamma_{i/S} = n_i \sum_{\sigma_m} p_i(\sigma_m)[\ln \Gamma_S(\sigma_m) - \ln \Gamma_i(\sigma_m)] + \ln \gamma_{i/S}^{SG} \quad (1)$$

Where $\gamma_{i/S}$ is the activity coefficient of the solute molecule i in the solvent S, n_i is the number of surface segments of molecule i, σ_m is the charge density of a segment m, $p_i(\sigma_m)$ is the probability of finding a segment with surface charge density σ_m, Γ_S is the segment activity coefficient and $RT \ln \Gamma_S(\sigma_m)$ is the free energy required to add a segment with charge density σ_m at a fixed position in the solution (or in the pure fluid i, for $\ln \Gamma_i(\sigma_m)$). The last term is the Staverman-Guggenheim combinatorial term, used to improve the calculations of the cavity formation free energy [7,8].

Although the great predictive power and elegance of the model theory, the COSMO-SAC is still not as quantitatively accurate as classical excess Gibbs energy model, such as UNIFAC [10] and UNIFAC(Do) [11]. Further refinements and improvements were proposed and implemented in the COSMO-SAC model to improve

its accuracy, with special attention to the works of Lin et al. [12], Wang and Sandler [13], Hsieh et al. [14], and Xiong et al. [15].

A different model was proposed by Soares and coworkers [16,17], the so-called Functional-Segment Activity Coefficient Model (F-SAC). It is still based on the group-contributions approach of models like UNIFAC and UNIQUAC, however, in the F-SAC model the interaction energy between the functional groups is obtained from the COSMO-SAC model. This method decreases the predictive capacity of the model, if compared to the COSMO-SAC by introducing a greater empiricism degree [16].

Additionally, the main difference between the F-SAC and the COSMO-SAC models is that the former relies on fitted molecular properties, while the latter obtains the molecular properties by quantum chemical calculations, such as the COSMO calculations.

In this work, the UNIFAC(LLE) [18], COSMO-SAC, and F-SAC models are used to predict the liquid-liquid equilibria (LLE) of 55 ternary mixtures. A total of 2184 experimental points for LLE phase compositions was collected, and 26 different species are contained in the 55 ternary systems. Table 1 presents the systems used in this work, their temperatures, number of experimental points available (NY) and their source, and the availability of the F-SAC model for the system. The F-SAC version used in this work is freely distributed by the Soares research group and can be found in their website (https://github.com/lvpp/f-sac); some of the species used in this work are not available in the open database.

Table 1. Ternary systems compared in this work.

System Number	System	$T\ [K]$	NY	F-SAC availability	Source
1	Water + Acetic Acid + Ethyl Acetate	[293.15, 313.15]	72	No	[19]
2	Water + Acetic Acid + Butyl Acetate	[293.15, 313.15]	66	No	
3	Water + Acetic Acid +Isobutyl Acetate	[293.15, 313.15]	60	No	
4	Water + Acetic Acid + Isoamyl Acetate	[293.15, 313.15]	60	No	
5	Water + Acetic Acid +Heptyl Acetate	[293.15, 313.15]	78	No	
6	Water + Butyric Acid + Butanal	[293.15, 308.15, 323.15]	162	No	[20]
7	Water + Butyric Acid + Butanol	[293.15, 308.15, 323.15]	144	No	

8	Methanol + Diisopropyl Ether + Water	[298]	42	No	[21]
9	Ethanol + Diisopropyl Ether + Water	[298]	42	No	
10	Propanol + Diisopropyl Ether + Water	[298]	36	No	
11	2-Propanol + Diisopropyl Ether + Water	[298]	42	No	
12	Butanol + Diisopropyl Ether + Water	[298]	30	No	
13	2-Butanol + Diisopropyl Ether + Water	[298]	30	No	
14	Isobutanol + Diisopropyl Ether + Water	[298]	24	No	
15	Tertbutanol + Diisopropyl Ether + Water	[298]	42	No	
16	Methanol + Heptene + Water	[298]	24	Yes	[22]
17	Ethanol + Heptene + Water	[298]	36	Yes	
18	Propanol + Heptene + Water	[298]	30	Yes	
19	2-Propanol + Heptene + Water	[298]	24	Yes	
20	Butanol + Heptene + Water	[298]	18	Yes	
21	2-Butanol + Heptene + Water	[298]	18	Yes	
22	Isobutanol + Heptene + Water	[298]	18	No	
23	Tertbutanol + Heptene + Water	[298]	36	No	
24	Methanol + O-Xylene + Water	[298]	36	Yes	[23]
25	Ethanol + O-Xylene + Water	[298]	36	Yes	
26	Propanol + O-Xylene + Water	[298]	48	Yes	
27	2-Propanol + O-Xylene + Water	[298]	36	Yes	
28	Butanol + O-Xylene + Water	[298]	30	Yes	
29	2-Butanol + O-Xylene + Water	[298]	24	Yes	
30	Isobutanol + O-Xylene + Water	[298]	30	Yes	
31	Tertbutanol + O-Xylene + Water	[298]	42	No	
32	Methanol + Mesitylene + Water	[298]	36	Yes	
33	Ethanol + Mesitylene + Water	[298]	42	Yes	
34	Propanol + Mesitylene + Water	[298]	48	Yes	
35	2-Propanol + Mesitylene + Water	[298]	30	Yes	
36	Butanol + Mesitylene + Water	[298]	30	Yes	
37	2-Butanol + Mesitylene + Water	[298]	30	Yes	
38	Isobutanol + Mesitylene + Water	[298]	30	Yes	
39	Tertbutanol + Mesitylene + Water	[298]	36	No	
40	Heptane + Water + Methanol	[298]	18	Yes	[24]
41	Heptane + Water + Ethanol	[298]	18	Yes	
42	Heptane + Water + Propanol	[298]	18	Yes	
43	Heptane + Water + 2-Propanol	[298]	18	No	
44	Heptane + Water + Butanol	[298]	18	Yes	
45	Heptane + Water + 2-Butanol	[298]	18	Yes	
46	Heptane + Water + Tertbutanol	[298]	24	No	
47	Heptane + Water + Pentanol	[298]	18	Yes	
48	Heptane + Water + 2-Pentanol	[298]	18	No	
49	Propanol + Water + Butanol	[310.93]	30	No	[25]

50	Propanol + Water + Benzene	[310.93]	36	No	
51	Propanol + Water + Heptane	[310.93]	24	No	
52	Propanol + Water + Hexane	[310.93]	30	No	
53	Butanol + Ethanol + Water	[298.15]	108	Yes	[26]
54	Isobutanol + Ethanol + Water	[293.15]	42	Yes	[27]
55	Tertbutanol + Ethanol + Water	[293.15]	48	Yes	

Several authors have reported different applications for the LLE calculations. For example, van Berlo et al. [26] reported the importance of LLE for processes, such as solvent extraction of biomolecules and precipitation in aqueous alkanol systems for the pharmaceutical industry. Bekri et al. [28] used LLE to evaluate the recovery of propionic acid, used in the esterification to produce thermoplastics and mold prevention in baking, from aqueous solutions with four different solvents. Roque and coworkers [19] studied the removal of acetic acid from an aqueous solution using different esters as solvents, since this carboxylic acid can decrease the ethanol production.

Kadir et al. [27] published an interesting work that reports the importance of the LLE in the production of neutral spirit, where the removal of the congeners (alcohols such as propyl, butyl, and amyl and their isomers) usually requires the addition of water to dislocate its equilibrium, allowing their removal through a simple stage decanter.

More recently, Liu and Zhang [29] reported the crescent use of computer-aided molecular methods to assist the solvent selection. The authors have successfully used the UNIFAC and the COSMO-SAC models as solvent screening methods for phenolic compounds removal from aromatic solutions.

A new and promising area for LLE study is the use of mixtures in diesel and biodiesel. Yoshimoto et al. [30] studied the efficiency of a diesel engine with different amount of 1-butanol in a diesel mixture. Atmanli [31] also compared the efficiency of ternary blends of diesel, biodiesel, and higher alcohols (propanol, n-butanol, and 1-pentanol). The biodiesel, besides being a renewable energy source, is sulfur free and offers potential reduction in CO2 emissions [30]. In this manner, to improve the efficiency of the biodiesel and to avoid phase-splitting, different alcohols are being used. Aguiar et al. [32] studied mixtures with different contents of diesel + ethanol + n-

butanol, in their work, however, no thermodynamics analysis were performed to obtain the LLE of the blends.

Our previous work was performed using only VLE and infinite-dilution activity coefficient (IDAC) for binaries mixtures [33]. Silveira and Salau [33] reported very good agreements with experimental data for the three models used in this work. The F-SAC was especially accurate for IDAC predictions. Since no extensive comparison between the UNIFAC(LLE), COSMO-SAC, and F-SAC models was found in literature, we extended the investigation to ternary LLE systems using the 3 referred excess Gibbs energy models.

The comparison among the 3 excess Gibbs energy models is performed in order to evaluate their accuracy in predicting the experimental molar fraction data from the 55 ternary systems studied in this work. In addition, the systems with similar structures and complexity are analyzed separately, and the performance of the models evaluated.

2. COMPUTATIONAL METHODS

As presented in Table 1, LLE data from 55 ternary systems were collected in literature. Some of the ternary systems have experimental data for different temperatures, however, none of the systems was experimentally measured in pressures different from the atmosphere. Given this reason, and since excess Gibbs energy models are being compared, a simple $\gamma - \gamma$ approach was chosen as sufficient. The $\gamma - \gamma$ approach, or the activity coefficient model approach, has been commonly used to describe LLE; unlike the $\varphi - \varphi$ approach, however, the activity coefficients method is unable to represent the pressure effects on the LLE problem [34–36].

The liquid-liquid equilibrium condition was established as by Equation 1.

$$x_i^I \gamma_i^I(T, P, \boldsymbol{x^I}) = x_i^{II} \gamma_i^{II}(T, P, \boldsymbol{x^{II}}) \quad (1)$$

Where x_i^I and γ_i^I are the molar fraction and activity coefficient of the component i in phase I (the same notation is valid for phase II), T and P are the temperature and

pressure of the system, and $\boldsymbol{x^I}$ and $\boldsymbol{x^{II}}$ are the vector of compositions of the phases I and II.

Considering the system at the same temperature and pressure conditions, to calculate the equilibrium solution becomes a hard task, given that when the mole fractions of the components are equal in both phase I and II, the activity coefficients will have the same value. Even though the equality is true, in this case, the solution is trivial, and it is not of our interest.

The numerical stability of LLE systems was studied in several works [35–39]. Usually, the stable solution is found by the analysis of the Gibbs free energy of the solutions. A particularly interesting work on this subject is Li's thesis [40], where the author evaluates different methods for the LLE calculation. In this work, we have considered only the stable and nontrivial solutions for the LLE calculations.

The equilibrium molar fractions were calculated using the Rachford-Rice method [41]. Although it is as method originally developed for vapor-liquid equilibrium (VLE) calculations, the Rachford-Rice can be used for LLE mole fractions predictions [42]. From the material balance of a *flash* problem, the equations 2 is obtained:

$$y_i = \frac{K_i z_i}{(K_i - 1)v + 1} \tag{2}$$

Where y_i and z_i are the vapor phase and feed compositions, K_i is the ratio y_i/x_i, and v is the number of moles in the vapor phase. Given that

$$\sum_{i=1}^{S} x_i = \sum_{i=1}^{S} y_i = 1 \tag{3}$$

Equation 2, thus, can be rewriting as a summation

$$\sum_{i=1}^{S} \frac{K_i z_i}{(K_i - 1)v + 1} - 1 = 0 \tag{4}$$

The same procedure can be used for LLE calculations, considering $y_i = x_i^I$ and $x_i = x_i^{II}$, and the K-value is then given by equation 5:

$$K_i = \gamma_i^{II}/\gamma_i^I \tag{5}$$

The activity coefficients on equation 5 can be obtained from any excess Gibbs energy model (in this work, for instance, the UNIFAC(LLE), COSMO-SAC, and F-SAC models). The equation 4 can be solved by any numerical method. In this work, we have

used the *fsolve* function, embedded in MATLAB, using the default Trust-Region Dogleg algorithm, which is a variant of the Powell dogleg method [43].

After obtaining v from equation 4, x_i^I and x_i^{II} are recalculated using equations 6a and 6b:

$$x_i^I = \frac{z_i}{\frac{1-v}{K_i}+v} \tag{6a}$$

$$x_i^{II} = \frac{z_i - v x_i^I}{1-v} \tag{6b}$$

The iteration procedure is conduced until convergence, as described in the Appendix A section.

As already mentioned, the activity coefficients used in equation 5 can be obtained from any excess Gibbs energy model. In this work, the UNIFAC(LLE) model was used as described by Fredenslund et al. [10] with the LLE parameters suggested by [18]; the COSMO-SAC version used was implemented in MATLAB, based on the implementation provided by Virginia Tech (COSMO-SAC-VT-2005, available at https://www.design.che.vt.edu/VT-Databases.html), which is based on the first version of the COSMO-SAC model [7] – the sigma-profile database provided by VT was also used; and the F-SAC version was that published by Soares et al. [16,17], available at https://github.com/lvpp/f-sac.

2.1 Statistical Analysis

Since no parameter estimation was conducted in this work, there is no need to use a theoretically robust objective function. The metric used to measure the goodness of each activity coefficient model was simply the absolute deviation of the calculated value from the experimental data, thus, the sum of the residuals for each system can be written as:

$$SR = \sum_{k=1}^{NY} \left| X_k^{calc} - X_k^{exp} \right| \tag{7}$$

Where SR is the sum of residuals, NY is the number of experimental points, and X_k^{calc} and X_k^{exp} are the calculated and experimental molar fraction for the experimental point k.

In addition to the sum of residuals, the average absolute deviation and the standard deviations (equations 8 and 9, respectively) will be presented in Table 2 (Section 3).

$$AAD = \frac{\sum_{k=1}^{NY}\left|X_k^{calc} - X_k^{exp}\right|}{NY} \quad (8)$$

$$SD = \sqrt{\frac{\sum_{k=1}^{NY}(X_k - \bar{X})^2}{NY-1}} \quad (9)$$

Where AAD and SD are the average absolute deviation and standard deviation, respectively, and $\bar{X}$ is the average value of the molar fractions residuals.

3. RESULTS AND DICUSSION

In an overall analysis, the UNIFAC(LLE) model was the most accurate among the 3 models tested, it presented the smallest values (sum of residuals, absolute average deviation, and standard deviation). Since some of the systems have different temperatures to be evaluated, there are, in fact, 64 systems (2 temperatures for systems from 1 to 5 and 3 temperatures for systems 6 and 7). The UNIFAC(LLE) presented the best results for 37 of the 64 systems, revealing a major accuracy, as presented in Table 2.

Table 2. Statistical results of the tested models.

	UNIFAC(LLE)			COSMO-SAC			F-SAC		
System	SR	AAD	SD	SR	AAD	SD	SR	AAD	SD
Sys 1a	1.4755	0.0410	0.0321	3.9605	0.1100	0.1155			
Sys 1b	1.7946	0.0498	0.0374	4.2647	0.1185	0.0962			
Sys 2a	1.0424	0.0290	0.0257	0.8946	0.0249	0.0302			
Sys 2b	0.7087	0.0236	0.0248	1.2675	0.0422	0.0452			
Sys 3a	0.6050	0.0202	0.0248	1.2298	0.0410	0.0427			

Sys 3b	0.4592	0.0153	0.0114	0.4592	0.0153	0.0114			
Sys 4a	0.9421	0.0314	0.0216	1.3280	0.0443	0.0392			
Sys 4b	0.8994	0.0300	0.0177	0.9424	0.0314	0.0233			
Sys 5a	1.6364	0.0390	0.0321	1.3249	0.0315	0.0259			
Sys 5b	1.3217	0.0367	0.0305	1.4447	0.0401	0.0349			
Sys 6a	0.9718	0.0180	0.0254	2.2434	0.0415	0.0637			
Sys 6b	1.2009	0.0222	0.0335	2.0359	0.0377	0.0591			
Sys 6c	2.0845	0.0386	0.0517	1.5718	0.0291	0.0374			
Sys 7a	0.8278	0.0172	0.0300	0.9553	0.0199	0.0252			
Sys 7b	1.0605	0.0221	0.0353	0.9692	0.0202	0.0222			
Sys 7c	1.3738	0.0286	0.0396	1.0088	0.0210	0.0212			
Sys 8	5.7927	0.1379	0.1853	4.8595	0.1157	0.1562			
Sys 9	6.0189	0.1433	0.1533	4.2794	0.1019	0.1602			
Sys 10	0.5522	0.0153	0.0136	1.1946	0.0332	0.0432			
Sys 11	0.4759	0.0113	0.0179	1.8906	0.0450	0.0472			
Sys 12	0.2924	0.0097	0.0139	1.1432	0.0381	0.0486			
Sys 13	0.4914	0.0164	0.0140	0.8413	0.0280	0.0352			
Sys 14	0.7767	0.0324	0.0344	0.4319	0.0180	0.0308			
Sys 15	2.2615	0.0538	0.0541	1.9271	0.0459	0.0418			
Sys 16	1.5200	0.0633	0.0891	5.1391	0.2141	0.1856	2.4590	0.1025	0.1076
Sys 17	2.3347	0.0649	0.0585	3.1583	0.0877	0.0834	3.8924	0.1081	0.0996
Sys 18	0.6987	0.0233	0.0200	3.1415	0.1047	0.1344	3.2120	0.1071	0.1032
Sys 19	2.0140	0.0839	0.0563	1.7091	0.0712	0.0685	3.5906	0.1496	0.1234
Sys 20	0.1615	0.0090	0.0130	0.2756	0.0153	0.0246	0.4179	0.0232	0.0330
Sys 21	0.2338	0.0130	0.0115	0.2788	0.0155	0.0128	0.5292	0.0294	0.0347
Sys 22	5.3750	0.2986	0.2054	0.1378	0.0077	0.0079			
Sys 23	2.1531	0.0598	0.0602	1.6220	0.0451	0.0432			
Sys 24	0.8373	0.0233	0.0259	2.9906	0.0831	0.0878	1.1277	0.0313	0.0402
Sys 25	0.8335	0.0232	0.0267	2.4310	0.0675	0.0556	2.7029	0.0751	0.0860
Sys 26	0.5600	0.0117	0.0123	0.8305	0.0173	0.0228	2.5105	0.0523	0.0766
Sys 27	0.4276	0.0119	0.0121	1.3766	0.0382	0.0432	3.0572	0.0849	0.0755
Sys 28	0.1777	0.0059	0.0101	0.6838	0.0228	0.0371	0.5331	0.0178	0.0299
Sys 29	0.1962	0.0082	0.0093	0.2459	0.0102	0.0128	0.5189	0.0216	0.0317
Sys 30	0.9707	0.0324	0.0349	0.2258	0.0075	0.0097	0.4203	0.0140	0.0209
Sys 31	1.9097	0.0455	0.0554	1.1669	0.0278	0.0307			
Sys 32	2.6852	0.0746	0.0742	3.4175	0.0949	0.0883	2.0128	0.0559	0.0812
Sys 33	1.3995	0.0333	0.0390	4.6628	0.1110	0.0935	2.6516	0.0631	0.1093
Sys 34	1.3201	0.0275	0.0341	1.9161	0.0399	0.0642	2.3383	0.0487	0.0645
Sys 35	2.8476	0.0949	0.1033	1.9361	0.0645	0.0653	3.0075	0.1003	0.1054

Sys 36	0.1204	0.0040	0.0067	0.5876	0.0196	0.0334	0.6433	0.0214	0.0345
Sys 37	0.2268	0.0076	0.0095	0.3177	0.0106	0.0123	0.5783	0.0193	0.0279
Sys 38	1.0183	0.0339	0.0344	0.2172	0.0072	0.0090	0.3548	0.0118	0.0174
Sys 39	1.6700	0.0464	0.0641	0.9048	0.0251	0.0340			
Sys 40	0.5184	0.0288	0.0258	1.4907	0.0828	0.1223	0.3546	0.0197	0.0291
Sys 41	0.2496	0.0139	0.0102	0.3830	0.0213	0.0205	0.9813	0.0545	0.0494
Sys 42	0.4686	0.0260	0.0163	0.3336	0.0185	0.0220	1.2861	0.0714	0.0580
Sys 43	0.1582	0.0088	0.0119	0.5328	0.0296	0.0354			
Sys 44	0.2042	0.0113	0.0105	0.1848	0.0103	0.0103	0.4632	0.0257	0.0448
Sys 45	0.2871	0.0160	0.0100	0.2593	0.0144	0.0149	0.3066	0.0170	0.0239
Sys 46	0.6410	0.0356	0.0390	0.3678	0.0204	0.0236			
Sys 47	0.2768	0.0154	0.0302	0.4081	0.0227	0.0415	0.0137	0.0008	0.0007
Sys 48	0.2460	0.0137	0.0193	0.3439	0.0191	0.0373			
Sys 49	2.0575	0.0686	0.0783	1.8165	0.0606	0.0682			
Sys 50	0.3987	0.0111	0.0112	0.6655	0.0185	0.0192			
Sys 51	1.7478	0.0728	0.0806	2.3903	0.0996	0.0820			
Sys 52	3.0896	0.0749	0.1073	1.8383	0.1212	0.1377			
Sys 53	5.6871	0.0527	0.0409	1.7759	0.0164	0.0228	7.5307	0.0697	0.0915
Sys 54	0.3484	0.0083	0.0103	1.6998	0.0405	0.0335	2.3423	0.0558	0.0697
Sys 55	0.0600	0.0013	0.0019	0.1221	0.0025	0.0031	2.0538	0.0428	0.0562

The performance of the UNIFAC(LLE) model was especially better than the other two models for systems containing alcohols such as Butanol, Isobutanol, and Tertbutanol; in addition, the presence of the referred alcohols and Propanol and 2-Propanol seem to affect the accuracy of both COSMO-SAC and F-SAC. Since the F-SAC uses the information provided by the COSMO-SAC model, this accuracy deterioration might be caused by the COSMO calculations, for instance, the sigma-profile or hydrogen bond descriptor.

Since the F-SAC model is not available for every ternary system used in this work, the summarized results presented in Table 3 are divided in the total summation of the values for both UNIFAC(LLE) and COSMO-SAC and the summation over these two models restricted to the systems that are available for F-SAC.

Table 3. Summarized results for comparison.

Model	Total SR	Total AAD
UNIFAC(LLE)	83.1963	2.4419
COSMO-SAC	96.4541	2.9016
UNIFAC(LLE) (restricted)	28.6837	0.8231
COSMO-SAC (restricted)	42.1990	1.3325
F-SAC	51.8907	1.4949

Although the good performance of both COSMO-SAC and F-SAC (which can be seen in the diagrams presented in the Supplementary Material), the UNIFAC(LLE) continues to offer the most accurate results for a wide range of molecules complexity.

Comparing only the restricted results, i.e., the results that are available for all the models, the COSMO-SAC model was roughly 10% more accurate than the F-SAC; the UNIFAC(LLE), however, presented and average absolute deviation almost 45% smaller than the F-SAC and roughly 40% smaller than the COSMO-SAC.

It also should be highlighted that the computational effort demanded by the simulations with the UNIFAC(LLE) model was much smaller than the alternatives.

The data used in this work allows certain analysis on the performance of the models as a function of the components of the systems. The first comparison is performed with the systems 19, 27, and 35 (2-Propanol + Heptene + Water, 2-Propanol + O-Xylene + Water, and 2-Propanol + Mesitylene + Water, respectively). The different hydrocarbons do not play a major role on the models performance, as can be seen in Figure 1.

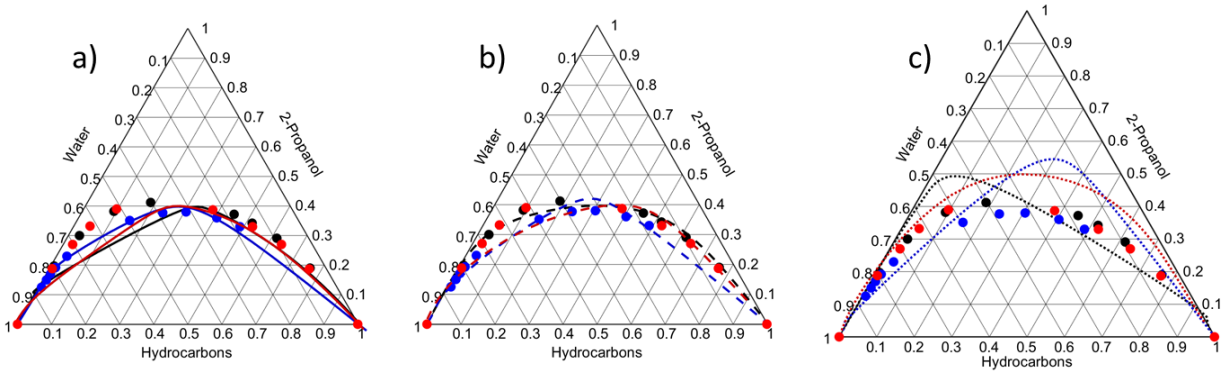

Figure 1. Models performance on different hydrocarbons (UNIFAC(LLE) (a), COSMO-SAC (b), and F-SAC (c)), the black curves represent the system 19, the blue curves represent the system 27, and the red curves represent the system 35.

The F-SAC model presents the most prominent differences when different hydrocarbons are used. Although the apparent difference, the accuracy of the F-SAC model was roughly the same for all the three systems, as can be seen in Table 4.

Table 4. 2-Propanol + Hydrocarbon + Water systems results.

		System 19 (Heptene)	System 27 (O-Xylene)	System 35 (Mesitylene)
UNIFAC(LLE)	SR	2.0140	0.4276	2.8476
	AAD	0.0839	0.0119	0.0949
COSMO-SAC	SR	1.7091	1.3766	1.9361
	AAD	0.0712	0.0382	0.0645
F-SAC	SR	3.5906	3.0572	3.0075
	AAD	0.1496	0.0849	0.1003

The COSMO-SAC model yielded accurate results for both systems 19 and 35, while the system 27 was better described by the UNIFAC(LLE) model.

The differences between the hydrocarbons seem to play a more important role in systems 20, 28, and 36 (Butanol + Heptene + Water, Butanol + O-Xylene + Water, and Butanol + Mesitylene + Water). As depicted in Figure 2, the linear hydrocarbon

heptene has a smaller region where the organic and aqueous phase coexist (a), while the systems with aromatic compounds (b and c, O-Xylene and Mesitylene, respectively) present a broader phase-envelope.

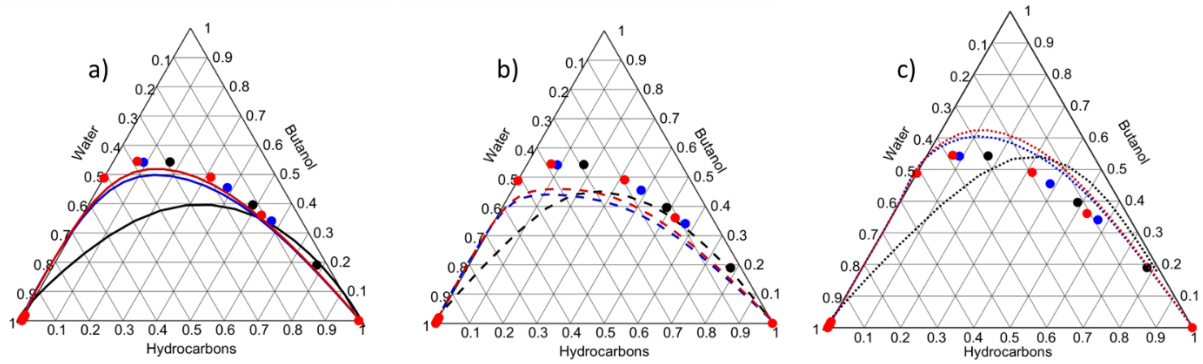

Figure 2. Models performance on different hydrocarbons (UNIFAC(LLE) (a), COSMO-SAC (b), and F-SAC (c)), the black curves represent the system 20, the blue curves represent the system 28, and the red curves represent the system 36.

Although qualitatively reliable (cf. Figure 2), both COSMO-SAC and F-SAC presented quantitatively results less accurate than those obtained by the use of UNIFAC(LLE), as demonstrated in Table 5.

Table 5. Butanol + Hydrocarbon + Water systems results.

		System 20 (Heptene)	System 28 (O-Xylene)	System 36 (Mesitylene)
UNIFAC(LLE)	SR	0.1615	0.1777	0.1204
	AAD	0.0090	0.0059	0.0040
COSMO-SAC	SR	0.2756	0.6838	0.5876
	AAD	0.0153	0.0228	0.0196
F-SAC	SR	0.4179	0.5331	0.6433
	AAD	0.0232	0.0178	0.0214

Likewise, the systems 21, 29, and 37 were analyzed. These systems are similar to the previous systems presented, they are composed by alcohol +

hydrocarbon + water. The alcohol now is 2-Butanol and the hydrocarbons are the same as the previous (heptene, o-xylene, and mesitylene). As depicted in figure 3, there are no major differences between the systems, neither between the model performances compared to their performance presented earlier.

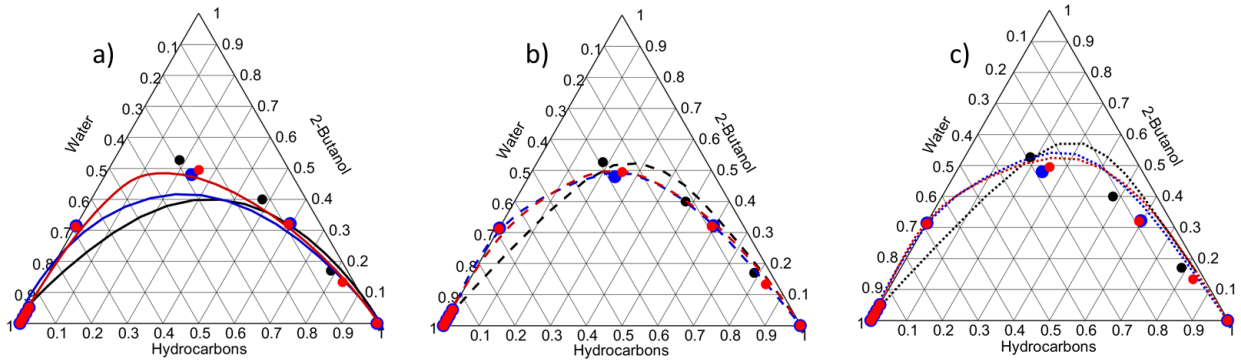

Figure 3. Models performance on different hydrocarbons (UNIFAC(LLE) (a), COSMO-SAC (b), and F-SAC (c)), the black curves represent the system 21, the blue curves represent the system 29, and the red curves represent the system 37.

Although the UNIFAC(LLE) model does not seem to properly calculate the inflection point of the 2-butanol + heptene + water system (system 21), its sum of residuals and absolute average deviation were still lower than those provided by both COSMO-SAC and F-SAC, as shown in Table 6.

Table 6. 2-Butanol + Hydrocarbon + Water systems results.

		System 21 (Heptene)	System 29 (O-Xylene)	System 37 (Mesitylene)
UNIFAC(LLE)	SR	0.2338	0.1961	0.2268
	AAD	0.0129	0.0081	0.0075
COSMO-SAC	SR	0.2787	0.2458	0.3177
	AAD	0.0154	0.0102	0.0105
F-SAC	SR	0.5292	0.5188	0.5783
	AAD	0.0294	0.0216	0.0192

Lastly, the systems containing ethanol + water (17, 25, 41, 53, 54, and 55) were investigated – the system number 9 was not considered here, since its results are not available for all models. The systems containing Isobutanol and Tertbutanol (54, 55) have shown great agreement with the experimental data; for the system containing Butanol (53), however, the UNIFAC(LLE) and the F-SAC models predictions accuracy decreased significantly. The results can be seen in Table 7.

The butanol + ethanol + water system is of special interest, since the butanol can be used as an additive to improve several properties of the ethanol fuel, such as the low heat value, which may provide better conditions for ignitions [32,44]. Thus, the COSMO-SAC model seems to be the most suitable for biofuels equilibrium calculations involving butanol + ethanol + water.

Table 7. Results for systems containing ethanol + water.

Nº	System	UNIFAC(LLE)		COSMO-SAC		F-SAC	
		SR	AAD	SR	AAD	SR	AAD
17	Ethanol + Heptene + Water	2.3346	0.0648	3.1583	0.0877	3.8923	0.1081
25	Ethanol + O-Xylene + Water	0.8334	0.0231	2.4310	0.0675	2.7029	0.0750
41	Heptane + Water + Ethanol	0.2495	0.0138	0.3830	0.0212	0.9813	0.0545
53	Butanol + Ethanol + Water	5.6870	0.0526	1.7759	0.0164	7.5307	0.0697
54	Isobutanol + Ethanol + Water	0.3484	0.0082	1.6998	0.0404	2.3423	0.0557
55	Tertbutanol + Ethanol + Water	0.0600	0.0012	0.1221	0.0025	2.0538	0.0427

The systems containing hydrocarbons as the third component were satisfactorily described by the three models. The system containing heptene, however, appeared to affect all the models, especially the UNIFAC(LLE) model, whose AAD value is roughly 50 times larger than its best performance.

The results for the systems 17 (worst predictions for all models), 53 (least accurate among the ethanol + water + alcohol systems), and 55 (best predictions for all models) are depicted in Figure 4. The remaining ternary diagrams are presented in the Supplementary Material.

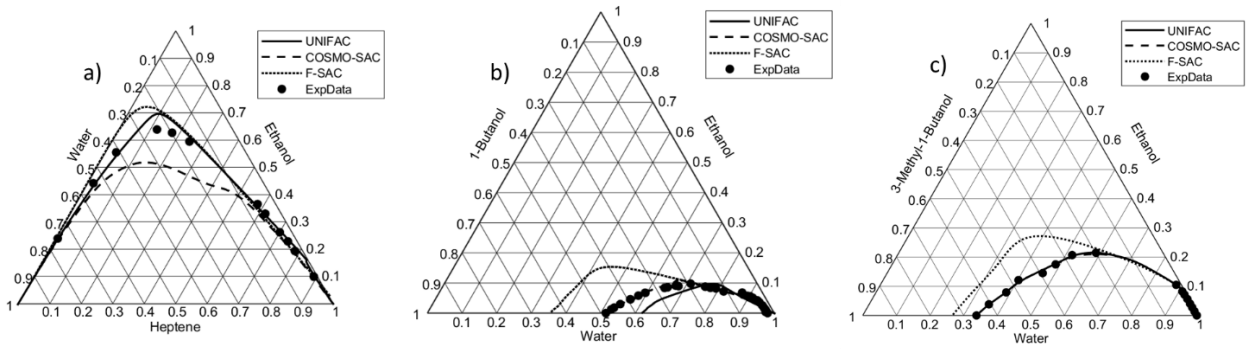

Figure 4. LLE diagrams for systems containing ethanol + water + (a) heptene (system 17), (b) 1-butanol (system 53), and (c) 3-methyl-1-butanol (tertbutanol, system 55).

Although UNIFAC was the model most affected by the introduction of the heptene in the system, the COSMO-SAC model was also greatly influenced by the alkene. The heptene sigma-profile used in this work was compared to that obtained by the COSMO-SAC (2013) [15] in order to verify if it was showing discrepancies. Figure 5 depicts the sigma-profile obtained from the VT database (used in this work) and that obtained from the COSMO-SAC (2013) software, provided by Xiong and Sandler [15].

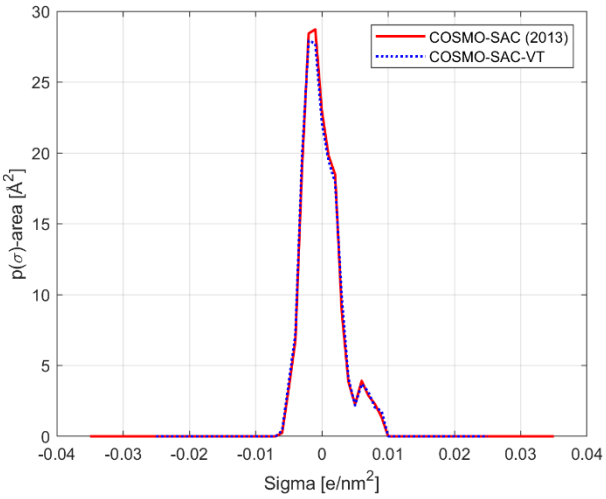

Figure 5. Heptene sigma-profiles comparison.

Perhaps one of the greatest differences between the COSMO-SAC 2013 and the version used in this work (2002) is that the former uses the sigma-profile divided

into: non-hydrogen bonding and hydrogen bonding contributions. However, in this case, heptene has no hydrogen bonding sites, hence, the sigma-profile is practically equal.

4. CONCLUSIONS

The UNIFAC, COSMO-SAC, and F-SAC models were used to describe the liquid-liquid equilibrium of 55 ternary systems containing water, alcohols, hydrocarbons, and ethers. The performance of each model was analyzed. The UNIFAC(LLE) model presented the most accurate results in an overall analysis, even though for several systems the COSMO-SAC model was the most precise. The F-SAC model also offered good predictions for several systems.

When the systems containing 2-propanol + water + hydrocarbons, butanol + water + hydrocarbons, and 2-butanol + water + hydrocarbons were analyzed, no great differences on the models performance were found when different hydrocarbons were used. The F-SAC model yielded more prominent differences among the hydrocarbons, and even these differences were not observed in every system.

Further, ternary systems containing ethanol + water + third component were analyzed. When the third component is butanol, both F-SAC and UNIFAC(LLE) presented a significant decrease in their accuracy compared to when other alcohols were used as third component, while the COSMO-SAC has maintained its level of accuracy, which suggests that the use of the latter model for bioethanol fuel blends with butanol provides the most reliable predictions.

When the third component was a hydrocarbon, the presence of heptene caused degeneracy in the predictions of all models. An investigation of the sigma-profile of the component was performed in order to verify if it was the cause of the COSMO-SAC predictions worsening, which was not confirmed.

Thus, the UNIFAC(LLE), although its own predictions flaws, is still the most reliable model among the three models tested for liquid-liquid equilibrium predictions for ternary systems. Further investigations using the several versions of COSMO-SAC and COSMO-RS models are still needed. For now, the UNIFAC(LLE) is the most

advisable model to be used for ternary LLE calculations, specially for acetic acid removal and aromatic compounds, due both its accuracy and computational effort.

Acknowledgements

The authors would like to thank to the Brazilian Coordination for the Improvement of Higher Education Personnel (CAPES) for the financial support.

Abbreviations

AAD – Average absolute deviation

COSMO-SAC – Conductor-like screening segment activity coefficient model

F-SAC – Functional segment activity coefficient model

IDAC – Infinite-Dilution Activity Coefficient

LLE – Liquid-liquid equilibrium

SD – Standard Deviation

SR – Sum of residuals

UNIQUAC – Universal Quasichemical theory

VLE – Vapor-liquid equilibrium

Nomenclature

K – Ratio between both the activity coeficiente of phases I and II

P – Pressure

T – Temperature

v – Number of moles in the light-phase

x – Molar fraction in liquid-phase

y – Molar fraction in vapor-phase

z – Feed composition

γ – Activity coefficient

Subscripts and Superscripts

$calc$ – Calculated value

exp – Experimental data

i – Component

I and II – Phases (e.g., aqueous and organic)

REFERENCES

[1] A. Klamt, G. Schüürmann, COSMO: a new approach to dielectric screening in solvents with explicit expressions for the screening energy and its gradient, J. Chem. Soc., Perkin Trans. 2. (1993) 799–805. doi:10.1039/P29930000799.

[2] A. Klamt, Conductor-like Screening Model for Real Solvents: A New Approach to the Quantitative Calculation of Solvation Phenomena, J. Phys. Chem. 99 (1995) 2224–2235. doi:10.1021/j100007a062.

[3] A. Klamt, The COSMO and COSMO-RS solvation models, Wiley Interdiscip. Rev. Comput. Mol. Sci. 8 (2018) 1–11. doi:10.1002/wcms.1338.

[4] A. Klamt, V. Jonas, T. Bürger, J.C.W. Lohrenz, Refinement and Parametrization of COSMO-RS, J. Phys. Chem. A. 102 (1998) 5074–5085. doi:10.1021/jp980017s.

[5] A. Klamt, COSMO-RS: From Quantum Chemistry to Fluid Phase Thermodynamics and Drug Design, Elsevier, 2005.

[6] A. Klamt, F. Eckert, COSMO-RS: a novel and efficient method for the a priori prediction of thermophysical data of liquids, Fluid Phase Equilib. 172 (2000) 43–72. doi:10.1016/S0378-3812(00)00357-5.

[7] S.-T. Lin, S.I. Sandler, A Priori Phase Equilibrium Prediction from a Segment Contribution Solvation Model, Ind. Eng. Chem. Res. 41 (2002) 899–913. doi:10.1021/ie001047w.

[8] S.T. Lin, S.I. Sandler, Infinite dilution activity coefficients from Ab initio solvation calculations, AIChE J. 45 (1999) 2606–2618. doi:10.1002/aic.690451217.

[9] A. Ben-Naim, Solvation Thermodynamics, Plenum Press, New York, 1987.

[10] A. Fredenslund, R.L. Jones, J.M. Prausnitz, Group-contribution estimation of activity coefficients in nonideal liquid mixtures, AIChE J. 21 (1975) 1086–1099. doi:10.1002/aic.690210607.

[11] U. Weidlich, J. Gmehling, A modified UNIFAC Model. 1. Prediction of VLE, hE, and y∞, Ind. Eng. Chem. Res. 26 (1987) 1372–1381. doi:10.1021/ie00067a018.

[12] S.T. Lin, J. Chang, S. Wang, W.A. Goddard, S.I. Sandler, Prediction of vapor pressures and enthalpies of vaporization using a COSMO solvation model, J. Phys. Chem. A. 108 (2004) 7429–7439. doi:10.1021/jp048813n.

[13] S. Wang, S.I. Sandler, C.C. Chen, Refinement of COSMO-SAC and the applications, Ind. Eng. Chem. Res. 46 (2007) 7275–7288. doi:10.1021/ie070465z.

[14] C.M. Hsieh, S.I. Sandler, S.T. Lin, Improvements of COSMO-SAC for vapor-liquid and liquid-liquid equilibrium predictions, Fluid Phase Equilib. 297 (2010) 90–97. doi:10.1016/j.fluid.2010.06.011.

[15] R. Xiong, S.I. Sandler, R.I. Burnett, An improvement to COSMO-SAC for predicting thermodynamic properties, Ind. Eng. Chem. Res. 53 (2014) 8265–8278. doi:10.1021/ie404410v.

[16] R. de P. Soares, R.P. Gerber, Functional-Segment Activity Coefficient Model. 1. Model Formulation, Ind. Eng. Chem. Res. 52 (2013) 11159–11171. doi:10.1021/ie400170a.

[17] R. de P. Soares, R.P. Gerber, L.F.K. Possani, P.B. Staudt, Functional-Segment Activity Coefficient Model. 2. Associating Mixtures, Ind. Eng. Chem. Res. 52 (2013) 11172–11181.

[18] T. Magnussen, P. Rasmussen, A. Fredenslund, Unifac Parameter Table for Prediction of Liquid-Liquid Equilibria, Ind. Eng. Chem. Process Des. Dev. 20 (1981) 331–339. doi:10.1021/i200013a024.

[19] L.R. Roque, R.R. Pinto, L.H. de Oliveira, S.C. Rabelo, Liquid-liquid equilibrium data for ternary systems of water + acetic acid+ acetate esters at 293.2 K and 303.2 K and ≈ 95 kPa, Fluid Phase Equilib. 463 (2018) 34–47. doi:10.1016/j.fluid.2018.02.003.

[20] C. Yu, S. Wu, Y. Zhao, Z. Zeng, W. Xue, Liquid-Liquid Equilibrium Data of Water + Butyric Acid + {Butanal or n-Butanol} Ternary Systems at 293.15, 308.15, and 323.15 K, J. Chem. Eng. Data. 62 (2017) 2244–2252. doi:10.1021/acs.jced.6b00941.

[21] T.M. Letcher, S. Ravindran, S.E. Radloff, Liquid-liquid equilibria for mixtures of an alkanol + diisopropyl ether + water at 25° C, Fluid Phase Equilib. 71 (1991) 177–188.

[22] T.M. Letcher, B.C. Bricknell, S.E. Radloff, J.D. Sewry, Liquid-liquid equilibria for mixtures of an alkanol + hept-1-ene + water at 25 C, J. Chem. Eng. Data. 39 (1994) 320–323.

[23] T.M. Letcher, P.M. Siswana, Liquid-liquid equilibria for mixtures of an alkanol + water + a methyl substituted benzene at 25??C, Fluid Phase Equilib. 74 (1992) 203–217. doi:10.1016/0378-3812(92)85062-D.

[24] T.M. Letcher, S. Wootton, B. Shuttleworth, C. Heyward, Phase equilibria for (n-heptane + water + an alcohol) at 298.2 K, J. Chem. Thermodyn. 18 (1986) 1037–1042. doi:10.1016/0021-9614(86)90017-0.

[25] J.F. McCants, J.H. Jones, W.H. Hopson, Ternary Solubility Data for Systems Involving 1-Propanol and Water, Ind. Eng. Chem. 45 (1953) 454–456. doi:10.1021/ie50518a054.

[26] M. van Berlo, M.T. Gude, L. a. M. van der Wielen, K.C. a. M. Luyben, Partition coefficients and solubilities of glycine in the ternary solvent system 1-butanol + ethanol + water, Ind. Eng. Chem. Res. 36 (1997) 2474–2482. doi:10.1021/ie960762w.

[27] S. Kadir, M. Decloux, P. Giampaoli, X. Joulia, Liquid–Liquid Equilibria of the Ternary Systems 3-Methyl-1-butanol + Ethanol + Water and 2-Methyl-1-propanol + Ethanol + Water at 293.15 K, J. Chem. Eng. Data. 53 (2008) 910–912. doi:10.1021/je700558x.

[28] S. Bekri, D. Özmen, A. Özmen, Correlation of Experimental Liquid-Liquid Equilibrium Data for Ternary Systems Using NRTL and GMDH-Type Neural Network, J. Chem. Eng. Data. 62 (2017) 1797–1805. doi:10.1021/acs.jced.6b00985.

[29] J.C. Thermodynamics, X. Liu, X. Zhang, Solvent screening and liquid-liquid measurement for extraction of phenols from aromatic hydrocarbon mixtures, J. Chem. Thermodyn. 129 (2019) 12–21. doi:10.1016/j.jct.2018.09.006.

[30] Y. Yoshimoto, E. Kinoshita, L. Shanbu, T. Ohmura, Influence of 1-butanol addition on diesel combustion with palm oil methyl ester/gas oil blends, Energy. 61 (2013) 44–51. doi:10.1016/j.energy.2012.11.039.

[31] A. Atmanli, Comparative analyses of diesel-waste oil biodiesel and propanol, n-butanol or 1-pentanol blends in a diesel engine, Fuel. 176 (2016) 209–215. doi:10.1016/j.fuel.2016.02.076.

[32] I.B.C. de Aguiar, T.R.M. Souza, M.A.M. Justino, A. de Oliveira, Performance and Emissions of a Diesel Engine Fueled By Diesel Oil-Ethanol-N-Butanol Blends, SAE Int. - Tech. Pap. Ser. (2017).

[33] C.L. Silveira, N.P.G. Salau, From Wilson to F-SAC: A comparative analysis of correlative and predictive activity coefficient models to determine VLE and IDAC of binary systems, Fluid Phase Equilib. 464 (2018) 1–11.

[34] G.N. Escobedo-Alvarado, S.I. Sandler, Study of EOS-Gex Mixing Rules for Liquid-Liquid Equilibria, AIChE J. 44 (1998) 1178–1187.

[35] M.L. Michelsen, The Isothermal Flash Problem. Part I. Stability, Fluid Phase Equilib. 9 (1982) 1–19.

[36] M.L. Michelsen, The Isothermal Flash Problem. Part II. Phase-Split Calculation, Fluid Phase Equilib. 9 (1982) 21–40.

[37] I.S.V. Segtovich, A.G. Barreto, F.W. Tavares, Simultaneous multiphase flash and stability analysis calculations including hydrates, Fluid Phase Equilib. 413 (2016) 196–208. doi:10.1016/j.fluid.2015.10.030.

[38] A.A. Izadpanah, M. Vafaie Sefti, F. Varaminian, Multi-component-multiphase flash calculations for systems containing gas hydrates by direct minimization of Gibbs free energy, Iran. J. Chem. Chem. Eng. 25 (2006) 27–34.

[39] S.K. Wasylkiewicz, L.N. Sridhar, M.F. Doherty, M.F. Malone, Global Stability Analysis and Calculation of Liquid−Liquid Equilibrium in Multicomponent Mixtures, Ind. Eng. Chem. Res. 35 (1996) 1395–1408. doi:10.1021/ie950049r.

[40] Z. Li, Thermodynamic Modelling of Liquid – liquid Equilibria Using the Nonrandom Two-Liquid Model and Its Applications, The University of Melbourne, 2015.

[41] H.H. Rachford, J.D. Rice, Procedure for Use of Electronic Digital Computers in Calculating Flash Vaporization Hydrocarbon Equilibrium, J. Pet. Technol. 4 (1952) 19–3. doi:10.2118/952327-G.

[42] L.F.K. Possani, Correlação Simultânea de IDAC, VLE e LLE com o Modelo F-SAC, (2014). http://www.lume.ufrgs.br/bitstream/handle/10183/107500/000945081.pdf?sequence=1.

[43] M.J.D. Powell, A Fortran subroutine for solving systems of nonlinear algebraic equations, (1968).

[44] A.C. Hansen, Q. Zhang, P.W.L. Lyne, Ethanol – diesel fuel blends — a review, 96 (2010) 277–285. doi:10.1016/j.biortech.2004.04.007.

APPENDIX A

LLE Flash Calculations Algorithm

1. z_i, T, and P are specified;
2. Initial guesses are given for x_i^I and x_i^{II};
3. γ_i^I and γ_i^{II} are calculated (using COSMO-SAC, F-SAC, or UNIFAC);
4. K_i is calculated ($K_i = \gamma_i^{II}/\gamma_i^I$);
5. v is calculated by: $1 - \sum_{i=1}^{NC} \frac{K_i z_i}{1+v(K_i-1)} = 0$;
6. Values for x_i^I and x_i^{II} are calculated using:

   $x_i^I = \frac{z_i}{\frac{1-v}{K_i}+v}$

   $x_i^{II} = \frac{z_i - v x_i^I}{1-v}$

7. If $\left|x_{i,old}^I - x_i^I\right| < \varepsilon$ and $\left|x_{i,old}^{II} - x_i^{II}\right| < \varepsilon$: END

   Else:

   $x_{i,new}^I = \frac{|x_{i,old}^I + x_i^I|}{2}$

   $x_{i,new}^{II} = \frac{|x_{i,old}^{II} + x_i^{II}|}{2}$

8. Return to step 3.

5 DAS REGRAS DE MISTURA: PREDIÇÕES DE ELV PARA SISTEMAS BINÁRIOS

On the mixing rules matter: the VLE predictions for binary systems.

Christian Luiz da Silveira[3]

Nina Paula Gonçalves Salau

Chemical Engineering Department
Universidade Federal de Santa Maria

ABSTRACT

Mixing rules are used to extend the range of applicability of both equations of state and excess Gibbs energy models. The equations of state are limited by the molecules complexity, whilst the excess Gibbs energy constraint is the range of temperature and pressure. Mixing rules allow the coupling of both types of thermodynamics models to overcome such limitations. In this work, the analysis of the performance of 5 excess Gibbs energy models using the Peng-Robinson equation of state and two of its variants with 3 different mixing rules – VDW1, HVOS, and WS. Great accuracy of the UNIFAC and UNIFAC(Do) models, especially when using the VDW1 mixing rule to couple with either PRSV or PRSV2, was obtained. The F-SAC model has provided reliable results as well. In addition, evaluations over the performance of the excess Gibbs energy, the equations of state, and the mixing rules were made separately, in order to better analyze their results. The COSMO-SAC model was greatly affected by the HVOS mixing rule, leading to very high objective function values.

Keywords: vapor-liquid equilibrium; mixing rules; COSMO-SAC; F-SAC; UNIFAC; Peng-Robinson.

[3] To whom all correspondence should be addressed. E−mail: christiansilveira86@gmail.com
Address: Chemical Engineering Department, UFSM − Av. Roraima, 1000, Cidade Universitária −Bairro Camobi. 97105-900 Santa Maria, RS − Brazil.
Phone: +55-55-3220-8448- Fax: +55-55-3220-8030.

1 INTRODUCTION

Equations of State (EOS) have been widely used in the industry. Mathias and Koltz [1] reported the “extremely effective” use of the EOS in industrial applications, such as modeling, design and thermodynamics properties predictions (density, fugacity, enthalpy, and entropy). The authors highlighted the surprisingly good performance of the EOS models, specially of those based on van der Waals, even though their weak theoretical basis [1].

The EOS, however, range from the virial equation (applicable only at low densities) to cubic EOS that, although their good performance for a wide range of temperature and pressure, can only be used for relatively simple mixtures, that do not hydrogen bond or otherwise associate. To avoid the limitation of the cubic EOS, excess Gibbs energy (EGE) models can be used for modeling low-pressure liquid-phase systems. In fact, they have been successfully used for molecules with wide degree of complexity, but they are mainly applicable to compressed liquids [2,3].

The use of mixing rules (MR) combining EOS and EGE models for extending their ranges of application has been extensively studied, and this approach has shown very good results, as can be seen in the works of Asselineau et al. [4], Wong and Sandler [5], Orbey and Sandler [6], Silveira and Sandler [2], and many others.

While several mixing rules have been developed throughout the years, some of these mixing rules seem to fail at different composition, temperature, and pressure conditions, either because of the range of applicability or because of the components of the mixture, like highly polar components [5,7–12].

Shibata and Sandler [13] depicted, in an easy method, the application of a mixing rule to expand the use of EOS from pure component to mixtures. The authors used this method in an example for the classic one-fluid rules of van der Waals, a very similar example was also presented by Wong and Sandler [5], as depicted in the Equations 1-4:

$$a_m = \sum_{i=1}^{NC} \sum_{j=1}^{NC} x_i x_j a_{ij} \quad (1)$$

$$b_m = \sum_{i=1}^{NC} \sum_{j=1}^{NC} x_i x_j b_{ij} \quad (2)$$

$$a_{ij} = a_{ji} = \sqrt{a_{ii}\, a_{jj}}\left(1 - k_{ij}\right) \quad (3)$$

$$b_{ij} = \frac{b_i + b_j}{2} \quad (4)$$

Where NC is the number of components, the subscripts i and j are the mixture components, a_{ii} and b_{ii} are the pure-component parameters of the EOS (e.g., Peng-Robinson), a_m and b_m are the mixture parameters, a_{ij} and b_{ij} are the cross-parameters, obtained by equations 3 and 4, and k_{ij} is the binary interaction parameter.

In this work, three different mixing rules are used: one-fluid van der Waals (VDW1), Huron-Vidal-Orbey-Sandler (HVOS), and Wong-Sandler (WS). Although there are several mixing rules nowadays [10,12,14–17], the three mixing rules aforementioned were chosen based on very simple criteria: the MRs should be very simple and easy to program computationally, they should be known and already extensively tested, and they should satisfy the quadratic dependency on composition of the second virial coefficient.

Even though the second virial coefficient composition dependency might have been considered unimportant for the calculation of phase behavior, the expression for fugacity coefficient of a species in a mixture reveals the dependency of the pressure

on the composition, consequently affecting the fugacity of the species [18]. Orbey and Sandler [18] argue that not only the Huron-Vidal mixing rule violates the aforementioned boundary of the second virial coefficient, but the well-known MHV1 and MHV2 as well. Hence, these rules, although very useful, were not included in this work.

The VDW1 [19] couples the EOS with the activity coefficient (AC) model through the excess Gibbs energy (Equation 5) and one binary-interaction parameter k_{ij}, the HVOS [6] uses the excess Helmholtz energy (EHE) instead of the Gibbs energy (Equation 6) but no binary-interaction parameter, and the WS [5] mixing rule uses the EHE with one k_{ij}.

$$\bar{G}_{\infty}^{ex} = C^{*}\left(\frac{a_m}{b_m} - \sum_{i=1}^{NC} x_i \frac{a_{ii}}{b_{ii}}\right) \tag{5}$$

$$\bar{A}_{\infty}^{ex} = C^{*}\left(\frac{a_m}{b_m} - \sum_{i=1}^{NC} x_i \frac{a_{ii}}{b_{ii}}\right) \tag{6}$$

Where $\bar{G}_{\infty}^{ex}$ and $\bar{A}_{\infty}^{ex}$ are the molar excess Gibbs and Helmholtz energies at infinite pressure, and C^{*} is a constant whose value depends on the EOS used. For the van der Waals EOS, C^{*} is -1; for the Peng-Robinson, C^{*} is -0.62323. Further details about how to obtain this constant can be found on Wong and Sandler work [5] (especially in the Appendix section).

Hence, to combine the EOS with the EGE model, the VDW1 mixing rule used is defined by equations 1-5. The WS mixing rule is defined by equations 7-9:

$$\frac{a_m}{b_m} = \left(\frac{\bar{A}_{\infty}^{ex}}{C^{*}} + \sum_i x_i \frac{a_i}{b_i}\right) \tag{7}$$

$$b_m = \frac{RT\ \sum_i \sum_j x_i x_j \left(b_m - \frac{a_m}{RT}\right)_{ij}}{RT - \left[\sum_i x_i \left(\frac{a_i}{b_i}\right) + \frac{\bar{A}_\infty^{ex}}{C^*}\right]} \quad (8)$$

Where

$$\left(b_m - \frac{a_m}{RT}\right)_{ij} = \frac{1}{2}\left(b_i + b_j\right) - \frac{\sqrt{a_i a_j}}{RT}\left(1 - k_{ij}\right) \quad (9)$$

Since the HVOS mixing rule does not contain a binary interaction parameter k_{ij}, this mixing rule is defined by equations 6,10-11:

$$\frac{a_m}{b_m} = RT\left\{\sum_i x_i \frac{a_i}{b_i RT} + \frac{1}{C^*}\left[\frac{\bar{A}_\infty^{ex}}{RT} + \sum_i x_i \ln\left(\frac{b_m}{b_i}\right)\right]\right\} \quad (10)$$

$$b_m = \sum_i x_i b_i \quad (11)$$

The use of Helmholtz instead of Gibbs energy on the WS Mixing Rule is justified by the Equation 12, which allows a theoretically correct extension from low to high pressure conditions, since the Helmholtz energy is a weak function of pressure.

$$Activity\ Coefficient\ Model = \bar{G}^{ex}(T, x, P = low) = \bar{A}^{ex}(T, x, P = low) = \bar{A}^{ex}(T, x, P = \infty) \quad (12)$$

The use of $\bar{G}^{ex}$, however, requires that the excess volume at infinite pressure be zero, and thus $\bar{G}^{ex}$ can be a finite number calculated through an EOS; otherwise the second term of Equation 13 becomes infinite, and so does the excess Gibbs free energy too; then $\bar{G}^{ex}$ is not related to an activity coefficient model [2,5].

$$\bar{G}^{ex} = \bar{A}^{ex} + P\bar{V}^{ex} \quad (13)$$

In this work, the original Peng-Robinson EOS [20] and two of its variants, PRSV [21] and PRSV2 [22], are coupled to activity coefficient models. This approach allows the extension of the applicability over a wide range of molecules complexity and of system conditions (e.g., temperature, pressure, and composition) with only one adjustable parameter, the binary interaction parameter k_{ij}, when using the VDW1 and WS, or no parameters when using the HVOS mixing rule.

5 excess Gibbs energy models were used to obtain the activity coefficient. The UNIQUAC [23] model was used as a reference, since it is the only correlative model used. The other models were UNIFAC [24], UNIFAC(Do) [25,26], COSMO-SAC [27–30], and F-SAC [31,32]. For further details on each of the 5 EGE models, the reader is directed to the cited literature. A brief review about each of the aforementioned models and their performances can be found in the work of Silveira and Salau [28].

The COSMO-SAC model coupled with the PRSV EOS has shown good results in the vapor-liquid equilibrium (VLE) predictions, as reported by Silveira and Sandler [2]. In this work, different and more recent EGE models are used to obtain the VLE predictions. Each activity coefficient model was associated to the 3 EOS through a MR, leading to a comprehensive combination of them all (45 different associations).

The performance of each of the associations is evaluated using experimental data available in literature for 32 binaries systems, i. e. a total of 6141 experimental points were used. The literature experimental data used in this work was isothermally obtained, therefore only a Bubble-point Pressure algorithm was used to calculate the

VLE. Hence, main goal of this work was to give to the reader directions on each system, and how each of the coupled models behave on the predictions.

2 MODELING, SIMULATION AND PARAMETER ESTIMATION

2.1 k_{ij} estimation method

The main idea of the use of mixing rules is to extend the applicability of both EOS and EGE models. It is usually easier to obtain information about a system at low temperature and pressure conditions, thus the binary interaction parameter k_{ij} of each system was estimated only at the lowest temperature of the isothermal VLE data obtained. This procedure was used by Silveira and Sandler [2] as well and the results can be seen in the Table A1, Appendix A, of their work.

After obtaining the k_{ij} parameters, the VLE calculations over the entire range of the available data was performed. Using this approach, the best fit may not be obtained; however, the situation where no access to data over larger ranges of temperature and pressure is granted was considered. The differences between these two parameter estimation procedures are reported by Silveira and Sandler [2].

Also, since the binary interaction parameter is considered independent of temperature, pressure, and composition, there is only one value of k_{ij} for each of the binaries.

The *lsqnonlin* function embedded in MATLAB® was used to perform the parameter optimization. The *lsqnonlin* function solves a nonlinear least-squares problem by the minimization of a specific Objective Function (e.g., Equation 14). The algorithm used in this case was the Levenberg-Marquardt [33] (LMA).

No boundaries were set during the k_{ij} parameter estimation, and different initial guesses were used for each optimization procedure, assuring the global minima of the objective function. The k_{ij} values will be presented in the Appendix section, Table A1.

2.2 Computational details

To perform the calculations necessary for this work, a Laptop with Intel® Core™ i7-6700HQ CPU @ 2.60GHz and 16.0 GB of RAM memory running on Windows 10 was used; with exception for the F-SAC activity coefficient calculations performed in a Laptop with Intel® Core™ i7-2720QM CPU @ 2.20GHz and 8.0 GB of RAM memory running on Kubuntu 16.04 LTS.

The objective function (OF) to be minimized in the optimization algorithm of the *lsqnonlin* function is represented by Equation 14

$$OF = \frac{\sum_{i=1}^{NP}\frac{\left|P_{exp,i}-P_{calc,i}\right|}{P_{exp,i}}+\sum_{i=1}^{NP}\frac{\left|y_{exp,i}-y_{calc,i}\right|}{y_{exp,i}}}{NY} \quad (14)$$

Where NY is the number of experimental points available for the system, the subscripts exp and $calc$ refer to the experimental and calculated values, respectively.

The number of available experimental points for each system can be seen in Table 1, as well as the experimental data source. The asymmetry ratio of the systems is also depicted, as it will be discussed in Section 3.1. It may be highlighted that all the pressure data obtained in literature was converted to bar before the calculations (1 bar = 10^5 Pa).

Table 1. Binaries systems and their number of experimental points and sources.

System Number	Component 1	Component 2	b_1/b_2	*NY*	Source
1	Acetone	Methanol	1.70	117	[34]
2	Acetone	Water	3.68	216	[34]
3	Butane	Methanol	1.77	138	[35,36]
4	Butanol	Decane	0.43	126	[37]
5	Butanol	Heptane	0.64	207	[37]
6	Butanol	Hexane	0.75	261	[37–39]
7	Butanol	Nonane	0.49	189	[37]
8	Butanol	Octane	0.55	120	[37]
9	Butanol	Pentane	0.91	171	[37]
10	Ethanol	Butane	0.74	171	[37]
11	Ethanol	Heptane	0.42	276	[37]
12	Ethanol	Hexane	0.49	150	[37]
13	Ethanol	Nonane	0.32	207	[37]
14	Ethanol	Octane	0.36	168	[37]
15	Ethanol	Pentane	0.60	204	[37]
16	Ethanol	Water	2.85	252	[40]
17	1-Pentanol	Heptane	0.76	387	[37,41]
18	Heptane	3-Methyl-1-Butanol	1.32	231	[41]
19	Methanol	Benzene	0.55	210	[42]
20	Methanol	Hexane	0.37	222	[37]
21	Methanol	Water	2.15	189	[34]
22	1-Pentanol	Decane	0.51	165	[37]
23	1-Pentanol	Hexane	0.89	153	[37]

24	1-Pentanol	Octane	0.65	153	[37]
25	1-Pentanol	Pentane	1.08	171	[37]
26	Pentane	Methanol	2.20	99	[43]
27	1-Propanol	Heptane	0.52	165	[37]
28	1-Propanol	Hexane	0.61	171	[37]
29	1-Propanol	Nonane	0.40	204	[37]
30	1-Propanol	Octane	0.45	252	[37]
31	1-Propanol	Undecane	0.32	165	[37]
32	2-Propanol	Water	3.63	231	[40]

2.3 The UNIQUAC optimization

The parameters necessary for the UNIQUAC calculation were not always available in literature, hence, it was necessary to estimate their values for some of the systems used. All the UNIQUAC binary interaction parameters, estimated and literature parameters, will be listed in Table 5, along with their source when applicable.

The estimation of the UNIQUAC parameters was performed using the modified Raoult's Law, as given by Equation 15

$$y_i = \frac{x_i \gamma_i P_i^{sat}}{P} \tag{15}$$

Where γ_i is the activity coefficient obtained by the UNIQUAC model and P_i^{sat} is the saturation pressure of the component i.

The *lsqnonlin* function with the LMA was used once again to estimate the binary parameters $(u_{21} - u_{11})$ and $(u_{12} - u_{22})$ of the UNIQUAC model.

3 RESULTS AND DISCUSSION

The results and discussion section will be divided in 5 parts: the first part will evaluate the performance solely of the mixing rules applied to the models; the second part will analyze the results obtained related to the EOS; the third part will focus on the activity coefficient models; the fourth part will discuss the temperature influence on the results, and the fifth and last part will analyze the overall results.

3.1 Mixing rules

To analyze the performance of the mixing rules, the summation over the objective function of every binary system for every combination of EOS-EGE model was used for each of mixing rule. For example, to evaluate the performance of the VDW1 mixing rule, the sum of the objective function value obtained in every binary system and every EOS-EGE combination (PR-UNIQUAC, PRSV-UNIQUAC, PRSV2-UNIQUAC, PR-UNIFAC, PRSV-UNIFAC, and so on) using only the VDW1 MR was used. The statistic results of these evaluations are presented in Table 2.

Table 2. Mixing rules results statistics.

MR	Sum of OF	Average	Average SD	Variance
VDW1	582.9883	1.4272	0.8375	6.4590
HVOS	2468.2964	5.1423	5.7904	133.7485
WS	611.6144	1.2742	0.6875	0.6537

It can be seen from Table 2 that the VDW1 was the mixing rule with the smallest OF value, followed by the WS. In fact, the average of the OF value obtained by the VDW1 is roughly 5% smaller than the one obtained by the WS, and the average of the standard deviation is also smaller for VDW1, thus the predictions of this mixing rule are more accurate. The HVOS performance, however, was very different from the other two. The unsatisfactory results of the HVOS suggested that the use of this mixing rule may be avoided; instead, VDW1 or WS may be used.

Furthermore, the performance of each mixing rule can be analyzed as a function of the number of carbons associated with the alcohols. To illustrate that, Figure 1 depicts the behavior of each mixing rule when the number of carbons of the alkane associated with an alcohol is varied.

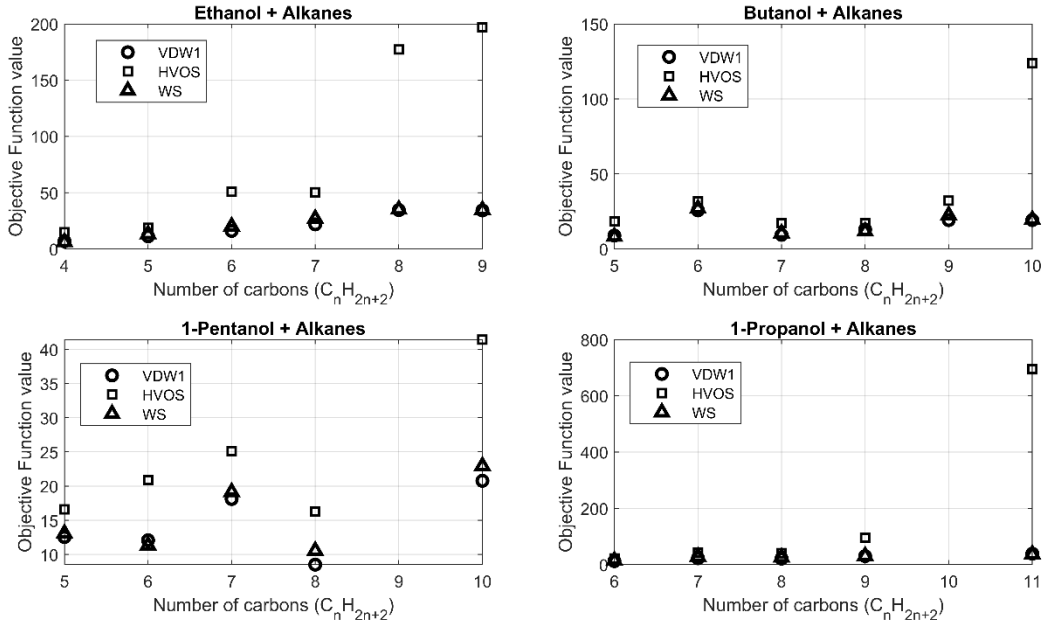

Figure 1. Mixing rules performance as a function of number of carbons.

It is perceivable from Figure 1 that when the number of carbons increases the errors also increase, especially if the HVOS mixing rule is used. Although all the mixing

rules seem to be similarly affected as the number of carbons increases, the HVOS mixing rule consistently presented the larger deviations - particularly when the alcohols are associated with the alkanes with larger carbon chain -, being roughly 4 times less accurate than the other mixing rules for the Ethanol + Nonane system, and more than 6 times less accurate for the 1-Propanol + Undecane system.

Additionally, an interesting relation to notice would be any correlation between the mixing rules and the nonideality or the asymmetry of the systems. One of the shortcomings of the van der Waals one-fluid mixing rules, as reported by Sandler and Orbey [44], is that they are applicable to mixtures that exhibit relatively moderate solution nonidealities. However, no trend was found when analyzing the results of the 32 systems with the 3 mixing rules tested (Table A2).

Concerning to the asymmetry of the system, Coutsikos et al. [45] reported a deterioration in the accuracy of the WS mixing rule as the asymmetry of the system increases, yet no evidence of such behavior was found in the systems tested in this work (Table A2). The degree of asymmetry was calculated by the ratio between the co-volume parameters of the components of the mixture, b_1/b_2. The larger the value of the ratio, the more asymmetric the system [45]. The asymmetry ratios of the systems are presented in Table 1.

3.2 Equations of state

When the EOS are analyzed, the differences are less noticeable. In their paper, Silveira and Sandler [2] found the PRSV, associated with either COSMO-SAC or NRTL through the WS mixing rule, to be the EOS that best predicted the VLE data. In the

present work, nevertheless, this advantage is not as evident; in fact, the PRSV2 offered the smallest value of the objective function, as shown in Table 3.

Table 3. EOS results statistics.

EOS	Sum of OF	Average	Average SD	Variance
PR	1315.0298	2.7396	2.4275	52.1770
PRSV	1175.4850	2.4489	2.3266	47.7854
PRSV2	1172.3844	2.4425	2.2542	45.0539

Although the PRSV performance was still good in this work, the PRSV2 outperformed the other two EOS, resulting in not only the smallest objective function value but also in the smallest average standard deviation and in the smallest residual average. However, the choice of the EOS caused small impact in the results, especially when compared to the MR choice impact. For instance, the PR was 12% less accurate than the PRSV2, while the PRSV was roughly 0.5% less accurate.

With respect to the alkanes size, Figure 2 depicts the OF of the EOS as a function of the number of carbons. It can be clearly seen that the three EOS tested are greatly affected by the number of carbons on the alkane chain. Except by the ethanol + alkanes and the 1-propanol + alkanes systems, the PR was the only EOS whose OF value was already high before reaching the larger carbon chain alkanes, while the other two EOS did not show the same trend.

With respect to the 1-pentanol + alkanes systems, no trend could be found; each EOS presented variations on its performance when the alkane size changed, however,

the PR presented residuals two to three times larger than the other EOS for the 1-pentanol + pentane, hexane, and heptane systems.

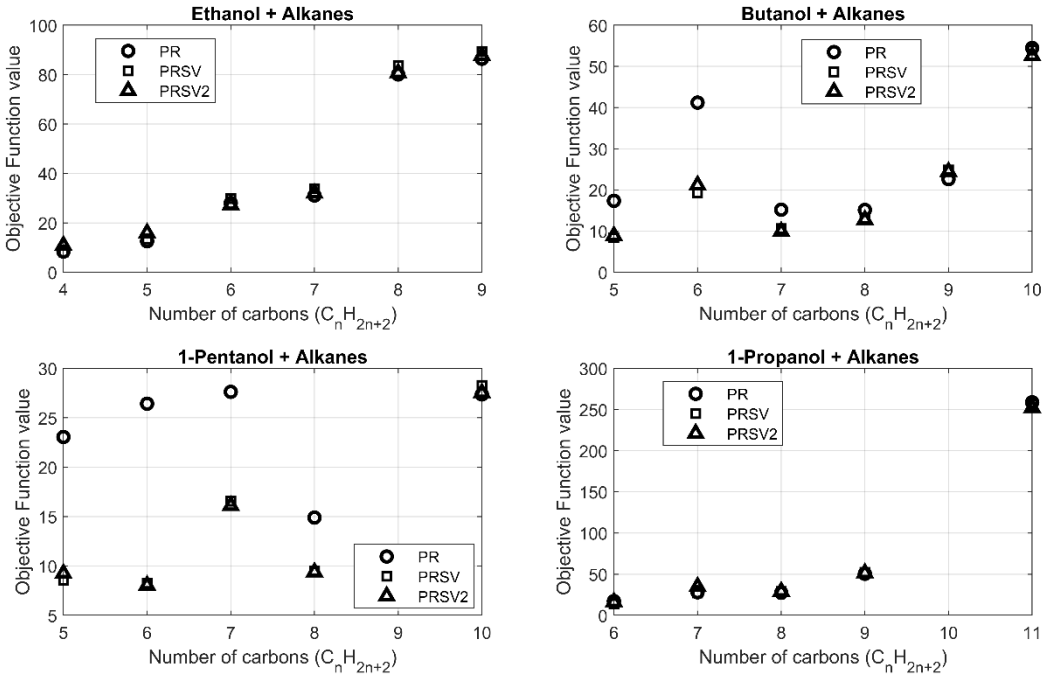

Figure 2. Equations of state performance as a function of number of carbons.

Moreover, no relations between the EOS and the symmetry of the system were found. Also, although the PRSV and PRSV2 improvements to the PR, the three EOS presented almost no difference in their residuals (Table A2 – Appendix). This result confirms the Stryjek and Vera conclusion that the selection of the mixing rule plays a more significant role in the VLE calculation [22].

3.3 Activity Coefficient models

The activity coefficient models were analyzed using the same approach that was used for the two previous items. In Table 4, it can be observed that the UNIQUAC

model was the one with the smallest objective function value. In fact, it is not surprising since, as explained in section 2.3, the UNIQUAC model parameters for several systems were estimated, using the same data used to validate the models. The parameters used in the UNIQUAC model are depicted in Table 5.

Table 4. EGE models results statistics.

Model	Sum of OF	Average	Average SD	Variance
UNIFAC	636.5647	2.2103	1.9639	27.8679
UNIFAC(Do)	690.8143	2.3987	2.1519	34.8852
UNIQUAC	503.9806	1.7499	0.9917	5.0749
COSMO-SAC	1120.0143	3.8889	4.3100	132.3748
F-SAC	711.5252	2.4706	2.3569	39.3377

If only the predictive models are analyzed (i.e. the other four EGE models besides the UNIQUAC), it can be perceived that the UNIFAC presented the smallest OF value, followed closely by both UNIFAC(Do) and F-SAC.

With respect to the COSMO-SAC model, the results were roughly twice as inaccurate than those obtained using the UNIFAC model. In fact, the largest errors obtained by the COSMO-SAC model were those provided by the predictions of the 1-Propanol + Undecane system using the HVOS mixing rule (independently of the EOS used). Those errors were responsible for roughly 28% of the inaccuracy of the COSMO-SAC accounted in Table 4.

Thus, the use of the HVOS together with the COSMO-SAC model, especially for the 1-Propanol + Undecane system, is unadvisable. In fact, the sum of the errors

obtained when the COSMO-SAC was coupled to an EOS through the HVOS mixing rule represents roughly 75% of the objective function value.

It is interesting to notice that, when the results are computed without the HVOS, each EGE model performance becomes significantly better, but the UNIFAC model is still the most accurate model, in this case followed by the F-SAC and the UNIFAC(Do), respectively. The COSMO-SAC is then 22.71% less accurate than the UNIFAC.

The good performance of the F-SAC model may be highlighted, since it is a recent and not extensively used model. The F-SAC OF values were of similar magnitude to the already well stablished UNIFAC and UNIFAC(Do) models, moreover, it greatly outperformed the COSMO-SAC model.

Table 5. UNIQUAC parameters.

Component 1	**Component 2**	$(u_{21} - u_{11})$	$(u_{12} - u_{22})$	**Source**
Acetone	Methanol	190.4200	-43.5060	[46]
Acetone	Water	-81.5607	-179.9613	[47]
Butane	Methanol	592.2400	50.9840	[36]
Butanol	Decane	502.2400	-91.5900	[48]
Butanol	Heptane	132.3760	-57.1649	*
Butanol	Hexane	968.6500	-327.3000	[48]
Butanol	Nonane	132.2177	-63.3723	*
Butanol	Octane	138.2312	-55.1164	*
Butanol	Pentane	129.7585	-68.5448	*
Ethanol	Butane	22.1920	267.1400	[36]
Ethanol	Heptane	159.9714	-31.0908	*
Ethanol	Hexane	-108.9300	1441.5700	[49]

Ethanol	Nonane	128.0757	-68.4950	*
Ethanol	Octane	136.2894	-58.5344	*
Ethanol	Pentane	-94.6100	913.5800	[48]
Ethanol	Water	1359.8000	-24.5040	[50]
1-Pentanol	Heptane	720.6200	-282.3700	[48]
Heptane	3-Methyl-1-Butanol	111.2084	-86.9980	*
Methanol	Benzene	-123.6900	935.0500	[51]
Methanol	Hexane	951.3500	1321.6000	*
Methanol	Water	-164.8000	256.6000	[52]
1-Pentanol	Decane	-74.8504	121.7240	*
1-Pentanol	Hexane	132.1393	-74.1561	*
1-Pentanol	Octane	129.0796	-66.6501	*
1-Pentanol	Pentane	306.2831	70.5908	*
Pentane	Methanol	0.1595	0.9963	[43]
1-Propanol	Heptane	394.8000	-73.3000	[53]
1-Propanol	Hexane	141.8699	-56.1505	*
1-Propanol	Nonane	127.7939	-68.6966	*
1-Propanol	Octane	139.7113	-55.3322	*
1-Propanol	Undecane	-198.9663	-436.2829	*
2-Propanol	Water	1319.9300	426.0200	[54]

*Estimated parameters

The influence of the alkanes size over the COSMO-SAC associated with an EOS is evident, as can be perceived in Figure 3. As increase the number of carbons increases, the errors of the COSMO-SAC model also increase, revealing a serious flaw

on its predictions. Although the same behavior is observed with the other activity coefficient models, they occur in a much smaller scale.

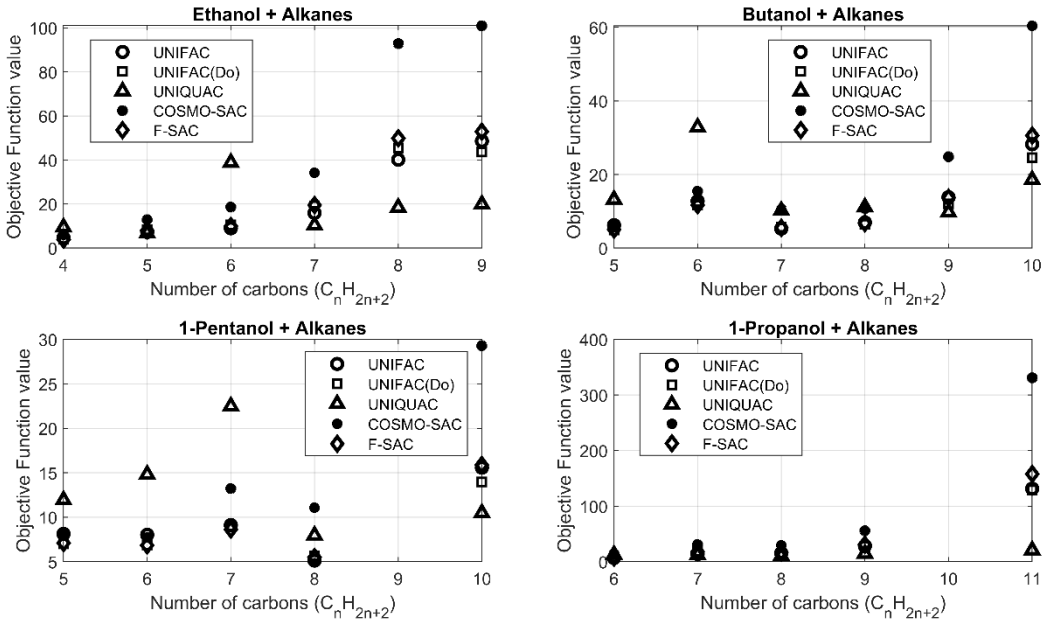

Figure 3. Activity coefficient models performance as a function of number of carbons.

Additionally and following the EOS results, the Activity Coefficient models did not show any specific behavior as the asymmetry of the systems increased nor when comparing systems of polar + polar, polar + weakly polar, or polar + non-polar components.

3.4 Temperature influence

In order to evaluate the influence of the temperature on the results, the performance of the models using the PR EOS and the WS Mixing Rule with the 5 different EGE models are analyzed. The EOS and the MR were randomly selected for this sections tests.

Figure 4 depicts the performance of the 5 mentioned combinations for each binary system used in this work at different temperatures.

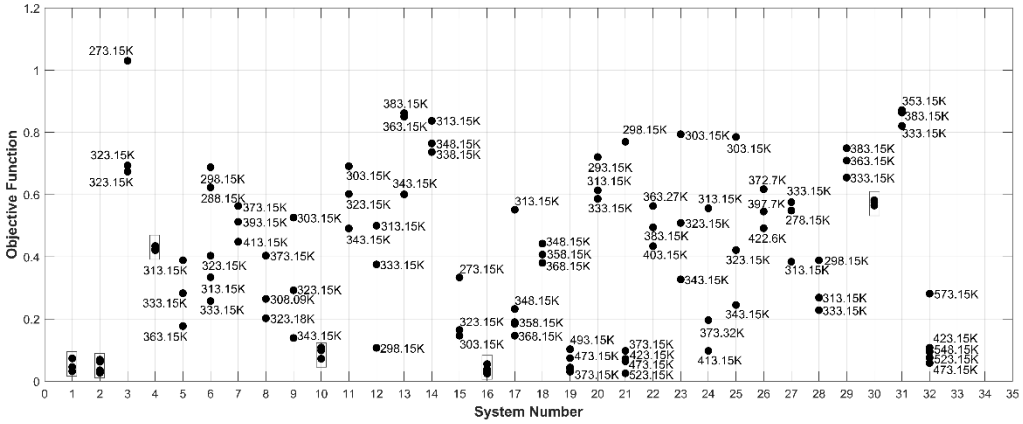

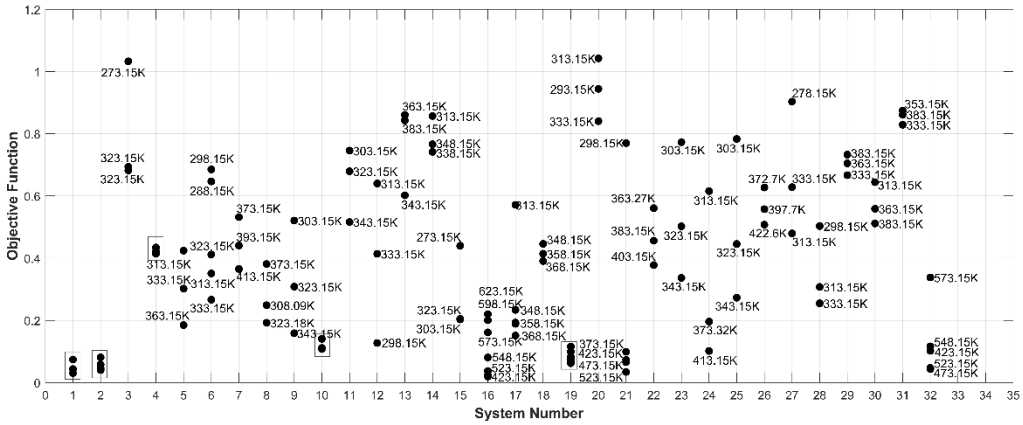

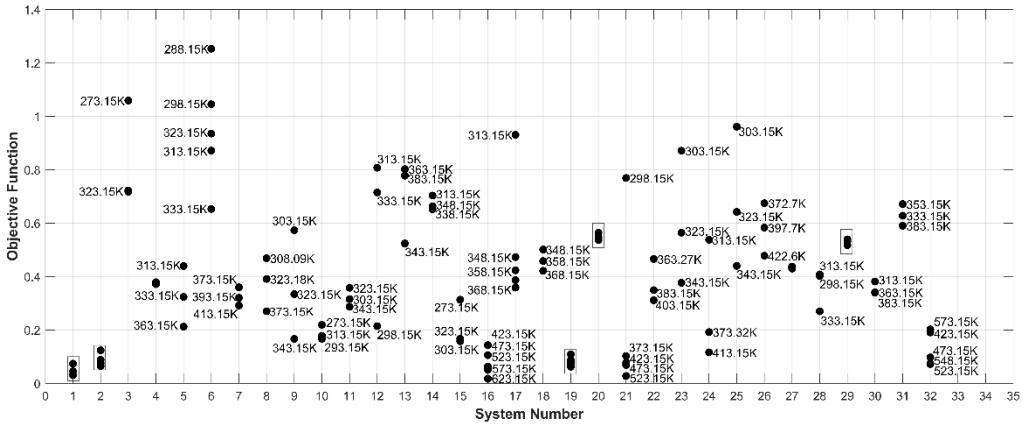

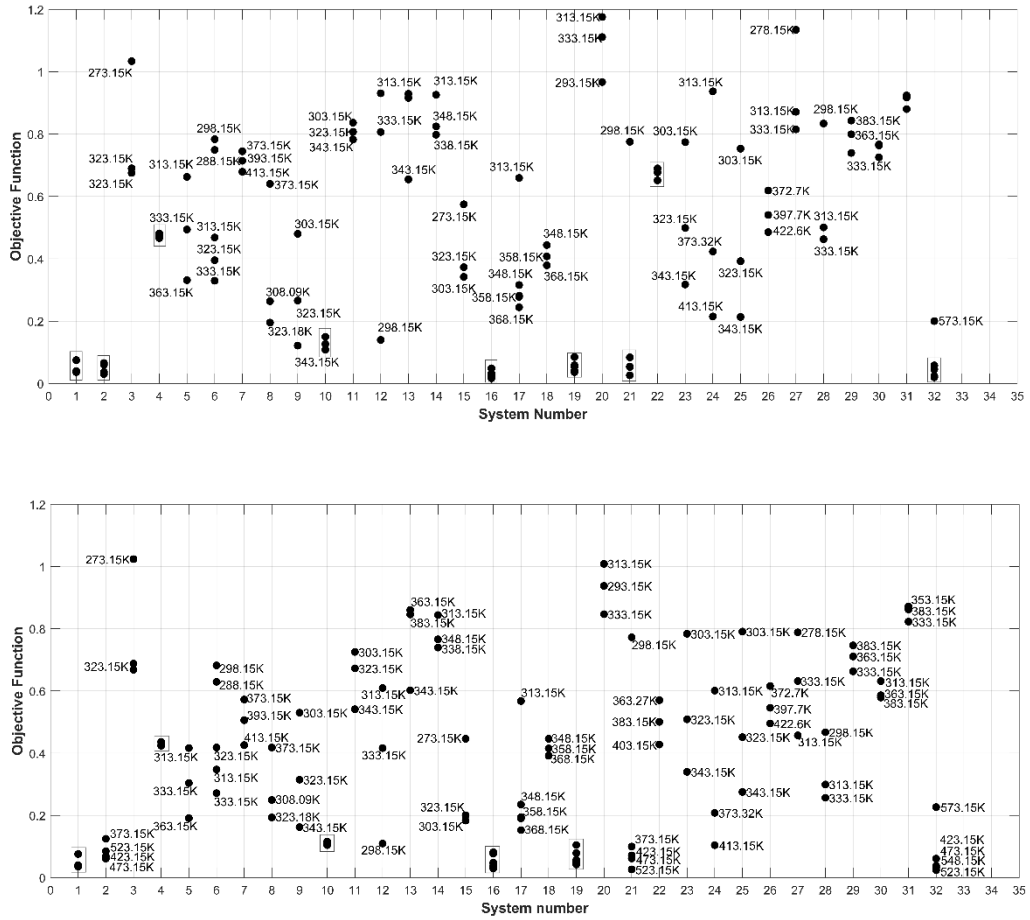

Figure 4. Evaluation of models performance at different temperatures (from top to down: UNIFAC, UNIFAC(Do), UNIQUAC, COSMO-SAC, and F-SAC + WS + PR).

The variations on the objective function value for each temperature are very similar for each of the models presented on Figure 4. The UNIQUAC model, for instance, presented larger differences in system 6, while the UNIFAC(Do) in the system 16, when compared to the others. However, those differences are very specific and no pattern can be stablish, as depicted in the Figure 4.

Moreover, the objective function value seems to behave differently for each system. For example, in the system 29 (1-Propanol + Nonane) the larger the temperature the bigger the errors; the system 7 (Butanol + Nonane), however, shows an opposite behavior; and the system 32 (2-Propanol + Water) presents larger

deviations for the highest temperature followed by the lowest temperature, for all the models except for the UNIFAC(Do).

It should be highlighted that this last alternating behavior was also found by Šerbanović et al. [55] when predicting the excess molar volume of some alcohol + aromatic mixtures.

3.5 Overall Analysis

Finally, an overall analysis was performed. It is perceivable from Table 6 that, as aforementioned, the UNIQUAC model offered very good results, probably because most of its parameters were estimated for this exact data set. Therefore, it should only be used as a reference, being unadvisable to compare it with the other models.

Table 6. Overall statistics.

Model	Mixing rule	EoS	Sum of OF	Average	Avg SD	Variance
UNIFAC	VDW1	PR	41.0971	1.2843	0.5241	0.4438
UNIFAC	VDW1	PRSV	33.9773	1.0618	0.5904	0.5072
UNIFAC	VDW1	PRSV2	35.0800	1.0962	0.5643	0.4737
UNIFAC	HVOS	PR	147.7539	4.6173	5.1904	87.2339
UNIFAC	HVOS	PRSV	134.8677	4.2146	4.9359	76.0208
UNIFAC	HVOS	PRSV2	132.3642	4.1364	4.7493	70.7219
UNIFAC	WS	PR	41.6873	1.3027	0.5876	0.4935
UNIFAC	WS	PRSV	34.2554	1.0705	0.6957	0.6168
UNIFAC	WS	PRSV2	35.4818	1.1088	0.6605	0.5627
UNIFAC(Do)	VDW1	PR	42.6223	1.3319	0.5278	0.4283
UNIFAC(Do)	VDW1	PRSV	35.4098	1.1066	0.5976	0.5223
UNIFAC(Do)	VDW1	PRSV2	36.3420	1.1357	0.5756	0.4921

UNIFAC(Do)	HVOS	PR	163.3794	5.1056	5.5764	112.5853
UNIFAC(Do)	HVOS	PRSV	148.0111	4.6253	5.2487	94.0985
UNIFAC(Do)	HVOS	PRSV2	145.4993	4.5469	5.0335	86.9001
UNIFAC(Do)	WS	PR	44.7100	1.3972	0.5890	0.5112
UNIFAC(Do)	WS	PRSV	36.9660	1.1552	0.7081	0.6671
UNIFAC(Do)	WS	PRSV2	37.8743	1.1836	0.6725	0.6192
UNIQUAC	VDW1	PR	42.7623	1.3363	0.5821	0.5886
UNIQUAC	VDW1	PRSV	36.0515	1.1266	0.5476	0.4506
UNIQUAC	VDW1	PRSV2	36.9885	1.1559	0.5314	0.4243
UNIQUAC	HVOS	PR	95.4346	2.9823	2.0051	15.7444
UNIQUAC	HVOS	PRSV	87.0713	2.7210	1.6367	11.9602
UNIQUAC	HVOS	PRSV2	85.5252	2.6727	1.5709	10.7649
UNIQUAC	WS	PR	44.3077	1.3846	0.6404	0.7999
UNIQUAC	WS	PRSV	37.4932	1.1717	0.5992	0.5540
UNIQUAC	WS	PRSV2	38.3462	1.1983	0.5879	0.5384
COSMO-SAC	VDW1	PR	47.5362	1.4855	0.6407	0.5880
COSMO-SAC	VDW1	PRSV	40.4819	1.2651	0.7506	0.7199
COSMO-SAC	VDW1	PRSV2	41.5164	1.2974	0.7176	0.6746
COSMO-SAC	HVOS	PR	293.4648	9.1708	10.4880	384.3546
COSMO-SAC	HVOS	PRSV	279.9345	8.7480	10.2905	369.9149
COSMO-SAC	HVOS	PRSV2	274.7150	8.5848	9.9497	352.8555
COSMO-SAC	WS	PR	52.1575	1.6299	0.7208	0.7666
COSMO-SAC	WS	PRSV	44.5260	1.3914	0.8280	0.9163
COSMO-SAC	WS	PRSV2	45.6820	1.4276	0.7935	0.8494
F-SAC	VDW1	PR	42.1533	1.3173	0.5425	0.4546
F-SAC	VDW1	PRSV	34.9276	1.0915	0.6196	0.5390
F-SAC	VDW1	PRSV2	36.0421	1.1263	0.5912	0.5000
F-SAC	HVOS	PR	171.8719	5.3710	6.1714	122.3155
F-SAC	HVOS	PRSV	155.0965	4.8468	5.8767	107.8060
F-SAC	HVOS	PRSV2	153.3070	4.7908	5.6479	100.6517
F-SAC	WS	PR	44.0914	1.3779	0.6134	0.5414
F-SAC	WS	PRSV	36.4151	1.1380	0.7321	0.6886
F-SAC	WS	PRSV2	37.6203	1.1756	0.6927	0.6265

In summary, the UNIFAC model coupled with the PRSV through the VDW1 mixing rule led to the best results, the smallest OF value and average residuals. However, several EOS + MR + EGE combinations offered reliable results as well. For example, the UNIFAC(Do) using the PRSV EOS and VDW1 MR, the F-SAC, again with the VDW1 and PRSV, also presented good performance.

It also should be noticed that the inaccuracy of the COSMO-SAC model presented in the last section is mainly because of its very poor results when associated to the HVOS MR. In fact, when the performance of the COSMO-SAC model associated to an EOS through the VDW1 MR is analyzed, it can be seen that its results are roughly 25% less accurate than the best performance of the UNIFAC model.

In order to simplify the results, only the k_{ij} values for UNIFAC, UNIFAC(Do), COSMO-SAC, and F-SAC are presented, and only for the VDW1 and WS mixing rules, since the HVOS has no binary interaction parameters. Because of the extension of the k_{ij} results table, these results are presented in Table A1 (Appendix).

It is interesting to notice, from Table A1, that the k_{ij} values obtained by the WS mixing rule are frequently lower than the k_{ij} estimated with the use of the VDW1 for both PR and PRSV EOS; however; the opposite happened when the PRSV EOS is used.

When the Table A1 is analyzed alongside Table A2, there is a small evidence that the objective function values are larger when the k_{ij} parameters found are more negative. This behavior can be seen in the Butane + Methanol, Ethanol + Nonane, Ethanol + Octane, 1-Propanol + Nonane, 1-Propanol + Octane, and 1-Propanol + Undecane systems.

Moreover, it can also be associated with the polarities of the molecules, given that that type of behavior was observed only when the alcohols were associated with alkanes proportionally larger than their own carbon chains.

The asymmetry of the molecules, however, seems to play no role in the k_{ij} parameter value or even in the performance of the associated models. This lack of correlation was also discussed in Section 3.1, and once again the relation reported by Coutsikos et al.[45] was not met.

CONCLUSIONS

The HVOS mixing rule presented a very poor performance, in fact the predictions of the VLE were greatly better when the VDW1 and the WS mixing rules were applied. The VDW1, however, was statistically better than the WS MR. Thus, the VDW1 is the most recommended mixing rule for the presented VLE binaries systems.

On the other hand, the equations of state choice caused only smalls impacts in the performance of the model, especially when compared to those observed when the mixing rules were changed. The PRSV2 was statistically better, however, the use of the PRSV EOS would affect by less than 0.5% the accuracy. To sum up, the PR presented the less accurate results and was 12% less accurate than the PRSV2.

Regarding to the choice of the excess Gibbs energy model, it greatly affected the results. In fact, the UNIFAC and UNIFAC(Do) performed better than the other excess Gibbs energy models. It should be noted, however, that the F-SAC model presented a great performance, its results were close to those obtained by the classical UNIFAC and UNIFAC(Do) models.

On the other hand, the results obtained with the COSMO-SAC model were the least accurate; although it should be mentioned that the performance of the model was heavily impeded by its coupling with the HVOS mixing rule. In fact, the objective function value of the COSMO-SAC model was 75% composed by errors when the model was associated with the EOS by the HVOS mixing rule. No specific trends were observed when the temperature in the systems were changed. The difference in the results when distinct temperatures were used was more sensitive to the system than to the model used.

Lastly, in an overall analysis, both UNIFAC and UNIFAC(Do) with the classical VDW1 mixing rule and a simple PRSV can lead to very good results. The F-SAC model seems promising as well, since it delivered reliable results, with errors of the same magnitude as the other two classical models. In this manner, the use of the UNIFAC model with the PRSV2 equations of state using the VDW1 mixing rules is the most advisable association.

The extension of these model associations to mixtures with three or more components is the subject of further work, especially for systems with wider ranges of temperature and pressure.

Abbreviations

COSMO-SAC – Conductor-like Screening Model Segment Activity Coefficient

EGE – Excess Gibbs Energy

EHE – Excess Helmholtz Energy

EOS – Equation of State

F-SAC – Functional-Segment Activity Coefficient Model

HVOS – Huron-Vidal-Orbey-Sandler mixing rule

LMA – Levenberg-Marquardt Algorithm

MR – Mixing Rule

NC – Number of components

NY – Number of experimental points

NRTL – Non-Random Two-Liquids Model

OF – Objective Function

PR – Peng-Robinson

PRSV – Peng-Robinson-Stryjek-Vera

PRSV2 – Peng-Robinson-Stryjek-Vera 2

SD – Standard Deviation

UNIFAC – UNIQUAC Functional-group Activity Coefficients

UNIFAC(Do) – Modified UNIFAC-Dortmund

UNIQUAC – Universal Quasichemical Theory

VDW1 – van der Waals mixing rule

VLE – Vapor-Liquid Equilibrium

WS – Wong-Sandler mixing rule

Symbols

A – Helmholtz energy

a – PR, PRSV, and PRSV2 parameter

b - PR, PRSV, and PRSV2 parameter

C^* - EOS-dependent constant

G – Gibbs energy

k_{ij} – Binary Interaction Parameter

P - Pressure

T – Temperature

V - Volume

x – Liquid-phase molar fraction

y – Vapor-phase molar fraction

γ – Activity coefficient

φ - Fugacity

Subscripts

$calc$ – Calculated value

exp – Experimental value

i, j – Component identification

m – Mixture

∞ - Infinite limit

Superscripts

$\bar{}$ - Molar property

ex – Excess property

L – Liquid-phase

sat – Saturation

V – Vapor-phase

ACKNOWLEDGMENTS

The authors would like to thank to the National Council for Improvement of Higher Education (CAPES - Brazil).

REFERENCES

[1] A. Klamt, G. Schüürmann, COSMO: a new approach to dielectric screening in solvents with explicit expressions for the screening energy and its gradient, J. Chem. Soc., Perkin Trans. 2. (1993) 799–805. doi:10.1039/P29930000799.

[2] A. Klamt, Conductor-like Screening Model for Real Solvents: A New Approach to the Quantitative Calculation of Solvation Phenomena, J. Phys. Chem. 99 (1995) 2224–2235. doi:10.1021/j100007a062.

[3] A. Klamt, The COSMO and COSMO-RS solvation models, Wiley Interdiscip. Rev. Comput. Mol. Sci. 8 (2018) 1–11. doi:10.1002/wcms.1338.

[4] A. Klamt, V. Jonas, T. Bürger, J.C.W. Lohrenz, Refinement and Parametrization of COSMO-RS, J. Phys. Chem. A. 102 (1998) 5074–5085. doi:10.1021/jp980017s.

[5] A. Klamt, COSMO-RS: From Quantum Chemistry to Fluid Phase Thermodynamics and Drug Design, Elsevier, 2005.

[6] A. Klamt, F. Eckert, COSMO-RS: a novel and efficient method for the a priori prediction of thermophysical data of liquids, Fluid Phase Equilib. 172 (2000) 43–72. doi:10.1016/S0378-3812(00)00357-5.

[7] S.-T. Lin, S.I. Sandler, A Priori Phase Equilibrium Prediction from a Segment Contribution Solvation Model, Ind. Eng. Chem. Res. 41 (2002) 899–913. doi:10.1021/ie001047w.

[8] S.T. Lin, S.I. Sandler, Infinite dilution activity coefficients from Ab initio solvation calculations, AIChE J. 45 (1999) 2606–2618. doi:10.1002/aic.690451217.

[9] A. Ben-Naim, Solvation Thermodynamics, Plenum Press, New York, 1987.

[10] A. Fredenslund, R.L. Jones, J.M. Prausnitz, Group-contribution estimation of activity coefficients in nonideal liquid mixtures, AIChE J. 21 (1975) 1086–1099. doi:10.1002/aic.690210607.

[11] U. Weidlich, J. Gmehling, A modified UNIFAC Model. 1. Prediction of VLE, hE, and y∞, Ind. Eng. Chem. Res. 26 (1987) 1372–1381. doi:10.1021/ie00067a018.

[12] S.T. Lin, J. Chang, S. Wang, W.A. Goddard, S.I. Sandler, Prediction of vapor pressures and enthalpies of vaporization using a COSMO solvation model, J. Phys. Chem. A. 108 (2004) 7429–7439. doi:10.1021/jp048813n.

[13] S. Wang, S.I. Sandler, C.C. Chen, Refinement of COSMO-SAC and the applications, Ind. Eng. Chem. Res. 46 (2007) 7275–7288. doi:10.1021/ie070465z.

[14] C.M. Hsieh, S.I. Sandler, S.T. Lin, Improvements of COSMO-SAC for vapor-liquid and liquid-liquid equilibrium predictions, Fluid Phase Equilib. 297 (2010) 90–97. doi:10.1016/j.fluid.2010.06.011.

[15] R. Xiong, S.I. Sandler, R.I. Burnett, An improvement to COSMO-SAC for predicting thermodynamic properties, Ind. Eng. Chem. Res. 53 (2014) 8265–8278. doi:10.1021/ie404410v.

[16] R. de P. Soares, R.P. Gerber, Functional-Segment Activity Coefficient Model. 1. Model Formulation, Ind. Eng. Chem. Res. 52 (2013) 11159–11171. doi:10.1021/ie400170a.

[17] R. de P. Soares, R.P. Gerber, L.F.K. Possani, P.B. Staudt, Functional-Segment Activity Coefficient Model. 2. Associating Mixtures, Ind. Eng. Chem. Res. 52 (2013) 11172–11181.

[18] T. Magnussen, P. Rasmussen, A. Fredenslund, Unifac Parameter Table for Prediction of Liquid-Liquid Equilibria, Ind. Eng. Chem. Process Des. Dev. 20 (1981) 331–339. doi:10.1021/i200013a024.

[19] L.R. Roque, R.R. Pinto, L.H. de Oliveira, S.C. Rabelo, Liquid-liquid equilibrium data for ternary systems of water + acetic acid+ acetate esters at 293.2 K and 303.2 K and ≈ 95 kPa, Fluid Phase Equilib. 463 (2018) 34–47. doi:10.1016/j.fluid.2018.02.003.

[20] C. Yu, S. Wu, Y. Zhao, Z. Zeng, W. Xue, Liquid-Liquid Equilibrium Data of Water + Butyric Acid + {Butanal or n-Butanol} Ternary Systems at 293.15, 308.15, and 323.15 K, J. Chem. Eng. Data. 62 (2017) 2244–2252. doi:10.1021/acs.jced.6b00941.

[21] T.M. Letcher, S. Ravindran, S.E. Radloff, Liquid-liquid equilibria for mixtures of an alkanol + diisopropyl ether + water at 25° C, Fluid Phase Equilib. 71 (1991) 177–188.

[22] T.M. Letcher, B.C. Bricknell, S.E. Radloff, J.D. Sewry, Liquid-liquid equilibria for mixtures of an alkanol + hept-1-ene + water at 25 C, J. Chem. Eng. Data. 39 (1994) 320–323.

[23] T.M. Letcher, P.M. Siswana, Liquid-liquid equilibria for mixtures of an alkanol + water + a methyl substituted benzene at 25??C, Fluid Phase Equilib. 74 (1992) 203–217. doi:10.1016/0378-3812(92)85062-D.

[24] T.M. Letcher, S. Wootton, B. Shuttleworth, C. Heyward, Phase equilibria for (n-heptane + water + an alcohol) at 298.2 K, J. Chem. Thermodyn. 18 (1986) 1037–1042. doi:10.1016/0021-9614(86)90017-0.

[25] J.F. McCants, J.H. Jones, W.H. Hopson, Ternary Solubility Data for Systems Involving 1-Propanol and Water, Ind. Eng. Chem. 45 (1953) 454–456. doi:10.1021/ie50518a054.

[26] M. van Berlo, M.T. Gude, L. a. M. van der Wielen, K.C. a. M. Luyben, Partition coefficients and solubilities of glycine in the ternary solvent system 1-butanol + ethanol + water, Ind. Eng. Chem. Res. 36 (1997) 2474–2482. doi:10.1021/ie960762w.

[27] S. Kadir, M. Decloux, P. Giampaoli, X. Joulia, Liquid–Liquid Equilibria of the Ternary Systems 3-Methyl-1-butanol + Ethanol + Water and 2-Methyl-1-propanol + Ethanol + Water at 293.15 K, J. Chem. Eng. Data. 53 (2008) 910–912. doi:10.1021/je700558x.

[28] S. Bekri, D. Özmen, A. Özmen, Correlation of Experimental Liquid-Liquid Equilibrium Data for Ternary Systems Using NRTL and GMDH-Type Neural Network, J. Chem. Eng. Data. 62 (2017) 1797–1805. doi:10.1021/acs.jced.6b00985.

[29] J.C. Thermodynamics, X. Liu, X. Zhang, Solvent screening and liquid-liquid measurement for extraction of phenols from aromatic hydrocarbon mixtures, J. Chem. Thermodyn. 129 (2019) 12–21. doi:10.1016/j.jct.2018.09.006.

[30] Y. Yoshimoto, E. Kinoshita, L. Shanbu, T. Ohmura, Influence of 1-butanol addition on diesel combustion with palm oil methyl ester/gas oil blends, Energy. 61 (2013) 44–51. doi:10.1016/j.energy.2012.11.039.

[31] A. Atmanli, Comparative analyses of diesel-waste oil biodiesel and propanol, n-butanol or 1-pentanol blends in a diesel engine, Fuel. 176 (2016) 209–215. doi:10.1016/j.fuel.2016.02.076.

[32] I.B.C. de Aguiar, T.R.M. Souza, M.A.M. Justino, A. de Oliveira, Performance and Emissions of a Diesel Engine Fueled By Diesel Oil-Ethanol-N-Butanol Blends, SAE Int. - Tech. Pap. Ser. (2017).

[33] C.L. Silveira, N.P.G. Salau, From Wilson to F-SAC: A comparative analysis of correlative and predictive activity coefficient models to determine VLE and IDAC of binary systems, Fluid Phase Equilib. 464 (2018) 1–11.

[34] G.N. Escobedo-Alvarado, S.I. Sandler, Study of EOS-Gex Mixing Rules for Liquid-Liquid Equilibria, AIChE J. 44 (1998) 1178–1187.

[35] M.L. Michelsen, The Isothermal Flash Problem. Part I. Stability, Fluid Phase Equilib. 9 (1982) 1–19.

[36] M.L. Michelsen, The Isothermal Flash Problem. Part II. Phase-Split Calculation, Fluid Phase Equilib. 9 (1982) 21–40.

[37] I.S.V. Segtovich, A.G. Barreto, F.W. Tavares, Simultaneous multiphase flash and stability analysis calculations including hydrates, Fluid Phase Equilib. 413 (2016) 196–208. doi:10.1016/j.fluid.2015.10.030.

[38] A.A. Izadpanah, M. Vafaie Sefti, F. Varaminian, Multi-component-multiphase flash calculations for systems containing gas hydrates by direct minimization of Gibbs free energy, Iran. J. Chem. Chem. Eng. 25 (2006) 27–34.

[39] S.K. Wasylkiewicz, L.N. Sridhar, M.F. Doherty, M.F. Malone, Global Stability Analysis and Calculation of Liquid−Liquid Equilibrium in Multicomponent Mixtures, Ind. Eng. Chem. Res. 35 (1996) 1395–1408. doi:10.1021/ie950049r.

[40] Z. Li, Thermodynamic Modelling of Liquid – liquid Equilibria Using the Nonrandom Two-Liquid Model and Its Applications, The University of Melbourne, 2015.

[41] H.H. Rachford, J.D. Rice, Procedure for Use of Electronic Digital Computers in Calculating Flash Vaporization Hydrocarbon Equilibrium, J. Pet. Technol. 4 (1952) 19–3. doi:10.2118/952327-G.

[42] L.F.K. Possani, Correlação Simultânea de IDAC, VLE e LLE com o Modelo F-SAC, (2014). http://www.lume.ufrgs.br/bitstream/handle/10183/107500/000945081.pdf?sequence=1.

[43] M.J.D. Powell, A Fortran subroutine for solving systems of nonlinear algebraic equations, (1968).

[44] A.C. Hansen, Q. Zhang, P.W.L. Lyne, Ethanol – diesel fuel blends — a review, 96 (2010) 277–285. doi:10.1016/j.biortech.2004.04.007.

APPENDIX

Table A1. Optimized k_{ij} values.

Component 1	Component 2	UNIFAC VDW1 PR	UNIFAC VDW1 PRSV	UNIFAC VDW1 PRSV2	UNIFAC WS PR	UNIFAC WS PRSV	UNIFAC WS PRSV2
Acetone	Methanol	0.21489±0.0017	0.21739±0.0017	0.20919±0.0025	0.21190±0.0021	0.23001±0.0023	0.23257±0.0026
Acetone	Water	0.41358±0.0038	0.23939±0.0024	0.41798±0.0043	0.24738±0.0022	0.41983±0.0048	0.25113±0.0025
Butane	Methanol	-1.8045±0.0820	-2.1399±0.0856	-1.7526±0.0731	-2.0862±0.0763	-1.7382±0.0693	-2.0711±0.0723
Butanol	Decane	-1.7371±0.0134	-2.1700±0.0189	-1.7064±0.0086	-2.1390±0.0141	-1.6814±0.0087	-2.1130±0.0141
Butanol	Heptane	0.33349±0.0018	0.12635±0.0043	0.39263±0.0021	0.19974±0.0003	0.37898±0.0013	0.17436±0.0023
Butanol	Hexane	0.37315±0.0045	0.15727±0.0032	0.37689±0.0032	0.18221±0.0031	0.36765±0.0038	0.16243±0.0036
Butanol	Nonane	0.34306±0.0081	0.05901±0.0365	0.39683±0.0029	0.09515±0.0297	0.38995±0.0032	0.12699±0.0235
Butanol	Octane	0.29040±0.0071	0.02890±0.0107	0.45027±0.0101	0.24954±0.0104	0.43566±0.0090	0.20399±0.0008
Butanol	Pentane	0.39454±0.0011	0.20888±0.0018	0.37251±0.0005	0.19856±0.0026	0.38208±0.0033	0.20627±0.0023
Ethanol	Butane	0.41055±0.0083	0.19984±0.0114	0.40267±0.0072	0.18727±0.0107	0.41652±0.0067	0.19338±0.0122
Ethanol	Heptane	0.50232±0.0011	-0.0736±0.0695	0.53545±0.0008	-0.0788±0.0736	0.52545±0.0023	-0.0029±0.0685
Ethanol	Hexane	0.50955±0.0036	0.27824±0.0075	0.51187±0.0019	0.28599±0.0074	0.49599±0.0015	0.27155±0.0046
Ethanol	Nonane	-1.8518±0.0310	-2.5843±0.0351	-1.8672±0.0318	-2.6015±0.0365	-1.8387±0.0288	-2.5763±0.0337
Ethanol	Octane	-1.4458±0.0248	-2.2560±0.0366	-1.4681±0.0280	-2.2823±0.0390	-1.4185±0.0281	-2.2364±0.0390
Ethanol	Pentane	0.49895±0.0048	0.26862±0.0014	0.49415±0.0049	0.26294±0.0013	0.48860±0.0053	0.26417±0.0033
Ethanol	Water	0.24807±0.0069	0.13500±0.0053	0.24570±0.0075	0.13237±0.0057	0.36422±0.0153	0.25559±0.0171
1-Pentanol	Heptane	0.33240±0.0011	0.13592±0.0013	0.36720±0.0014	0.19219±0.0008	0.34887±0.0006	0.17634±0.0016
Heptane	3-Methyl-1Butanol	-0.0599±0.0221	-0.2545±0.0223	-0.1841±0.0294	-0.3861±0.0278	-0.1605±0.0263	-0.3494±0.0274
Methanol	Benzene	0.40136±0.0037	0.26130±0.0023	0.41111±0.0042	0.26602±0.0019	0.40336±0.0030	0.26604±0.0035
Methanol	Hexane	0.61046±0.0001	0.36206±0.0040	0.60708±0.0002	0.36558±0.0027	0.59245±0.0017	0.34688±0.0040

Methanol	Water	0.09189±0.0111	0.00825±0.0115	0.11194±0.0111	0.02847±0.0110	0.10145±0.0091	0.01813±0.0092
1-Pentanol	Decane	-0.0595±0.0710	-0.4064±0.1004	0.05397±0.0695	-0.3125±0.1073	0.07379±0.0639	-0.2681±0.1067
1-Pentanol	Hexane	0.35828±0.0029	0.18420±0.0010	0.36458±0.0028	0.19144±0.0009	0.33782±0.0004	0.15687±0.0033
1-Pentanol	Octane	0.25151±0.0019	0.04660±0.0085	0.32545±0.0099	0.14576±0.0058	0.32266±0.0090	0.14778±0.0064
1-Pentanol	Pentane	0.39651±0.0042	0.23684±0.0018	0.36051±0.0017	0.20890±0.0014	0.35452±0.0011	0.20513±0.0032
Pentane	Methanol	-0.3066±0.0487	-0.5614±0.0460	-0.3316±0.0490	-0.5966±0.0433	-0.2970±0.0501	-0.5568±0.0457
1-Propanol	Heptane	0.39355±0.0051	0.09974±0.0088	0.45819±0.0022	0.21476±0.0071	0.36527±0.0170	0.05328±0.0378
1-Propanol	Hexane	0.41315±0.0015	0.19769±0.0026	0.42913±0.0002	0.21097±0.0052	0.39533±0.0033	0.18367±0.0061
1-Propanol	Nonane	-0.8645±0.0358	-1.6185±0.0410	-0.8659±0.0333	-1.6176±0.0380	-0.8319±0.0339	-1.5893±0.0385
1-Propanol	Octane	0.37258±0.0091	-0.0297±0.0259	0.48099±0.0047	0.09860±0.0301	0.42663±0.0068	0.06597±0.0152
1-Propanol	Undecane	-3.0815±0.0645	-3.6796±0.0650	-3.0798±0.0580	-3.6773±0.0587	-3.0484±0.0621	-3.6461±0.0627
2-Propanol	Water	0.43931±0.0109	0.34438±0.0091	0.44610±0.0065	0.35100±0.0051	0.51843±0.0082	0.43035±0.0093

Component 1	**Component 2**	**UNIFAC(Do) VDW1 PR**	**UNIFAC(Do) VDW1 PRSV**	**UNIFAC(Do) VDW1 PRSV2**	**UNIFAC(Do) WS PR**	**UNIFAC(Do) WS PRSV**	**UNIFAC(Do) WS PRSV2**
Acetone	Methanol	0.15504±0.0043	0.11769±0.0072	0.14804±0.0022	0.11376±0.0053	0.17005±0.0058	0.13257±0.0082
Acetone	Water	0.48838±0.0046	0.37093±0.0110	0.49207±0.0041	0.37663±0.0107	0.49403±0.0039	0.37911±0.0103
Butane	Methanol	-1.8724±0.0826	-2.2474±0.0870	-1.8202±0.0736	-2.1929±0.0774	-1.8056±0.0697	-2.1774±0.0735
Butanol	Decane	-1.6517±0.0217	-2.0331±0.0322	-1.6210±0.0169	-2.0021±0.0274	-1.5962±0.0169	-1.9764±0.0274
Butanol	Heptane	0.32178±0.0037	0.10470±0.0074	0.37815±0.0008	0.17531±0.0034	0.36168±0.0010	0.15281±0.0051
Butanol	Hexane	0.33704±0.0044	0.09115±0.0048	0.34850±0.0029	0.12117±0.0033	0.33932±0.0046	0.09584±0.0045
Butanol	Nonane	0.38391±0.0091	0.22230±0.0206	0.43218±0.0006	0.26101±0.0132	0.42625±0.0009	0.28272±0.0073
Butanol	Octane	0.29090±0.0096	0.04669±0.0162	0.45343±0.0084	0.24956±0.0034	0.43543±0.0062	0.20776±0.0032
Butanol	Pentane	0.33976±0.0009	0.13376±0.0026	0.32140±0.0017	0.10662±0.0043	0.32682±0.0018	0.11012±0.0041
Ethanol	Butane	0.35083±0.0088	0.08760±0.0142	0.34457±0.0088	0.07985±0.0139	0.35210±0.0086	0.09244±0.0121
Ethanol	Heptane	0.48387±0.0036	-0.4824±0.0981	0.50470±0.0061	-0.4918±0.1012	0.51021±0.0038	-0.2748±0.1073
Ethanol	Hexane	0.48767±0.0040	0.21167±0.0160	0.49245±0.0032	0.21912±0.0152	0.47260±0.0034	0.22785±0.0074
Ethanol	Nonane	-1.7283±0.0484	-2.4077±0.0598	-1.7441±0.0491	-2.4252±0.0611	-1.7152±0.0462	-2.3997±0.0585
Ethanol	Octane	-1.5397±0.0443	-2.3718±0.0603	-1.5615±0.0475	-2.3885±0.0604	-1.5129±0.0478	-2.3448±0.0608
Ethanol	Pentane	0.46222±0.0040	0.18215±0.0041	0.45682±0.0046	0.18153±0.0046	0.45129±0.0048	0.17334±0.0038
Ethanol	Water	0.40713±0.0045	0.40426±0.0146	0.40490±0.0040	0.40283±0.0136	0.50204±0.0215	0.49048±0.0305
1-Pentanol	Heptane	0.32509±0.0024	0.11548±0.0033	0.34838±0.0008	0.16812±0.0022	0.33164±0.0009	0.14853±0.0033
Heptane	3-Methyl-1Butanol	-0.0985±0.0230	-0.3106±0.0232	-0.2228±0.0298	-0.4431±0.0287	-0.1934±0.0279	-0.4073±0.0283
Methanol	Benzene	0.43724±0.0026	0.32568±0.0041	0.44632±0.0028	0.33807±0.0039	0.43766±0.0024	0.32760±0.0040
Methanol	Hexane	0.59683±0.0035	-0.5889±0.1681	0.60694±0.0007	-0.7254±0.1686	0.59177±0.0020	-0.4832±0.1828
Methanol	Water	0.10950±0.0104	0.03698±0.0112	0.12989±0.0098	0.05747±0.0097	0.11905±0.0079	0.04685±0.0083
1-Pentanol	Decane	-0.0071±0.0701	-0.3010±0.1025	0.11047±0.0672	-0.2063±0.1094	0.12551±0.0604	-0.1811±0.1062
1-Pentanol	Hexane	0.32355±0.0027	0.12774±0.0007	0.32432±0.0019	0.11685±0.0011	0.29585±0.0010	0.08797±0.0040
1-Pentanol	Octane	0.26375±0.0070	0.06888±0.0194	0.33808±0.0045	0.17457±0.0036	0.33715±0.0045	0.17414±0.0047
1-Pentanol	Pentane	0.32331±0.0022	0.13746±0.0021	0.30037±0.0010	0.10356±0.0025	0.29739±0.0022	0.09971±0.0040
Pentane	Methanol	-0.3139±0.0522	-0.5863±0.0468	-0.3494±0.0492	-0.6214±0.0443	-0.3153±0.0501	-0.5729±0.0493
1-Propanol	Heptane	0.36676±0.0063	-0.0861±0.0391	0.42513±0.0051	0.12792±0.0133	0.34095±0.0205	-0.1817±0.0924
1-Propanol	Hexane	0.38860±0.0034	0.11850±0.0116	0.39055±0.0035	0.16028±0.0058	0.36920±0.0045	0.11944±0.0117
1-Propanol	Nonane	-0.7679±0.0630	-1.5075±0.0744	-0.7709±0.0600	-1.5068±0.0712	-0.7337±0.0612	-1.4776±0.0720
1-Propanol	Octane	0.37469±0.0128	-0.1157±0.0591	0.48200±0.0009	0.03592±0.0424	0.43409±0.0092	-0.0140±0.0616
1-Propanol	Undecane	-3.0182±0.0843	-3.5828±0.0957	-3.0162±0.0779	-3.5806±0.0893	-2.9851±0.0819	-3.5494±0.0934
2-Propanol	Water	0.50379±0.0016	0.44411±0.0060	0.50398±0.0016	0.44853±0.0097	0.56484±0.0139	0.50535±0.0206

Component 1	**Component 2**	**UNIQUAC VDW1 PR**	**UNIQUAC VDW1 PRSV**	**UNIQUAC VDW1 PRSV2**	**UNIQUAC WS PR**	**UNIQUAC WS PRSV**	**UNIQUAC WS PRSV2**
Acetone	Methanol	0.18206±0.0016	0.16299±0.0018	0.17411±0.0019	0.15544±0.0014	0.19643±0.0027	0.17823±0.0031
Acetone	Water	0.65076±0.0078	0.63390±0.0080	0.65649±0.0083	0.63387±0.0085	0.65720±0.0086	0.63564±0.0088
Butane	Methanol	-1.6508±0.0817	-1.8958±0.0848	-1.5999±0.0730	-1.8440±0.0755	-1.5858±0.0692	-1.8293±0.0717
Butanol	Decane	-1.4954±0.0077	-1.7823±0.0099	-1.4647±0.0031	-1.7517±0.0052	-1.4405±0.0031	-1.7265±0.0052
Butanol	Heptane	0.57158±0.0029	0.52254±0.0011	0.59136±0.0035	0.54438±0.0024	0.58016±0.0034	0.53494±0.0030
Butanol	Hexane	0.36835±0.0089	0.11752±0.0176	0.34795±0.0103	0.09395±0.0199	0.34746±0.0100	0.06639±0.0214
Butanol	Nonane	0.52801±0.0032	0.49827±0.0036	0.56710±0.0043	0.53443±0.0041	0.56373±0.0049	0.53249±0.0046
Butanol	Octane	0.54170±0.0017	0.48952±0.0016	0.65342±0.0104	0.60601±0.0096	0.65601±0.0122	0.60371±0.0109
Butanol	Pentane	0.60057±0.0036	0.56654±0.0024	0.56980±0.0022	0.53788±0.0017	0.57648±0.0043	0.54509±0.0034
Ethanol	Butane	0.50839±0.0069	0.37205±0.0106	0.50109±0.0070	0.36530±0.0107	0.51209±0.0067	0.37066±0.0106
Ethanol	Heptane	0.72650±0.0020	0.67629±0.0016	0.74915±0.0021	0.70182±0.0017	0.74574±0.0009	0.69560±0.0004

Ethanol	Hexane	0.24282±0.0085	-0.8734±0.1331	0.26631±0.0071	-0.8551±0.1357	0.25094±0.0075	-0.8181±0.1268
Ethanol	Nonane	-0.3644±0.0361	-0.3768±0.0362	-0.3900±0.0357	-0.4023±0.0358	-0.3473±0.0337	-0.3597±0.0338
Ethanol	Octane	0.66388±0.0023	0.60773±0.0111	0.70093±0.0011	0.56154±0.0324	0.73019±0.0013	0.70762±0.0009
Ethanol	Pentane	0.40427±0.0040	0.08562±0.0044	0.39951±0.0043	0.08039±0.0033	0.39684±0.0053	0.07734±0.0053
Ethanol	Water	0.13565±0.0052	-0.0417±0.0054	0.13203±0.0054	-0.0491±0.0037	0.25910±0.0196	0.09265±0.0271
1-Pentanol	Heptane	0.38996±0.0012	0.20033±0.0029	0.35451±0.0008	0.18010±0.0028	0.35393±0.0021	0.16168±0.0046
Heptane	3-Methyl-1Butanol	0.21849±0.0216	0.18682±0.0212	0.12374±0.0309	0.08751±0.0301	0.15320±0.0280	0.11912±0.0279
Methanol	Benzene	0.44984±0.0043	0.34588±0.0024	0.45660±0.0047	0.35412±0.0030	0.45063±0.0038	0.34670±0.0024
Methanol	Hexane	0.78652±0.0004	0.68459±0.0014	0.78715±0.0005	0.68436±0.0023	0.77495±0.0010	0.66265±0.0031
Methanol	Water	0.10071±0.0117	0.02334±0.0127	0.12161±0.0118	0.0439±0.0122	0.11025±0.0098	0.03317±0.0104
1-Pentanol	Decane	0.38656±0.0111	0.34140±0.0173	0.53986±0.0081	0.51802±0.0079	0.53008±0.0079	0.50835±0.0078
1-Pentanol	Hexane	0.55983±0.0045	0.52901±0.0037	0.56211±0.0049	0.52507±0.0042	0.53272±0.0017	0.49686±0.0013
1-Pentanol	Octane	0.46854±0.0052	0.43071±0.0043	0.51679±0.0124	0.47648±0.0109	0.51378±0.0115	0.47325±0.0102
1-Pentanol	Pentane	0.27523±0.0031	-0.0001±0.0086	0.17313±0.0072	-0.1258±0.0179	0.16459±0.0074	-0.1317±0.0198
Pentane	Methanol	0.35372±0.0720	0.42392±0.0655	0.27215±0.0584	0.38662±0.0665	0.36285±0.0743	0.43327±0.0679
1-Propanol	Heptane	0.46044±0.0063	0.26995±0.0085	0.48580±0.0069	0.29684±0.0100	0.44941±0.0087	0.25499±0.0103
1-Propanol	Hexane	0.66765±0.0050	0.62702±0.0052	0.64880±0.0010	0.60406±0.0020	0.64029±0.0038	0.59917±0.0038
1-Propanol	Nonane	0.53615±0.0109	0.50498±0.0140	0.64712±0.0043	0.62809±0.0037	0.63588±0.0036	0.61533±0.0042
1-Propanol	Octane	0.59095±0.0038	0.55405±0.0048	0.67526±0.0070	0.63857±0.0063	0.63300±0.0033	0.59678±0.0037
1-Propanol	Undecane	0.18030±0.1062	1.19957±0.0062	0.15072±0.1112	1.22013±0.0082	0.18281±0.1062	1.21960±0.0084
2-Propanol	Water	0.24305±0.0057	0.05622±0.0058	0.24848±0.0029	0.05819±0.0068	0.33492±0.0129	0.11634±0.0204

Component 1	**Component 2**	**COSMO-SAC VDW1 PR**	**COSMO-SAC VDW1 PRSV**	**COSMO-SAC VDW1 PRSV2**	**COSMO-SAC WS PR**	**COSMO-SAC WS PRSV**	**COSMO-SAC WS PRSV2**
Acetone	Methanol	0.15041±0.0031	0.11754±0.0029	0.14720±0.0017	0.10908±0.0023	0.16644±0.0040	0.13216±0.0054
Acetone	Water	0.46678±0.0067	0.32910±0.0057	0.46946±0.0061	0.33084±0.0062	0.47195±0.0067	0.33702±0.0067
Butane	Methanol	-1.7241±0.0810	-2.0122±0.0838	-1.6727±0.0723	-1.9591±0.0747	-1.6585±0.0685	-1.9441±0.0708
Butanol	Decane	-2.0990±0.0197	-2.7509±0.0292	-2.0681±0.0149	-2.7196±0.0242	-2.0423±0.0150	-2.6922±0.0242
Butanol	Heptane	0.36116±0.0021	0.15148±0.0066	0.42236±0.0023	0.24701±0.0007	0.39848±0.0004	0.22728±0.0018
Butanol	Hexane	0.38402±0.0034	0.19550±0.0038	0.40752±0.0027	0.22151±0.0033	0.39126±0.0036	0.19507±0.0043
Butanol	Nonane	-0.0035±0.0542	-1.1729±0.0452	-0.0010±0.0510	-1.1752±0.0432	0.03852±0.0458	-1.1573±0.0405
Butanol	Octane	0.28102±0.0135	-0.2644±0.1181	0.44398±0.0254	-0.0914±0.1374	0.43984±0.0210	-0.1173±0.1289
Butanol	Pentane	0.41135±0.0011	0.23678±0.0017	0.39187±0.0002	0.23341±0.0016	0.40114±0.0027	0.23506±0.0020
Ethanol	Butane	0.43435±0.0067	0.24032±0.0104	0.42666±0.0069	0.23021±0.0099	0.43693±0.0067	0.23603±0.0112
Ethanol	Heptane	-0.0832±0.0745	-1.7435±0.0634	-0.0653±0.0814	-1.7531±0.0660	0.14162±0.0860	-1.6700±0.0663
Ethanol	Hexane	0.51773±0.0111	-0.0867±0.1219	0.51642±0.0094	-0.0795±0.1223	0.52971±0.0015	-0.0475±0.1109
Ethanol	Nonane	-2.4986±0.0322	-3.5338±0.0407	-2.5159±0.0335	-3.5430±0.0416	-2.4912±0.0309	-3.5224±0.0391
Ethanol	Octane	-2.2063±0.0294	-3.1518±0.0308	-2.2231±0.0294	-3.1557±0.0325	-2.1815±0.0296	-3.1120±0.0327
Ethanol	Pentane	0.52779±0.0044	0.31104±0.0021	0.52330±0.0044	0.30853±0.0024	0.52072±0.0052	0.28462±0.0063
Ethanol	Water	0.26406±0.0074	0.15555±0.0062	0.26045±0.0082	0.15197±0.0071	0.37643±0.0145	0.27458±0.0160
1-Pentanol	Heptane	0.34844±0.0006	0.14277±0.0012	0.38577±0.0010	0.22674±0.0007	0.37053±0.0005	0.20966±0.0013
Heptane	3-Methyl-1Butanol	-0.0381±0.0227	-0.2149±0.0238	-0.1652±0.0295	-0.3553±0.0283	-0.1392±0.0269	-0.3205±0.0276
Methanol	Benzene	0.45588±0.0046	0.36291±0.0018	0.46652±0.0051	0.36982±0.0022	0.46273±0.0039	0.36020±0.0022
Methanol	Hexane	-0.0611±0.1570	-2.1247±0.0499	-0.0845±0.1647	-2.1818±0.0552	-0.0810±0.1605	-2.1170±0.0564
Methanol	Water	0.08434±0.0094	0.00499±0.0095	0.10807±0.0100	0.03027±0.0084	0.09416±0.0078	0.01352±0.0067
1-Pentanol	Decane	-0.5235±0.1103	-1.5217±0.0952	-0.4835±0.1118	-1.4807±0.0870	-0.4140±0.1148	-1.4478±0.0877
1-Pentanol	Hexane	0.38208±0.0042	0.20975±0.0001	0.38433±0.0027	0.22037±0.0005	0.35597±0.0007	0.19168±0.0025
1-Pentanol	Octane	0.27110±0.0017	0.02845±0.0202	0.34805±0.0099	0.17640±0.0057	0.34132±0.0083	0.16785±0.0030
1-Pentanol	Pentane	0.40508±0.0038	0.25331±0.0018	0.37349±0.0021	0.23430±0.0004	0.36503±0.0013	0.22777±0.0028
Pentane	Methanol	-0.2176±0.0560	-0.4493±0.0489	-0.2557±0.0522	-0.4849±0.0460	-0.2214±0.0532	-0.4325±0.0526
1-Propanol	Heptane	0.29520±0.0331	-1.0595±0.0878	0.41150±0.0170	-0.8329±0.1013	0.24717±0.0350	-1.1086±0.1099
1-Propanol	Hexane	0.44108±0.0013	0.14261±0.0262	0.44964±0.0031	0.26112±0.0056	0.42741±0.0033	0.15885±0.0259
1-Propanol	Nonane	-1.6351±0.0417	-2.6671±0.0545	-1.6343±0.0387	-2.6591±0.0502	-1.6024±0.0397	-2.6344±0.0507
1-Propanol	Octane	-0.2183±0.0233	-1.5846±0.0327	0.04934±0.0557	-1.5546±0.0280	-0.1517±0.0192	-1.5579±0.0317
1-Propanol	Undecane	-3.5984±0.0580	-4.4428±0.0714	-3.5962±0.0517	-4.4347±0.0665	-3.5652±0.0559	-4.4094±0.0693
2-Propanol	Water	0.39957±0.0092	0.27453±0.0062	0.41139±0.0064	0.28033±0.0046	0.46347±0.0096	0.33423±0.0143

Component 1	**Component 2**	**F-SAC VDW1 PR**	**F-SAC VDW1 PRSV**	**F-SAC VDW1 PRSV2**	**F-SAC WS PR**	**F-SAC WS PRSV**	**F-SAC WS PRSV2**
Acetone	Methanol	0.12337±0.0037	0.07390±0.0051	0.12115±0.0012	0.06636±0.0044	0.13985±0.0051	0.08876±0.0078

Acetone	Water	0.35086±0.0023	0.13244±0.0040	0.34987±0.0020	0.13242±0.0032	0.35060±0.0019	0.13443±0.0029
Butane	Methanol	-1.8359±0.0820	-2.1895±0.0858	-1.7838±0.0731	-2.1353±0.0765	-1.7693±0.0693	-2.1200±0.0725
Butanol	Decane	-1.7792±0.0133	-2.2376±0.0190	-1.7484±0.0087	-2.2066±0.0143	-1.7233±0.0089	-2.1804±0.0145
Butanol	Heptane	0.30264±0.0040	0.07246±0.0077	0.35981±0.0006	0.14368±0.0036	0.34264±0.0009	0.12038±0.0054
Butanol	Hexane	0.32692±0.0049	0.06767±0.0059	0.33343±0.0030	0.09552±0.0042	0.32283±0.0040	0.06917±0.0053
Butanol	Nonane	0.33805±0.0093	0.03513±0.0397	0.39328±0.0019	0.06257±0.0369	0.38673±0.0024	0.09223±0.0317
Butanol	Octane	0.26649±0.0066	-0.0179±0.0138	0.42893±0.0086	0.20097±0.0055	0.40938±0.0063	0.15667±0.0041
Butanol	Pentane	0.33774±0.0019	0.13029±0.0046	0.31804±0.0021	0.09886±0.0055	0.32245±0.0021	0.10569±0.0048
Ethanol	Butane	0.34673±0.0096	0.07880±0.0160	0.33991±0.0095	0.07083±0.0157	0.34542±0.0101	0.08177±0.0142
Ethanol	Heptane	0.45203±0.0043	-0.5427±0.0917	0.47317±0.0068	-0.5445±0.0961	0.47904±0.0041	-0.3761±0.0980
Ethanol	Hexane	0.46600±0.0043	0.16834±0.0167	0.47073±0.0036	0.17507±0.0157	0.45054±0.0037	0.18273±0.0085
Ethanol	Nonane	-1.9141±0.0399	-2.6774±0.0482	-1.9291±0.0406	-2.6945±0.0496	-1.9005±0.0375	-2.6692±0.0469
Ethanol	Octane	-1.6283±0.0376	-2.5009±0.0520	-1.6495±0.0408	-2.5176±0.0521	-1.6013±0.0410	-2.4739±0.0525
Ethanol	Pentane	0.44369±0.0034	0.14944±0.0065	0.44097±0.0039	0.14436±0.0070	0.43366±0.0040	0.13766±0.0063
Ethanol	Water	0.27997±0.0062	0.18730±0.0047	0.27426±0.0067	0.18232±0.0052	0.38763±0.0153	0.30344±0.0179
1-Pentanol	Heptane	0.31293±0.0021	0.08849±0.0030	0.33395±0.0007	0.14714±0.0025	0.31805±0.0012	0.12552±0.0035
Heptane	3-Methyl-1Butanol	-0.1267±0.0235	-0.3579±0.0228	-0.2566±0.0290	-0.4927±0.0278	-0.2237±0.0279	-0.4574±0.0274
Methanol	Benzene	0.42522±0.0030	0.30472±0.0032	0.43602±0.0036	0.31864±0.0029	0.42954±0.0024	0.31574±0.0044
Methanol	Hexane	0.56274±0.0036	-0.5953±0.1696	0.57065±0.0011	-0.7358±0.1689	0.55376±0.0026	-0.5351±0.1806
Methanol	Water	0.10167±0.0092	0.02512±0.0081	0.12148±0.0096	0.04589±0.0084	0.11102±0.0075	0.03407±0.0061
1-Pentanol	Decane	-0.0826±0.0777	-0.4466±0.1094	0.02895±0.0776	-0.3628±0.1149	0.04412±0.0717	-0.3096±0.1154
1-Pentanol	Hexane	0.31615±0.0018	0.11703±0.0004	0.31566±0.0011	0.09973±0.0025	0.28679±0.0016	0.07502±0.0049
1-Pentanol	Octane	0.23507±0.0051	0.01754±0.0167	0.31008±0.0056	0.12140±0.0014	0.30828±0.0054	0.12464±0.0008
1-Pentanol	Pentane	0.32224±0.0016	0.13911±0.0029	0.30102±0.0014	0.10395±0.0037	0.29814±0.0027	0.10048±0.0052
Pentane	Methanol	-0.3198±0.0522	-0.5973±0.0464	-0.3563±0.0489	-0.6324±0.0439	-0.3215±0.0500	-0.5810±0.0498
1-Propanol	Heptane	0.33746±0.0065	-0.0585±0.0206	0.39713±0.0062	0.09203±0.0132	0.31323±0.0198	-0.1505±0.0666
1-Propanol	Hexane	0.37105±0.0040	0.07694±0.0151	0.37268±0.0042	0.13139±0.0070	0.35052±0.0053	0.07770±0.0150
1-Propanol	Nonane	-0.9507±0.0490	-1.7371±0.0592	-0.9515±0.0463	-1.7353±0.0560	-0.9181±0.0471	-1.7074±0.0567
1-Propanol	Octane	0.33672±0.0121	-0.3177±0.0473	0.45026±0.0013	-0.1923±0.0330	0.39874±0.0087	-0.2412±0.0440
1-Propanol	Undecane	-3.1560±0.0741	-3.7983±0.0808	-3.1539±0.0677	-3.7960±0.0744	-3.1224±0.0718	-3.7648±0.0785
2-Propanol	Water	0.40979±0.0081	0.28094±0.0032	0.41883±0.0049	0.28559±0.0014	0.47472±0.0099	0.34441±0.0155

Table A2. Objective function value for all systems and all combinations.

(File Table_B.xlsx)

Appendix B - Algorithm

As mentioned in the introduction section, the VLE calculations were performed using simple Bubble-point Pressure algorithm, with the fugacities calculated by the mixing rules and the equilibrium composition given by Equation B1

$$y_i = \frac{x_i \varphi_i^L}{\varphi_i^V} \tag{B1}$$

Where y_i and x_i are the molar fractions of vapor and liquid phases of component i, respectively, and φ_i is the fugacity of component i, where the superscripts L and V denote liquid and vapor-phase, respectively. The algorithm for the VLE calculations used in this work is illustrated in Figure B1.

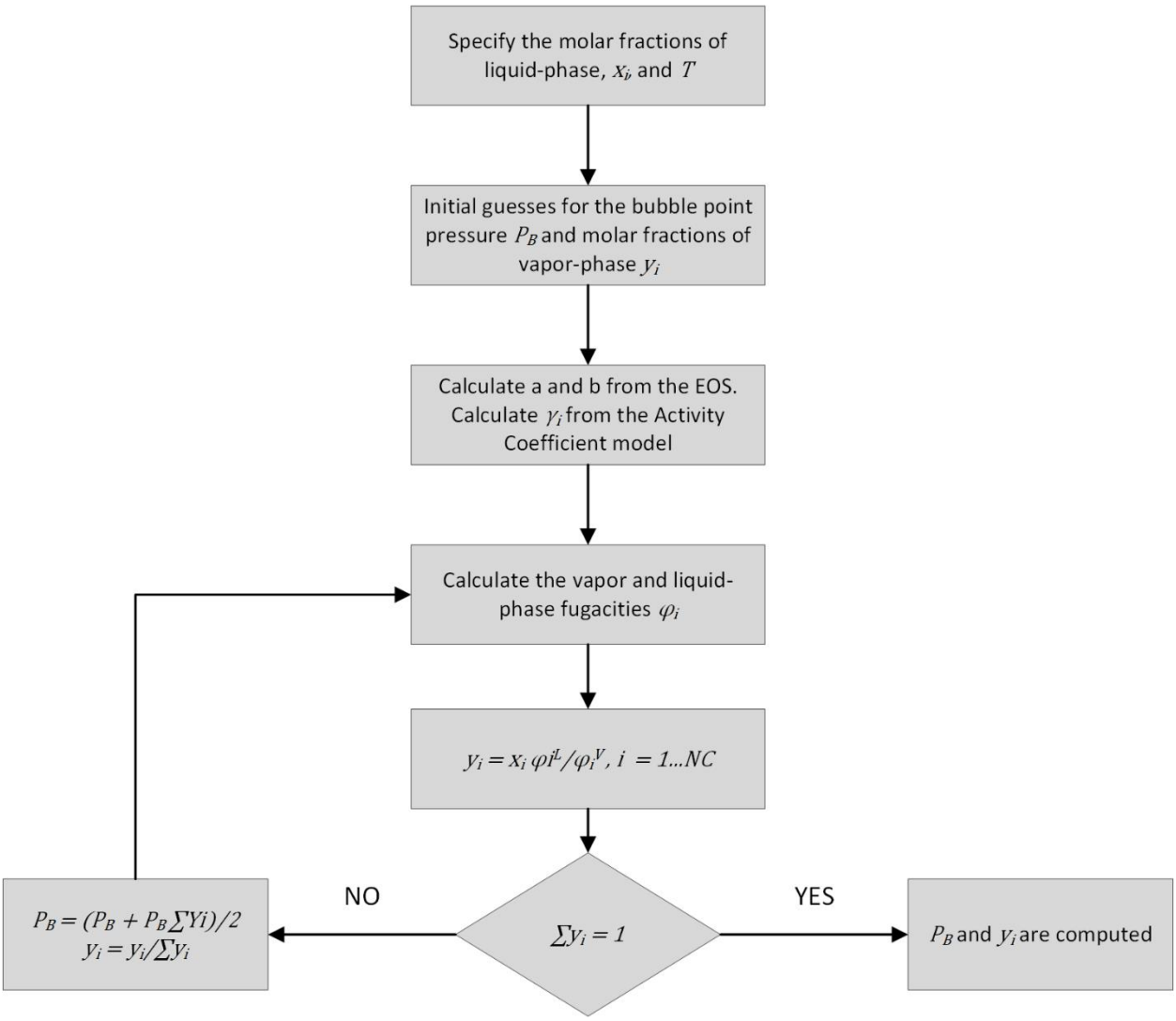

Figure B1. Flow diagram of the VLE algorithm.

For the mixing rules calculations, the algorithms were based on those published by Orbey and Sandler [56].

6 DISCUSSÃO

Diversos sistemas foram utilizados para a avaliação de diferentes tipos de cálculos de equilíbrio (ELV, ELL e ELLV) que foram realizados a partir de diferentes modelos de energia de Gibbs em excesso ou suas associações com equações cúbicas de estado através de regras de mistura. Neste capítulo, buscou-se discorrer sobre os principais resultados encontrados em cada um dos capítulos apresentados como resultados e discussões gerais.

Os modelos de EGE utilizados para predições de ELV podem ser divididos em modelos correlativos e modelos preditivos (capítulo 6). Os modelos correlativos forneceram resultados satisfatórios e próximos, exceto pelo modelo Wilson com parâmetros da literatura. Os modelos NRTL e UNIQUAC apresentaram bons resultados, sendo o modelo NRTL cerca de 8% mais preciso que o modelo UNIQUAC, mesmo com parâmetros otimizados.

Quando os modelos preditivos são comparados, os melhores resultados foram obtidos com o modelo COSMO-SAC, sendo este cerca de 45% mais preciso que o bem conhecido modelo UNIFAC. Deve-se destacar também que o modelo F-SAC obteve um desempenho com precisão 11% maior que aquela alcançada pelo modelo UNIFAC com parâmetros de literatura.

O modelo UNIFAC com parâmetros otimizados apresentou uma melhoria significativa no seu desempenho. O modelo com parâmetros ótimos foi cerca de 40% mais preciso que o modelo com os parâmetros originais. É interessante notar que a precisão dos modelos com parâmetros otimizados aumentou principalmente nas predições das pressões de equilíbrio, possivelmente devido à magnitude dos resíduos da pressão, uma vez que estes são maiores que aqueles das composições da fase vapor, assim, o estimador busca minimizar os erros, dando maior peso às predições de pressão.

Os dados utilizados para a estimação, no entanto, foram os mesmos utilizados para a validação, o que torna a comparação tendenciosa. Dessa maneira, dados de coeficiente de atividade em diluição infinita foram coletados na literatura para realizar a comparação entre todos os modelos, com e sem parâmetros otimizados.

O modelo F-SAC apresentou os melhores resultados para a predição dos coeficientes de atividade em diluição infinita. Esse resultado é surpreendente, pois o modelo F-SAC, ainda que sem nenhum parâmetro otimizado e com uma base preditiva significativa, foi mais preciso que os modelos mais utilizados na literatura. O sucesso do modelo F-SAC para predições de coeficientes de atividade em diluição infinita se deve, provavelmente, ao fato de que os parâmetros desse modelo foram estimados com base em dados de diluição infinita. Os modelos UNIQUAC (com parâmetros de literatura) e COSMO-SAC (sem parâmetros otimizados) foram bastante precisos nas predições de diluição infinita também, seguidos pelo modelo UNIFAC com parâmetros estimados no trabalho (capítulo 6).

A precisão oferecida pelo modelo F-SAC, no entanto, não continuou quando sistemas ternários de ELL foram avaliados. Os resultados dos modelos F-SAC, COSMO-SAC e UNIFAC-LLE foram comparados para diversos sistemas ternários, nos quais o modelo UNIFAC-LLE se mostrou mais preciso, seguido do modelo COSMO-SAC. O modelo UNIFAC-LLE foi parametrizado especialmente para cálculos de equilíbrio líquido-líquido, portanto, esperava-se que este modelo seja mais preciso que os demais, cujos parâmetros são universais.

O modelo UNIFAC(Do), ou UNIFAC-Dortmund, uma modificação do já citado modelo UNIFAC, foi utilizado para a modelagem e simulação de uma coluna de destilação para separação de uma mistura quaternária de 1-Butanol + Etanol + Acetona + Água. Esse sistema é comumente obtido após um processo ABE (Acetona + 1-Butanol + Etanol), onde busca-se a obtenção de 1-butanol como combustível renovável. A mistura aquosa de 1-Butanol + Etanol + Acetone + Água é comum, sendo que a água forma azeótropo com o butanol (heterogêneo) e com o etanol (homogêneo).

Os binários do sistema foram testados separadamente e foram corretamente preditos pelo modelo UNIFAC(Do), assim, passou-se à simulação da coluna de destilação em batelada. Os resultados sugerem que apenas com uma unidade de destilação, é possível obter um produto de fundo composto apenas de 1-Butanol e água e, dependendo das condições, apenas traços de Etanol (que é retirado como produto de topo juntamente com a acetona).

O comportamento do ELV dessa mistura foi avaliado com dados experimentais disponíveis na literatura, validando o desempenho do modelo termodinâmicos e do algoritmo BOL T (chamado no capítulo 8 de *Bubble-T Algorithm*).

O 1-butanol é, posteriormente, purificado por meio de decantação (processo extrativo de equilíbrio líquido-líquido), onde, através da adição de água em excesso consegue-se deslocar o equilíbrio da mistura, ocasionando a divisão do sistema em duas fases: uma fase rica em água e a outra contendo a maior parte do 1-butanol.

Continuando a investigação dos métodos de resolução de problemas de equilíbrio de fases, uma comparação extensa entre diversos modelos de energia de Gibbs em excesso, equações de estado cúbicas e regras de mistura foi realizada e apresentada no capítulo 9.

Assim, 3 regras de mistura foram utilizadas para associar 5 modelos diferentes de EGE a 3 equações cúbicas de estado e realizar predições de ELV sob diferentes condições de pressão e temperatura. Os melhores resultados foram obtidos pela associação UNIFAC + VDW1 + PRSV, porém, outras associações ofereceram resultados quase tão bons quanto a citada anteriormente.

A regra de mistura de VDW1, quando comparada às outras duas utilizadas, apresentou resultados mais precisos, seguida da regra de mistura de WS. Na verdade, essa diferença de precisão de resultados é de apenas 5%. Quando o desempenho das regras de mistura é avaliado em misturas binárias de álcoois com alcanos de diferentes tamanhos de cadeias carbônicas, nota-se uma deterioração nos resultados das 3 regras, principalmente na regra de HVOS, que apresentou os piores resultados entre as 3. Deve-se notar que assimetria e não-idealidade dos sistemas parecem afetar muito pouco VDW1 e WS.

Entre as equações cúbicas de estados, as diferenças de resultados foram muito menores para sistemas de diferentes tamanhos de alcanos. PRSV2 apresentou os menores resíduos, porém, foi apenas 0.5% mais preciso que PRSV (e 12% mais preciso que PR), dessa forma, PRSV2 não apresentou melhorias significativas em relação a PRSV. As 3 equações, no entanto, foram bastante afetadas pelo número de carbonos no alcano da mistura.

Quando essa análise é estendida aos modelos de EGE, podemos perceber que apenas o modelo COSMO-SAC sofreu influências significativas do número de carbonos nos alcanos dos sistemas binários, possivelmente por algum problema na associação do modelo com as equações de estado através da regra HVOS, uma vez que o COSMO-SAC foi o modelo que sofreu maior influência dessa regra de mistura. Por exemplo, quando todos os resultados são comparados, o modelo UNIFAC apresentou o melhor desempenho, seguido pelos modelos UNIFAC(Do) (que foi 8% menos preciso), F-SAC (11% menos preciso) e COSMO-SAC (75% menos preciso). Quando os resultados obtidos com o uso de HVOS são omitidos, a ordem e as precisões se alteram, assim obtemos: UNIFAC, F-SAC (4.36% menos preciso), UNIFAC(Do) (6.48% menos preciso) e COSMO-SAC (22.71% menos preciso).

Também se investigou o papel da temperatura do sistema e o desempenho dos modelos para as diferentes condições experimentais. A única tendência que se observou foi a dos valores de k_{ij} serem geralmente menores quando otimizados para a regra de mistura WS do que para VDW1, e essa tendência se inverte quando PRSV é utilizada na associação.

Além disso, quando álcoois estão associados a alcanos com cadeias carbônicas muito maiores que a do próprio álcool, k_{ij} produzem resultados menos precisos, ainda que otimizados. Dessa maneira, é interessante que se proceda à uma investigação de regiões de convergência dos parâmetros para mínimos locais e globais, o que pode ser escopo de trabalhos futuros.

Tendo comparado, testado e avaliado diversos métodos para a obtenção do equilíbrio de fases, um trabalho completamente *a priori* foi proposto. O equilíbrio líquido-líquido de uma mistura de 1-Butanol + Etanol + Diesel foi estudado para diferentes condições de pressão e temperatura, uma vez que essa mistura pode ser utilizada como *blend* de combustível, mas apenas em algumas regiões do planeta, uma vez que a mistura precisa ser homogênea, e a região de uso afeta a pressão (nível do mar) e temperatura.

Observou-se que valores plausíveis para o parâmetro de interação binária k_{ij} residem entre 0.0 e 0.2, uma vez que valores maiores e menores descaracterizam completamente uma curva de equilíbrio. Os efeitos de temperatura parecem ser completamente negligenciáveis numa faixa de -20 a 20°C. Os efeitos da pressão, no

entanto, são mais importantes; à medida que a pressão do sistema aumenta, o envelope de fases diminui, revelando maior miscibilidade da mistura, ou seja, em lugares cuja pressão atmosférica é mais baixa a separação de fases da mistura é maior. Ainda assim, os limites do envelope de fases parecem ser fracamente afetados tanto pela temperatura quanto pela pressão.

Percebe-se que os modelos de energia de Gibbs em excesso analisados neste trabalho podem fornecer resultados mais ou menos precisos, dependendo de uma série de fatores como: os componentes que compõem o sistema, as condições de temperatura e pressão, o quão perto ou longe se está da diluição infinita e a regra de mistura utilizada.

Não houve um modelo absolutamente melhor, sendo que modelos como UNIFAC, COSMO-SAC e F-SAC podem ser utilizados para diferentes situações, dependendo dos dados experimentais disponíveis e de fatores como os relacionados anteriormente.

7 CONCLUSÕES

O trabalho apresentado mostrou cálculos de equilíbrios de fases (líquido-vapor, líquido-líquido ou líquido-líquido-vapor) utilizando diferentes modelos de energia de Gibbs em excesso (também conhecidos como modelos de coeficiente de atividade). Esses mesmos modelos também foram aplicados em diferentes regras de misturas para novas avaliações.

O modelo UNIFAC se mostrou um dos modelos mais confiáveis para a predição dos diferentes sistemas apresentados neste trabalho. O modelo apresentou resultados satisfatórios (ainda que não tenham sido os melhores) para predições de ELV em sistemas binários. No entanto, os modelos COSMO-SAC e F-SAC se mostraram mais precisos para cálculos de ELV para sistemas binários e para predição de coeficientes de atividade em diluição infinita (neste caso, os dois modelos superaram até mesmo o modelo UNIFAC com parâmetros otimizados para os mesmos sistemas com dados ELV).

Esse resultado, contudo, não se mantém verdadeiro quando regras de mistura são utilizadas. O modelo COSMO-SAC apresenta incompatibilidade com a regra de mistura HVOS, e mesmo quando avaliado sem os resultados obtidos através desta regra de mistura, ele continua sendo menos preciso que o UNIFAC quando regras de mistura foram utilizadas.

Também, pode-se ressaltar que as regras de mistura VDW1 e WS podem ser utilizadas com tranquilidade, enquanto a HVOS deve ser cautelosamente utilizada, uma vez que os resultados apresentados mostraram sérios desvios dos dados experimentais quando essa regra foi utilizada.

O tamanho das cadeias carbônicas dos alcanos associados aos álcoois testados parecem ter pouca influência sobre a equação de estado cúbica utilizada, muita influência sobre as regras de mistura e quase nenhuma sobre os modelos de energia de Gibbs em excesso, exceto pelo modelo COSMO-SAC, que teve suas predições deterioradas com o aumento das cadeias carbônicas dos alcanos.

A temperatura parece não apresentar grandes efeitos sobre os modelos de coeficiente de atividade na predição de equilíbrio líquido-vapor com regras de mistura,

uma vez que os desvios foram praticamente os mesmos para todos. A mesma conclusão pode ser observada nos cálculos de equilíbrio líquido-líquido de um sistema ternário de 1-Butanol + Etanol + Diesel com o uso de regras de mistura: a temperatura teve pouca importância no equilíbrio das fases líquidas, mas o envelope de fases foi afetado moderadamente pela variação de pressão no sistema. Aproveitando a capacidade preditiva do método, cálculos *a priori* revelaram um mapeamento de regiões de pressão, temperatura e composição onde a mistura ternária referida possui uma única fase e regiões em que a separação ocorre.

Os modelos COSMO-SAC e UNIFAC-LLE ofereceram boas predições para equilíbrio líquido-líquido e, ainda que o modelo F-SAC tenha apresentado resultados qualitativamente interessantes, quantitativamente os dois primeiros foram mais acurados. A performance na predição de ELL dos modelos UNIFAC-LLE, COSMO-SAC e F-SAC foi testada em 55 sistemas ternários, revelando a maior precisão do primeiro.

Os extensivos testes com os diversos modelos e algoritmos permitiram o emprego do modelo UNIFAC(Do) na modelagem e simulação de uma coluna de destilação operada em batelada. Os resultados promissores mostram que a modificação do modelo UNIFAC é, também, um modelo confiável para o uso em modelos matemáticos de processos de separação que envolvem equilíbrio de fases líquido-vapor.

Dessa maneira, o uso dos modelos F-SAC, COSMO-SAC e UNIFAC é aconselhável para diversos cálculos de equilíbrio de fases. Quando regras de mistura são utilizadas, o modelo UNIFAC parece ser mais robusto, mantendo sua precisão. As regras de mistura VDW1 e WS forneceram resultados bastante satisfatórios, sendo ambas regras passíveis de aplicação em sistemas. Além disso, a equação cúbica de estado PRSV parece ser a melhor opção quando a associação com modelos de coeficiente de atividade é necessária, uma vez que possui menos parâmetros e quase a mesma precisão que sua modificação PRSV2.

Diversos trabalhos futuros podem vir a ser desenvolvidos a partir dos resultados apresentados nesta tese, como por exemplo: análise de sensibilidade paramétrica, análise dos mínimos globais e locais das funções, validação dos modelos

aplicados em destilação e dos cálculos de equilíbrio *a priori*, e o desenvolvimento de interfaces gráficas que facilitam o uso dos modelos em sala de aula, entre outros.

APÊNDICE A – FLUXOGRAMA PARA CÁLCULO DE ELV COM REGRAS DE MISTURA

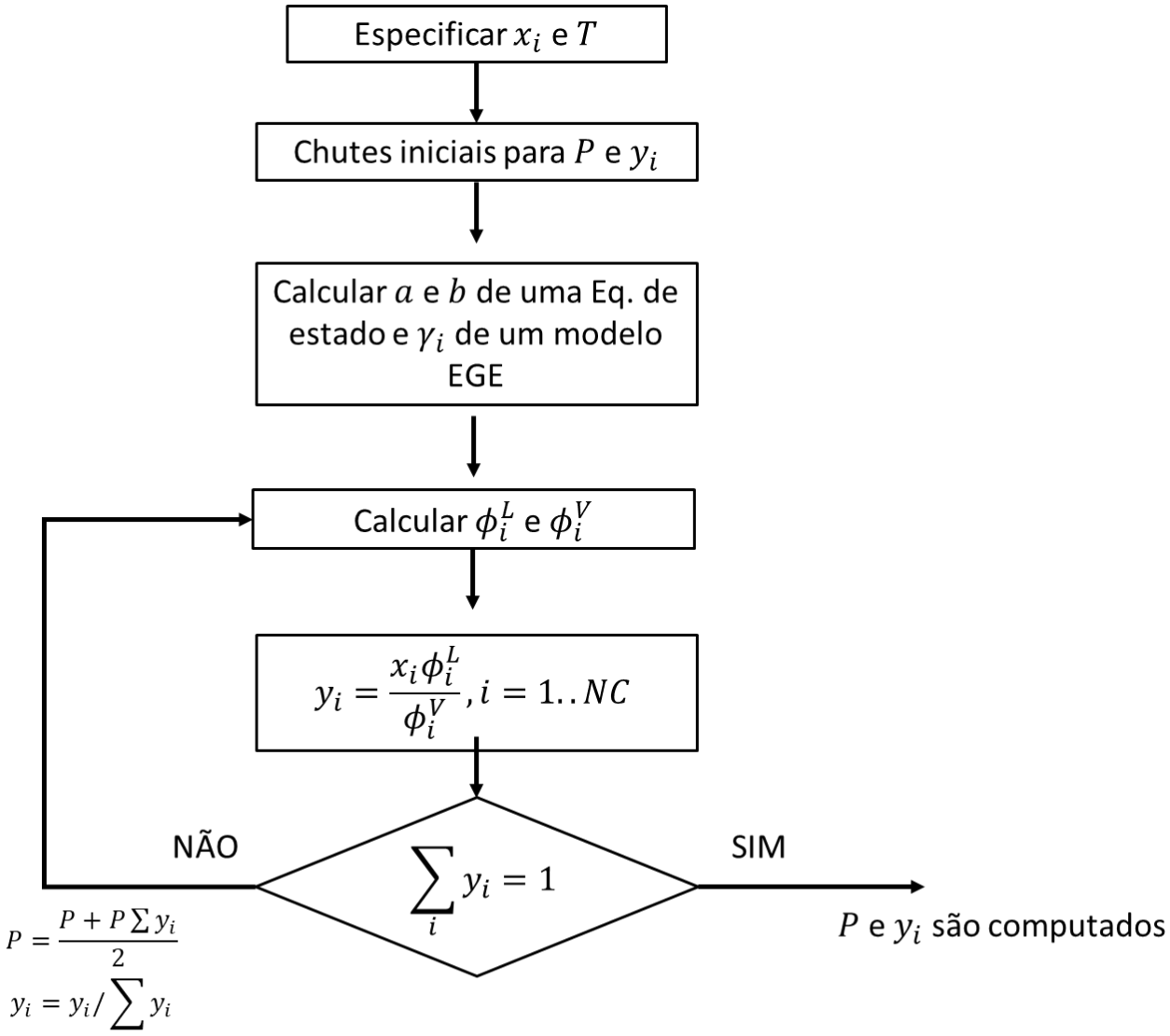

APÊNDICE B – FLUXOGRAMA PARA CÁLCULO FLASH DE ELL

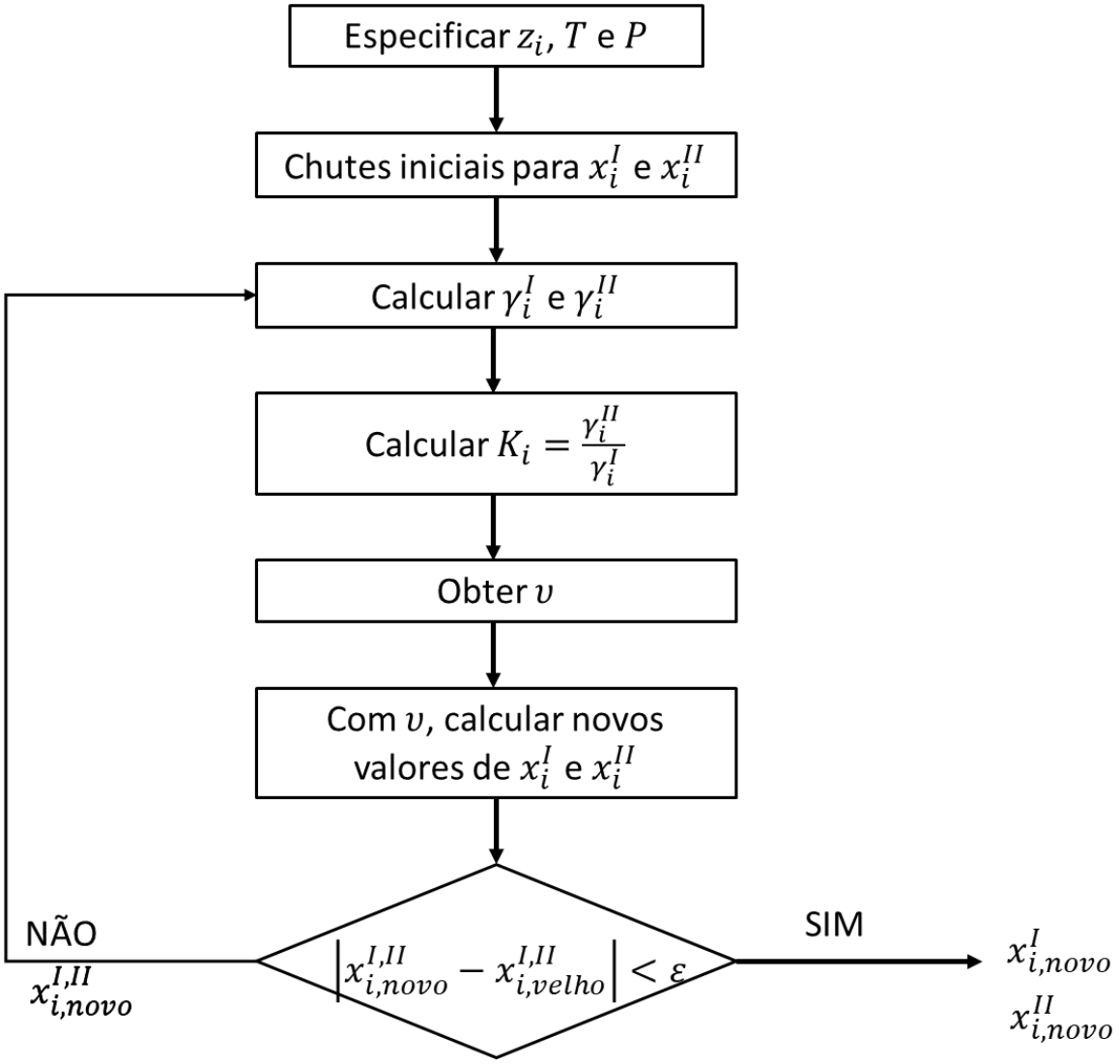

APÊNDICE C – FLUXOGRAMA PARA CÁLCULO DE ELL COM REGRAS DE MISTURA

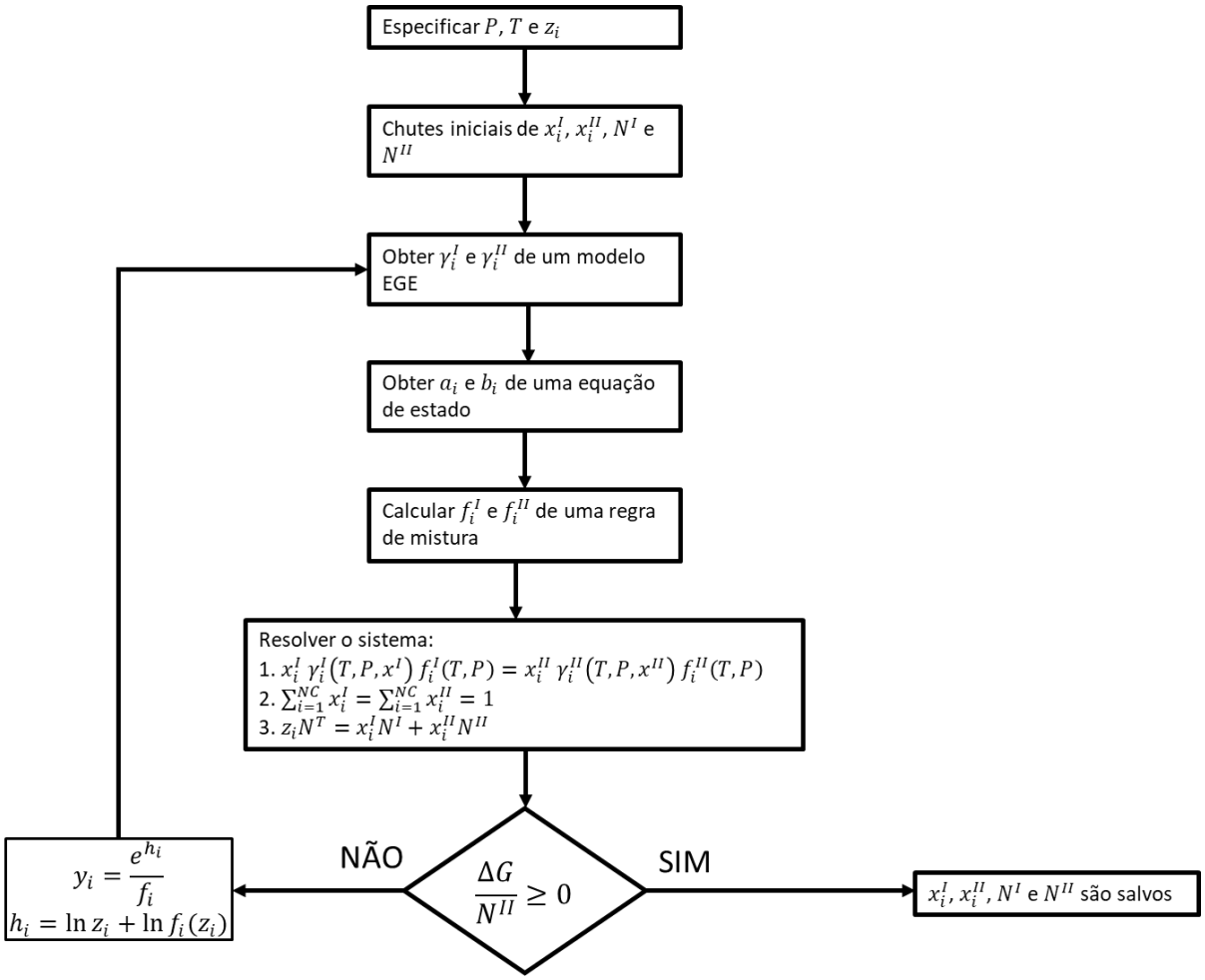

APÊNDICE D – PARÂMETROS

Tabela D1. Parâmetros das equações cúbicas de estado

	a	b	α	k
VDW	$0.4218\frac{R^2T_c^2}{P_c}$	$0.125\frac{RT_c}{P_c}$		
RK	$0.4278\frac{R^2T_c^{2.5}}{P_c}$	$0.0867\frac{RT_c}{P_c}$		
SRK	$0.4278\frac{R^2T_c^2}{P_c}$	$0.0867\frac{RT_c}{P_c}$	$\left[1+k\left(1-\sqrt{T_r}\right)\right]^2$	$0.4851+1.5517\omega-0.1561\omega^2$
PR	$0.4572\frac{R^2T_c^2}{P_c}$	$0.0778\frac{RT_c}{P_c}$	$\left[1+k\left(1-\sqrt{T_r}\right)\right]^2$	$0.37464+1.54226\omega-0.26992\omega^2$
PRSV	$0.4572\frac{R^2T_c^2}{P_c}$	$0.0778\frac{RT_c}{P_c}$	$\left[1+k\left(1-\sqrt{T_r}\right)\right]^2$	$0.37889+1.4897153\omega-0.17131848\omega^2+0.0196554\omega^3+k_1(1+\sqrt{T_r})(0.7-T_r)$
PRSV2	$0.4572\frac{R^2T_c^2}{P_c}$	$0.0778\frac{RT_c}{P_c}$	$\left[1+k\left(1-\sqrt{T_r}\right)\right]^2$	$0.37889+1.4897153\omega-0.17131848\omega^2+0.0196554\omega^3+\left[k_1+k_2(k_3-T_r)(1-\sqrt{T_r})\right]\times(1-\sqrt{T_r})(0.7-T_r)$

$$T_r=\frac{T}{T_c}$$

APÊNDICE E – EXTENDING THE RANGE OF APPLICABILITY

AIChE

THERMODYNAMICS AND MOLECULAR-SCALE PHENOMENA

Extending the Range of COSMO-SAC to High Temperatures and High Pressures

Christian L. Silveira
Dept. of Chemical Engineering, Universidade Federal de Santa Maria, Santa Maria, RS 97105-900, Brazil

Stanley I. Sandler
Dept. of Chemical and Biomolecular Engineering, University of Delaware, Newark, DE 19716

DOI 10.1002/aic.16043
Published online December 12, 2017 in Wiley Online Library (wileyonlinelibrary.com)

The range of the predictive Gibbs energy of solvation model, COSMO-SAC, is extended to large ranges of density, pressure, and temperature for very nonideal mixtures by combining it with an equation of state (EOS) using the Wong-Sandler mixing rule. The accuracy of isothermal vapor-liquid equilibria (VLE) calculations based on using the predictive COSMO-SAC model and separately the correlative NRTL model is compared, each combined with three different forms of the Peng-Robinson equation of state. All the models considered require the value of the EOS mixing rule binary parameter k_{ij}. The NRTL model also requires three other parameters obtained from correlation low pressure VLE data. The PRSV + COSMO-SAC model is showed, with its one adjustable parameter obtained from low temperature data leads good predictions at much higher temperatures and pressures. © 2017 American Institute of Chemical Engineers *AIChE J*, 64: 1806–1813, 2018

Keywords: conductor-like screening model—segment activity coefficient, Wong-Sandler mixing rule, vapor-liquid equilibria, nonideal mixtures, high pressure

Introduction

Two different types of chemical thermodynamic models are generally used in industrial applications. One is equations of state (EOS) that range from the virial equation, that is applicable only at low density, to multiparameter extended virial equations (that can be difficult to use for mixtures and for routine engineering calculations), and cubic EOS that are frequently used for engineering calculations, but only for relatively simple mixtures that do not hydrogen bond or otherwise associate. The second type of model is activity coefficient or equivalently excess Gibbs energy models that can be used for liquid mixtures of a wide degree of complexity by suitable parameterization, but are mainly applicable to liquids. Wong et al.[1] discuss the applicability of these different classes of models at different conditions.

A question that arises with EOS is the mixing rules (MRs) to be used when extending a pure component EOS to mixtures. Usually such MRs are formulated to be quadratically dependent on mole fraction to satisfy the low-density boundary condition on the second virial coefficient known from statistical mechanics. Huron and Vidal[2] reported that classical MRs are only really effective for nonpolar gas mixtures. Huron et al.[3] and Asselineau et al.[4] showed that fitting the binary parameter contained in the MRs using experimental data can extend the range of applicability of cubic EOS to mixtures that are slightly polar.

Wong and Sandler[5] proposed a new MR that simultaneously satisfies the quadratic composition dependence of the second virial coefficient at low density, and behaves like an activity coefficient (solvation free energy) model at high density. For brevity, we will refer to this as the WS mixing rule, or simply as WSMR. Previous to this, Huron and Vidal[2] had proposed a MR by equating the excess Gibbs energy at infinite pressure calculated from an EOS to the excess Gibbs energy of an activity coefficient model for liquids. This approach has two main problems. The first is that it requires that the excess volume V^E at infinite pressure to be 0, otherwise the term PV^E in the expression for excess Gibbs energy G^E becomes infinite and then is not related to an activity coefficient model. The second is that their MR does not satisfy the requirement that the second virial coefficient be a quadratic function of composition so that the low density compositional behavior of the EOS can be problematic. In the same fashion, Holderbaum and Gmehling[6] proposed the predictive Soave-Redlich-Kwong using both the Soave-Redlich-Kwong EOS and the UNIFAC method; however, this approach was made using the Gibbs energy as well. The WS mixing rule uses the Helmholtz energy that is virtually independent of the liquid density and so is much less dependent on pressure than the Gibbs energy.[5] Consequently, at liquid density the following equality is used

Additional Supporting Information may be found in the online version of this article.

Correspondence concerning this article should be addressed to C. L. Silveira at christiansilveira86@gmail.com.

$$\text{Activity Coefficient Model} \equiv \underline{G}^E(T,x,P=\text{low}) = \underline{A}^E(T,x,P=\text{low}) = \underline{A}^E(T,x,P=\infty) \quad (1)$$

so that the common liquid-phase excess Gibbs energy models can be used at high pressure when the Helmholtz energy is used in the EOS boundary condition.

Several different MRs have been proposed in recent last years. Voutsas et al.[7] proposed a so-called universal mixing rule (UMR) for cubic EOS, coupling it with the UNIFAC activity coefficient model, and claiming its applicability for both symmetric and asymmetric systems. Staudt and Soares[8] proposed the self-consistent Gibbs excess mixing rule (SCMR) and claim that it can predict with more accuracy the excess Gibbs energy than other MRs—such as UMR, UGMR,[9] and MHV-1.[10] In their work, the SCMR was tested with a COSMO-SAC version implemented and parametrized by Gerber and Soares.[11] Even though these rules provide good results, they are more difficult to implement and furthermore the requirement that the second virial coefficient be a quadratic function of composition is not met so that their behavior at low density is uncertain. In contrast, use of the MR of Wong and Sandler allows a cubic EOS to produce the proper composition dependence of the second virial coefficient at low density and behave like an activity coefficient model at liquid densities. Previous calculations have shown that it is reasonably accurate over this range of densities. The details of this seamless combination of an EOS and activity coefficient models are described in Ref. 5.

In that reference the Peng-Robinson EOS was combined with various activity coefficient models with correlated parameters to make good predictions of vapor-liquid and vapor-liquid-liquid equilibria over wide ranges of temperature and pressure. Here, we want to extend this work by making it almost completely predictive (requiring only the single EOS binary interaction parameter k_{ij}) by replacing the activity coefficient model parameters that have been correlated to low pressure VLE data with a predictive model based on quantum mechanics.

The predictive activity coefficient model we use is COSMO-SAC proposed by Lin and Sandler[12] and refined and improved by Lin et al.,[13] Wang et al.,[14] and Hsieh et al.[15] for VLE and LLE predictions, and most recently by Xiong et al.[16] The main advantage of the COSMO-SAC over UNIFAC[17] and modified UNIFAC[18] is its small number of adjustable parameters, that it can distinguish between isomers having the same numbers of each functional group, there are no arbitrary choices of how to divide a molecule into functional groups, and that no new functional groups need to be defined for new classes of compounds. Further, as there are only nine universal adjustable parameters in COSMO-SAC,[16] there is no need for a difficult parameter estimation procedure with extremely large experimental data sets as required when introducing a new functional group in the UNIFAC and modified UNIFAC models. The disadvantage of COSMO-SAC is that a quantum mechanical density functional calculation of the charge density on the surface of each molecule must be done. However, this needs to be done only once for each molecule and stored in a data bank for future use with mixtures containing this molecule. Our current data bank contains over 2100 molecules; consequently, the user of the COSMO-SAC method needs to know nothing about the underlying quantum mechanical calculations. Also, COSMO-SAC calculations are very fast, indeed almost as fast as UNIFAC calculations, and are easily incorporated into chemical process calculations as has been done in the Aspen simulator.

In this work, the COSMO-SAC model used to predict the Gibbs energy of solvation, and thereby liquid-phase activity coefficients, is coupled with the original cubic EOS of Peng-Robinson and two of its variants, PRSV[19] and PRSV2,[20] using the WS mixing rule. This approach allows the combined model to be used to estimate the phase behavior of nonideal systems over wide ranges of temperature, pressure, and

Table 1. Critical Properties and NRTL Parameters Used in the Tested Systems

Systems	T_C (K)	P_C (kPa)	ω	α	a_{12} (cal/mol)	a_{21} (cal/mol)	Exp. Data Source	NRTL Parameters Source	NP
Acetone (1)	508.1	4701	0.309	0.3000	924.2000	863.1000	21	22	117
Methanol (2)	512.6	8096	0.559						
Methanol (1)	512.6	8096	0.559	0.2600	−786.5000	2153.6000	21	23	153
Water (2)	647.3	22048	0.3438						
2-propanol (1)	508.4	4764	0.6637	0.3000	6900.8100	77.4900	24	25	231
Water (2)	647.3	22048	0.3438						
Methanol (1)	512.6	8096	0.559	0.4858	777.3744	1142.1594	26	27	210
Benzene (2)	562.1	4894	0.212						
Acetone (1)	508.1	4701	0.309	0.4200	2609.2000	3164.1000	21	23	216
Water (2)	647.3	22048	0.3438						
Ethanol (1)	516.2	6383	0.635	0.3000	88.0000	976.0000	24	28	252
Water (2)	647.3	22048	0.3438						
Butane (1)	425.15	3792	0.199	0.4240	1678.2112	1045.5487	27,29	27	138
Methanol (2)	512.6	8096	0.559						
Butanol (1)	562.98	4412	0.595	−1.1217	1905.4000	1816.3000	30	30[a]	126
n-Decane (2)	618.45	2123	0.484						
Butanol (1)	562.98	4412	0.595	0.2000	−62.2000	−1002.4000	31,32	33	93
n-Hexane (2)	507.43	3012	0.305						
Heptane (1)	540.26	2736	0.351	−1.1732	1267.7400	2112.9200	34	34[a]	183
1-Pentanol (2)	586.15	3880	0.675						
Heptane (1)	540.26	2736	0.351	−1.2376	1223.0500	2041.0300	34	34[a]	231
3-Methyl-1-butanol (2)	579.45	3880	0.556						
Pentane (1)	469.65	3369	0.249	0.2884	1036.9000	1035.9000	35	[b]	99
Methanol (2)	512.6	8096	0.559						

[a]The values shown in Table 1 are the mean values; the authors reported, however, one value for each parameter for each temperature.
[b]The values presented in Table 1 are estimated values.
The (a) and (b) notes are referring exclusively to the NRTL parameters, i.e., alpha, a12, and a21.

Table 2. WS MR Binary Interaction Parameter k_{ij} for Every System and Every Model Tested, and vdW Binary Interaction Parameter k_{ij} for the PRSV

Systems	PR + COSMO-SAC	PRSV + COSMO-SAC	PRSV2 + COSMO-SAC	PR + NRTL	PRSV + NRTL	PRSV2 + NRTL	PRSV
Acetone (1) Methanol (2)	0.0684 ± 0.0003	0.1150 ± 0.0005	0.0469 ± 0.0011	0.0218 ± 0.0002	0.0752 ± 0.0005	0.0001 ± 0.0006	0.0100 ± 0.0002
Methanol (1) Water (2)	0.0299 ± 0.0004	0.0387 ± 0.0007	0.0470 ± 0.0003	0.1477 ± 0.0004	0.1562 ± 0.0008	0.1593 ± 0.0007	−0.0657 ± 0.0003
2-Propanol (1) Water (2)	0.2270 ± 0.0016	0.2603 ± 0.0009	0.3859 ± 0.0033	0.3023 ± 0.0008	0.3266 ± 0.0002	0.4984 ± 0.0050	−0.1153 ± 0.0006
Methanol (1) Benzene (2)	0.3130 ± 0.0006	0.3360 ± 0.0008	0.3020 ± 0.0008	0.4521 ± 0.0009	0.4830 ± 0.0011	0.4397 ± 0.0012	0.1289 ± 0.0003
Acetone (1) Water (2)	0.3049 ± 0.0015	0.3077 ± 0.0011	0.3238 ± 0.0009	0.3702 ± 0.0003	0.3732 ± 0.0003	0.3845 ± 0.0007	−0.1417 ± 0.0011
Ethanol (1) Water (2)	0.1390 ± 0.0011	0.1455 ± 0.0011	0.2474 ± 0.0034	0.3474 ± 0.0010	0.3523 ± 0.0010	0.4930 ± 0.0032	−0.0648 ± 0.0002
Butane (1) Methanol (2)	0.3209 ± 0.0010	0.3146 ± 0.0009	0.3414 ± 0.0012	0.6152 ± 0.0015	0.6090 ± 0.0015	0.6300 ± 0.0014	0.0435 ± 0.0008
Butanol (1) Decane (2)	0.3002 ± 0.0017	0.3945 ± 0.0004	0.3885 ± 0.0003	0.2704 ± 0.0022	0.3596 ± 0.0001	0.3561 ± 0.0001	0.0503 ± 0.0001
Butanol (1) Hexane (2)	0.2057 ± 0.0013	0.2305 ± 0.0011	0.1880 ± 0.0013	0.7367 ± 0.0013	0.7520 ± 0.0005	0.7195 ± 0.0007	0.0545 ± 0.0008
Heptane (1) 1-Pentanol (2)	0.2486 ± 0.0002	0.2768 ± 0.0001	0.2578 ± 0.0003	0.1865 ± 0.0003	0.2213 ± 0.0001	0.2100 ± 0.0006	0.0676 ± 0.0001
Heptane (1) 3-Methyl-1-butanol (2)	0.1576 ± 0.0001	0.2061 ± 0.0001	0.1701 ± 0.0001	0.1384 ± 0.0004	0.1795 ± 0.0002	0.1416 ± 0.0006	0.0801 ± 0.0001
Pentane (1) Methanol (2)	0.4423 ± 0.0003	0.4528 ± 0.0006	0.4478 ± 0.0002	0.7198 ± 0.0003	0.7353 ± 0.0002	0.7293 ± 0.0004	0.1348 ± 0.0009

Table 3. Results of the PR Models with COSMO-SAC and NRTL Models

		AR y_1	AR P	RMSD y_1	RMSD P (kPa)	AAD y_1	AAD P (kPa)
PR + COSMO-SAC	Average	0.0366	0.0247	0.0232	53.6806	0.0178	44.4392
	SD	0.0447	0.0191	0.0130	69.0470	0.0097	56.8509
PRSV + COSMO-SAC	Average	0.0303	0.0207	0.0210	46.8379	0.0159	37.4417
	SD	0.0276	0.0138	0.0131	60.5534	0.0090	45.9674
PRSV2 + COSMO-SAC	Average	0.0370	0.0329	0.0250	110.2049	0.0193	91.6942
	SD	0.0378	0.0256	0.0145	168.6857	0.0105	138.0353
PR + NRTL	Average	0.0642	0.0369	0.0362	86.4260	0.0280	68.7552
	SD	0.0712	0.0263	0.0161	103.3108	0.0132	81.9116
PRSV + NRTL	Average	0.0593	0.0355	0.0345	89.2364	0.0246	71.8044
	SD	0.0659	0.0272	0.0177	113.7380	0.0137	91.8354
PRSV2 + NRTL	Average	0.0571	0.0504	0.0371	159.0369	0.0285	140.3782
	SD	0.0465	0.0420	0.0181	246.7748	0.0139	226.3571
PRSV	Average	0.0532	0.0576	0.0460	89.4638	0.0329	68.3999
	SD	0.0484	0.0614	0.0376	95.1454	0.0246	68.8985
COSMO-SAC	Average	0.4893	0.3123	0.2128	1776.6120	0.1774	1760.7601
	SD	1.0133	0.3146	0.1437	3315.6352	0.1473	3312.0084

composition with only one adjustable parameter, the cubic EOS binary interaction parameter k_{ij} of the WSMR. This parameter is independent of the state variables. The PRSV model has one adjustable parameter while PRSV2 model modifies the temperature dependence of the attractive term of the PRSV model has three adjustable parameters for better VLE predictions.

The results of using the COSMO-SAC model with each of the three versions of the PR EOS with the WSMR combined with the NRTL model with its three additional parameters obtained from the correlation of low pressure phase behavior data are compared here. The results are also compared with those from the PRSV EOS with quadratic van der Waals MR. (Note that the value of k_{ij} parameter in the quadratic vdW MR is different from the values obtained with the WSMR.) The results obtained here are for high pressure, high temperature experimental VLE data reported in the literature for 12 different binary systems (2049 experimental points) over a wide range of temperature and pressure.

Computational Details

The experimental data for VLE for the 12 binary systems tested in this work were obtained from literature: acetone + methanol at 100, 150, and 200°C; methanol + water at 100, 150, 200, and 250°C; 2-propanol + water at 150, 200, 250, 275, and 300°C; methanol + benzene at 100, 120, 140, 160, 180, 200, and 220°C; acetone + water at 100, 150, 200, and 250°C; ethanol + water at 150, 200, 250, 275, 300, 325, and 350°C; *n*-butane + methanol at 0 and 50°C; butanol + *n*-decane at 85, 100, and 115°C; butanol + *n*-hexane at 25 and 50°C; heptane + 1-pentanol at 75, 85, and 95°C; heptane + 3-methyl-1-butanol at 75, 85, and 95°C; and pentane + methanol at 100, 125, and 150°C. The critical properties, acentric factors, NRTL parameters used and their source, and the number of experimental points available (NP) for each binary system are listed in Table 1.

A Levenberg-Marquardt algorithm[36] implemented in a MATLAB® function was used to estimate the WS mixing rule binary interaction parameter k_{ij} for each system and for each of the combined equation of state + activity coefficient models. For each model, two different sets of k_{ij} values were obtained. In the first set, a single value of k_{ij} was obtained by minimizing the error between calculated and experimental values for each system at the lowest temperature at which data were available, then there was no further adjustment of this parameter. The value of this parameter was then used to make VLE estimations at all higher temperatures for which data

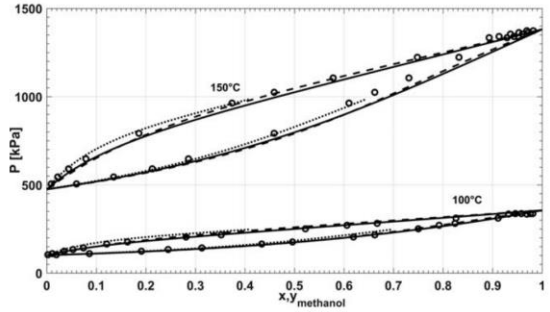

Figure 1. Diagram for low temperature and pressure conditions for the methanol + water system predictions with the PRSV + COSMO-SAC, PRSV + NRTL, and PRSV models (PRSV + COSMO-SAC—solid line, PRSV + NRTL—dashed line, PRSV—dotted line).

Experimental data.[21]

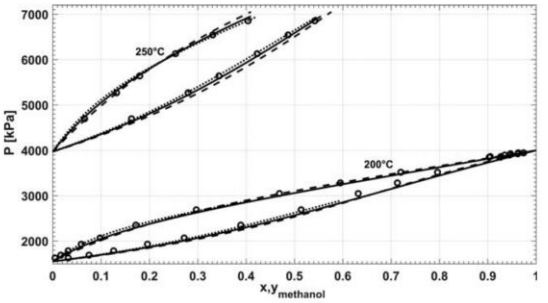

Figure 2. Diagram for high temperature and pressure conditions for the methanol + water system predictions with the PRSV + COSMO-SAC, PRSV + NRTL, and PRSV models (PRSV + COSMO-SAC—solid line, PRSV + NRTL—dashed line, PRSV—dotted line).

Experimental data.[21]

were available. In the second set, a single value of k_{ij} was obtained as the best fit parameter for the data at all temperatures for each mixture. The k_{ij} values obtained for each system by both methods are in Table 2 (and Supporting Information Table A1, Appendix A). As this parameter is considered independent of temperature, pressure, and composition for each binary system, there is only a single value for each of the two fitting methods and separately for each model. It is interesting to note that the values of the k_{ij} parameters are uniformly lower using COSMO-SAC than the NRTL model.

After the estimation of the k_{ij} parameter, the average relative deviation (ARD), the root mean square deviation (RMSD), and the average absolute deviation (AAD) were computed for each system vapor-phase composition and absolute pressure for the whole VLE data set. The VLE calculations, for the fixed liquid compositions reported in the literature, were performed using a simple bubble-point algorithm. The tolerance criterion used was

$$1-\sum_{i=1}^{NP} y_i \leq 1\times10^{-8} \tag{2}$$

Results

The final results obtained with the use of the estimated MR binary interaction parameter k_{ij} can be seen in Table 3 (and Supporting Information Table A2, Appendix A). In this table, the following abbreviations are used

$$\text{AR} = \text{average relative deviation} = \frac{\sum_{i=1}^{NP} |\theta_{i,\text{exp}} - \theta_{i,\text{calc}}|}{\theta_{i,\text{exp}}} \tag{3}$$

$$\text{RMSD} = \text{root mean square deviation} = \frac{\sum_{i=1}^{NP} \sqrt{\left(\theta_{i,\text{exp}} - \theta_{i,\text{calc}}\right)^2}}{\text{NP}} \tag{4}$$

and

$$\text{Average absolute deviation} = \frac{\sum_{i=1}^{NP} |\theta_{i,\text{exp}} - \theta_{i,\text{calc}}|}{\text{NP}} \tag{5}$$

with θ being either the vapor composition or pressure, NP the number of points, and the subscripts exp and calc indicating the experimental and calculated values, respectively. The SD indicates the standard deviation of the obtained results; so, even though it may not hold significant statistical meaning for the RMSD and AAD for pressure, because it has different order of magnitude depending on the system and its conditions, it does measure the SD for the vapor-phase fraction results and all AR results.

As can be seen in the Table 3, the combination of the PRSV + COSMO-SAC model yields the best results, having the lowest average relative deviations and RMSDs for both vapor-phase composition and pressure. Indeed, this model has approximately half the deviations from experiment in pressure and vapor composition than other studied models. We also see that the combination of the PRSV model with either activity coefficient model produced better results than with either the PR or PRSV2 EOS. It is noticeable that the combination of the completely predictive COSMO-SAC activity coefficient model with the EOSs produced better results than the EOS combined with the correlative NRTL model. It is somewhat surprising that the use of the PRSV2 EOS with either of the COSMO-SAC and NRTL models produced the worst results as the PRSV2 modification of the Peng-Robinson EOS was developed especially for VLE calculations.

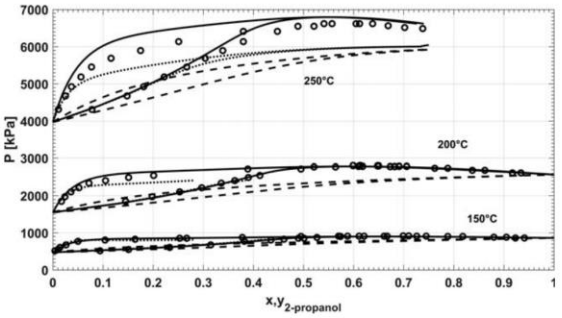

Figure 3. Diagram for low temperature and pressure conditions for the 2-propanol + water system predictions with the PRSV + COSMO-SAC, PRSV + NRTL, and PRSV models (PRSV + COSMO-SAC—solid line, PRSV + NRTL—dashed line, PRSV—dotted line).

Experimental data.[24]

It can also be seen in Table 3 that the results obtained with the use of the COSMO-SAC model alone are not satisfying. The COSMO-SAC is particularly interesting for low pressure systems, hence good predictions are obtained for systems that the temperature and pressure do not raise too much—butanol (1)/decane (2), butanol (1)/hexane (2), and pentane (1)/methanol (2); systems that have wider range of T and P conditions are not well described by the COSMO-SAC alone when more severe conditions are reached.

It should be noted that the COSMO-SAC model performance for mixtures that contain water is lower than for the other mixtures. The COSMO-SAC model is still in need of some improvements in the hydrogen bonding energy term, which may be the reason why, even for low temperature and pressure conditions, the model is not satisfactorily accurate. So, in these cases, we may see the binary interaction parameter k_{ij} sort of "fixing" the COSMO-SAC performance.

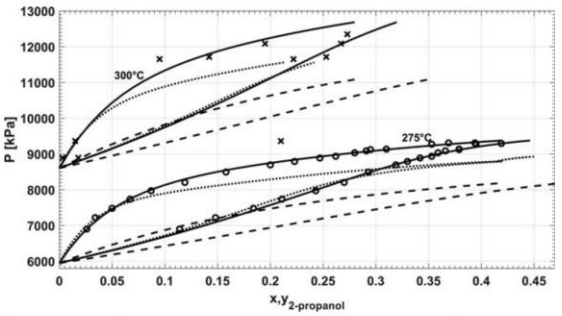

Figure 4. Diagram for high temperature and pressure conditions for the 2-propanol + water system predictions with the PRSV + COSMO-SAC, PRSV + NRTL, and PRSV models (PRSV + COSMO-SAC—solid line, PRSV + NRTL—dashed line, PRSV—dotted line).

Experimental data.[24]

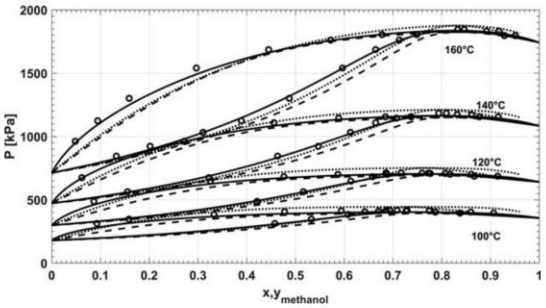

Figure 5. Diagram for low temperature and pressure conditions for the methanol + benzene system predictions with the PRSV + COSMO-SAC, PRSV + NRTL), and PRSV models (PRSV + COSMO-SAC—solid line, PRSV + NRTL—dashed line, PRSV—dotted line).

Experimental data.[26]

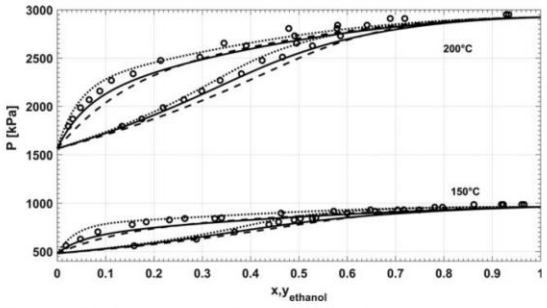

Figure 7. Diagram for low temperature and pressure conditions for the ethanol + water system predictions with the PRSV + COSMO-SAC, PRSV + NRTL, and PRSV models (PRSV + COSMO-SAC—solid line, PRSV + NRTL—dashed line, PRSV—dotted line).

Experimental data.[24]

As the PRSV EOS provided better estimations with both COSMO-SAC and NRTL than the other EOS, as it can be seen in Table 3, for visual simplicity it is only these that are presented in the following graphs. Also, only 4 of the 12 systems are shown, and these systems were chosen because of the wider range of temperature and pressure in their experimental data. More detailed information on all the systems studied here is provided in the Supporting Information Appendices.

As can be seen in Figures 1–8, the PRSV + NRTL model provides reasonable estimations of the phase behavior at high temperatures and pressures, however, even better results are obtained using the PRSV + COSMO-SAC approach. The results using the value of k_{ij} obtained only with the lowest temperature data, can be seen in Figures 5–8 (Supporting Information Appendix B). Also, it should be noted that all the COSMO-SAC + EOS methods have only one adjustable parameter, the k_{ij} of the EOS MR. Using the NRTL model in any of the MRs requires not only a value of k_{ij} to be adjusted, but also the NRTL parameters α, a_{12}, and a_{21}, the values of which are referenced in Table 1, and have been obtained from correlating low-pressure VLE data.

The results obtained with the use of the PRSV EOS with the simple quadratic MR, as can be seen in Figures 1–9 (and Supporting Information Figures B1–B9, Appendix B), given the simplicity of the method, are very good only for the ethanol-water system. However, for the other systems it tends to not be as good. For example, for the 2-propanol-water system, this model yields good predictions at low pressures, but as the pressure rises its predictions become less accurate.

Systems containing 2-propanol are also known to be difficultly represented by the UNIFAC model, which is one of the best activity coefficient models available. In this manner, we have performed a simulation only for that system using the UNIFAC model. The UNIFAC model alone does not provide results as accurate as the PR + COSMO-SAC or PRSV + COSMO-SAC, and its performance, compared to the other models, for the 2-propanol + water system can be seen in Supporting Information Table A3 (Appendix A). The comparison between UNIFAC and COSMO-SAC, however, reveals that the first is still more accurate, even though the COSMO-SAC performance was also satisfactory. The sum of the AR for all temperatures of the 2-propanol + water system of the UNIFAC model results in

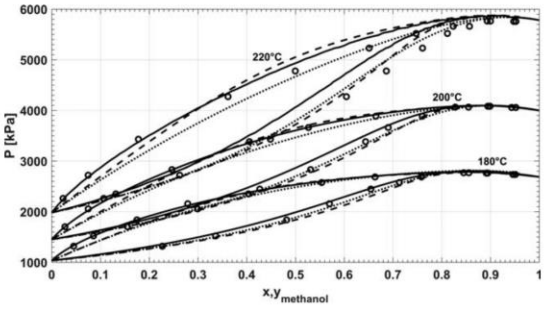

Figure 6. Diagram for high temperature and pressure conditions for the methanol + benzene system predictions with the PRSV + COSMO-SAC, PRSV + NRTL, and PRSV models (PRSV + COSMO-SAC—solid line, PRSV + NRTL—dashed line, PRSV—dotted line).

Experimental data.[26]

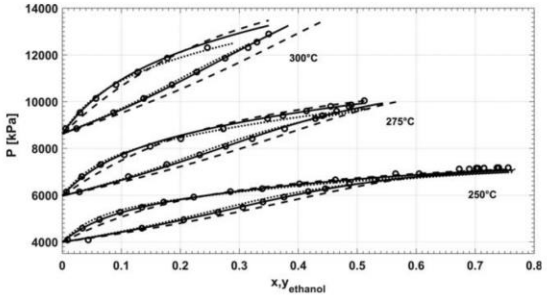

Figure 8. Diagram for mean temperature and pressure conditions for the ethanol + water system predictions with the PRSV + COSMO-SAC, PRSV + NRTL, and PRSV models (PRSV + COSMO-SAC—solid line, PRSV + NRTL—dashed line, PRSV—dotted line).

Experimental data.[24]

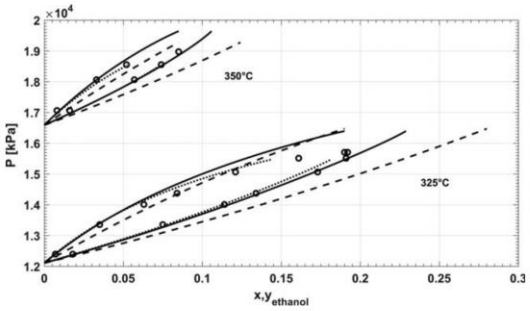

Figure 9. Diagram for high temperature and pressure conditions for the ethanol + water system predictions with the PRSV + COSMO-SAC, PRSV + NRTL, and PRSV models (PRSV + COSMO-SAC—solid line, PRSV + NRTL—dashed line, PRSV—dotted line).

Experimental data.[24]

1.2216 and 0.1580, while the COSMO-SAC results are 3.7440 and 2.3700, revealing that the UNIFAC is better when compared solely to the COSMO-SAC model for this system.

The data for the systems 2-propanol + water (Figure 2) and ethanol + water (Figure 4) extend temperature ranges of over 150°C to pressure ranges of over 10,000 kPa. Also, in these two systems, it can be clearly seen that as the temperature and pressure increases there is the largest difference between PRSV + COSMO-SAC and PRSV + NRTL methods, with noticeably better performance of the PRSV + COSMO-SAC model. Analyzing the results presented in Table 3 and Figures 1–8, it can be concluded that the PRSV + COSMO-SAC model is, among the tested approaches, the best for vapor-liquid equilibria (VLE) calculations over large ranges of temperature and pressure. Its wide range of applicability for non-ideal mixtures, from pressures of less than 100 kPa to over 10,000 kPa, makes it a useful tool for engineering purposes, overcoming the separate limitations of EOS and activity coefficients models.

Also, it should be noted that using a single value of the binary interaction parameter k_{ij} fit to only the lowest temperature data results in estimations at higher temperatures and pressures that are only slightly less accurate than using the value obtained by correlating data over the whole temperature range, as can be seen in Supporting Information Table A2 (Appendix A) and Supporting Information Figures B1–B9 (Appendix B).

Conclusions

While many EOS MRs have been suggested over the years, such as the van der Waals MR, can be applied to fairly simple mixtures (hydrocarbons or inorganic gases), the WSMR is an alternative to extend the applicability of EOS to more complex mixtures and over wide ranges of temperature and pressure while meeting the boundary conditions at both low and high density. The use of an EOS model combined with an activity coefficient model through the WSMR provides a wider range of applicability, being able to predict VLE behavior of non-ideal mixtures from low density conditions to very high pressure and temperature, and even close to the mixture critical points as shown in Figures 1–4.

We have shown here that once a value of the MR binary interaction parameter k_{ij} is obtained for a system, it can be used to make good VLE predictions at all temperatures, pressures, and compositions. It was also shown that the PRSV + COSMO-SAC model provided the best results of the models considered, having the smallest average deviations and RMSD values and, therefore, resulting in VLE behavior closest to the experimental data. Even though the PRSV + NRTL model and the PRSV EOS also provided relatively good results, it was shown that the PRSV + COSMO-SAC model is still somewhat better with about half the average error. Also, the PRSV + COSMO-SAC model requires only one adjustable parameter while the PRSV + NRTL model requires four.

The combination of the original PR EOS with the two activity coefficient models considered here provided fairly good results, they were not as good as using the PRSV equation, and both were better than using PRSV2 model. Therefore, we conclude that the use of the WS mixing rule with the PRSV + COSMO-SAC model provided the best results in the study here, and therefore is a useful method for extending the COSMO-SAC free energy solvation model to predict VLE data over large ranges of temperature and pressure.

We also see that obtaining the value of the k_{ij} binary interaction parameter for the PRSV + COSMO-SAC model by correlating data at only a single temperature allows reasonably accurate estimations of VLE over a wide range of temperatures and pressures, including near the mixture critical point.

Acknowledgment

Christian would like to thank to Nina P. G. Salau for the intellectual support and the incentive.

Notation

Abbreviations

AAD = average absolute deviation
AR = average relative deviation
COSMO-SAC = conductor-like screening model—segment activity coefficient
EOS = equation of state
LLE = liquid-liquid equilibrium
MHV-1 = modified Huron-Vidal mixing rule
MR = mixing-rule
NP = number of experimental points
NRTL = nonrandom two liquid model
PR = Peng-Robinson
PRSV = Peng-Robinson-Stryjek-Vera
RSMD = root mean square deviation
SCMR = self-consistent Gibbs excess mixing rule
SD = standard deviation
UGMR = universal and generic mixing rule
UMR = universal mixing rule
UNIFAC = UNIQUAC functional-group activity coefficients
UNIQUAC = universal quasi-chemical activity coefficients
VLE = vapor-liquid equilibrium
WS = Wong-Sandler
WSMR = Wong-Sandler mixing rule

Literature Cited

1. Wong DSH, Orbey H, Sandler SI. Equation of state mixing rule for nonideal mixtures using available activity coefficient model parameters and that allows extrapolation over large ranges of temperature and pressure. *Ind Eng Chem Res*. 1992;31(8):2033–2039.
2. Huron M, Vidal J. New mixing rules in simple equations of state for representing vapour-liquid equilibria of strongly non-ideal mixtures. *Fluid Phase Equilib*. 1979;3(4):255–271.
3. Huron M, Dufour G, Vidal J. Vapour-liquid equilibrium and critical locus curve calculations with the Soave equation for hydrocarbons

systems with carbon dioxide and hydrogen sulphide. *Fluid Phase Equilib.* 1977;1(4):247–265.
4. Asselineau L, Bogdanić G, Vidal J. Calculation of thermodynamic properties and vapor-liquid equilibria of refrigerants. *Chem Eng Sci.* 1978;33(9):1269–1276.
5. Wong DSH, Sandler SI. A theoretically correct mixing rule for cubic equations of state. *AIChE J.* 1992;38(5):671–680.
6. Holderbaum T, Gmehling J. PSRK: a group contribution equation of state based on UNIFAC. *Fluid Phase Equilib.* 1991;70(2–3):251–265.
7. Voutsas E, Magoulas K, Tassios D. Universal mixing rule for cubic equations of state applicable to symmetric and asymmetric systems: results with the Peng-Robinson equation of state. *Ind Eng Chem Res.* 2004;43(19):6238–6246.
8. Staudt PB, Soares RP. A self-consistent Gibbs excess mixing rule for cubic equations of state. *Fluid Phase Equilib.* 2012;334:76–88.
9. Staudt PB, Soares RP, Secchi AR, Cardozo NSM. A new cubic equation of state for prediction of VLE of polymer solutions. *Fluid Phase Equilib.* 2010;295(1):38–45.
10. Michelsen ML. A modified Huron-Vidal mixing rule for cubic equations of state. *Fluid Phase Equilib.* 1990;60(1–2):213–219.
11. Gerber RP, Soares RP. Assessing the reliability of predictive activity coefficient models for molecules consisting of several functional groups. *Braz J Chem Eng.* 2013;30(1):1–11.
12. Lin S, Sandler SI. A priori phase equilibrium prediction from a segment contribution solvation model. *Ind Eng Chem Res.* 2002;41(5): 899–913.
13. Lin S, Chang J, Wang S, Goddard WA, Sandler SI. Prediction of vapor pressures and enthalpies of vaporization using a COSMO solvation model. *J Phys Chem.* 2004;108(36):7429–7439.
14. Wang S, Sandler SI, Chen C. Refinement of COSMO-SAC and the applications. *Ind Eng Chem Res.* 2007;46(22):7275–7288.
15. Hsieh C, Sandler SI, Lin S. Improvements of COSMO-SAC for vapor-liquid and liquid-liquid equilibrium predictions. *Fluid Phase Equilib.* 2010;297(1):90–97.
16. Xiong R, Sandler SI, Burnett RI. An improvement to COSMO-SAC for predicting thermodynamic properties. *Ind Eng Chem Res.* 2014; 53(19):8265–8278.
17. Fredenslund A, Jones RL, Prausnitz JM. Group-contribution estimation of activity coefficients in nonideal liquid mixtures. *AIChE J.* 1975;21(6):1086–1099.
18. Weidlich U, Gmehling J. A modified UNIFAC model. 1. Prediction of VLE, h^E, and γ^∞. *Ind Eng Chem Res.* 1987;26(7):1372–1381.
19. Stryjek R, Vera JH. PRSV: an improved Peng-Robinson equation of state for pure compounds and mixtures. *Can J Chem Eng.* 1986; 64(2):323–333.
20. Stryjek R, Vera JH. PRSV2: a cubic equation of state for accurate vapor-liquid equilibria calculations. *Can J Chem Eng.* 1986;64(5):820–826.
21. Griswold J, Wong SY. Phase-equilibria of the acetone-methanol-water system from 100°C into the critical region. *Chem Eng Prog Symp Ser.* 1952;48(3):18–34.
22. Chen X, Yang B, Abdeltawab AA, Al-Deyab SS, Yu G, Yong X. Isobaric vapor-liquid equilibrium for acetone + methanol + phosphate ionic liquids. *J Chem Eng Data.* 2015;60(3):612–620.
23. Toikka A, Naumkin P, Penkova A. Approximation and analysis of pervaporation of binary mixtures using nonequilibrium thermodynamics approach. *Chem Eng Res Des.* 2015;104:669–680.
24. Barr-David F, Dodge BF. Vapor-liquid equilibrium at high pressures: the systems ethanol-water and 2-propanol-water. *J Chem Eng Data.* 1959;4(2):107–121.
25. Zhang Z, Zhang L, Zhang Q, Sun D, Pan F, Dai S, Li W. Separation of 2-propanol and water azeotropic system using ionic liquid as entrainers. *Fluid Phase Equilib.* 2016;412:94–100.
26. Butcher KL, Medani MS. Thermodynamic properties of methanol-benzene mixtures at elevated temperatures. *J Appl Chem.* 1968;18: 100–107.
27. Gmehling J, Onken U. Vapor-liquid equilibrium data collection. Alcohols: Methanol. Supplement 5. *DECHEMA – Chemistry Data Series, Vol. 1, Part 2g*. Frankfurt: DECHEMA, 2005.
28. Renon H, Prausnitz JM. Estimation of parameters for the NRTL equation for excess Gibbs energies of strongly nonideal liquid mixtures. *Ind Eng Chem Process Des Dev.* 1969;8(3):413–419.
29. Moilanen P, Uusi-Kyyny P, Pokki J, Pakkanen M, Aittamaa J. Vapor-liquid equilibrium for butane + methanol, + ethanol, + 2-propanol, + 2-butanol, and + 2-methyl-2-propanol (TBA) at 323 K. *J Chem Eng Data.* 2008;53(1):83–88.
30. Bernatová S, Linek J, Wichterle I. Vapour-liquid equilibrium in the butyl alcohol – n-decane system at 85, 100 and 115°C. *Fluid Phase Equilib.* 1992;74:127–132.
31. Heintz A, Dolch E, Lichtenthaler RN. New experimental VLE-data for alkanol/alkane mixtures and their description by an extended real association (ERAS) model. *Fluid Phase Equilib.* 1986;27:61–79.
32. Rodriguez V, Pardo J, López MC, Royo FM, Urieta JS. Vapor pressures of binary mixtures of hexane + 1-butanol, + 2-butanol, + 2-methyl-1-propanol, or 2+methyl-2-propanol at 298.15 K. *J Chem Eng Data.* 1993;38(3):350–352.
33. Gomis V, Font A, Saquete MD, García-Cano J. LLE, VLE and VLLE data for the water – n-butanol – n-hxane system at atmospheric pressure. *Fluid Phase Equilib.* 2012;316:135–140.
34. Máchová I, Linek J, Wichterle I. Vapour—liquid equilibria in the heptane - 1-pentanol and heptane - 3-methyl-1-butanol systems at 75, 85 and 95°C. *Fluid Phase Equilib.* 1988;41(3):257–267.
35. Wilsak RA, Campbell SW, Thodos G. Vapor-liquid equilibrium measurements for the n-pentane – methanol system at 372.7, 397.7 and 422.6 K. *Fluid Phase Equilib.* 1987;33:157–171.
36. Moré JJ. The Levenberg-Marquardt Algorithm: implementation and theory. *Numer Anal Lect Notes Math.* 1977;630:105–116.

Manuscript received Dec. 8, 2016, and revision received Sep. 26, 2017.

REFERÊNCIAS

ABBOTT, M. M. Cubic Equation of State: An Interpretive Review. **Equations of State in Engineering and Research**, p. 47–70, 1979.

ABRAMS, D. S.; PRAUSNITZ, J. M. Statistical thermodynamics of liquid mixtures: A new expression for the excess Gibbs energy of partly or completely miscible systems. **AIChE Journal**, v. 21, n. 1, p. 116–128, 1975.

AQAR, D. Y.; RAHMANIAN, N.; MUJTABA, I. M. Feasibility of integrated batch reactive distillation columns for the optimal synthesis of ethyl benzoate. **Chemical Engineering and Processing: Process Intensification**, v. 122, n. August, p. 10–20, 2017.

ARCE, A.; DOMINGUEZ, A.; TOJO, J. Vapor-liquid equilibrium of the system metanol + benzene + cyclohexane at 760 mmHg. **Journal of Chemistry & Engineering Data**, v. 44, p. 661–665, 1999.

ASHRAF, F. A.; VERA, J. Vapor-Liquid Equilibria for the Ternary System n-Heptane/n-Propanol/1-Chlorobutane and its Constituent Binaries at 318.15 and 338.15 K. **The Canadian Journal of Chemical Engineering**, v. 59, n. February, p. 89–95, 1981.

ASSELINEAU, L.; BOGDANIC, G.; VIDAL, J. Calculation of thermodynamic properties and vapor-liquid equilibria of refrigerants. **Chemical Engineering Science**, v. 33, p. 1269–1276, 1978.

ATMANLI, A. Comparative analyses of diesel-waste oil biodiesel and propanol, n-butanol or 1-pentanol blends in a diesel engine. **Fuel**, v. 176, p. 209–215, 2016.

BANERJEE, S.; JANA, A. K. Observer-based extended generic model control of a reactive batch distillation. **Chemical Engineering Science**, v. 179, p. 185–197, 2018.

BARR-DAVID, F.; DODGE, B. F. Vapor-Liquid Equilibrium at High Pressures. The Systems Ethanol - Water and 2-Propanol - Water. **Journal of Chemical & Engineering Data**, v. 4, n. 2, p. 107–121, 1959.

BERGMANN, D. L.; ECKERT, C. A. Measurement of limiting activity

coefficients for aqueous systems by differential ebuliometry. **Fluid Phase Equilibria**, v. 63, p. 141–150, 1991.

BERNATOVÁ, S.; LINEK, J.; WICHTERLE, I. Vapour-liquid equilibrium in the butyl alcohol – n-decane system at 85, 100 and 115°C. **Fluid Phase Equilibria**, v. 74, p. 127–132, 1992.

BHARTI, A.; BANERJEE, T. Enhancement of bio-oil derived chemicals in aqueous phase using ionic liquids: Experimental and COSMO-SAC predictions using a modified hydrogen bonding expression. **Fluid Phase Equilibria**, v. 400, p. 27–37, 2015.

BRITTO, R. F.; MARTINS, C. A. Experimental analysis of a diesel engine operating in Diesel-Ethanol Dual-Fuel mode. **Fuel**, v. 134, n. May, p. 140–150, 2014.

BUTCHER, K. L.; MEDANI, M. S. Thermodynamic properties of methanol–benzene mixtures at elevated temperatures. **Journal of Applied Chemistry**, v. 18, n. 4, p. 100–107, 1968.

CAMERETTI, L. F.; SADOWSKI, G. Modeling of aqueous electrolyte solutions with perturbed-chain statistical associated fluids theory. **Industrial & Engineering Chemistry Research**, v. 44, p. 3355–3362, 2005.

CHAPMAN, W. G. et al. SAFT: Equation-of-state solution model for associating fluids. **Fluid Phase Equilibria**, v. 52, n. C, p. 31–38, 1989.

CHEN, Y. et al. Screening solvents to extract phenol from aqueous solutions by the COSMO-SAC model and extraction process simulation. **Fluid Phase Equilibria**, v. 451, p. 12–24, 2017.

COUTSIKOS, P.; KALOSPIROS, N. S.; TASSIOS, D. P. Capabilities and limitations of the Wong-Sandler mixing rules. **Fluid Phase Equilibria**, v. 108, n. 1–2, p. 59–78, 1995.

DE AGUIAR, I. B. C. et al. Performance and Emissions of a Diesel Engine Fueled By Diesel Oil-Ethanol-N-Butanol Blends. **SAE International - Technical Paper Series**, 2017.

DERR, E. L.; DEAL, C. H. Analytical solutions of groups: correlation of activity coefficients through structural groups parameters. **Chemical Engineering**

Symposium Series, v. 32, p. 3–40, 1969.

DOHNAL, V.; VRBKA, P. Limiting activity coefficients in the 1-alkanol + n-alkane systems: Survey, critical evaluation and recommended values, interpretation in terms of association models. **Fluid Phase Equilibria**, v. 133, n. 1–2, p. 73–87, 1997.

DOMENECH, S.; ENJALBERT, M. **Program for simulating batch rectification as a unit operationComputers and Chemical Engineering**, 1981.

Dortmund Data Bank - Vapor-Liquid Equilibrium Data - Ethanol + Water + 1-Butanol VLE Data. Disponível em: <http://www.ddbst.com/en/EED/VLE/VLE Ethanol%3B1-Butanol%3BWater.php>.

E, J. et al. Effect of different technologies on combustion and emissions of the diesel engine fueled with biodiesel: A review. **Renewable and Sustainable Energy Reviews**, v. 80, p. 620–647, 2017.

ENDLER, I.; HRADETZKY, G.; BITTRICH, H. J. Grenzaktivitätskoeffizienten in binären Systemen Benzen-Alkanol. **J. Prakt. Chem.**, v. 327, p. 693–697, 1985.

ESCOBEDO-ALVARADO, G. N.; SANDLER, S. I. Study of EOS-Gex Mixing Rules for Liquid-Liquid Equilibria. **AIChE Journal**, v. 44, n. 5, p. 1178–1187, 1998.

ESPANANI, R.; MILLER, A.; JACOBY, W. Prediction of vapor-liquid equilibria for mixtures of low boiling point compounds using Wong-Sandler mixing rule and EOS/GE model. **Chemical Engineering Science**, v. 152, p. 343–350, 2016.

FAÚNDEZ, C. A.; VALDERRAMA, J. O. Low pressure vapor – liquid equilibrium in ethanol + congener mixtures using the Wong – Sandler mixing rule. **Thermochimica Acta**, v. 490, p. 37–42, 2009.

FRANCO, A. L. C. et al. Soil carbon, nitrogen and phosphorus changes under sugarcane expansion in Brazil. **Science of the Total Environment**, v. 515–516, p. 30–38, 2015.

FREDENSLUND, A. et al. Computerized Design of Multicomponent Distillation Columns Using the UNIFAC Group Contribution Method for Calculation of Activity Coefficients. **Industrial & Engineering Chemistry Process Design and Development**, v. 16, n. 4, p. 450–462, 1977.

FREDENSLUND, A.; JONES, R. L.; PRAUSNITZ, J. M. Group-contribution estimation of activity coefficients in nonideal liquid mixtures. **AIChE Journal**, v. 21, n. 6, p. 1086–1099, 1975.

GERBER, R. P.; SOARES, R. D. P. Prediction of infinite-dilution activity coefficients using UNIFAC and COSMO-SAC variants. **Industrial and Engineering Chemistry Research**, v. 49, n. 16, p. 7488–7496, 2010.

GERBER, R. P.; SOARES, R. DE P. Functional-Segment Activity Coefficient Model. 1. Model Formulation. **Industrial & Engineering Chemistry Research**, v. 52, p. 1159–11171, 2013.

GIAKOUMIS, E. G. et al. Exhaust emissions with ethanol or n-butanol diesel fuel blends during transient operation: A review. **Renewable and Sustainable Energy Reviews**, v. 17, p. 170–190, 2013.

GMEHLING, J.; LI, J.; SCHILLER, M. A modified UNIFAC model. 2. Present parameter matrix and results for different thermodynamic properties. **Industrial & Engineering Chemistry Research**, v. 32, n. 1, p. 178–193, 1993.

GMEHLING, J.; ONKEN, U. **Vapor-liquid equilibrium data collection. Alcohols: methanol. Supplement 5 - DECHEMA - Chemistry Data Series 1(2g)**. [s.l: s.n.].

GOMIS, V.; RUIZ, F.; ASENSI, J. C. The application of ultrasound in the determination of isobaric vapour-liquid-liquid equilibrium data. **Fluid Phase Equilibria**, v. 172, n. 2, p. 245–259, 2000.

GÓRAL, M. et al. Recommended vapor-liquid equilibrium data. Part 1: Binary n-alkanol-n-alkane systems. **Journal of Physical and Chemical Reference Data**, v. 31, n. 3, p. 701–748, 2002.

GRISWOLD, J.; WONG, S. Y. Phase-equilibria of the acetone-methanol-water system from 100°C into the critical region. **Chemical Engineering Progress Symposium Series**, v. 48, n. 3, p. 18–34, 1952.

GROSS, J.; SADOWSKI, G. Perturbed-chain SAFT: An equation of state based on a perturbation theory for chain molecules. **Industrial and Engineering Chemistry Research**, v. 40, n. 4, p. 1244–1260, 2001.

HANSEN, A. C.; ZHANG, Q.; LYNE, P. W. L. Ethanol – diesel fuel blends — a review. v. 96, n. 2005, p. 277–285, 2010.

HEGELY, L.; LANG, P. Optimization of a batch extractive distillation process with recycling off-cuts. **Journal of Cleaner Production**, v. 136, p. 99–110, 2016.

HEINTZ, A.; DOLCH, E.; LICHTENTHALER, R. N. New experimental VLE-data for alkanol/alkane mixtures and their description by an extended real association (ERAS) model. **Fluid Phase Equilibria**, v. 27, n. C, p. 61–79, 1986.

HSIEH, C. M.; LIN, S. T. First-principles prediction of phase equilibria using the PR + COSMOSAC equation of state. **Asia-Pacific Journal of Chemical Engineering**, v. 7, n. SUPPL. 1, p. 1, 2012.

HSIEH, C. M.; SANDLER, S. I.; LIN, S. T. Improvements of COSMO-SAC for vapor-liquid and liquid-liquid equilibrium predictions. **Fluid Phase Equilibria**, v. 297, n. 1, p. 90–97, 2010.

HURON, M. J.; VIDAL, J. New Mixing Rules In Simple Equations Of State For Representing Vapour-Liquid Equilibria Of Strongly Non-Ideal Mixtures. **Fluid Phase Equil.**, v. 3, n. August 1978, p. 255, 1979.

IGLESIAS, M.; ORGE, B.; MARINO, G. Vapor - Liquid Equilibria for the Ternary System Acetone + Methanol + Water at 101 . 325 kPa. p. 661–665, 1999.

IPCC. **Climate Change, 2007. The Physical Science Basis**. [s.l.] Cambridge University Press, 2007. v. 53

IZADPANAH, A. A.; VAFAIE SEFTI, M.; VARAMINIAN, F. Multi-component-multiphase flash calculations for systems containing gas hydrates by direct minimization of Gibbs free energy. **Iranian Journal of Chemistry and Chemical Engineering**, v. 25, n. 3, p. 27–34, 2006.

JANSSENS, I. R. **Butanol scoping study: opportunities and threats for developing countries**. [s.l: s.n.]. Disponível em: <http://bioenergyforumfact.org/sites/default/files/2016-10/35. Butanol scoping study - opportunities and threats for developing countries.pdf>.

JIA, H. et al. Effect of thermodynamic parameters on prediction of phase behavior and process design of extractive distillation. **Chinese Journal of Chemical**

Engineering, v. 26, n. 5, p. 993–1002, 2018.

KADIR, S. et al. Liquid–Liquid Equilibria of the Ternary Systems 3-Methyl-1-butanol + Ethanol + Water and 2-Methyl-1-propanol + Ethanol + Water at 293.15 K. **Journal of Chemical & Engineering Data**, v. 53, n. 4, p. 910–912, 2008.

KAMIHAMA, N. et al. Isobaric Vapor–Liquid Equilibria for Ethanol + Water + Ethylene Glycol and Its Constituent Three Binary Systems. **Journal of Chemical & Engineering Data**, v. 57, n. 2, p. 339–344, 2012.

KAN, İ.; ÖZALP, A.; ÖZALP, Ü. **Limits on the predictive thermodynamic models, Wilson and UNIQUAC in multicomponent phase equilibria of ethanol-benzene-heptane and hexane-ethanol-benzeneCommunications, Faculty Of Science, University of Ankara Series B Chemistry and Chemical Engineering**, 1996. Disponível em: <http://dergiler.ankara.edu.tr/dergiler/31/1402/15875.pdf>

KARABEKTAS, M.; HOSOZ, M. Performance and emission characteristics of a diesel engine using isobutanol-diesel fuel blends. **Renewable Energy**, v. 34, n. 6, p. 1554–1559, 2009.

KHALIFE, E. et al. Impacts of additives on performance and emission characteristics of diesel engines during steady state operation. **Progress in Energy and Combustion Science**, v. 59, p. 32–78, 2017.

KIM, H. N.; CHOI, B. C. Effect of ethanol-diesel blend fuels on emission and particle size distribution in a common-rail direct injection diesel engine with warm-up catalytic converter. **Renewable Energy**, v. 33, n. 10, p. 2222–2228, 2008.

KLAMT, A. Conductor-like Screening Model for Real Solvents: A New Approach to the Quantitative Calculation of Solvation Phenomena. **Journal of Physical Chemistry**, v. 99, n. 7, p. 2224–2235, 1995.

KLAMT, A.; ECKERT, F. COSMO-RS: a novel and efficient method for the a priori prediction of thermophysical data of liquids. **Fluid Phase Equilibria**, v. 172, n. 1, p. 43–72, 2000.

KLAMT, A.; SCHÜÜRMANN, G. COSMO: a new approach to dielectric screening in solvents with explicit expressions for the screening energy and its gradient. **J. Chem. Soc., Perkin Trans. 2**, n. 5, p. 799–805, 1993.

KOJIMA, K.; ZHANG, S.; HIAKI, T. **Measuring methods of infinite dilution activity coefficients and a database for systems including waterFluid Phase Equilibria**, 1997.

KOSUGE, H.; IWAKABE, K. Estimation of isobaric vapor-liquid-liquid equilibria for partially miscible mixture of ternary system. **Fluid Phase Equilibria**, v. 233, n. 1, p. 47–55, 2005.

KURAMOCHI, H. et al. Application of UNIFAC models for prediction of vapor-liquid and liquid-liquid equilibria relevant to separation and purification processes of crude biodiesel fuel. **Fuel**, v. 88, n. 8, p. 1472–1477, 2009.

KURZIN, A. V et al. Activity Coefficients of Methanol and Water in the Reaction of Potassium Hydroxide Methanolysis. **Journal of Chemical Engineering Data**, v. 48, p. 344–346, 2003.

LAGARIAS, J. C. et al. Convergence Properties of the Nelder--Mead Simplex Method in Low Dimensions. **SIAM Journal on Optimization**, v. 9, n. 1, p. 112–147, 1998.

LANDAU, I.; BELFER, A. J.; LOCKE, D. C. Measurement of limiting activity coefficients using non-steady-state gas chromatography. **Industrial & Engineering Chemistry Research**, v. 30, p. 1900–1906, 1991.

LAPUERTA, M.; ARMAS, O.; GARCÍA-CONTRERAS, R. Stability of diesel-bioethanol blends for use in diesel engines. **Fuel**, v. 86, n. 10–11, p. 1351–1357, 2007.

LETYANINA, I.; TSVETOV, N.; TOIKKA, A. **Application of the UNIFAC models for prediction and description of excess molar enthalpies for binary mixtures of n-propanol, acetic acid, n-propyl acetate, and waterFluid Phase Equilibria**, 2016.

LI, Z. **Thermodynamic Modelling of Liquid – liquid Equilibria Using the Nonrandom Two-Liquid Model and Its Applications**. [s.l.] The University of Melbourne, 2015.

LIN, S.-T.; SANDLER, S. I. A Priori Phase Equilibrium Prediction from a Segment Contribution Solvation Model. **Industrial & Engineering Chemistry Research**, v. 41, n. 5, p. 899–913, 2002.

LIN, S. T. et al. Prediction of miscibility gaps in water/ether mixtures using COSMO-SAC model. **Fluid Phase Equilibria**, v. 310, n. 1–2, p. 19–24, 2011.

LIU, H.; HU, B.; JIN, C. Effects of different alcohols additives on solubility of hydrous ethanol/diesel fuel blends. **Fuel**, v. 184, p. 440–448, 2016.

LO, K. M.; CHIEN, I. L. **Efficient separation method for tert-butanol dehydration via extractive distillationJournal of the Taiwan Institute of Chemical Engineers**, 2017.

LOPEZ-SAUCEDO, E. S. et al. Rigorous modeling, simulation and optimization of a conventional and nonconventional batch reactive distillation column: A comparative study of dynamic optimization approaches. **Chemical Engineering Research and Design**, v. 111, p. 83–99, 2016.

LUEDECKE, D.; PRAUSNITZ, J. M. **Phase equilibria for strongly nonideal mixtures from an equation of state with density-dependent mixing rulesFluid Phase Equilibria**, 1985.

LUYBEN, W. L. Control of the Heterogeneous Azeotropic n -Butanol/Water Distillation System. **Energy & Fuels**, v. 22, n. 6, p. 4249–4258, 2008.

MÁCHOVÁ, I.; LINEK, J.; WICHTERLE, I. Vapour-liquid equilibria in the heptane – 1-pentanol and heptane – 3-methyl-1-butanol systems at 75, 85 and 95°C. **Fluid Phase Equilibria**, v. 41, p. 257–267, 1988.

MAGNUSSEN, T.; RASMUSSEN, P.; FREDENSLUND, A. Unifac Parameter Table for Prediction of Liquid-Liquid Equilibria. **Industrial and Engineering Chemistry Process Design and Development**, v. 20, n. 2, p. 331–339, 1981.

MARZAL, P.; MONTÓN, J. B.; RODRIGO, M. A. Isobaric Vapor−Liquid Equilibria of the Water + 2-Propanol System at 30, 60, and 100 kPa. **Journal of Chemical Engineering Data**, v. 41, p. 608–611, 1996.

MASOUDI, N.; ZACCOUR, G. Adapting to climate change: Is cooperation good for the environment? **Economics Letters**, v. 153, p. 1–5, 2017.

MATHIAS, P. M.; KLOTZ, H. C. Take a closer look at thermodynamic property models. **Chemical Engineering Progress**, n. January 1994, p. 67–75, 1994.

MATHIAS, P. M.; KLOTZ, H. C.; PRAUSNITZ, J. M. Equation-of-State mixing rules for multicomponent mixtures: the problem of invariance. **Fluid Phase Equilibria**, v. 67, n. C, p. 31–44, 1991.

MICHELSEN, M. L. The Isothermal Flash Problem. Part I. Stability. **Fluid Phase Equilibria**, v. 9, p. 1–19, 1982a.

MICHELSEN, M. L. The Isothermal Flash Problem. Part II. Phase-Split Calculation. **Fluid Phase Equilibria**, v. 9, p. 21–40, 1982b.

MICHELSEN, M. L. A method for incorporating excess Gibbs energy models in equations of state. **Fluid Phase Equilibria**, v. 60, n. 1–2, p. 47–58, 1990.

MIYANO, Y.; NAKANISHI, K.; FUKUCHI, K. Henry's constants of butane, isobutane, 1-butene and isobutene in methanol at 255-320 K. **Fluid Phase Equilibria**, v. 208, n. 1–2, p. 223–238, 2003.

MOHAMMADI, A. et al. Fuel Injection Strategy for Clean Diesel Engine Using Ethanol Blended Diesel Fuel. **SAE International - Technical Paper Series**, 2005.

MOILANEN, P. et al. Vapor-liquid equilibrium for butane + methanol, + ethanol, + 2-propanol, + 2-butanol, and + 2-methyl-2-propanol (TBA) at 323 K. **Journal of Chemical and Engineering Data**, v. 53, n. 1, p. 83–88, 2008.

MORE, J. **The Levenberg-Marquardt Algorithm: implementation and theory**. Conference on Numerical Analysis1. **Anais**...University of Dundee, Scotland: 1977

NDABA, B.; CHIYANZU, I.; MARX, S. N-Butanol derived from biochemical and chemical routes: A review. **Biotechnology Reports**, v. 8, p. 1–9, 2015.

NEBIG, S.; GMEHLING, J. Measurements of different thermodynamic properties of systems containing ionic liquids and correlation of these properties using modified UNIFAC (Dortmund). **Fluid Phase Equilibria**, v. 294, n. 1–2, p. 206–212, 2010.

NEBIG, S.; LIEBERT, V.; GMEHLING, J. Measurement and prediction of activity coefficients at infinite dilution (γ∞), vapor-liquid equilibria (VLE) and excess enthalpies (HE) of binary systems with 1,1-dialkyl-pyrrolidinium bis(trifluoromethylsulfonyl)imide using mod. UNIFAC (Dortmund). **Fluid Phase**

Equilibria, v. 277, n. 1, p. 61–67, 2009.

NELDER, J. A.; MEAD, R. **A simplex method for function minimizationComputer Journal**, 1964. Disponível em: <http://apps.isiknowledge.com.gate6.inist.fr/full_record.do?product=WOS&search_mode=GeneralSearch&qid=2&SID=R1L1cN2N12FbagJN87d&page=1&doc=2>

ONG, H. C.; MAHLIA, T. M. I.; MASJUKI, H. H. A review on energy scenario and sustainable energy in Malaysia. **Renewable and Sustainable Energy Reviews**, v. 15, n. 1, p. 639–647, 2011.

ORBEY, H.; SANDLER, S. I. On the combination of equation of state and excess free energy models. **Fluid Phase Equilibria**, v. 111, n. 1, p. 53–70, 1995.

ORBEY, H.; SANDLER, S. I. A comparison of Huron-Vidal type mixing rules of mixtures of compounds with large size differences, and a new mixing rule. **Fluid Phase Equilibria**, v. 132, n. 1–2, p. 1–14, 1997.

ORBEY, H.; SANDLER, S. I. **Modeling Vapor-Liquid Equilibria: cubic equations of state and their mixing rules**. 1. ed. [s.l.] Cambridge University Press, 1998.

ORGANIZATION OF THE PETROLEUM EXPORTING COUNTRIES - OPEC. **Monthly Oil Market Report 12**. [s.l: s.n.]. Disponível em: <www.opec.org>.

OSUOLALE, F. N.; ZHANG, J. Thermodynamic optimization of atmospheric distillation unit. **Computers and Chemical Engineering**, v. 103, p. 201–209, 2017.

PANAGIOTOPOULOS, A. Z.; REID, R. C. New mixing rule for cubic equations of state for highly polar, asymmetric systems. **ACS Symposium Series**, n. 300, p. 571–582, 1986.

PATRASCU, I.; BILDEA, C. S.; KISS, A. A. Eco-efficient butanol separation in the ABE fermentation process. **Separation and Purification Technology**, v. 177, p. 49–61, 2017.

PELLEGRINI, L. A. et al. Prediction of vapor–liquid equilibrium for reservoir mixtures with cubic equations of state: Binary interaction parameters for acidic gases. **Fluid Phase Equilibria**, v. 326, p. 45–49, 2012.

PENG, D.-Y.; ROBINSON, D. B. A New Two-Constant Equation of State. **Industrial & Engineering Chemistry Fundamentals**, v. 15, n. 1, p. 59–64, 1976.

PINZI, S. et al. Castor oil enhanced effect on fuel ethanol-diesel fuel blend properties. **Applied Energy**, v. 224, n. January, p. 409–416, 2018.

PIVIDAL, K. A.; BIRTIGH, A.; SANDLER, S. I. Infinite Dilution Activity Coefficients for Oxygenate Systems Determined Using a Differential Static Cell. **Journal of Chemical & Engineering Data**, v. 37, p. 484–487, 1992.

POSSANI, L. F. K. Correlação Simultânea de IDAC, VLE e LLE com o Modelo F-SAC. 2014.

RACHFORD, H. H.; RICE, J. D. Procedure for Use of Electronic Digital Computers in Calculating Flash Vaporization Hydrocarbon Equilibrium. **Journal of Petroleum Technology**, v. 4, n. 10, p. 19–3, 1952.

REDLICH, O.; KWONG, J. N. S. On The Thermodynamics of Solutions. V. An Equation of State. Fugacities of Gaseous Solutions. **Chemical Reviews**, v. 44, n. 1, p. 233–244, 1949.

RENON, H.; PRAUSNITZ, J. M. Local compositions in thermodynamics excess functions for liquids mixtures. **AIChE J.**, v. 14, n. 1, p. 135–144, 1968.

RODRIGUEZ, V. et al. Vapor pressures of binary mixtures of hexane + 1-butanol, + 2-butanol, + 2-methyl-1-propanol, or + 2-methyl-2-propanol at 298.15 K. **Journal of Chemical Engineering Data**, v. 38, n. 1, p. 350–352, 1993.

SANDLER, S. I. **Chemical, Biochemical, and Engineering Thermodynamics**. 4. ed. [s.l.] John Wiley & Sons, Inc., 2006.

SANDLER, S. I.; ORBEY, H. 9 Mixing and combining rules. **Experimental Thermodynamics**, v. 5, p. 321–357, 2000.

SANTOS, D. et al. Vapor-Liquid Equilibrium Calculations for Alcohol and Hydrocarbon Mixtures Using COSMO-SAC, NRTL, and UNIQUAC Models. **Brazilian Journal of Petroleum and Gas**, v. 8, n. 4, p. 127–137, 2014.

SATGÉ DE CARO, P. et al. Interest of combining an additive with diesel-ethanol blends for use in diesel engines. **Fuel**, v. 80, n. 4, p. 565–574, 2001.

SCHMIDT, T. W. **Determination of Infinite Dilution Activity Coefficients (gamma infinite) using molecular beamsUS-Patent**, 1980.

SCHWARTZENTRUBER, J.; RENON, H. Equations of state: how to reconcile flexible mixing rules, the virial coefficient constraint and the “michelsen-Kistenmacher syndrome” for multicomponent systems. **Fluid Phase Equilibria**, v. 67, n. C, p. 99–110, 1991.

SCOTT, R. L. Corresponding states treatment of nonelectrolyte solutions. **The Journal of Chemical Physics**, v. 25, n. 2, p. 193–205, 1956.

SEGTOVICH, I. S. V.; BARRETO, A. G.; TAVARES, F. W. Simultaneous multiphase flash and stability analysis calculations including hydrates. **Fluid Phase Equilibria**, v. 413, p. 196–208, 2016.

ŠERBANOVIĆ, S. P. et al. Effect of temperature on the excess molar volumes of some alcohol + aromatic mixtures and modelling by cubic EOS mixing rules. **Fluid Phase Equilibria**, v. 239, n. 1, p. 69–82, 2006.

SHAMPINE, L. F.; REICHELT, M. W. The MATLAB ODE Suite. **SIAM Journal on Scientific Computing**, v. 18, n. 1, p. 1–22, 1997.

SHI, X. et al. Emission reduction potential of using ethanol-biodiesel-diesel fuel blend on a heavy-duty diesel engine. **Atmospheric Environment**, v. 40, n. 14, p. 2567–2574, 2006.

SHIBATA, S. K.; SANDLER, S. I. Critical evaluation of equation of state mixing rules for the prediction of high-pressure phase equilibria. **Industrial & Engineering Chemistry Research**, v. 28, n. 12, p. 1893–1898, 1989.

SILVEIRA, C. L.; SALAU, N. P. G. From Wilson to F-SAC: A comparative analysis of correlative and predictive activity coefficient models to determine VLE and IDAC of binary systems. **Fluid Phase Equilibria**, v. 464, p. 1–11, 2018.

SILVEIRA, C. L.; SANDLER, S. I. Extending the range of COSMO-SAC to high temperatures and high pressures. **AIChE Journal**, n. February, p. 2012–2014, 2017.

SKJOLD-JORGENSEN, S. et al. Vapor-Liquid Equilibria by UNIFAC Group Contribution. Revision and Extension. **Industrial & Engineering Chemistry Process Design and Development**, v. 18, n. 4, p. 714–722, 1979.

SMITH, J. M.; VAN NESS, H. C.; ABBOTT, M. M. **Introdução à Termodinâmica da Engenharia Química**. 7a. ed. Rio de Janeiro: LTC, 2007.

SOARES, R. DE P. et al. Functional-Segment Activity Coefficient Model. 2. Associating Mixtures. **Industrial & Engineering Chemistry Research**, v. 52, n. 32, p. 11172–11181, 2013.

SOARES, R. DE P.; GERBER, R. P. Functional-Segment Activity Coefficient Model. 1. Model Formulation. **Industrial & Engineering Chemistry Research**, v. 52, n. 32, p. 11159–11171, 2013.

SOAVE, G. Equilibrium constants from a modified Redlich-Kwong equation of state. **Chemical Engineering Science**, v. 27, n. 6, p. 1197–1203, 1972.

SOAVE, G.; GAMBA, S.; PELLEGRINI, L. A. SRK equation of state: Predicting binary interaction parameters of hydrocarbons and related compounds. **Fluid Phase Equilibria**, v. 299, p. 285–293, 2010.

SOUTO, R. M. L. O. et al. Rigorous thermodynamic evaluation of the extractive distillation process. **Chemical Engineering Research and Design**, v. 133, p. 195–203, 2018.

STAVROU, M.; BARDOW, A.; GROSS, J. **Estimation of the binary interaction parameter kijof the PC-SAFT Equation of State based on pure component parameters using a QSPR methodFluid Phase Equilibria**, 2016.

STOJKOVIC, M.; GERBAUD, V.; SHCHERBAKOVA, N. Cyclic operation as optimal control reflux policy of binary mixture batch distillation. **Computers and Chemical Engineering**, v. 108, p. 98–111, 2018.

STRYJEK, R.; VERA, J. H. PRSV: An improved peng—Robinson equation of state for pure compounds and mixtures. **The Canadian Journal of Chemical Engineering**, v. 64, n. 2, p. 323–333, 1986a.

STRYJEK, R.; VERA, J. H. PRSV2: A cubic equation of state for accurate vapor-liquid equilibria calculations. **The Canadian Journal of Chemical Engineering**, v. 64, n. 5, p. 820–826, 1986b.

STRYJEK, R.; VERA, J. H. PRSV — An improved peng-Robinson equation of state with new mixing rules for strongly nonideal mixtures. **The Canadian Journal of**

Chemical Engineering, v. 64, n. 2, p. 334–340, 1986c.

SULEMAN, H. et al. Thermodynamic modelling of liquid-liquid extraction systems involving ionic liquids: A new approach. **Journal of Molecular Liquids**, v. 252, p. 18–23, 2018.

THAKRE, N.; JANA, A. K. Modeling phase equilibrium with a modified Wong-Sandler mixing rule for natural gas hydrates: Experimental validation. **Applied Energy**, v. 205, n. August, p. 749–760, 2017.

THOMAS, E. R. et al. Limiting activity coefficients of nonpolar and polar solutes in both volatile and nonvolatile solvents by gas chromatography. **Journal of Chemical & Engineering Data**, v. 27, p. 399–405, 1982.

TORRES-JIMENEZ, E. et al. Physical and chemical properties of ethanol-diesel fuel blends. **Fuel**, v. 90, n. 2, p. 795–802, 2011.

TU, C.-H.; WU, Y.-S.; LIU, T.-L. Vapor-liquid equilibria of the ternary system methanol + acetone + methyl vinyl ketone at atmospheric pressure. **Fluid Phase Equilibria**, v. 131, p. 181–188, 1997.

U.S DEPARMENT OF ENERGY. **Alternative Fuels Data Center – Fuel Properties Comparison**. Disponível em: <https://www.afdc.energy.gov/fuels/fuel_comparison_chart.pdf>.

VALDERRAMA, J. O. The State of the Cubic Equations of State. **Industrial & Engineering Chemistry Research**, v. 42, n. 8, p. 1603–1618, 2003.

VALDERRAMA, O.; ZAVALETA, J. Generalized binary interaction parameters in the Wong – Sandler mixing rules for mixtures containing n -alkanols and carbon dioxide. v. 234, p. 136–143, 2005.

VAN BERLO, M. et al. Partition coefficients and solubilities of glycine in the ternary solvent system 1-butanol + ethanol + water. **Industrial & Engineering Chemistry Research**, v. 36, n. 6, p. 2474–2482, 1997.

WAALS, VAN DER. De continuiteit van den gasen Vloeistoftoestand. p. 136, 1873.

WALLINGTON, T. J.; LAMBERT, C. K.; RUONA, W. C. Diesel vehicles and

sustainable mobility in the U.S. **Energy Policy**, v. 54, p. 47–53, 2013.

WANG, S.; SANDLER, S. I.; CHEN, C. C. Refinement of COSMO-SAC and the applications. **Industrial and Engineering Chemistry Research**, v. 46, n. 22, p. 7275–7288, 2007.

WASYLKIEWICZ, S. K. et al. Global Stability Analysis and Calculation of Liquid−Liquid Equilibrium in Multicomponent Mixtures. **Industrial & Engineering Chemistry Research**, v. 35, n. 4, p. 1395–1408, 1996.

WEIDLICH, U.; GMEHLING, J. A modified UNIFAC Model. 1. Prediction of VLE, hE, and y∞. **Industrial & Engineering Chemistry Research**, v. 26, p. 1372–1381, 1987.

WILSAK, R. A.; CAMPBELL, S. W.; THODOS, G. Vapor-liquid equilibrium measurements for the n-pentane-methanol-acetone ternary at 372.7 K and their prediction from the constituent binaries. **Fluid Phase Equilibria**, v. 33, n. 1–2, p. 173–190, 1987.

WILSON, G. M. Vapor-Liquid Equilibrium. XI. A New Expression for the Excess Free Energy of Mixing. **Journal of the American Chemical Society**, v. 86, n. 2, p. 127–130, 1964.

WONG, D. S. H.; ORBEY, H.; SANDLER, S. I. Equation of state mixing rule for nonideal mixtures using available activity coefficient model parameters and that allows extrapolation over large ranges of temperature and pressure. **Industrial & Engineering Chemistry Research**, v. 31, n. 8, p. 2033–2039, 1992.

WONG, D. S. H.; SANDLER, S. I. A theoretically correct mixing rule for cubic equations of state. **AIChE Journal**, v. 38, n. 5, p. 671–680, 1992.

XING-CAI, L. et al. Effect of cetane number improver on heat release rate and emissions of high speed diesel engine fueled with ethanol-diesel blend fuel. **Fuel**, v. 83, n. 14–15 SPEC. ISS., p. 2013–2020, 2004.

XIONG, R.; SANDLER, S. I.; BURNETT, R. I. An improvement to COSMO-SAC for predicting thermodynamic properties. **Industrial and Engineering Chemistry Research**, v. 53, n. 19, p. 8265–8278, 2014.

XU, D. et al. Measurement and thermodynamic modelling of ternary liquid-

liquid equilibrium for extraction of thioglycolic acid from aqueous solution with different solvents. **Journal of Chemical Thermodynamics**, v. 113, p. 229–235, 2017.

XUE, Z.; MU, T.; GMEHLING, J. Comparison of the a Priori COSMO-RS models and group contribution methods: Original UNIFAC, modified UNIFAC(Do), and modified UNIFAC(Do) consortium. **Industrial and Engineering Chemistry Research**, v. 51, n. 36, p. 11809–11817, 2012.

YANG, C. et al. Experimental measurement and thermodynamic modelling of liquid-liquid equilibria for the separation of 1,2-dichloroethane from cyclohexane using various extractants. **Journal of Molecular Liquids**, v. 252, p. 263–270, 2018.

YOSHIMOTO, Y. et al. Influence of 1-butanol addition on diesel combustion with palm oil methyl ester/gas oil blends. **Energy**, v. 61, p. 44–51, 2013.

ZHU, L. et al. Emissions characteristics of a diesel engine operating on biodiesel and biodiesel blended with ethanol and methanol. **Science of the Total Environment**, v. 408, n. 4, p. 914–921, 2010.